

AD-A136 342

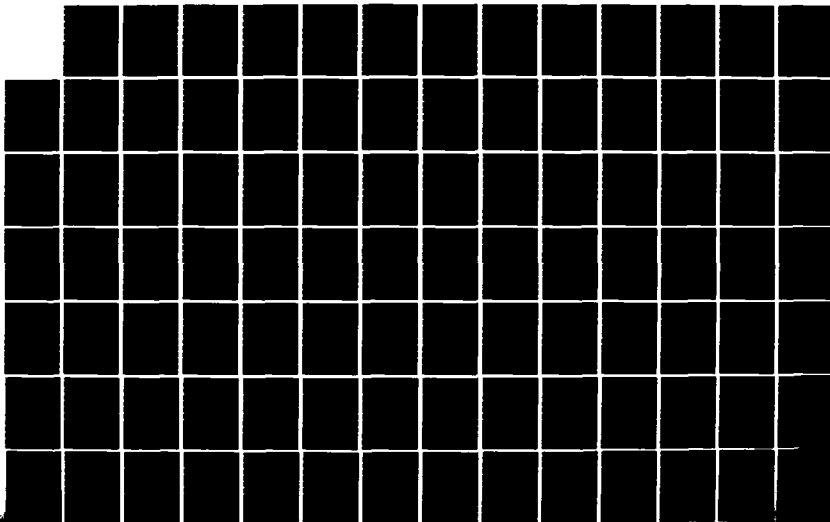
IDENTIFICATION OF DAMAGE IN HYSTERETIC STRUCTURES(U)
NEW MEXICO UNIV ALBUQUERQUE DEPT OF CIVIL ENGINEERING
M L WANG ET AL. JUL 83 AFOSR-TR-83-1230 AFOSR-81-0086

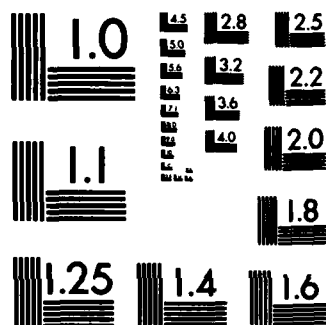
1/3

UNCLASSIFIED

F/G 13/13

NL





MICROCOPY RESOLUTION TEST CHART
NATIONAL BUREAU OF STANDARDS-1963-A

IDENTIFICATION OF DAMAGE IN HYSTERETIC STRUCTURES

Prepared by

Department of Civil Engineering

The University of New Mexico
Albuquerque, New Mexico 87131

by

Ming-Liang Wang
Thomas L. Paez
Frederick D. Ju

Prepared for

The Office of Scientific Naval Research
Bolling Air Force Base
Washington, D.C.

July 1983

DTIC

DEC 27 1983

E

Approved for public release
Distribution unlimited.

83 12 27 001

A136342

DTIC FILE COPY

UNCLASSIFIED

SECURITY CLASSIFICATION OF THIS PAGE (When Data Entered)

REPORT DOCUMENTATION PAGE		READ INSTRUCTIONS BEFORE COMPLETING FORM
1. REPORT NUMBER AFOSR-TR- 83 - 1230	2. GOVT ACCESSION NO.	3. RECIPIENT'S CATALOG NUMBER
4. TITLE (and Subtitle) IDENTIFICATION OF DAMAGE IN HYSTERETIC STRUCTURES		5. TYPE OF REPORT & PERIOD COVERED ANNUAL 1 Feb 82 - 28 Feb 83
		6. PERFORMING ORG. REPORT NUMBER
7. AUTHOR(s) MING-LIANG WANG THOMAS L PAEZ FREDERICK D JU		8. CONTRACT OR GRANT NUMBER(s) AFOSR-81-0086
9. PERFORMING ORGANIZATION NAME AND ADDRESS UNIVERSITY OF NEW MEXICO DEPT OF CIVIL ENGINEERING ALBUQUERQUE, NM 87131		10. PROGRAM ELEMENT, PROJECT, TASK AREA & WORK UNIT NUMBERS 61102F 2307/C2
11. CONTROLLING OFFICE NAME AND ADDRESS AIR FORCE OFFICE OF SCIENTIFIC RESEARCH/NA BOLLING AFB, DC 20332		12. REPORT DATE July 1983
		13. NUMBER OF PAGES 207
14. MONITORING AGENCY NAME & ADDRESS (if different from Controlling Office)		15. SECURITY CLASS. (of this report) Unclassified
		15a. DECLASSIFICATION/DOWNGRADING SCHEDULE
16. DISTRIBUTION STATEMENT (of this Report) Approved for Public Release; Distribution Unlimited.		
17. DISTRIBUTION STATEMENT (of the abstract entered in Block 20, if different from Report)		
18. SUPPLEMENTARY NOTES		
19. KEY WORDS (Continue on reverse side if necessary and identify by block number) SHOCK VIBRATION TESTING INELASTIC STRUCTURES LEAST FAVORABLE RESPONSE PEAK RESPONSE ENERGY DISSIPATION		
20. ABSTRACT (Continue on reverse side if necessary and identify by block number) In structural engineering it is imperative to design each system to survive the inputs anticipated over the design life of the structure. Strong motion inputs cause systems to execute nonlinear responses, and during the strong motion responses, structures accumulate damage. Therefore, the capability to model nonlinear responses and to assess the damage level in a structure is essential for optimal design. Techniques for the diagnosis of damage in inelastic structures have been developed. The dissipated energy in mechanical systems is taken as a measure of damage accumulation. Two models		

DD FORM 1 JAN 73 1473

EDITION OF 1 NOV 65 IS OBSOLETE

UNCLASSIFIED

SECURITY CLASSIFICATION OF THIS PAGE (When Data Entered)

83 12 27 001

UNCLASSIFIED

SECURITY CLASSIFICATION OF THIS PAGE(When Data Entered)

for the simulation of damaged structural response have been developed. Both the single-degree-of-freedom and multi-degree-of-freedom systems were included in the analysis. The objective of this study is to use these models to estimate the amount of energy dissipated due to a strong motion input. The results show that structural damage can be predicted, even in the presence of measurement noise.

UNCLASSIFIED

SECURITY CLASSIFICATION OF THIS PAGE(When Data Entered)

ACKNOWLEDGEMENT

The authors gratefully acknowledge the support provided by the United States Air Force for this investigation. This study was supported under Grant No. AFOSR-81-0086. The concrete experiments were performed at the University of New Mexico Engineering Research Institute. Permission to use their equipment is acknowledged. The concrete experiments were partially supported by the Civil Engineering Department at the University of New Mexico. The authors express their appreciation for this support.

Accession For	
NTIS GRA&I	<input checked="" type="checkbox"/>
DTIC TAB	<input type="checkbox"/>
Unannounced	<input type="checkbox"/>
Justification	
By	
Distribution/	
Availability Codes	
Dist	Avail and/or Special
A-1	



AIR FORCE OFFICE OF SCIENTIFIC RESEARCH (AFOSR)
 NOTICE OF TRANSMITTAL TO DTIC
 This technical report has been approved for release to the
 DTIC and is available for distribution.
 MATTHEW J. K...
 Chief, Technical Information Division



ABSTRACT

In structural engineering it is imperative to design each system to survive the inputs anticipated over the design life of the structure. Strong motion inputs cause systems to execute nonlinear responses, and during the strong motion responses, structures accumulate damage. Therefore, the capability to model nonlinear responses and to assess the damage level in a structure is essential for optimal design.

Techniques for the diagnosis of damage in inelastic structures have been developed. The dissipated energy in mechanical systems is taken as a measure of damage accumulation. Two models for the simulation of damaged structural response have been developed. Both the single-degree-of-freedom and multi-degree-of-freedom systems were included in the analysis. The objective of this study is to use these models to estimate the amount of energy dissipated due to a strong motion input.

The results show that structural damage can be predicted, even in the presence of measurement noise.




TABLE OF CONTENTS

<u>Chapter</u>		<u>Page</u>
1	INTRODUCTION	1
	1.0 Introduction	1
	1.1 Literature Review	2
	1.2 Objective	7
2	HIGH ORDER EQUIVALENT LINEARIZATION	9
	2.1 Model	9
3	IDENTIFICATION OF PARAMETERS IN THE TIME DOMAIN . . .	15
	3.0 Time Domain Approach	15
	3.1 Formulation	15
4	IDENTIFICATION OF PARAMETERS IN FREQUENCY DOMAIN . . .	20
	4.0 Identification of Parameters	20
	4.1 Second Order System	20
	4.2 Third Order Equation	24
5	SYSTEM WITH TIME-VARYING PARAMETERS	31
	5.0 Time-Varying Parameters Model	31
	5.1 Identification Procedure	35
6	IDENTIFICATION OF MULTI-DEGREE-OF-FREEDOM SYSTEM . . .	39
	6.0 M.D.F. System Model	39
	6.1 Identification Procedure	48
7.	ENERGY DISSIPATED RELATED TO CONCRETE DAMAGE	51
	7.0 Introduction	51
	7.1 Discussion of Results	54

TABLE OF CONTENTS (Concluded)

<u>Chapter</u>	<u>Page</u>
8 NUMERICAL EXAMPLES	65
8.0 Data Description	65
8.1 Example 1	67
8.2 Example 2	81
8.3 Example 3	103
8.4 Example 4	106
9 SUMMARY AND CONCLUSION	127
REFERENCES	130
APPENDIX - COMPUTER PROGRAMS	138

LIST OF FIGURES

<u>Figure</u>		<u>Page</u>
<u>2-1</u>	Total restoring force versus displacement for second-order system	11
2-2	Total restoring force versus displacement for third-order system	12
6-1	Multi-degree-of-freedom shear column frames	40
7-1	Idealized first and second cycles	55
7-2	Test configuration	55
7-3	Stress-strain diagram for test specimen number 3WE#7	56
7-4	Initial modulus versus accumulated energy dissipated for a typical concrete specimen	57
7-5	Typical stress-strain diagram for a concrete test specimen under cyclic load. Peak stress 90 percent of failure stress for Batch#3 (14 days curing)	59
7-6	Typical stress-strain diagram for a concrete test specimen under cyclic load. Peak stress 90 percent of failure stress for Batch #2 (28 days curing)	60
7-7	Typical stress-strain diagram for a concrete test specimen under cyclic load. Peak stress 90 percent of failure stress for Batch #3 (14 days curing)	61
7-8	Percent decrease in residual strength versus energy dissipated in concrete specimen (14 days curing)	62
7-9	Residual strength versus energy dissipated in concrete specimens (28 days curing)	63
8-1a	Decaying exponential forcing function for Example 1	68
8-1b	Derivative of forcing function in Figure 8-1a	68
8-2a	Response of a linear system to the force in Figure 8-1a. $k_y = \infty$	70

LIST OF FIGURES (Continued)

<u>Figure</u>		<u>Page</u>
8-2b	Spring restoring force versus displacement for linear system	70
8-3a	Response of nonlinear system to the force in Figure 8-1a. $k_y = 7000$	71
8-3b	Spring restoring force versus displacement for nonlinear system	71
8-4a	Response of nonlinear system to the force in Figure 8-1a. $k_y = 5000$	73
8-4b	Spring restoring force versus displacement for nonlinear system	73
8-5a	Displacement response of identified system to force in Figure 8-1a. (Case 2)	74
8-5b	Spring plus damper restoring force versus displacement for identified system. (Case 2)	74
8-6a	Displacement response of identified system to force in Figure 8-1a. (Case 3)	75
8-6b	Spring plus damper restoring force versus displacement for identified system. (Case 3)	75
8-7a	Displacement response of identified system to force in Figure 8-1a. (Case 4)	76
8-7b	Spring plus damper restoring force versus displacement for identified system. (Case 4)	76
8-8a	Displacement response of identified system to force in Figure 8-1a. (Case 7)	77
8-9a	Displacement response of identified system to force in Figure 8-1a. (Case 8)	78
8-9b	Total restoring force versus displacement for identified system. (Case 8)	78

LIST OF FIGURES (Continued)

<u>Figure</u>		<u>Page</u>
8-10	The comparison between measured response (light line) and identified response (dark line) for both second-order (Case 3) and third-order (Case 7) approximate systems. (The identified responses are practically the same.)	79
8-11a	The comparison between measured response (light line) and identified response for second-order system. (Case 3)	82
8-11b	The comparison between measured response (light line) and identified response for third-order system. (Case 7)	83
8-12	Signal used to simulate the actual input in Examples 2 and 3	88
8-13	Signal used to simulate the measured input (includes 6% noise)	88
8-14	Signal used to simulate the measured input (includes 10% noise)	89
8-15	Displacement response of nonlinear SDF system to force in Figure 8-12 (Case 2)	91
8-16	Spring restoring force versus displacement for nonlinear system (Case 2)	92
8-17	Spring plus damper restoring force versus displacement (Case 2)	92
8-18	Signal used to simulate measured displacement response. Signal of Figure 8-15 plus 6% noise	93
8-19	Signal used to simulate measured displacement response (10% noise)	93
8-20	Displacement response of nonlinear system to the force in Figure 8-12 for Case 4	94
8-21	Displacement response (Case 4) plus 10% noise	94

LIST OF FIGURES (Continued)

<u>Figure</u>		<u>Page</u>
8-22	Spring restoring force versus displacement for nonlinear system (Case 4)	95
8-23	A realization of $Q(\omega)$	98
8-24	A realization of $Q(\omega) + \epsilon(\omega)$	98
8-25	The comparison between noise-free response (solid) and second-order identified response (dot) for Case 2	100
8-26	The comparison between noise-free response (heavy) and third-order identified response (light) for Case 2	101
8-27	The comparison between noise-free response (heavy) and second-order time varying parameters identified response for Case 2	101
8-28	Comparison between actual response (thin line) and model (method 3) response (thick line)	102
8-29	Comparison between actual response (thin line) and model (method 5) response (thick line)	102
8-30	Comparison between actual response (thin line) and model (method 6) response (thick line)	105
8-31	Displacement response of second-order time varying parameter system to force in Figure 8-12 (Case 5)	105
8-32	Total restoring force versus displacement for time varying parameter system (Case 5)	107
8-33	The comparison between measured response (light) and the identified response (dark) by method 6 for Case 5	107
8-34	Total restoring force versus displacement after the identification by using method 6 for Case 5	108

LIST OF FIGURES (Continued)

<u>Figure</u>		<u>Page</u>
8-35	Comparison between measured response (heavy) and second-order identified response (light) using method 3 for Case 5	108
8-36	Comparison between measured response (heavy) and third-order response (light) using method 4 for Case 5	109
8-37	Typical input used to represent forcing function in Example 4	110
8-38	Input including eight percent noise	110
8-39	Relative displacement response between base and mass 1 in 2DF structure (Case 1)	112
8-40	Relative displacement response between mass 1 and mass 2 in 2DF structure (Case 1, linear)	112
8-41	Relative displacement response between base and mass 1 in 2DF structure. Case 2, nonlinear)	113
8-42	Relative displacement response between mass 1 and mass 2 in 2DF structure (Case 2)	113
8-43	Relative displacement response between base and mass 1 in 2DF structure plus 10 percent noise (corresponding to Figure 8-41)	114
8-44	Relative displacement response between mass 1 and mass 2 in 2DF structure plus 15 percent noise (corresponding to Figure 8-42)	114
8-45	Comparison of second order model and actual relative displacement between base and mass 1 (Case 1)	117
8-46	Comparison of second order model and actual relative displacement response between mass 1 and mass 2 (Case 1)	118
8-47	Comparison of third order model and actual relative displacement response between base and mass 1 (Case 1)	119

LIST OF FIGURES (Concluded)

<u>Figure</u>		<u>Page</u>
8-48	Comparison of third order model and actual relative displacement response between mass 1 and mass 2 (Case 1)	120
8-49	Comparison of second order model and actual relative displacement response between base and mass 1 (Case 2)	122
8-50	Comparison of second order model and actual relative displacement response between mass 1 and mass 2 (Case 2)	123
8-51	Comparison of third order model and actual relative displacement response between base and mass 1 (Case 2)	124
8-52	Comparison of third order model and actual relative displacement response between mass 1 and mass 2 (Case 2)	125

LIST OF TABLES

<u>Table</u>		<u>Page</u>
7.1	CONCRETE MIX DETAILS	53
8.1	PARAMETERS AND RESULTS FOR EXAMPLE 1	80
8.2	PARAMETERS OF THE FORCING FUNCTION	87
8.3a	SYSTEM PARAMETERS	87
8.3b	ENERGY DISSIPATION FOR CASE 1 THROUGH CASE 4	90
8.4	IDENTIFIED PARAMETERS AND ENERGY DISSIPATED FOR CASE 1	96
8.5	IDENTIFIED PARAMETERS AND ENERGY DISSIPATED FOR CASE 2	96
8.6	IDENTIFIED PARAMETERS AND ENERGY DISSIPATED FOR CASE 3	97
8.7	IDENTIFIED PARAMETERS AND ENERGY DISSIPATED FOR CASE 4	97
8.8	IDENTIFIED PARAMETERS AND ENERGY DISSIPATED FOR CASE 1 WITH TEN PERCENT NOISE TO SIGNAL RATIO	99
8.9	IDENTIFIED PARAMETERS AND ENERGY DISSIPATED FOR CASE 4 WITH TEN PERCENT NOISE TO SIGNAL RATIO	103
8.10	SYSTEM PARAMETERS FOR CASE 5	103
8.11	IDENTIFIED PARAMETERS AND ENERGY DISSIPATED FOR CASE 5 WITH SIX PERCENT NOISE TO SIGNAL RATIO	104
8.12	IDENTIFIED PARAMETERS AND ENERGY DISSIPATED FOR CASE 5 WITH SIX PERCENT NOISE TO SIGNAL RATIO	104
8.13	PARAMETERS OF THE FORCING FUNCTION	106
8.14	SYSTEM PARAMETERS (CASES 1 AND 2)	111
8.15	ENERGY DISSIPATION	111
8.16	IDENTIFIED PARAMETERS AND ENERGY DISSIPATED FOR CASE 1 WITHOUT NOISE	115

LIST OF TABLES (Concluded)

<u>Table</u>		<u>Page</u>
8.17	IDENTIFIED PARAMETERS AND ENERGY DISSIPATED FOR CASE 1 WITHOUT NOISE	115
8.18	IDENTIFIED PARAMETERS AND ENERGY DISSIPATED FOR NONLINEAR (CASE 2) WITHOUT NOISE	116
8.19	IDENTIFIED PARAMETERS AND ENERGY DISSIPATED FOR CASE 2 WITH NOISE	116

CHAPTER 1

INTRODUCTION

1.0 Introduction

When a structure is excited by an external force, it executes a response determined by the characteristics of both the input and the structure. One could predict the exact response of a structure, characterized by its geometry and its mechanical properties, if he could predict inputs exactly; if he had a perfect model for the structure; and if the mathematical computations were correct. However, since inputs are random, one cannot perfectly characterize complex structures, and since mathematical models are not perfect, one can only estimate the response of a structure.

In structural analysis it is necessary to assess the response of a structure to dynamic loads, such as blasts and earthquakes. This procedure, of course, requires the use of a dynamic model which will permit accurate prediction of the response of a structure. These structural models are generally chosen to fit experimental data and to simplify mathematical computations.

Most existing structures were designed based on a static model, and although dynamic properties may be considered in their design, the design parameters may be inadequate to predict the response to dynamic load correctly. Considerable work has been performed on identifying the parameters of mathematical models from dynamic experimental data, and various approaches have been proposed for predicting system parameters based on experimental data.

These identified parameters can be used to predict the dynamic response of a structure to a different excitation than that used to test it. The identified parameters also can be used to calculate the energy dissipation in a hysteretic structure caused by strong excitation.

The energy dissipated by a structure during a strong motion response is an indication of the structural damage. It is important to predict how much damage occurs in a structure due to strong motion because the level of damage is related to the likelihood of structural failure. When damage does occur, it can appear in different forms, such as cracks, permanent deformation, or change in characteristic frequency.

In practice, it may be difficult to assess the damage extent and location in a complex structure after an extreme excitation. For example, in a nuclear power plant or buried protection structure, it may be difficult to assess damage. This difficulty may arise due to the number of elements in a structure or the scale of individual structure members.

A certain degree of damage is usually unavoidable when structures are subjected to strong motion; therefore, estimation of structural damage is necessary for proper design. At present, the exact criteria useful in judging the failure of a structural system are not available. It is known that some of the measures of structural response related to the occurrence of failure are peak response, energy dissipation, plastic deformation, etc. In fact, the failure criteria of any practical material are a complicated function of many measures of response.

In this study models are established for single-degree-of-freedom (SDF) and multi-degree-of-freedom (MDF) damageable structures. Signals that can be used to simulate measured data are generated. These are used to identify the parameters of the structural models. Finally, damage measures are computed for the simulated systems and their mathematical models.

1.1 Literature Review

The present investigation establishes mathematical models for the simulation of damaged structural response. The mathematical models are

proposed, then signals which can be used to simulate the input and response of damaged structures are generated. These signals are used to identify the model parameters. There are two broad areas in the literature that are concerned with concepts important in this study. These are (1) mathematical models for damaged structural systems, and (2) the identification of structural system parameters. Some papers from the literature in both these areas are briefly discussed below.

Part of the energy dissipated by a structure is dissipated due to hysteretic behavior of the structural material. The equation governing the hysteretic response of a lumped mass system is a second-order, nonlinear, ordinary differential equation with history-dependent stiffness term. Two models which may approximate the nonlinear system will be proposed in this study. These are

1. High-order equivalent linear system;
2. Time-varying parameter linear system.

The first model considered in this investigation is a high-order equivalent linear system. It is assumed that the nonlinear hysteretic system is approximately governed by a high-order equivalent system. This model is motivated by studies summarized in the literature. For example, Lutes and Hsieh [1] used a third-order linear system to approximate a SDF oscillator with bilinear hysteretic yielding behavior, excited by stationary white noise. In the linear system, certain parameters were chosen so that the root mean square displacement and velocity matched empirical values for the nonlinear system. They showed that the third-order system gives a better overall prediction of response buildup than does either the linear SDF system or a two-mode system.

Lutes [2] used a different type of equivalent linear system to approximate the nonlinear system. All the methods Lutes considered defined the equivalence either in terms of response displacement level, velocity level, frequency, or a combination of these. He found that

a particular equivalent linear system can generally only be expected to match a limited number of response statistics of a particular non-linear system with a particular type of excitation.

Wen [3] and Wen and Baber [5, 6] have used the equivalent linearization method to approximately represent the response of a hysteretic SDF system. They showed that the third order, linear, differential equation provided a satisfactory representation of the inelastic, hysteretic systems. This closed form linearization is relatively simple to formulate which allows ready extension to multi-degree-of-freedom (MDF) systems. They showed that the equivalent linearization method gives satisfactory results at all response levels for response analysis of MDF deteriorating or non-deteriorating systems under random excitation.

Another study by Wafa [7] demonstrated that the peak response for an hysteretic SDF system excited by random inputs is closely predicted by a third order, linear equivalent system. Recent work [8] has also shown that the high-order linear equivalent model provides a good approximation to the hysteretic system when the energy dissipated and frequency shift are concerns. Significantly, the results established that the parameters of a higher order system can be identified by using a frequency domain method even when noise is present both in the forcing and response signals. In contrast, the time domain approach yields poor results in the presence of noise. Because of the frequency domain's preferable application, it will be used to do the most analysis.

The second model is motivated by the fact that structures may exhibit time-variant nonlinear response to strong motion. This implies that structure deterioration was in progress during the large amplitude motion. Such a phenomenon has been recognized and studied in the past. For example, Udawadia and Trifunac [9] and Iemura and Jennings [10] carried out an analysis to characterize such behavior in

terms of a quasi-time-variant linear formulation based on the data obtained from the San Fernando earthquake of February 9, 1971.

In another study Townsend and Hanson [11] demonstrate time-varying hysteretic loops by the experimental test of reinforced concrete beam-column and T-shaped specimens under different loading conditions. In addition, Uzumeri [12] has also shown the same behavior for an experimental study of cast-in-place reinforced concrete beam-column joints subjected to simulated seismic loading.

Based on the above referenced investigations involving time-varying parameters systems, we anticipate that the time-varying parameter model will provide a good representation of a hysteretic system.

Many papers in the literature address the problem of damage assessment; however, few of these treat the mathematical quantification of damage measures. In the following, some papers which discuss damage analysis in both quantitative and non-quantitative ways are discussed.

To assess structural damage, it is necessary to first define and quantify the damage. Yao [13] has examined various definitions of structural damage and reviewed available methods for damage assessment. In 1971, Wiggins and Moran [14] developed a procedure for grading existing buildings in Long Beach, California. Damage is assessed on a point basis, and a total of up to 180 points is assigned to each structure according to the evaluation of structural components of five types. In 1975, Culver et al [15] proposed the field evaluation method (FEM) which is applicable even when building plans are unavailable. In 1980, Bresler et al [16] described their structural and fire evaluation model, which was developed to provide a broad overview of potential safety problems for more than 10,000 buildings for a government agency in the United States. Recently, Ishizuka, Fu, and Yao [17, 18, 19] suggested a rule-based damage assessment system called SPERIL Version I. All these systems are primarily based on professional experience and engineering judgment in the decision making process.

A more mathematical quantification of damage in structures has been used by Ang, and Wen [20]. They used the hysteretic energy absorbed and the maximum structural distortion as the function of structural damage. Others who published in this area are Rudd, Yang and Manning [21], Yao [22], Toussi and Yao [23, 24], Chen and Yao [25] and Yao, Toussi, and Sozen [26].

An important aspect of the present study is the method used to identify the parameters of the damaged structure. The literature on structural identification, in general, is very broad. A few of the papers closely related to the present investigation are reviewed here.

The historical development of research in the area of system identification is summarized in the works of Astrom and Eykhoff [27], Bekey [28], Bowles and Straeter [29] and Collins, Young, and Keifling [30]. Many survey papers have been written. For example, Collings, et al [30], Sage [31], Rodeman and Yao [32], Chen [33], Hart and Yao [34], Ting, Chen, and Yao [35] and Liu and Yao [36] present surveys of structural identification.

The potential for change in structural characteristics due to the accumulation of damage exists and can be investigated through observation of structural parameters. Signature analysis techniques have been used to predict cracking in bridges by Cole [37, 38].

One important area in system identification permits the analyst to characterize system modes. An early paper by Kennedy and Pancu [39] shows how model parameters can be obtained from a vector representation of the steady-state response in the complex plane. Later papers in the same area were written by Bert [40], Bert and Clary [41], Smith [45], and Trail-Nash [46]. Some of the difficulties encountered in applying the techniques developed in the above papers are described by Nord [47].

The least squares approach to the identification of system parameters has been developed in many studies, and is applied in both the time and frequency domains. (This technique is used in the present study.) Some papers that have been written on the subject of least squares parameter estimation are those of Distefano and Rath [48, 49], Flannelly and Berman [50], Hart and Yao [34], Ibanez [51], Ibrahim [53-58], Milne [59], Raggett, Rodeman, and Yao [32], Ting, Chen, and Yao [35], Udawadia and Shaw [61], and Wells [62]. Brieman [63] shows that for a linear time invariant system, the least square prediction is optimal. The technique for using the least squares parameter identification in the frequency domain was presented by Ibanez [51, 52]. Wang, Paez, and Ju [8, 66, 67] found that frequency domain approach is well suited to the identification of parameters for high order linear models and time varying linear models.

The effects caused by measurement noise can be important in the identification of structural system parameters. Kandianis [68] considered that effect for linear structural systems. His theoretical development considered white noise random input. The studies by Wang, Paez, and Ju [8, 66, 67] show that the parameters of higher order linear and time varying linear models can be accurately predicted even in the presence of noise.

1.2 Objective

The determination of the system parameters from suitable experimental observations is a fundamental problem in engineering. Obtaining a good representation of a system requires all the proper information, such as well measured data and a suitable model.

The objective of this study is to justify two possible models to characterize the behavior of a system. The relative merits for each model are discussed. Extensive numerical experimentation using simulated data is also presented in order to investigate their feasibility and accuracy. This study will demonstrate how well the system parameters can be identified with and without noise in the measurements.

Once the parameters are known, the energy dissipated by the system can be computed. Based on the computed results, one can compare how well the models performed for a given set of data. The ultimate goal of this study is to establish structural models useful for other purposes, such as prediction, design, control, and damage assessment.

The present research has been aimed at the analysis of damage accumulation in concrete structures. It is assumed that when a concrete structure dissipates energy, it accumulates damage. To justify this assumption some physical experiments have been performed. Specifically, concrete cylinders have been subjected to cyclic loading. The energy dissipated in each cylinder was measured and the level of residual strength in each cylinder was determined after the load cycling was completed. The residual strength was plotted versus energy dissipated. When the reduction in strength is taken as a measure of damage, this plot reveals the damage caused by energy dissipation.

CHAPTER 2

HIGH ORDER EQUIVALENT LINEARIZATION

2.1 Model

The differential equation governing the response of a single-degree-of-freedom (SDF) system is

$$m\ddot{z} + u = f \quad (2-1)$$

where m is the mass of the structure, f is the forcing function, z is the displacement response, dots denote differentiation with respect to time, and u is the restoring force of the structure. Equation (2-1) can be used to model the actual system in which u can be a very complicated function. In the present study, the hysteretic restoring force, u , is modeled by using the equation

$$\sum_{j=0}^M c_j u^{(j)} = c_{M+1} \ddot{z} + z \quad (2-2)$$

where the c_j , $j = 0, 1, \dots, M+1$ are the constants governing the system restoring force characteristics, where $u^{(j)}$ denotes the j th time derivative of u , and M is a constant denoting the order of approximation provided by the linear system. The reason for using this model to represent the hysteretics system is that it displays a hysteretic character that can be made to match the character of an inelastic structure.

Combine Equations 2-1 and 2-2 in the following way. Solve Equation 2-1 for u , then take derivatives of the resulting expression. Use these in Equation 2-2; the result is

$$\frac{1}{c_0} \ddot{z} + \frac{c_{M+1}}{c_0} \ddot{z} + \sum_{j=1}^M \frac{c_j}{c_0} \left(-f^{(j)} + m z^{(j+2)} \right) = f - m\ddot{z} \quad (2-3)$$

where $f^{(j)}$ is the j th derivative of f , and $z^{(j+2)}$ is the $(j+2)$ th derivative of z . To simplify the identification procedure, Equation 2-3 was divided by c_0 . This particular arrangement is chosen since c_0 should never be 0 for the systems under consideration.

Consider the case where M is equal to 0. The model in Equations 2.1 and 2.2 becomes

$$m\ddot{z} + \frac{c_1}{c_0} \dot{z} + \frac{1}{c_0} z = f \quad (2-4)$$

This is simply the second-order linear differential equation governing the SDF system. However, when the response of the actual system is linear and damping is viscous, the model of Equation (2-4) represents the actual system. The restoring force function for this system is $u = (c_1/c_0)\dot{z} + (1/c_0)z$. This model displays the hysteretic behavior as shown in Figure (2-1).

When the constant M is chosen as 1 in equation 2-2, the model becomes

$$\begin{aligned} m\ddot{z} + u &= f \\ c_0 u + c_1 \dot{u} &= c_2 \dot{z} + z \end{aligned} \quad (2-5)$$

Combining these equations results in

$$\frac{c_1}{c_0} \ddot{m}\ddot{z} + m\ddot{z} + \frac{c_2}{c_0} \dot{z} + \frac{1}{c_0} z = f + \frac{c_1}{c_0} \dot{f} \quad (2-6)$$

The parameters of the system in Equation (2-6) can be chosen so that the model represents the hysteretic system as well as possible.

For example, Figure (2-2) shows the hysteretic properties for an SDF system by plotting the restoring force versus displacement. The parameters for the system and the forcing input

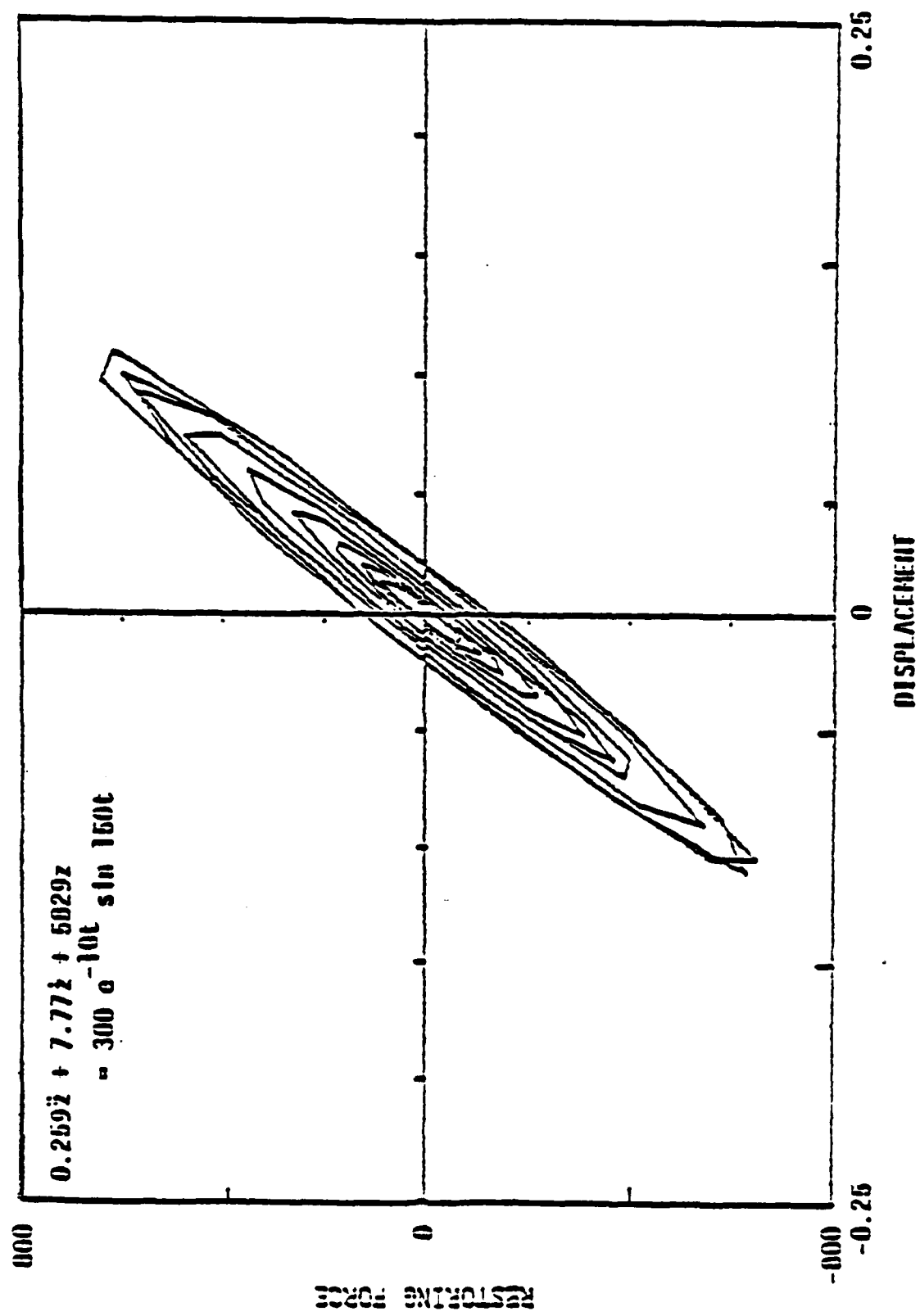


Figure 2-1. Total restoring force versus displacement for second-order system.

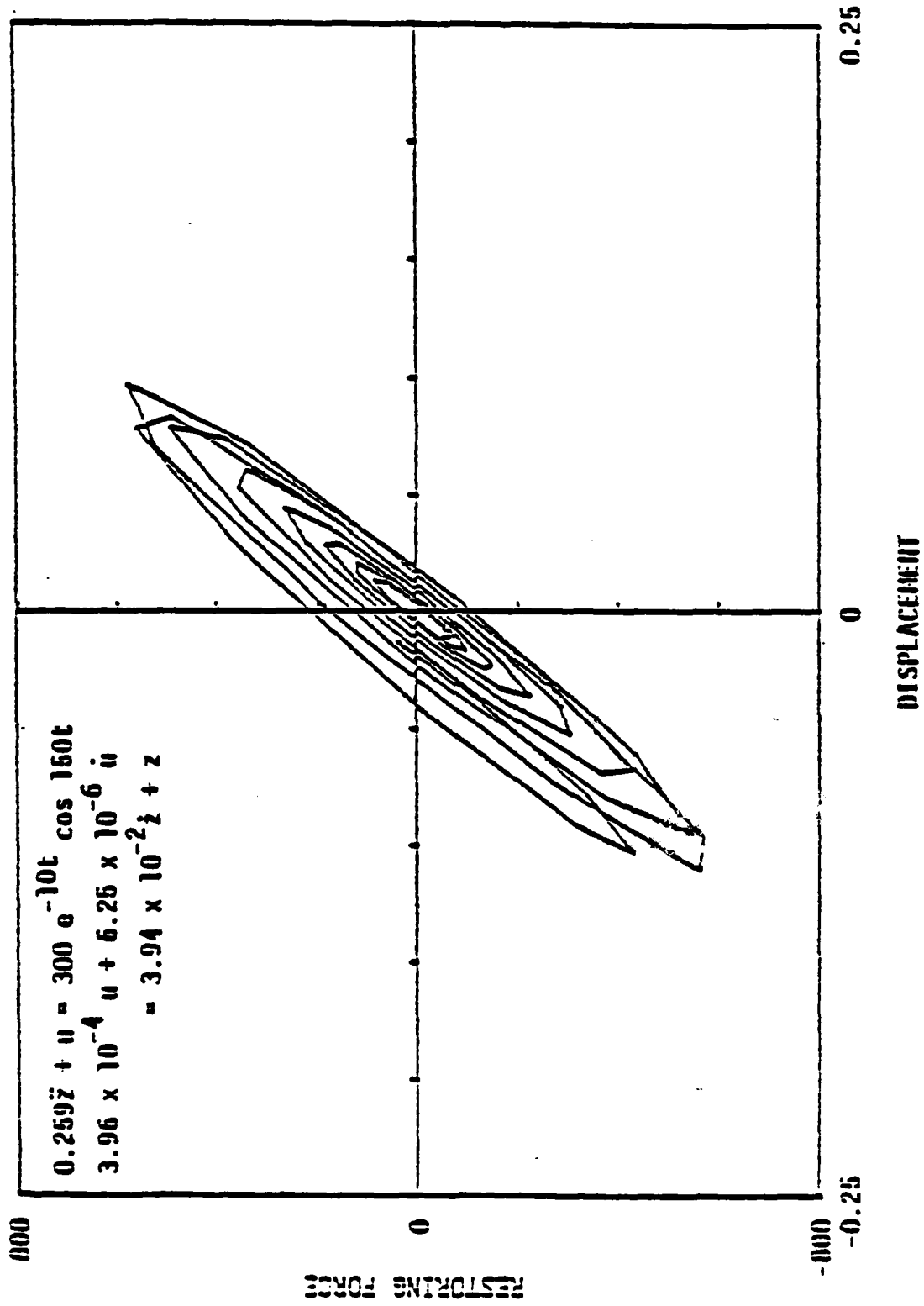


Figure 2-2. Total restoring force versus displacement for third-order system.

are given in Figures (2-2). This study will consider both the equations (2-4) and (2-6).

The parameters can be identified by using the least-square identification criterion. Since most observed data include a certain percentage of noise, the frequency domain approach will be used to perform the parameter identification.

It is anticipated that as the order, M , of the model in Equation 2-2 is increased, the response of a hysteretic system can be matched with increasing accuracy. However, for practical reasons involving estimation accuracy for system parameters, very high order linear system models cannot be used to simulate hysteretic system behavior.

Before considering the problem of parameter estimation for the system of Equation 2-2, note that we anticipate calculating a set of parameters with values in a specific range. For example, when $M = 0$ and Equation 2-4 is the model for system response, we anticipate finding values $1/c_0 > 0$ and $c_1/c_0 > 0$ (i.e., $c_0 > 0$ and $c_1 > 0$). These values guarantee that the model has positive stiffness and damping, as we know the real system must. When $M = 1$ and Equation 2-5 models the system response, we anticipate finding values $c_0 > 0$, $c_1 > 0$, and $c_2 > 0$. These values guarantee that the model response will be stable.

The energy dissipated by the systems described in this section can be computed using Equation 2-1 or 2-2. In the terms of Equation 2-1, the energy dissipated by a system is

$$E_D = \int_{z(0)}^{z(T)} u \, dz \quad (2-7)$$

where $z(0)$ is the system displacement at time 0, $z(T)$ is the system displacement at time T , and T is the time through which the energy computation is executed. This formula provides the area enclosed in the hysteresis loops generated by the system

response. For example, Equation 2-7 could be used to compute the area enclosed by the hysteresis loop of Figure 2-1. This equation can be transformed into terms more convenient for computation. Note that the integral of Equation 2-7 is written in terms of the displacement variable z . The variable of integration can be transformed to a time variable yielding the following expression.

$$E_D = \int_0^T u \dot{z} dt \quad (2-7a)$$

Finally, Equation 2-1 can be used to obtain

$$E_D = \int_0^T (f - m\ddot{z}) \dot{z} dt \quad (2-7b)$$

When the input and response for an SDF system are measured, Equation 2-7b can be used to directly compute the energy dissipated by a system. When the response is computed, for example by solving Equations 2-5, then the input and system parameters are used to find z and its derivatives. The input, f , and computed response, z , are used in Equation 2-7b to determine the energy dissipated.

Numerical examples where we compute the parameters of linear systems equivalent to bilinear, hysteretic systems are presented in Chapter 8. In these examples, the energy dissipated by each system is computed and the results are compared.

CHAPTER 3

IDENTIFICATION OF PARAMETERS IN THE TIME DOMAIN

3.0 Time Domain Approach

The time domain parameter identification procedure is used to introduce the identification procedures for the models described in Chapter 2. Though time domain approach is not used extensively in this investigation, the method can still be effective under certain circumstances. Particularly, the time domain identification process is useful when the measured input and response contain little or no noise.

Measured input and response data from a structural system are used to estimate the system parameters. The measured input data can be a base acceleration, force or a pressure function. In the following, the measured response data are assumed to be given as acceleration values. This assumption is realistic since structure response acceleration is often measured during an experiment or test by accelerometers installed in the structure.

3.1 Formulation

Consider Equation 2-3 and let z_ℓ , \dot{z}_ℓ , and $z_\ell^{(j)}$, $\ell=0, \dots, n-1$, be the response displacement, velocity, and j th derivatives of the displacement at time, $t_\ell = \ell\Delta t$, $\ell = 0, \dots, n-1$. Let f_ℓ and $f_\ell^{(j)}$, $\ell = 0, \dots, n-1$, be the force at time t_ℓ , $\ell = 0, \dots, n-1$ and its j th derivative. Then Equation 2-3 can be written at time t_ℓ to obtain

$$\frac{1}{c_0} z_\ell + \frac{c_{M+1}}{c_0} \dot{z}_\ell + \sum_{j=1}^M \frac{c_j}{c_0} \left(-f_\ell^{(j)} + m z_\ell^{(j+2)} \right) = f_\ell - m \ddot{z}_\ell$$

$\ell=0, \dots, n-1 \quad (3-1)$

The reason for normalizing with respect to c_0 is that c_0 should never be 0 for the system under consideration.

The notation in this equation can be simplified by taking

$$a_0 = \frac{1}{c_0}, a_1 = \frac{c_{M+1}}{c_0}, a_{j+1} = \frac{c_j}{c_0}, j = 1, \dots, M \quad (3-2)$$

Equation 3-1 can be written as

$$a_0 z_l + a_1 \dot{z}_l + \sum_{j=1}^M a_{j+1} \left(-f_l^{(j)} + m z_l^{(j+2)} \right) = f_l - m \ddot{z}_l, \quad l = 0, \dots, n-1 \quad (3-3)$$

The notation in this equation can be simplified by defining

$$\{z_l\} = \left[z_l \dot{z}_l \left(-\ddot{f}_l + m \ddot{z}_l \right) \dots \left(-f_l^{(M)} + m z_l^{(M+2)} \right) \right] \quad l = 0, \dots, n-1 \quad (3-4)$$

$$\{a\} = (a_0 \ a_1 \ a_2 \dots a_{M+1})^T \quad (3-5)$$

where the T superscript refers to matrix transposition. Using these expressions in Equation 3-3 yields the relation

$$\{z_l\} \{a\} = f_l - m \ddot{z}_l, \quad l = 0, \dots, n-1 \quad (3-6)$$

This is the equation governing the linear system response at time t_l .

The notation can be further simplified by defining

$$[Z_f] = \begin{bmatrix} \{z_0\} \\ \{z_1\} \\ \vdots \\ \{z_{n-1}\} \end{bmatrix}, \quad \{f_z\} = \begin{Bmatrix} f_0 - m \ddot{z}_0 \\ f_1 - m \ddot{z}_1 \\ \vdots \\ f_{n-1} - m \ddot{z}_{n-1} \end{Bmatrix} \quad (3-7)$$

Using this expression, the sequence of Equation 3-6, for $l = 0, \dots, n-1$, can be written

$$[Z_f] \{a\} = \{f_z\} \quad (3-8)$$

This equation governs the linear system response at all times. When (1) the system from which the data were measured is truly linear, (2) there is no noise in the measured data, and (3) the derivatives and integrals of f_l and z_l , $l = 0, \dots, n-1$, are known exactly, Equation 3-8 can be satisfied exactly by the measured data and a set of coefficients. In general, these conditions cannot be satisfied exactly, therefore, an error term should be included in Equation 3-8. Define the error vector as

$$\begin{aligned} \{\epsilon\} &= (\epsilon_0 \ \epsilon_1 \ \dots \ \epsilon_{n-1})^T \\ &= [Z_f] \{a\} - \{f_z\} \end{aligned} \quad (3-9)$$

The element ϵ_l , $l=0, \dots, n-1$, designates the error term at time t_l . This error quantifies the data nonlinearity, the measurement noise, and the inaccuracy of the derivatives and integrals of \ddot{z}_l and f_l . In Equation 3-9 $[Z_f]$ and $\{f_z\}$ will be treated as known quantities which can be measured during an experiment. The error vector in Equation 3-9 thus becomes a function of the system parameters, $\{a\}$.

The next step is to identify the parameters of the system model. A least squares approach is adopted in this investigation.

An overall measure of the mismatch between the measured data and the model in Equation 3-8 is established as follows.

$$\epsilon^2 = \{\epsilon\}^T \{\epsilon\} = (\{a\}^T [Z_f]^T - \{f_z\}^T) ([Z_f] \{a\} - \{f_z\}) \quad (3-10)$$

This is referred to as the squared error between the measured data and the system model. This error can be minimized through the proper choice of the parameter vector $\{a\}$. This can be done by letting

$$\frac{\partial \epsilon^2}{\partial a_0^2} = 0 = \frac{\partial \epsilon^2}{\partial a_1^2} = \dots = \frac{\partial \epsilon^2}{\partial a_{M+1}^2}, \quad (3-11)$$

and solving this sequence of equations for the a_j , $j=0, \dots, M+1$. This solution can be executed and the result, in vector form, is

$$\{a\} = \left(\begin{bmatrix} Z_f \end{bmatrix}^T \begin{bmatrix} Z_f \end{bmatrix} \right)^{-1} \begin{bmatrix} Z_f \end{bmatrix}^T \{f_z\} \quad (3-12)$$

The parameter vector chosen above is the best estimate of the system parameters in a least squares sense. If the quantity, ϵ^2/n (where ϵ^2 is computed using Equations 3-9 and 3-10), is relatively small, then Equation 3-3 accurately represents the measured system. If this is not true, then the model of Equation 3-3 is inadequate.

The ϵ^2 will be equal to zero if the measured data are noise free, the system is linear, and the computed derivatives and integrals of the measured data are exact. Failure to meet one or more of these requirements will cause ϵ^2 to be nonzero. In practice, the parameter identification procedure outlined above can only be used effectively when there is little or no noise in the measurements. The method is particularly effective when the parameter M is set to 0 because this model will not, in general, require the computation of derivatives of \ddot{z} and f . However, when noise is present and $M = 1$, the procedure loses its accuracy. If the measured raw data, \ddot{z}_ℓ and f_ℓ , $\ell=0, \dots, n-1$, are used to obtain the derivatives through numerical differentiation, then the estimated values of \ddot{z} and f may be very poor due to amplification of the effects of noise.

In view of this, alternate procedures for parameter identification in the presence of noise must be established. The following chapters develop a frequency domain approach to the identification of system parameters.

CHAPTER 4

IDENTIFICATION OF PARAMETERS IN FREQUENCY DOMAIN

4.0 Identification of Parameters

The problem of parameter identification can be posed as one class in the broader topic of optimization. The object of parameter identification is to make inferences about the real world and mathematical models on the basis of measured input data. The measured data in this study were assumed available, and were simulated to represent the field data.

First, it is assumed that there is no noise present in the measured data. Then, noise data are introduced. Note that the measured response data are given as acceleration values. This is realistic since the structural response acceleration is often the measured quantity in an experimental test.

4.1 Second Order System

Now, consider the second-order model, Equation 2-4, Equation 2-4 can be simplified by taking

$$\frac{1}{c_0} = a_0, \quad a_1 = \frac{c_1}{c_0} \quad (4-1)$$

The equation governing motion of the system becomes

$$m\ddot{z} + a_1\dot{z} + a_0z = f \quad (4-2)$$

Fourier transform both sides to obtain

$$m(i\omega)^2 Z(\omega) + a_1(i\omega)Z(\omega) + a_0Z(\omega) = F(\omega) \quad (4-3)$$

where

$$\begin{aligned}
 Z(\omega) &= \int_{-\infty}^{\infty} z(t) e^{-i\omega t} dt \quad -\infty < \omega < \infty \\
 F(\omega) &= \int_{-\infty}^{\infty} f(t) e^{-i\omega t} dt \quad -\infty < \omega < \infty
 \end{aligned}
 \tag{4-4}$$

are the Fourier transforms of $z(t)$ and $f(t)$, respectively. This equation can be rearranged and combined with $Z(\omega)$ and $F(\omega)$ terms on one side of the equation to obtain

$$(-m\omega^2 + a_0 + a_1 i\omega) = \frac{F}{Z} \tag{4-5}$$

Multiply each side of the equation by its complex conjugate to obtain the modulus squared.

$$|-m\omega^2 + a_0 + a_1 i\omega|^2 = \frac{|F|^2}{|Z|^2} \tag{4-6}$$

Evaluate the left side and let $|F|^2/|Z|^2$ equal $Q(\omega)$ to obtain

$$(a_0 - m\omega^2)^2 + (a_1\omega)^2 = Q(\omega) \tag{4-7}$$

This equation can be used to identify the parameters of second-order linear system. However, this equation is exactly satisfied if and only if: 1) the system under consideration is linear; 2) all measurements are noise free; and, 3) the Fourier transforms of $\ddot{z}(t)$ and $f(t)$ used in Equation (4-7) are exact. When these requirements are not satisfied, Equation (4-7) will include an error term (or noise term). This practical case is usually the one that needs the most attention.

When noise is present on the measured input and response, Equation (4-7) can be written as

$$(a_0 - m\omega^2)^2 + (a_1\omega)^2 = Q(\omega) + \epsilon(\omega) \tag{4-8}$$

Note from Equation 4-2 that a_0 is the equivalent stiffness and a_1 is the equivalent damping for the second-order linear system. Therefore, a_0 is greater in magnitude than a_1 . In view of this and the form of Equation 4-8, a_0 can be estimated by noting the frequency where $Q(\omega) + \epsilon(\omega)$ is a minimum whenever the equivalent damping factor is much less than 1 (say less than 0.2). This will be true in most civil engineering systems.

Denote the frequency where $Q(\omega) + \epsilon(\omega)$ is a minimum by ω_m . Equation 4-8 shows that, approximately,

$$a_0 = m\omega_m^2 \quad (4-9)$$

since the first term on the left is approximately zero when $Q(\omega) + \epsilon(\omega)$ is a minimum. Substitute Equation 4-9 into Equation 4-8; this yields

$$m^2(\omega_m^2 - \omega^2) + (a_1\omega)^2 = Q(\omega) + \epsilon(\omega) \quad (4-10)$$

Now, it is necessary to find the coefficient a_1 which minimizes the $\epsilon(\omega)$.

The coefficients a_1 can be evaluated using a least-squares approach, where the integral of $\epsilon^2(\omega)$ over a specific range of frequencies is minimized. Based on Equation 4-10, set

$$\int_{\omega_a}^{\omega_b} \left(a_1^2 \omega^2 + m^2(\omega_m^2 - \omega^2) - Q(\omega) \right)^2 d\omega = \epsilon^2(\omega) \quad (4-11)$$

where ω_a and ω_b are lower and upper bound frequencies, respectively. This frequency band is chosen so that the system response behavior can be fully characterized. It is anticipated

that the frequency band includes the natural frequency for a linear or slightly non-linear system. For a highly nonlinear system, the characteristic frequency, ω_m , will shift. However, the frequency band can be located by finding the frequency where $Q(\omega) + \epsilon(\omega)$ is a minimum, and selecting the frequency band around this frequency.

In general, the lower frequency, ω_a , is located at a point where its corresponding $Q(\omega_a) + \epsilon(\omega_a)$ value is about 5 times as great as the minimum value of $Q(\omega) + \epsilon(\omega)$; and ω_b is the higher frequency where $Q(\omega_b) + \epsilon(\omega_b)$ is about 5 times greater than the minimum value of $Q(\omega) + \epsilon(\omega)$. This method is used to select ω_a and ω_b based on an approximate linear analysis. When ω_a and ω_b are chosen in this manner, the interval (ω_a , ω_b) will be approximately the half power bandwidth of the system. This frequency interval reflects the characteristics of the system.

Take the first partial derivative of ϵ^2 with respect to a_1^2 , and set it equal to 0. The result is

$$\frac{\partial \epsilon^2}{\partial a_1^2} = 2 \int_{\omega_a}^{\omega_b} \left(a_1^2 \omega^2 + m^2 (\omega_m^2 - \omega^2)^2 - Q(\omega) \right) \omega^2 d\omega = 0 \quad (4-12)$$

Simplify this to obtain

$$a_1^2 \int_{\omega_b}^{\omega_a} \omega^4 d\omega = \int_{\omega_a}^{\omega_b} \left(Q(\omega) - m^2 (\omega_m^2 - \omega^2)^2 \right) \omega^2 d\omega \quad (4-12a)$$

Integrate the equation where possible to get

$$a_1^2 = \frac{5}{\omega_b^5 - \omega_a^5} \left\{ \int_{\omega_a}^{\omega_b} \omega^2 Q(\omega) d\omega - m^2 \left[\frac{\omega_m^4}{3} (\omega_b^3 - \omega_a^3) - \frac{2}{5} \omega_m^5 (\omega_b^5 - \omega_a^5) + \frac{1}{7} (\omega_b^7 - \omega_a^7) \right] \right\} \quad (4-13)$$

Let $\omega_a = q_a \omega_m$

$$\omega_b = q_b \omega_m \quad (4-14)$$

where q_a is a coefficient less than one and q_b is a coefficient greater than one. This equation can be further simplified

$$a_1^2 = \frac{\omega_m^2}{q_b^5 - q_a^5} \left\{ \frac{5}{\omega_m^7} \int_{\omega_a}^{\omega_b} \omega^2 Q(\omega) d\omega + m^2 \left[-\frac{5}{3} (q_b^3 - q_a^3) + 2(q_b^5 - q_a^5) - \frac{5}{7} (q_b^7 - q_a^7) \right] \right\} \quad (4-15)$$

This equation provides the value of a_1 . This is the best estimator in the least-squares sense. All the parameters in this equation are known except the integral of the $\omega^2 Q(\omega)$ term which can be evaluated numerically.

4.2 Third Order Equation

The second-order linear ordinary differential equation may not be considered an accurate representation of the hysteretic system. It is hoped that the third-order linear system may improve the accuracy in some sense.

Equation 2-6 can be simplified by taking

$$\frac{1}{c_0} = a_0, \quad \frac{c_2}{c_0} = a_1, \quad \frac{c_1}{c_0} = a_2 \quad (4-16)$$

Then Equation 2-6 becomes

$$ma_2 \ddot{z} + m\dot{z} + a_1 \dot{z} + a_0 z = f + a_2 \dot{f} \quad (4-17)$$

Fourier transform both sides to get

$$\frac{(ma_2 (i\omega)^3 + m(i\omega)^2 + a_1 (i\omega) + a_0)}{(1 + a_2 (i\omega))} = \frac{F}{Z} \quad (4-18)$$

The symbols used in this equation have the same meaning as in earlier equations. Multiply each side of the equation by its complex conjugate to yield the modulus squared

$$\frac{|-ima_2\omega^3 - m\omega^2 + ia_1\omega + a_2|^2}{|1 + ia_2\omega|^2} = \frac{|F|^2}{|Z|^2} \quad (4-19)$$

Evaluate the left hand side and let $|F|^2/|Z|^2$ be replaced by $Q(\omega)$ to obtain

$$\frac{(a_0 - m\omega^2)^2 + \omega^2 (a_1 - m\omega^2 a_2)^2}{1 + (a_2\omega)^2} = Q(\omega) \quad (4-20)$$

This equation governs a third-order linear system in the frequency domain. Measured data can satisfy this equation exactly if and only if: 1) the system under consideration is linear; 2) all measurements are noise free; and, 3) the Fourier transforms used to define $Q(\omega)$ are exact. These conditions, however, are not usually met. In fact, the purpose of this investigation is to use the higher-order linear system to represent an hysteretic system. Therefore, measured data do not usually satisfy the

above equation. To account for this explicitly, Equation 4-20 is written

$$\frac{(a_0 - m\omega^2)^2 + \omega^2(a_1 - m\omega^2 a_2)^2}{1 + (a_2\omega)^2} = Q(\omega) + \epsilon(\omega) \quad (4-21)$$

$\epsilon(\omega)$ is a noise term which must be minimized by the proper choice of system parameters. This equation can be used to identify the system parameters following several approaches. Two of these are summarized below. One approach approximates certain terms in Equation 4-20 to obtain estimates for the system parameters, while the other approach uses a search technique to estimate system parameters.

The first method to be investigated is an approximate technique. When a_2 is small compared to the characteristic frequency, ω_m of an SDF system, the $(a_2\omega)^2$ term in the denominator can be neglected. This is usually true when nonlinear deformation is not too large. Eliminate the $(a_2\omega)^2$ term in Equation 4-21 to obtain

$$(a_0 - m\omega^2)^2 + \omega^2(a_1 - m\omega^2 a_2)^2 = Q(\omega) + \epsilon(\omega) \quad (4-22)$$

When a_1 and a_2 are small compared to a_0 (which is usually the case, the minimum of the left-hand side occurs near the frequency

$$\omega = \sqrt{\frac{a_0}{m}} \quad (4-23)$$

As previously described, the characteristic frequency, ω_m , can be found when the $Q(\omega) + \epsilon(\omega)$ term is a minimum. In terms of ω_m , a_0 can be written

$$a_0 = m\omega_m^2 \quad (4-24)$$

Expand the second term on the left side of Equation 4-22 and use the result of Equation 4-24. Neglect the $m^2 \omega^4 a_2^2$ term. Then Equation 4-22 becomes

$$m^2 (\omega_m^2 - \omega_k^2)^2 + \omega^2 (a_1^2 - 2m\omega^2 a_1 a_2) = Q(\omega) + \epsilon(\omega) \quad (4-25)$$

$$\text{Let } a_1^2 = b_1 \text{ and } a_1 a_2 = b_2, \text{ then} \quad (4-26)$$

$$\omega^2 (b_1 - 2m\omega^2 b_2) - (Q(\omega) - m^2 (\omega_m^2 - \omega^2)^2) = \epsilon(\omega) \quad (4-27)$$

When this expression is evaluated at the discrete frequency

$\omega = \omega_k$, the result is

$$\omega_k^2 (b_1 - 2m\omega_k^2 b_2) - (Q_k - m^2 (\omega_m^2 - \omega_k^2)^2) = \epsilon_k \quad (4-28)$$

The system parameters, a_1 and a_2 , can now be identified as those which minimize the sum of the squares of the ϵ_k terms in Equation 4-28. Consider a sequence of discrete frequencies uniformly spaced in the interval (ω_a, ω_b) . These are ω_a , $\omega_a + \Delta\omega$, $\omega_a + 2\Delta\omega$, etc. Define

$$\{b\} = (b_1 \ b_2)^T \quad (4-29a)$$

$$[x_1] = \begin{bmatrix} \omega_a & -2m\omega_a^4 \\ \omega_a + \Delta\omega & -2m(\omega_a + \Delta\omega)^4 \\ \omega_a + 2\Delta\omega & -2m(\omega_a + 2\Delta\omega)^4 \\ \vdots & \vdots \\ \vdots & \vdots \\ \omega_b & -2m\omega_b^4 \end{bmatrix} \quad (4-29b)$$

$$\{x_2\} = \begin{Bmatrix} Q_{\omega_a} & -m^2(\omega_m^2 - \omega_a^2)^2 \\ Q_{\omega_a+\Delta\omega} & -m^2(\omega_m^2 - (\omega_a+\Delta\omega)^2)^2 \\ Q_{\omega_a+2\Delta\omega} & -m^2(\omega_m^2 - (\omega_a+2\Delta\omega)^2)^2 \\ \vdots & \vdots \\ Q_{\omega_b} & -m^2(\omega_m^2 - \omega_b^2)^2 \end{Bmatrix}$$

$$\{\epsilon\} = (\epsilon_{\omega_a} \quad \epsilon_{\omega_a+\Delta\omega} \dots \epsilon_{\omega_b}) \quad (4-29d)$$

Note $\Delta\omega$ is equal to $(2\pi/T)$ and T is the total duration of the excitation. (ω_a, ω_b) defines the range of frequencies over which the system is analyzed. As in the identification of parameters of the second-order linear system, only a portion of the frequency range is used in the parameter identification.

This frequency range can be chosen as before. In terms of the matrices defined above, Equation 4-27 can be written at discrete frequencies as

$$[x_1] \{b\} - \{x_2\} = \{\epsilon\} \quad (4-30)$$

The vector $\{b\}$ can be found by minimizing the sum of the squares of $\{\epsilon\}$. This is $\epsilon^2 = \{\epsilon\}^T \{\epsilon\}$. The vector $\{b\}$ which minimizes ϵ^2 is

$$\{b\} = ([x_1]^T [x_1])^{-1} [x_1]^T \{x_2\} \quad (4-31)$$

When b_1 and b_2 have been computed, a_1 and a_2 can be found from Equation 4-26.

$$a_1 = \sqrt{b_1}, \quad a_2 = b_2/a_1 \quad (4-32)$$

This solution provides approximate values for the parameters in the third-order linear system which represents the hysteretic system.

Another approach can be used for the estimation of parameters in the higher order linear system. This is a search procedure which iteratively estimates the parameter values. Equation 4-21 can be rewritten

$$\epsilon(\omega) = Q(\omega) - \frac{(a_0 - m\omega)^2 + \omega (a_1 - m\omega a_2)^2}{1 + (a_2\omega)^2} \quad (4-33)$$

This quantity is a measure of the mismatch between the measured data, reflected in $Q(\omega)$, and the model, reflected in the second term on the right side of Equation 4-33.

This mismatch can be either positive or negative and can be used to define one measure of the difference between the model and the measured data over a range of frequencies. This measure is

$$\epsilon^2 = \sum_k \epsilon(\omega_k) \quad (4-34)$$

where the sum is taken over those discrete frequencies in the interval (ω_a, ω_b) . This is the square error of the model. This error is minimized, however, when the model parameters are chosen to satisfy the sequence of equations

$$\frac{\partial \epsilon^2}{\partial a_0} = 0 = \frac{\partial \epsilon^2}{\partial a_1} = \frac{\partial \epsilon^2}{\partial a_2} \quad (4-35)$$

The parameters a_0 , a_1 , and a_2 , which satisfy these equations establish a model which is optimal in a least squares sense.

Equations 4-35 can be solved numerically using a search technique. A computer program was written to solve Equation

4-35. The program, included in the appendix, uses Newton's method to search for the solution. The analysis procedure followed in the computer program is identical to that used in solution of the problem summarized in the following section. The steps in the solution procedure are listed at the end of Chapter 5.

CHAPTER 5

SYSTEM WITH TIME-VARYING PARAMETERS

5.0 Time-Varying Parameters Model

Structures may exhibit time-variant nonlinear response to strong motion excitation. Time-varying structural properties were not considered in the previous chapters. In this chapter, a structure is modeled as a time variant single-degree-of-freedom (SDF) oscillator, and a methodology is introduced to determine its parameters using the observed data. It is important to introduce a technique which can be applied when noise is present in the measured data.

To demonstrate this procedure, consider an SDF linear system with mass m . Let the damping and stiffness parameters for this system be time varying. Its equation of motion is

$$m\ddot{z} + C(t)\dot{z} + K(t)z = f \quad (5-1)$$

in which z is the displacement response of the system; $C(t)$ and $K(t)$ are time variant damping and stiffness functions of the system, respectively; and f is the forcing function. It is proposed that this equation be used to model the behavior of a system governed by Equation 2-1. Observe the system from time 0 to T and assume that $z(0) = 0$ and $\dot{z}(0) = 0$.

The functions $C(t)$ and $K(t)$ are assumed to have the form

$$\begin{aligned} C(t) &= (1 + \alpha t) c_0 \\ K(t) &= (1 + \beta t) k_0 \end{aligned} \quad (5-2)$$

Here, c_0 and k_0 are the damping constant and the stiffness constant, respectively. α and β are constant coefficients which are usually much less than one.

In many practical cases, it is observed that the structure displays an increase in damping and a decrease in stiffness when the structure excites an inelastic response. This implies α is a positive constant and β is a negative constant.

In this study, although α and β will be considered as small values, they will be large enough to influence the system's properties. This permits treatment of Equation 5-1 as a perturbed differential equation. When α and β are both equal to 0 (unperturbed), the equation 5-1 is simply a second-order differential equation with constant coefficients which can be easily solved.

The solution of Equation 5-1 can be written in the form (for example reference 82)

$$z = z_0 + \alpha z_\alpha + \beta z_\beta + \text{high-order terms} \quad (5-3)$$

Since α and β are small, the high-order terms will be neglected. Substituting Equation 5-3 into 5-1 and expanding yields

$$m(\ddot{z}_0 + \alpha \ddot{z}_\alpha + \beta \ddot{z}_\beta) + c_0 (1 + \alpha t) (\dot{z}_0 + \alpha \dot{z}_\alpha + \beta \dot{z}_\beta) + k_0 (1 + \beta t) (z_0 + \alpha z_\alpha + \beta z_\beta) = f \quad (5-4)$$

Moving the force term to the left side of the equation, grouping coefficients of the terms, 1, α , and β , then equating the coefficients to zero results in

$$m\ddot{z}_0 + c_0\dot{z}_0 + k_0z_0 = f \quad (5-5a)$$

$$m\ddot{z}_\alpha + c_0\dot{z}_\alpha + k_0z_\alpha = -c_0t\dot{z}_0 \quad (5-5b)$$

$$m\ddot{z}_\beta + c_0\dot{z}_\beta + k_0z_\beta = -k_0tz_0 \quad (5-5c)$$

These equations approximately govern the system's response when time variation of the parameters is linear, as shown in Equation

5-2. If the excitation and the system's response are known, then these equations can be used with a time domain parameter identification procedure to estimate the system parameters. However, when a time-domain parameter identification approach is used, problems arise if noise is present in the measured input and response signals (see Reference 8).

A frequency domain approach to the identification of system parameters is pursued. Therefore, the equations of motion are transformed to the frequency domain.

Let

$$Z_0(\omega) = \int_{-\infty}^{\infty} z_0(t) e^{-i\omega t} dt \quad (5-6a)$$

$$Z_\alpha(\omega) = \int_{-\infty}^{\infty} z_\alpha(t) e^{-i\omega t} dt \quad (5-6b)$$

$$Z_\beta(\omega) = \int_{-\infty}^{\infty} z_\beta(t) e^{-i\omega t} dt \quad (5-6c)$$

define the Fourier transforms of $z_0(t)$, $z_\alpha(t)$, and $z_\beta(t)$.

And let

$$z_0(t) = \frac{1}{2\pi} \int_{-\infty}^{\infty} Z_0(\omega) e^{i\omega t} d\omega \quad (5-7a)$$

$$z_\alpha(t) = \frac{1}{2\pi} \int_{-\infty}^{\infty} Z_\alpha(\omega) e^{i\omega t} d\omega \quad (5-7b)$$

$$z_\beta(t) = \frac{1}{2\pi} \int_{-\infty}^{\infty} Z_\beta(\omega) e^{i\omega t} d\omega \quad (5-7c)$$

define the inverse Fourier transforms. Then the Fourier transform of Equation 5-3 is

$$Z(\omega) = Z_0 + \alpha Z_\alpha + \beta Z_\beta \quad (5-8)$$

It can be shown that the Fourier transform of Equations 5-5a through 5-5c are given by

$$-m\omega^2 Z_0(\omega) + c_0 i\omega Z_0(\omega) + k_0 Z_0(\omega) = F(\omega) \quad (5-9a)$$

$$-m\omega^2 Z_\alpha(\omega) + c_0 i\omega Z_\alpha(\omega) + k_0 Z_\alpha(\omega) = c_0 \left(Z_0(\omega) + \omega Z'_0(\omega) \right) \quad (5-9b)$$

$$-m\omega^2 Z_\beta(\omega) + c_0 i\omega Z_\beta(\omega) + k_0 Z_\beta(\omega) = -i k_0 Z'_0(\omega) \quad (5-9c)$$

Now solve the Equations 5-9 simultaneously. The result is

$$Z_0(\omega) = H(\omega) F(\omega) \quad (5-10a)$$

$$Z_\alpha(\omega) = c_0 H(\omega) \left(H(\omega) F(\omega) + \omega (H'(\omega) F(\omega) + H(\omega) F'(\omega)) \right) \quad (5-10b)$$

$$Z_\beta(\omega) = -i k_0 H(\omega) \left(H'(\omega) F(\omega) + H(\omega) F'(\omega) \right) \quad (5-10c)$$

where $H(\omega)$ is frequency response function and $H'(\omega)$ is its first derivative. These can be written in the forms

$$H(\omega) = [(k_0 - m\omega^2) + i(\omega c_0)]^{-1} \quad (5-11a)$$

$$H'(\omega) = (2m\omega - ic_0) [(k_0 - m\omega^2) + i(\omega c_0)]^{-2} \quad (5-11b)$$

$F(\omega)$ is the Fourier transform of $f(t)$ and $F'(\omega)$ is its derivative.

$$F(\omega) = \int_{-\infty}^{\infty} f(t) e^{-i\omega t} dt \quad (5-12a)$$

$$F'(\omega) = -i \int_{-\infty}^{\infty} t f(t) e^{-i\omega t} dt \quad (5-12b)$$

Substitute the results from Equations 5-10 into Equation 5-8. This yields

$$\begin{aligned} Z(\omega) = & H(\omega)F(\omega) + \alpha c_0 \left(H(\omega) H(\omega)F(\omega) + \omega(H'(\omega)F(\omega) \right. \\ & \left. + H(\omega)F'(\omega)) \right) + (-ik_0\beta) H(\omega) \left(H'(\omega)F(\omega) + H(\omega)F'(\omega) \right) \end{aligned} \quad (5-13)$$

This is the approximate frequency domain expression for the solution of Equation 5-1. It is considered accurate when both α and β are small. The displacement response also can be obtained by inverse Fourier transformation of the Equation 5-13. Equation 5-13 is used in the identification process. Its use will finally lead to the estimation of the parameters from a sequence of measured data.

5.1 Identification Procedure

The method described above provides the solution for the Equation 5-1 in the frequency domain. When the measured values of $f(t)$ are used to estimate $F(\omega)$ and the result is used in Equation 5-13 to obtain $Z(\omega)$, this $Z(\omega)$ will not, in general, match the $Z(\omega)$ estimated from the measured $Z(t)$. Moreover, the calculated $|Z(\omega)|$ will not match the $|Z(\omega)|$ obtained from measurement. The reasons for this mismatch are that (1) noise is inevitably present in the measured input and response. (2) the mathematical model is linear, yet the measured data come from nonlinear structures and (3) the discrete Fourier transform of a time series is used to represent the continuous Fourier transform. In the following, a brief theoretical background is presented together with the simple description of the procedure for finding the unknown parameters.

An equation defining the mismatch between the measured data and the model of Equation 5-1 can be established. Let $|Z^{(m)}(\omega)|$ be the modulus of the Fourier transform of the measured structural response data. Let $|Z(\omega)|$ be the modulus of the function obtained when the Fourier transform of the measured input data is used in Equation 5-13. The difference between these function is defined

$$\epsilon(\omega) = |Z(\omega)| - |Z^{(m)}(\omega)| \quad (5-14)$$

When the discrete Fourier transform is used to approximate the continuous Fourier transform of a measured or theoretical signal, it is defined at a discrete set of frequencies, $\omega_k = k\Delta\omega$, $k = 0, 1, \dots, n-1$. Here n and $\Delta\omega$ relate to the time signal $z(t)$ and its discretization. It is assumed that $z(t)$ is available on the interval $(0, T)$ and is represented by the discrete set of values z_j , $j=0, \dots, n-1$. Thus, n is the number of points where the signal is represented. $\Delta\omega$ is given by $2\pi/T$. At a particular frequency $\omega = \omega_k$, Equation 5-14 becomes

$$\epsilon_k = |Z_k(\omega)| - |Z_k^{(m)}(\omega)| \quad (5-15)$$

ϵ_k can be positive or negative. A quantity which is always non-negative and which summarizes the differences between the measured, $|Z_k^{(m)}|$, and the theoretical, $|Z_k|$, structural responses in the frequency domain over a range of frequencies is given by

$$\epsilon^2 = \sum_k \epsilon_k^2 \quad (5-16)$$

This is the square error between measured data and the model. This error can be minimized by properly choosing the parameters, k_0 , c_0 , α , and β . A method that chooses the parameters this way is a least squares method.

The range of index values, k , over which the above sum is taken, is not specified in Equation 5-16. Equation 5-16 need not be summed from 0 to n . Rather, the summation should be carried out over the range of frequencies which includes those values of Z_k containing significant information on the behavior of the system. In general, this is the band of frequencies surrounding the characteristic frequency of the system.

Now, one can choose k_0 , c_0 , α , and β , as those constants which satisfy

$$\frac{\partial \epsilon^2}{\partial k_0} = \frac{\partial \epsilon^2}{\partial c_0} = \frac{\partial \epsilon^2}{\partial \alpha} = \frac{\partial \epsilon^2}{\partial \beta} = 0 \quad (5-17)$$

The k_0 , c_0 , α , and β , can be located using a search technique. To simplify the analysis, Newton's method is used to minimize ϵ^2 with respect to k_0 , c_0 , α , and β .

Newton's method converges very rapidly once an iterate is fairly close to the solution. The formal simplicity and its great speed are the reasons why Newton's method is used in this study.

To assure convergence in the numerical analysis, it is important to choose the initial iterate properly. A more detailed discussion of the numerical procedures will be presented later, in the numerical examples.

The steps in the numerical analysis are as follows:

1. Make the initial guesses at the parameter values, k_0 , c_0 , α , and β .
2. Choose the computation increments Δk_0 , Δc_0 , $\Delta \alpha$, and $\Delta \beta$.
3. Choose the desired accuracy measure (used to judge convergence).

4. Compute the partial first and second derivatives of ϵ^2 with respect to k_0 using central difference formulas.
5. Use Newton's method to minimize ϵ^2 with respect to k_0 .
6. Repeat steps 4 and 5, this time minimizing with respect to c_0 , then α , then β .
7. Check the result to convergence.
 - a. If convergence has occurred, then stop the analysis.
 - b. If convergence has not occurred, then repeat steps 4 through 6.

A computer program to execute the procedure described above has been written. This program is named PUR and a listing is included in the Appendix.

CHAPTER 6

IDENTIFICATION OF MULTI-DEGREE-OF-FREEDOM SYSTEM

6.0 M.D.F. System Model

The restoring force model developed in the Equation 2-2 of Chapter 2 can be extended for use in the modeling of a multi-degree-of-freedom (MDF) system. In the present investigation a shear beam type MDF structure will be considered. Figure 6-1 shows the type of structure under investigation. In this system the mass, m_j , is connected to masses m_{j-1} and m_{j+1} by the elements denoted k_j and k_{j+1} .

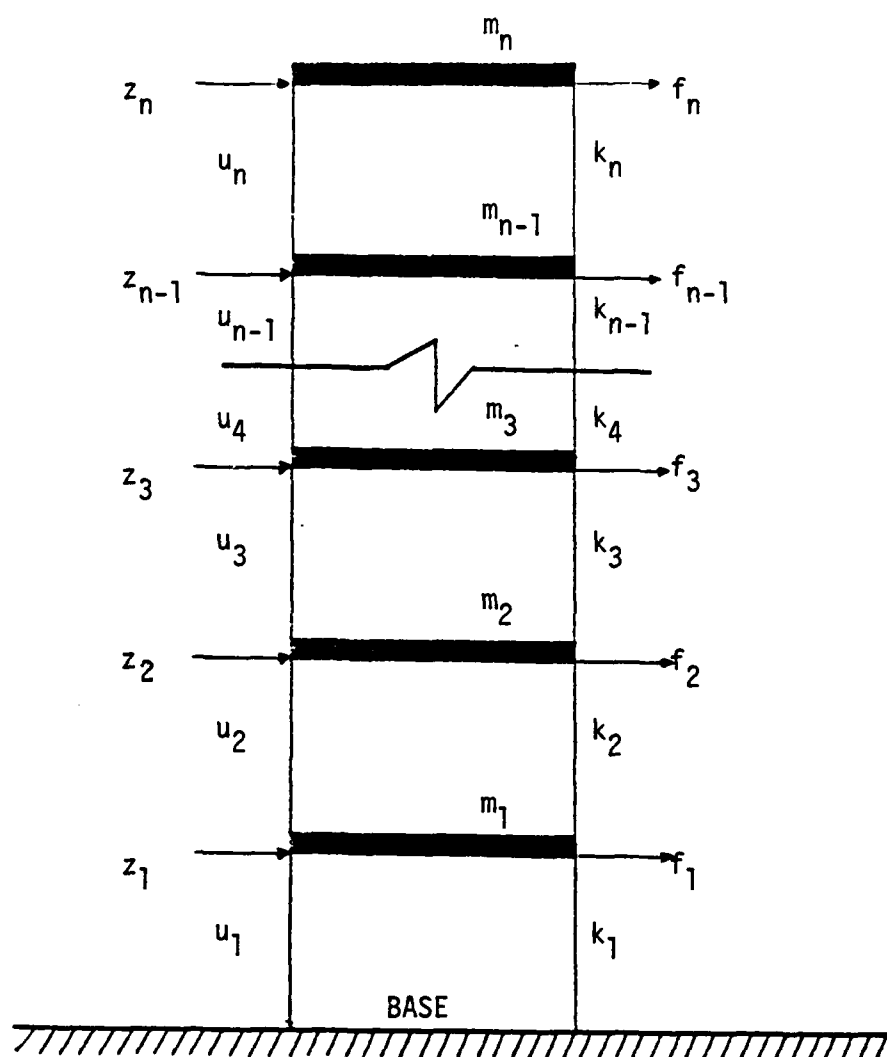
The equation of motion governing the response of a linear mass excited undamped MDF system is

$$[m] \{\ddot{z}\} + [k] \{z\} = \{f\} \quad (6-1)$$

where m and k are the mass and stiffness matrices, respectively, and are written in the form

$$[m] = \begin{bmatrix} m_1 & & & & & \\ & m_2 & & & & \\ & & m_3 & & & \\ & & & \ddots & & \\ & & & & \ddots & \\ & 0 & & & & \ddots \\ & & & & & & m_n \end{bmatrix} \quad (6-1a)$$

$$[k] = \begin{bmatrix} k_1+k_2 & -k_2 & 0 & \cdot & \cdot & \cdot & 0 \\ -k_2 & k_2+k_3 & -k_3 & & & & \cdot \\ 0 & -k_3 & & & & & \cdot \\ \cdot & & & \cdot & & & \cdot \\ \cdot & & & & \ddots & & \cdot \\ \cdot & & & & & & -k_n \\ 0 & \cdot & \cdot & & & -k_n & k_n \end{bmatrix} \quad (6-1b)$$



m : Mass
 k : Stiffness
 u : Restoring Force
 z : Displacement
 f : Forcing Function

Figure 6-1. Multi-degree-of-freedom shear column frame.

n is the number of degrees of freedom of the MDF system in Figure 6-1. The restoring force in this expression is $[k] \{z\}$ and this expression is valid as long as the response remains linear. When the response is inelastic then $[k] \{z\}$ must be replaced by a vector reflecting the time dependent characteristic of the restoring force.

In the present application it will be convenient to rewrite the equation of motion in terms of relative displacements. Let y_j , $j=2, \dots, n$, denote the relative displacement between the $j-1$ th and j th masses, and let y_1 denote the relative displacement between mass, m_1 , and the ground. Then the relation can be written

$$\{z\} = [A] \{y\} \quad (6-2)$$

where

$$[A] = \begin{bmatrix} 1 & 0 & 0 & \cdot & \cdot & \cdot & 0 \\ 1 & 1 & 0 & & & & 0 \\ 1 & 1 & 1 & & & & 0 \\ \cdot & \cdot & \cdot & \cdot & & & \cdot \\ \cdot & \cdot & \cdot & & \cdot & & \cdot \\ \cdot & \cdot & \cdot & & & \cdot & \cdot \\ 1 & 1 & 1 & \cdot & \cdot & \cdot & 1 \end{bmatrix} \quad (6-3)$$

Equation 6-2 provides an expression for $\{z\}$, and this result can be used in Equation 6-1 to obtain an alternate expression for the equation of motion. This is

$$[M] \{\ddot{y}\} + [K] \{y\} = \{f\} \quad (6-4)$$

where

$$[M] = [m] [A] = \begin{bmatrix} m_1 & 0 & 0 & \cdot & \cdot & \cdot & 0 \\ m_2 & m_2 & 0 & \cdot & \cdot & \cdot & 0 \\ m_3 & m_3 & m_3 & \cdot & & & \cdot \\ \cdot & \cdot & \cdot & & & & \cdot \\ \cdot & \cdot & \cdot & & & & \cdot \\ \cdot & \cdot & \cdot & & & & \cdot \\ m_n & m_n & m_n & \cdot & \cdot & \cdot & m_n \end{bmatrix} \quad (6-4a)$$

$$[K] = [k] [A] = \begin{bmatrix} k_1 & -k_2 & 0 & \cdot & \cdot & \cdot & 0 \\ 0 & k_2 & -k_3 & 0 & & & \\ 0 & 0 & k_3 & -k_4 & & & \\ \cdot & \cdot & \cdot & \cdot & & & \\ \cdot & \cdot & \cdot & \cdot & \cdot & & \\ \cdot & \cdot & \cdot & \cdot & \cdot & \cdot & \\ \cdot & \cdot & \cdot & \cdot & \cdot & \cdot & -k_n \\ 0 & 0 & 0 & \cdot & \cdot & \cdot & k_n \end{bmatrix} \quad (6-4b)$$

The term $[k] \{y\}$ in Equation 6-4 can be expanded to obtain the expression

$$[K] \{y\} = \begin{Bmatrix} k_1 y_1 - k_2 y_2 \\ k_2 y_2 - k_3 y_3 \\ k_3 y_3 - k_4 y_4 \\ \cdot \\ \cdot \\ \cdot \\ \cdot \\ k_n y_n \end{Bmatrix} \quad (6-5)$$

Note that the restoring force applied to mass j is $k_j y_j - k_{j+1} y_{j+1}$. The objective in this investigation is to replace the simple

linear restoring force with a high order linear model. Therefore in Equation 6-5 each of the terms $k_j y_j$ will be replaced with a term u_j . Each term u_j is governed by a differential equation. Let $[U]$ and $\{R\}$ be defined as follows

$$[U] = \begin{bmatrix} u_1 & -u_2 & 0 & \cdot & \cdot & \cdot & 0 \\ 0 & u_2 & -u_3 & & & & \\ 0 & 0 & u_3 & -u_4 & & & \\ \cdot & \cdot & \cdot & \cdot & \cdot & & \\ \cdot & \cdot & & & & \cdot & -u_n \\ \cdot & \cdot & & & & \cdot & u_n \\ 0 & 0 & \cdot & \cdot & \cdot & \cdot & \end{bmatrix} \quad (6-6)$$

$$\{R\} = \begin{bmatrix} 1 \\ 1 \\ 1 \\ \cdot \\ \cdot \\ \cdot \\ 1 \end{bmatrix} \quad (6-7)$$

Then the differential equation governing the motion becomes

$$[M] \{\ddot{y}\} + [U] \{R\} = \{f\} \quad (6-8)$$

Each u_i , $i=1, \dots, n$, is governed by an equation of the form

$$\sum_{j=0}^M c_{ij} u_i^{(j)} = c_{i,M+1} y_i + \dot{y}_i \quad (6-9)$$

where c_{ij} , $i=1, \dots, n$, $j=0, \dots, M+1$, are the parameters which characterize the restoring force. The superscript (j) refers to the j th derivative of u_i with respect to time. This equation is analogous to Equation 2-2 for the SDF system.

Equation 6-9 can be written in matrix form using the following expression. Let

$$[C_j] = \begin{bmatrix} c_{1j} & 0 & 0 & \cdot & \cdot & \cdot & 0 \\ 0 & c_{2j} & 0 & & & & 0 \\ 0 & 0 & c_{3j} & & & & 0 \\ \cdot & & & \cdot & & & \cdot \\ \cdot & & & & \cdot & & \cdot \\ \cdot & & & & & \cdot & \cdot \\ 0 & 0 & 0 & \cdot & \cdot & \cdot & c_{nj} \end{bmatrix}, \quad j=0, \dots, M+1 \quad (6-10)$$

Then the sequence of Equation 6-9 can be expressed

$$\sum_{j=0}^M [C_j] \{u^{(j)}\} = [C_{M+1}] \{y\} + \{y\} \quad (6-11)$$

where $\{u^{(j)}\}$ is the jth derivative of the vector

$$\{u\} = \begin{Bmatrix} u_1 \\ u_2 \\ u_3 \\ \cdot \\ \cdot \\ \cdot \\ u_n \end{Bmatrix} \quad (6-12)$$

To obtain the differential equation approximately governing the motion of an MDF system, it is necessary to combine Equation 6-8 and 6-11. Rearrange Equation 6-8 to obtain

$$[U] \{R\} = \{f\} - [M] \{\ddot{y}\} \quad (6-13)$$

Let

$$\{D\} = \begin{bmatrix} 1 & 1 & 1 & \cdot & \cdot & \cdot & 1 \\ 0 & 1 & 1 & & & & 1 \\ 0 & 0 & 1 & & & & \cdot \\ \cdot & & & \cdot & & & \cdot \\ \cdot & & & & \cdot & & \cdot \\ \cdot & & & & & \cdot & \cdot \\ 0 & 0 & 0 & \cdot & \cdot & \cdot & 1 \end{bmatrix} \quad (6-14)$$

Premultiply both sides of Equation 6-16 by $[D]$; the result is

$$[D] [U] \{R\} = [D] \left[\{f\} - [M] \{\ddot{y}\} \right] \quad (6-15)$$

But the left side of Equation 6-15 is simply equal to $\{u\}$.

Therefore

$$\{u\} = [D] \left[\{f\} - [M] \{\ddot{y}\} \right] \quad (6-16)$$

and the j th derivative of $\{u\}$ is

$$\left\{ u^{(j)} \right\} = [D] \left[\left\{ f^{(j)} \right\} - [M] \left\{ y^{(j+2)} \right\} \right] \quad (6-17)$$

This expression can be used in Equation 6-11 to obtain

$$\sum_{j=0}^M [C_j] [D] \left[\left\{ f^{(j)} \right\} - [M] \left\{ y^{(j+2)} \right\} \right] = [C_{M+1}] \{\dot{y}\} + \{y\} \quad (6-18)$$

Upon rearrangement this expression becomes

$$\begin{aligned} & \left(\sum_{j=0}^M [C_j] [D] [M] \left\{ y^{(j+2)} \right\} \right) + [C_{M+1}] \{\dot{y}\} + \{y\} \\ & = \sum_{j=0}^M [C_j] [D] \left\{ f^{(j)} \right\} \end{aligned} \quad (6-19)$$

This is the equation assumed to govern motion of the inelastic MDF system. The element restoring forces of the MDF system are governed by Equation 6-9. The governing equation for the MDF system is analogous to Equation 2-4, the governing equation for the SDF system.

When the parameters appearing in Equation 6-19 are known and the input is specified, the equation of motion can be solved and its solution provides the structural response approximation. Several measurements of structural responses can be evaluated. For example, the response displacement, velocity and acceleration at all structural degrees of freedom can be formed. Beyond this, other measures of structure response, such as energy dissipated by the structure, can be determined. Later, numerical examples of structural response computation will be given.

The objective of this investigation is to perform structural parameter identification for inelastic structures. Equation 6-19 could be used to execute such an identification, using measured data, but the presence of the higher derivatives of both input and response precludes the practical application of this approach. (See Reference 8). A better approach to the parameter identification problem is in the frequency domain. Therefore, Equation 6-19 is transformed. Fourier transformation of both sides of Equation 6-19 yields the expression

$$\begin{aligned} & \left[\left(\sum_{j=0}^M [C_j] [D] [M] (i\omega)^{j+2} \right) + (i\omega)[C_{M+1}] + [I] \right] \{Y\} \\ & = \left[\sum_{j=0}^M [C_j][D] (i\omega)^j \right] \{F\} \end{aligned} \quad (6-20)$$

where

$$\{Y(\omega)\} = \int_{-\infty}^{\infty} \{y(t)\} e^{-i\omega t} dt \quad (6-20a)$$

$$\{F(\omega)\} = \int_{-\infty}^{\infty} \{f(t)\} \bar{e}^{i\omega t} dt \quad (6-20b)$$

To use this equation for parameter identification, the following notation is established. Let

$$\begin{aligned} [H(\omega)] &= \left[\left(\sum_{j=0}^M [C_j] [D] [M] (i\omega)^{j+2} \right) + (i\omega) [C_{M+1}] + [I] \right]^{-1} \\ &\times \left[\sum_{j=0}^M [C_j] [D] (i\omega)^j \right] \end{aligned} \quad (6-21)$$

The components in $[H(\omega)]$ can be denoted

$$[H(\omega)] = \begin{bmatrix} H_{11}(\omega) & H_{12}(\omega) & \cdots & H_{1n}(\omega) \\ H_{21}(\omega) & H_{22}(\omega) & & H_{2n}(\omega) \\ \cdot & & & \cdot \\ \cdot & & & \cdot \\ \cdot & & & \cdot \\ H_{n1}(\omega) & H_{n2}(\omega) & \cdots & H_{nn}(\omega) \end{bmatrix} \quad (6-22)$$

Then Equation 6-23 can be expressed as

$$\{Y\} = [H] \{F\} \quad (6-23)$$

The jth term in the vector $\{Y\}$ is

$$Y_j(\omega) = \sum_{k=1}^n H_{jk}(\omega) F_k(\omega) \quad (6-24)$$

This is the Fourier Transform of the structure response at the jth degree of freedom of the structure. The modulus of the response at this degree of freedom is

$$|Y_j(\omega)| = \left| \sum_{k=1}^n H_{jk}(\omega) F_k(\omega) \right|, \quad j=1, \dots, n \quad (6-25)$$

6.1 Identification Procedure

Equation 6-25 can be used to execute the identification of the structural model parameters. If the structural system under consideration is linear with governing equation given by Equation 6-19, and if its input and response can be measured exactly, without noise, and if the Fourier Transform of these signals is performed exactly, then measured data can satisfy Equation 6-25. But, in general, measured data are noisy. The Fourier Transform used in practical computation is the Fast Fourier Transform (FFT). And the model of Equation 6-19 does not precisely characterize the structural system. Therefore, Equation 6-25 will not generally be exactly satisfied where $Y_j(\omega)$ and $F_k(\omega)$ are obtained using measured data. In view of this the following expression can be written

$$\epsilon_j(\omega) = |Y_j(\omega)| - \left| \sum_{k=1}^n H_{jk}(\omega) F_k(\omega) \right| \quad (6-26)$$

This is an error term and it characterizes the differences between the measured response data, and the response that would be predicted by the model, Equation 6-20.

A least squares approach can be used to minimize this error. Let

$$\epsilon_j^2 = \int_{\omega_a}^{\omega_b} \epsilon_j^2(\omega) d\omega \quad (6-27)$$

define the squared error of the model in the frequency domain at degree of freedom j . The integration is taken over a range of frequency values such as ω_a through ω_b . These limits are usually chosen to include the frequencies where the system displays power.

A measure of the model error at all degrees of freedom is obtained by summing the ϵ_j^2 at all points.

$$\epsilon^2 = \sum_{j=1}^n \epsilon_j^2 \quad (6-28)$$

This quantity reflects the model error in the entire system. This error can be minimized with respect to the model parameters c_{ij} , $i=1, \dots, n$, $j=0, \dots, M+1$, by solving the sequence of equation

$$\frac{\partial \epsilon^2}{\partial c_{ij}} = 0, \quad i=1, \dots, n, \quad j=0, \dots, M+1 \quad (6-29)$$

for the c_{ij} . The solution yields the system parameters which best characterize the model in a least squares sense.

Because of the complexity of the system model, the computation used to solve Equation 6-29 must be executed numerically. This computation is a search for the minimum value of ϵ^2 in the $n \times (M+2)$ dimension space of system parameters, c_{ij} , $i=1, \dots, n$, $j=0, \dots, M$. The search can be carried out in one of two ways. First, a search can be executed wherein the quantity ϵ^2 is minimized sequentially with respect to each of the parameters c_{ij} . For example, ϵ^2 can be minimized with respect to c_{11} then c_{12} , then c_{13} etc. The minimizing sequence is repeated as many times as necessary to obtain convergence in ϵ^2 .

The second approach to minimization of ϵ^2 is the gradient search technique. In this technique, the gradient of ϵ^2 is computed at a point in the c_{ij} space. This information is used to choose a new set of parameters where ϵ^2 will be smaller than its original value. At the newly adjusted point, ϵ^2 and its gradient are recomputed, and this process is repeated until ϵ^2 is near its minimum.

In the present investigation the former analytical approach is adopted. Numerical examples in Chapter 8 shows how a least squares computer program can be used to identify the parameters of an MDF structure.

CHAPTER 7

ENERGY DISSIPATED RELATED TO CONCRETE DAMAGE

7.0 Introduction

This presentation describes and evaluates an experimental study of the strength reduction and behavior of plain concrete subjected to cyclic loading. It is recognized that concrete is damaged by application of stresses lower than the ultimate stress. The concrete fracture process begins at very low stress and is continuous.

The damage caused by loading to small stresses is slight and each subsequent loading over the same stress range produces a negligible increase in damage. However, as the loading stress is increased, more damage occurs. Stresses with peak values in the range of 40 percent to 100 percent of the ultimate stress produce considerable damage and subsequent loading over the same range cannot be neglected. In practical situations, when a severe excitation is applied to a structure, it is not uncommon for the peak stress to go beyond the 50 percent level of ultimate stress.

When loading is repeated, damage accumulates in a concrete specimen; consequently it no longer retains its original strength. This concept suggests that it might be useful to attempt a quantitative evaluation of damage occurring in concrete during the cyclic loading. The objective of this study is to demonstrate that concrete damage and strength reduction are related to energy dissipation under repeated loading.

When energy is dissipated during loading and unloading, an hysteresis loop is formed in the stress-strain curve as shown in Figure 7-1. The area enclosed represents the total energy dissipated during one cycle of loading. This dissipated energy may be classified into two parts, namely, damage and damping energy

dissipation. However, the total accumulated energy dissipation is of primary interest in this experimental study. A more detailed discussion of the energy dissipation mechanism is given in Reference [69].

There are many methods that can be used to detect and assess damage in concrete. Among the most frequently used techniques are those which assess change in initial elastic modulus, and those which measure acoustic emissions, change in pulse velocity, and energy dissipation. In the present study, the dissipated energy method will be adopted. Attention will be focused on this means for measuring damage because of its intuitive relationship with the energy dissipation of an hysteretic structure under dynamic loads. Other methods may be considered as in References [69, 70, and 71].

In the present investigation a sequence of physical experiments was performed. In each experiment a concrete cylinder (specifications given below) was loaded in uniaxial compression. The load applied to each cylinder was a cyclic load, and the energy dissipated was calculated. This was done by plotting the stress versus strain diagram and by determining the area enclosed within the hysteresis loops. Varying amounts of energy were dissipated in the various test specimens, and upon completion of cyclic testing each specimen was loaded to failure in order to determine its residual strength. For each test specimen, dissipated energy and residual strength were recorded and the relation between these quantities was established.

More details of the testing procedure are given below, together with fresh concrete properties observed during the mixing. These may provide a useful reference for the concretes used in the test.

The concrete specimens tested in this investigation have the mix details and plastic properties of fresh concrete as shown in Table 7-1.

TABLE 7-1.
Concrete Mix Details

Type of Cement	W/C Ratio	Aggregate Cement Ratio	Ratio of Coarse:Fine Aggregate	Maximum Aggregate Size (in)
Type 1 A	0.53	4.8	60:40	3/4

Plastic Properties of Fresh Concrete

Mix No.	Slump (in)	Air %	Room Temperature (degrees C)	Unit Weight lb/ft ³
2 WE	4	3.5	27	145.8
3 WE	4 1/4	4	30	148.96

The specimens were all cast in 6-in x 12-in steel cylinder molds. The concrete mix proportions were constant for all the specimens. The specimens were tested at a constant loading rate of 1000 lb/sec in a RIEHLE compression testing machine. The force versus strain results of each test were plotted with an x-y electronic recorder. This recorder was connected by an electronic compressometer which is properly designed for this specific purpose as shown in Figure 7-2. The test machine was properly calibrated before the test.

To ensure a uniform displacement of the specimens, thin sulfur caps on the two end surfaces of the specimens were employed and were allowed to harden before testing. Specimens were cured in water in the curing tank at 25°C for 14 days and 28 days.

In assessing the energy dissipated and residual strength, specimens were subjected to a series of cycles of loading and unloading. The specimens were loaded up to a value in the range of stress, 90 - 94 percent of the ultimate stress. This ensured that damage occurred for every cycle of loading. At the end of each cycle of loading and unloading, the testing machine was returned to a rest position, and reloading was commenced immediately. To ensure that concrete characteristics would be as nearly uniform as possible, all the tests in each sequence were run in one day.

7.1 Discussion of Results

Numerous physical experiments were conducted in this investigation and characteristics of concrete accumulating damage can be derived from the individual tests and all the tests, jointly. In the following section the characteristics of individual tests are discussed first; then damage characteristics related to the entire test sequence are discussed.

A typical stress-strain diagram obtained during one experiment is shown in Figure 7-3. A number of characteristic features can be extracted from this result. On the initial cycle the specimen was loaded to a stress near its ultimate (95 to 98 percent). It can be seen that the most significant change in behavior between consecutive loading cycles occurs between the first and second cycle.

The first loading curve shows more curvature than the following reloading curves in which curvature tends to diminish. The reloading curves show progressively decreasing slopes. This may be attributed to structural degradation of the specimen.

Another measure of degradation can be established by plotting the initial elastic modulus for a particular cycle versus energy dissipation prior to that cycle. This is shown in Figure 7-4. As the energy dissipated gradually increases, the initial elastic modulus diminishes.

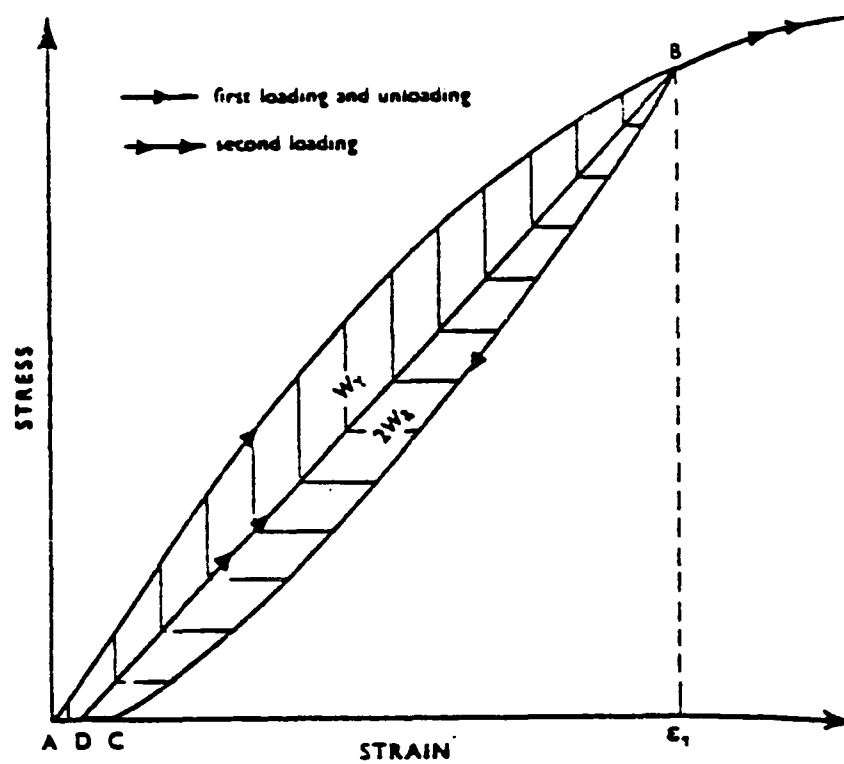


Figure 7-1. Idealized first and second cycles.

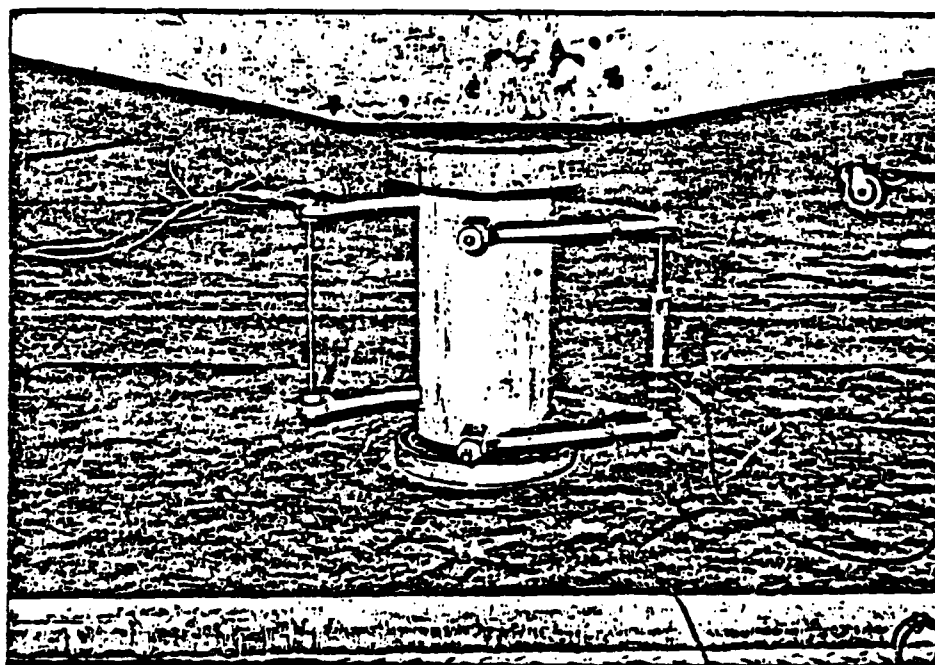


Figure 7-2. Test configuration.

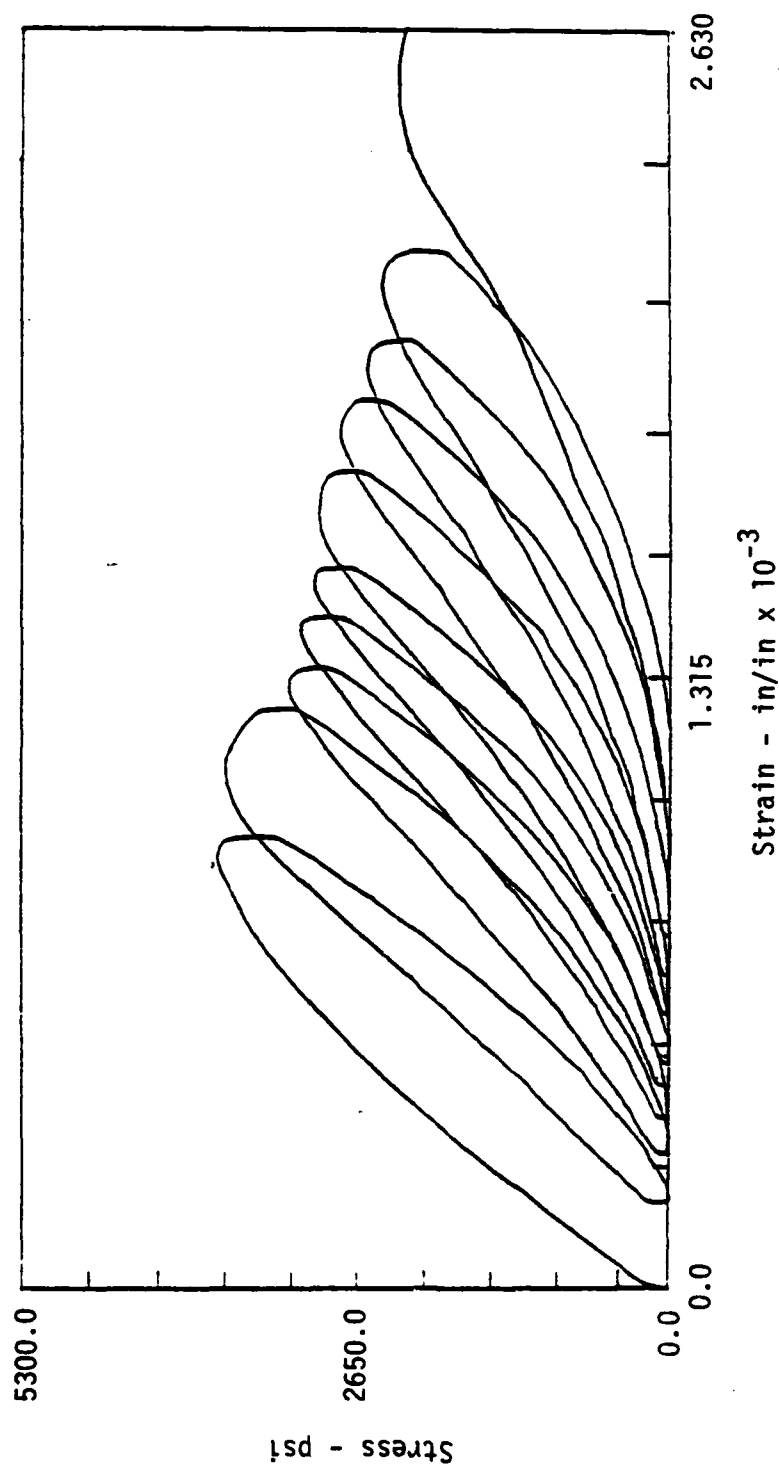


Figure 7-3. Stress-strain diagram for test specimen number 3WE#7.

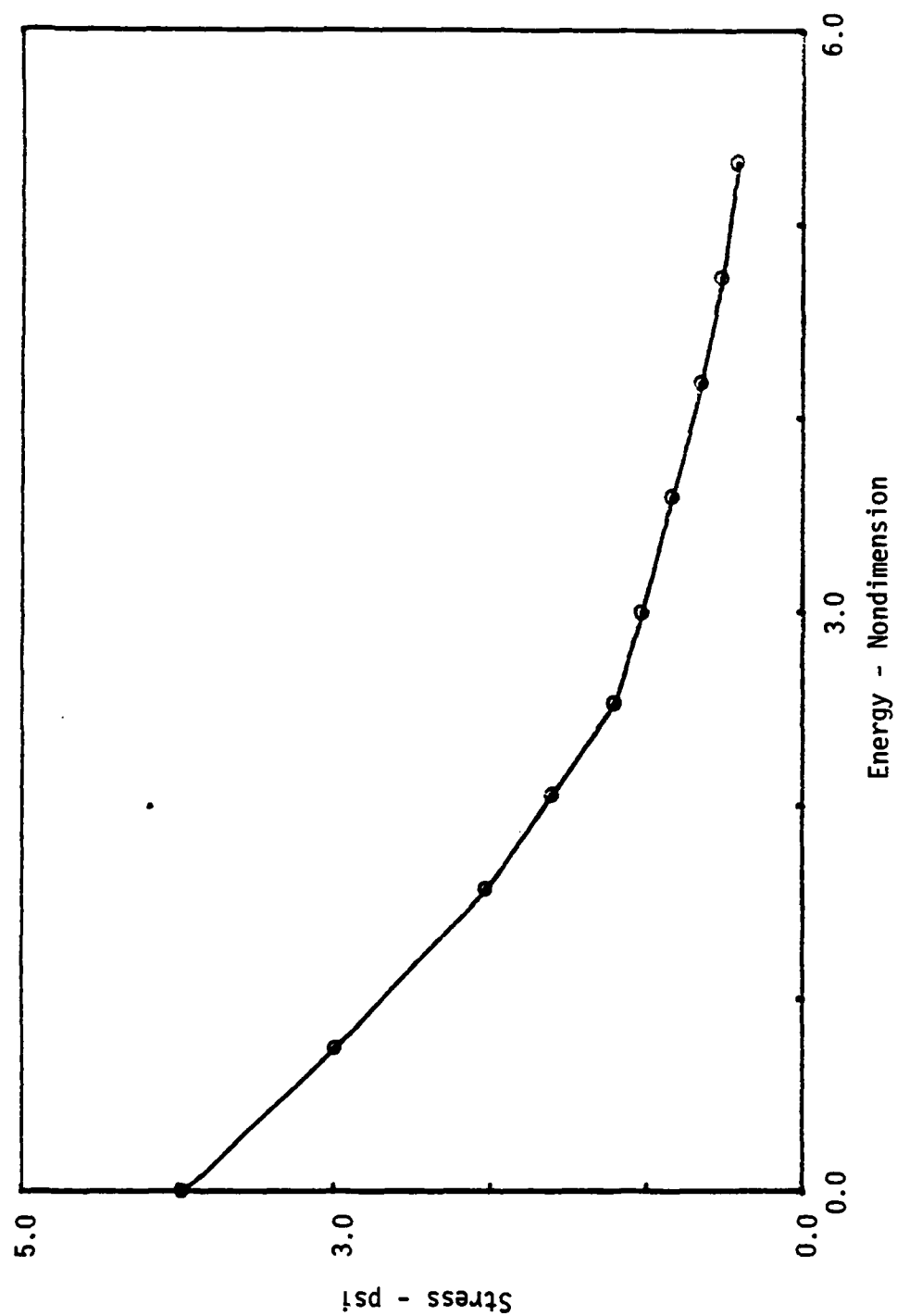


Figure 7-4. Initial modulus versus accumulated energy dissipated for a typical concrete specimen.

The above discussion was based on one typical sample. A similar discussion could be given for the other samples. Figures 7-5, 7-6, and 7-7 show the stress-strain curves for some other specimens tested during this investigation.

Some general characteristics of the accumulation of damage in concrete specimens can be derived from the entire collection of results. A total of 24 concrete specimens were tested in this investigation.

As noted earlier, the specimens were subjected to cyclic loadings inducing different amounts of energy dissipation in the various cylinders. Not all specimens were cycled to failure. At least, three of the specimens were tested for the determination of the ultimate strength. Other specimens, however, were cycled till failure. The remainder of the specimens were cycled till a certain amount of energy was dissipated; then these were loaded to failure in order to find their residual strength.

Using these data, a characteristic of the specimens can be extracted. The total energy dissipated by each particular specimen was plotted against the residual strength of the specimen as shown in Figure 7-9. Another result can be illustrated by plotting the total energy dissipated versus percentage of decrease in strength as shown in Figure 7-8. Both diagrams show a decrease in strength as the total energy dissipated is increased. Since only a limited number of specimens were tested, no direct mathematical expression relating the residual strength to the total energy dissipated was obtained. While such a relation could be established, further testing is required to derive a general relationship. However, the present results provide the information needed to conclude that energy dissipation is truly related to the residual strength.

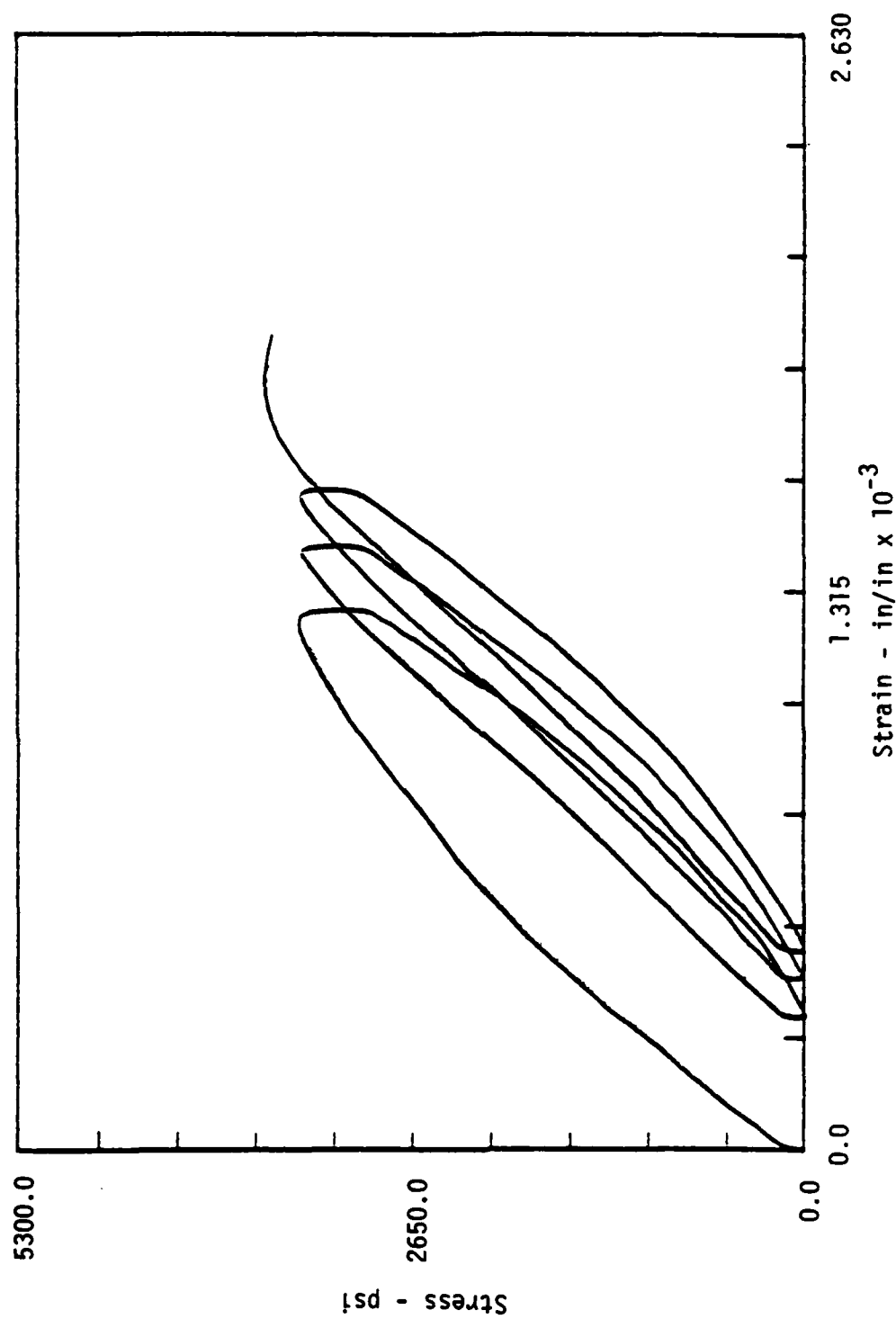


Figure 7-5. Typical stress-strain diagram for a concrete test specimen under cyclic load. Peak stress 90 percent of failure stress for Batch #3 (14 days curing).

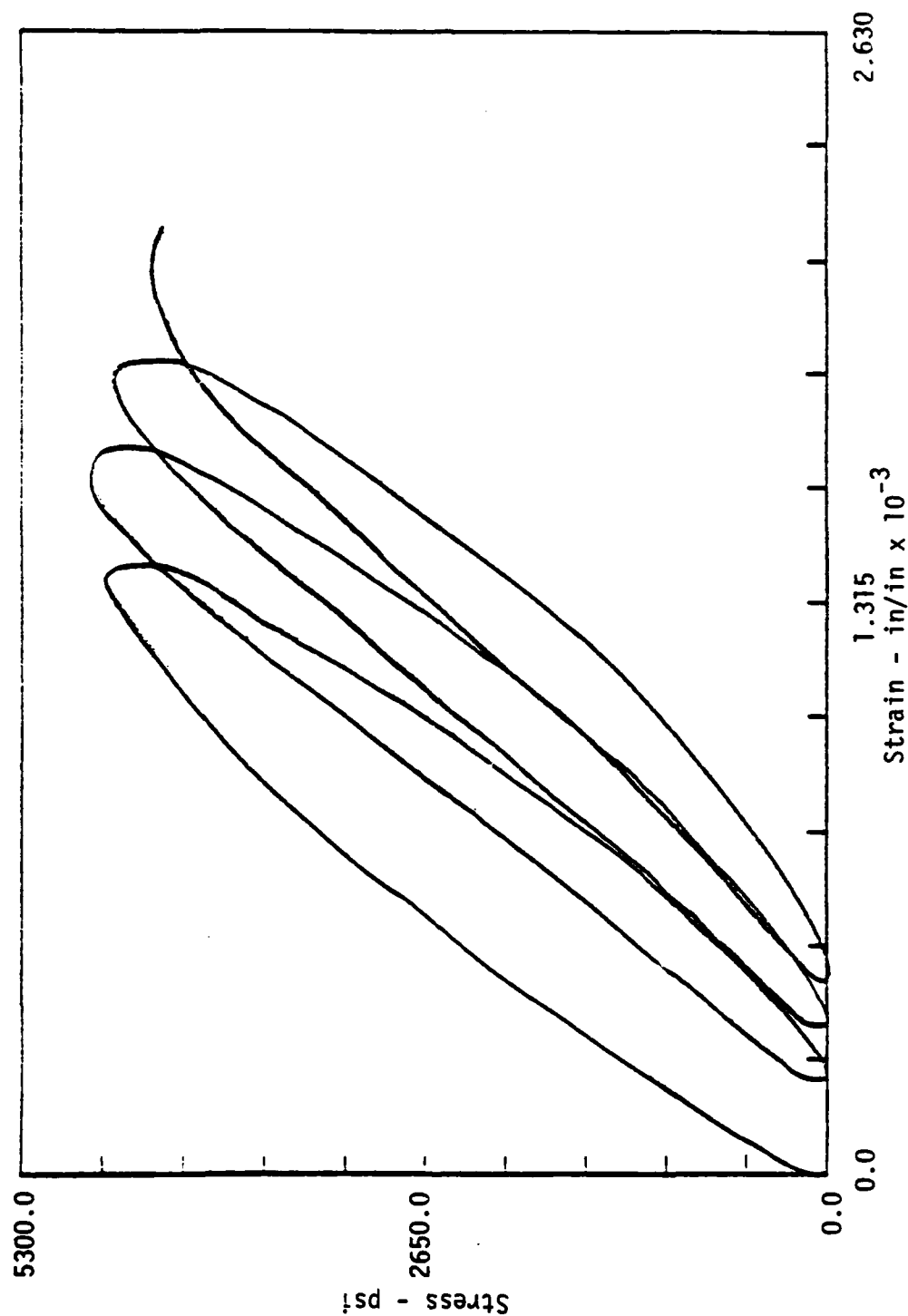


Figure 7-6. Typical stress-strain diagram for a concrete test specimen under cyclic load. Peak stress 90 percent of failure stress for Batch #2 (28 days curing).

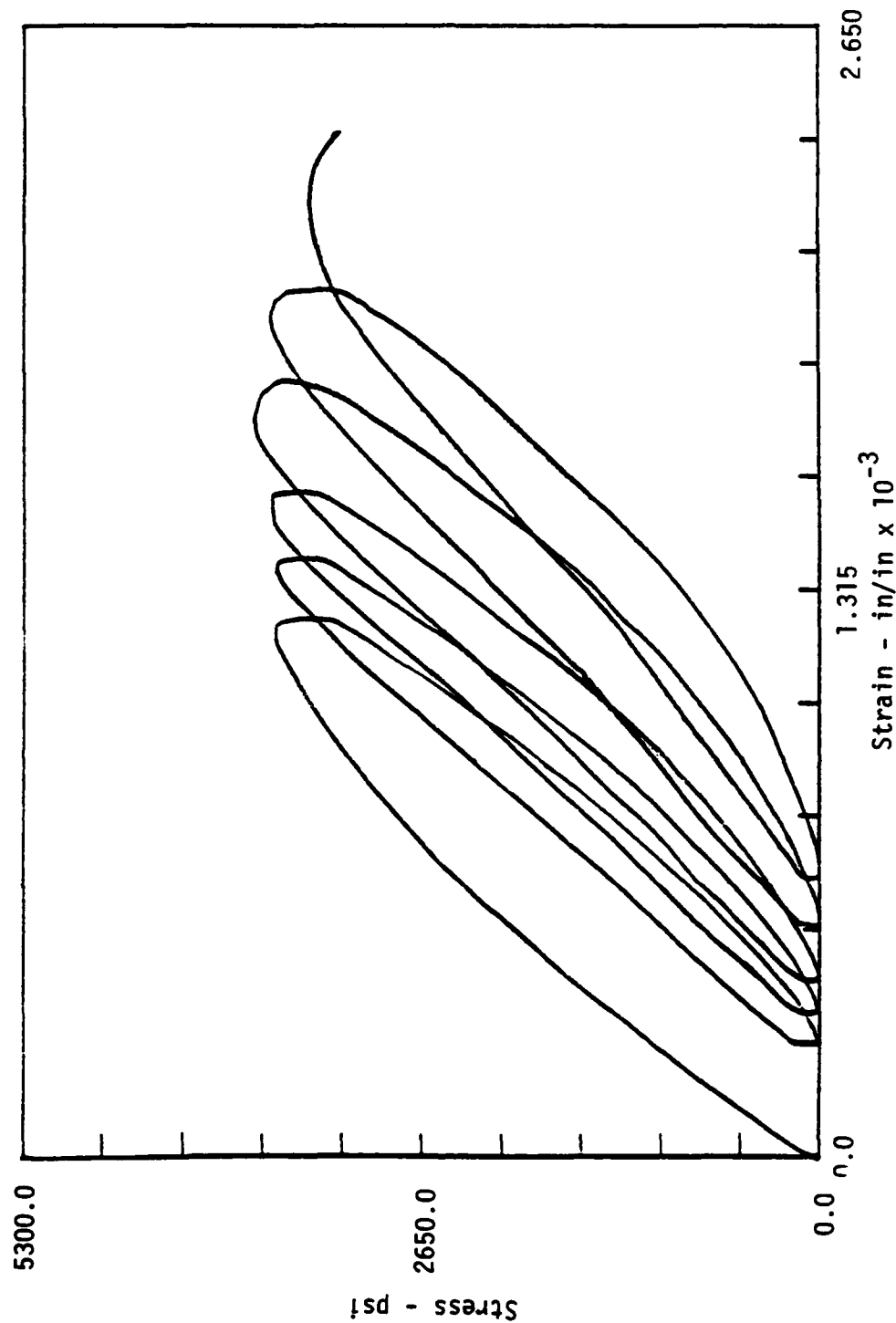


Figure 7-7. Typical stress-strain diagram for a concrete test specimen under cyclic load. Peak stress 90 percent of failure stress for Batch #3 (14 days curing).

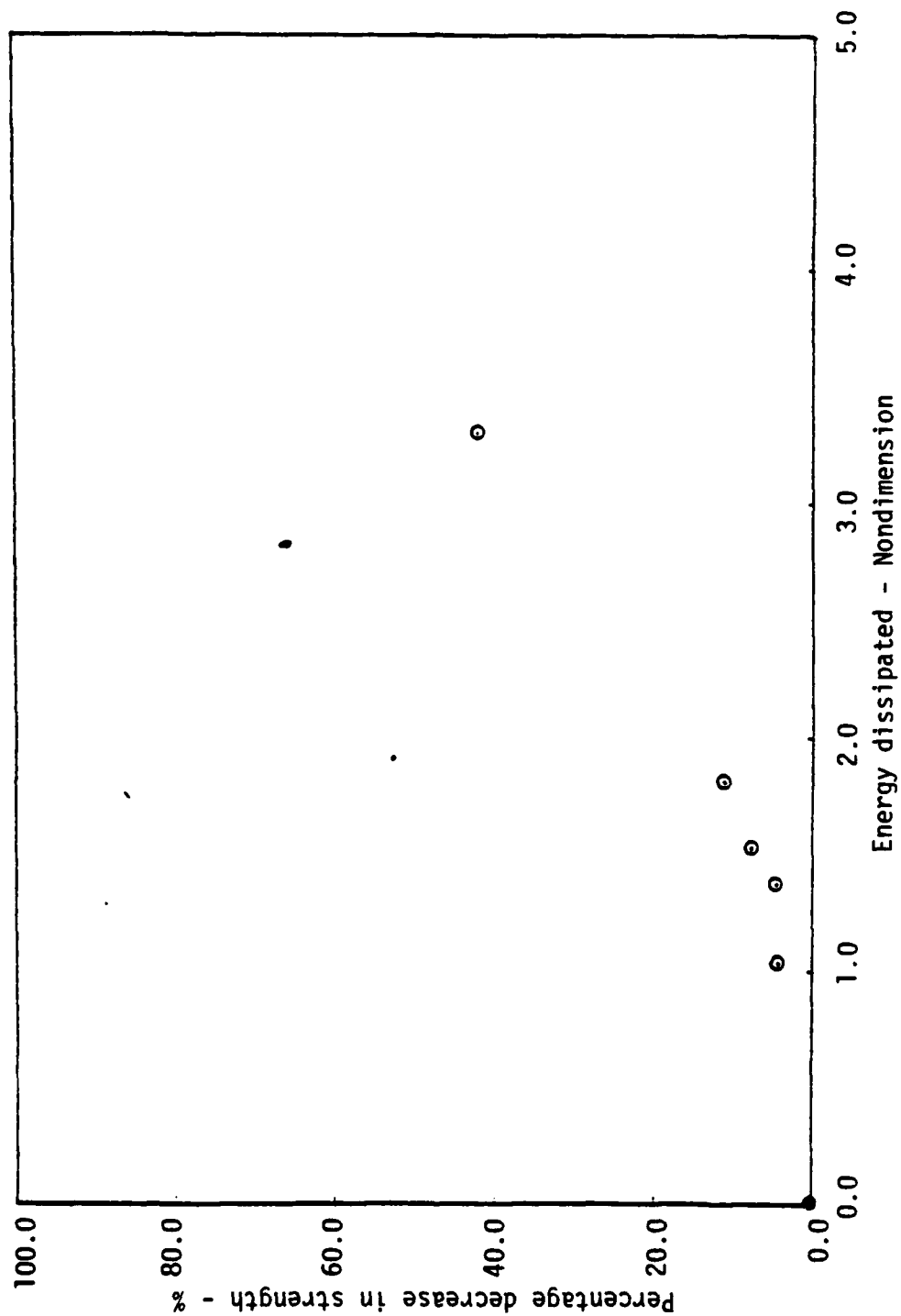


Figure 7-8. Percent decrease in residual strength versus energy dissipated in concrete specimen (14 day curing).

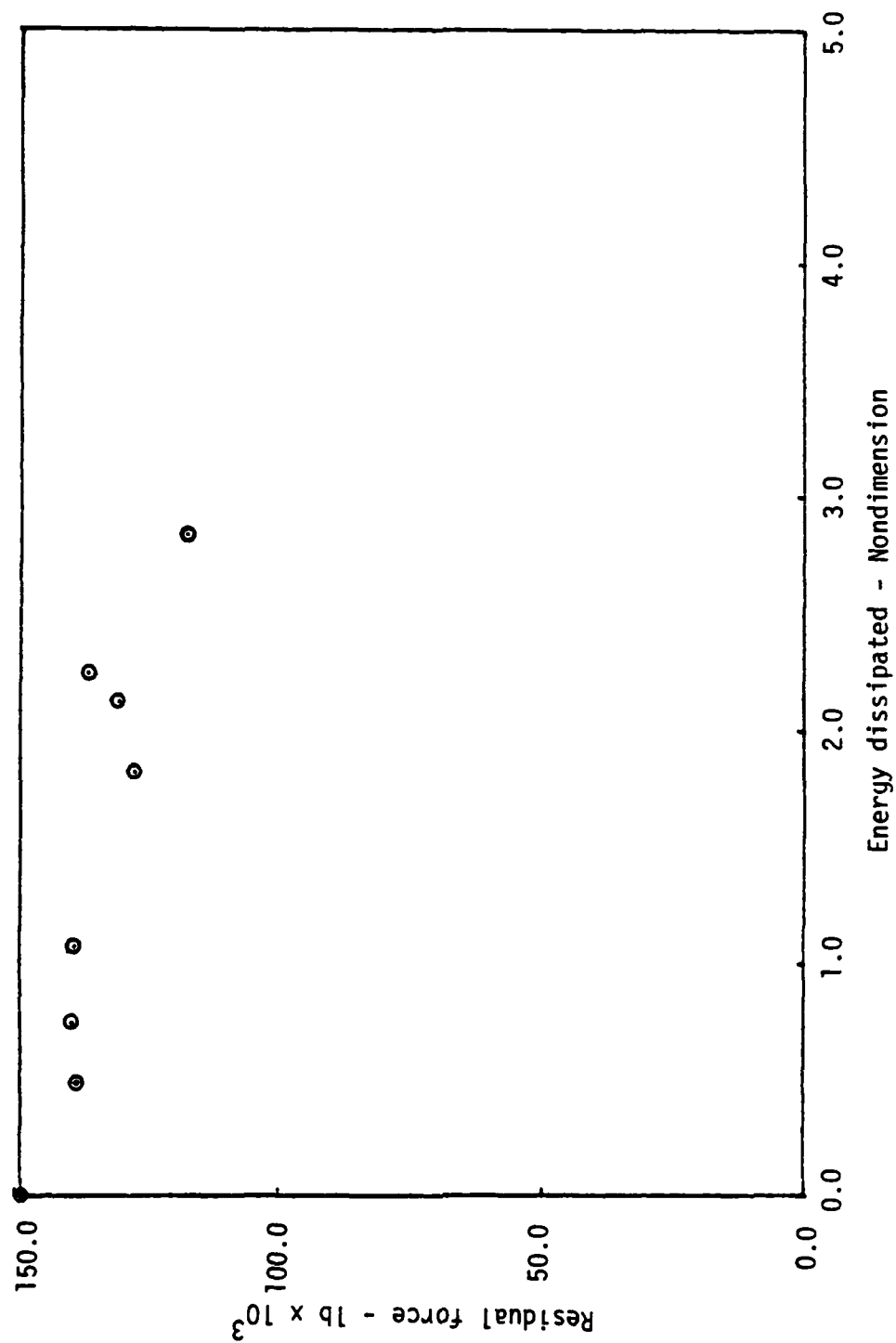


Figure 7-9. Residual strength versus energy dissipated in concrete specimens (28 day curing).

The experimental technique described above provides an approach for the estimation of damage in concrete. Based on the physical experiments, the following conclusions can be made:

1. The most significant change in the properties of the concrete occur between the first cycle and second cycle when loading in the first cycle is severe.
2. The initial elastic modulus of the specimens gradually diminishes as energy is dissipated. This implies that the damage of concrete under cyclic loading occurs progressively.
3. The energy dissipated in a concrete specimen is adversely related to residual strength. As the energy dissipated increases, the residual strength decreases. Therefore, energy dissipated may be used to predict the damage of a structure under a severe loading. Moreover, total energy dissipated may be considered as an indicator of the degree of damage in an hysteretic structure.

Some restrictions apply to the above conclusions. The work is limited to behavior in uniaxial compression. Other types of loading are possible and further tests are required to characterize damage under general loading. It has been assumed that the creep effect is small enough to be neglected in this investigation.

CHAPTER 8

NUMERICAL EXAMPLES

8.0 Data Description

In this chapter numerical examples are presented which demonstrate the use of the analytic procedures developed in the previous chapters. The first set of examples demonstrates the identification of the model parameters for linear and hysteretic, single-degree-of-freedom (SDF) structures both when measurement noise is and is not present. One example demonstrating the time domain approach to parameter identification is summarized. Two examples showing the frequency domain approach are presented.

Another example demonstrates the application of the analysis presented in Chapter 6. The frequency domain approach is used to identify the parameters of a multi-degree-of-freedom (MDF) structure.

The input used to excite the SDF system in all numerical examples is a decaying exponential, oscillatory function. It is generated using the formula

$$f(t) = e^{-\alpha t} \left[\sum_{j=1}^N c_j \cos(\omega_j t - \phi_j) \right] \quad 0 \leq t \leq T \quad (8-1)$$

where α , c_j , $j=1, \dots, N$, and ω_j , $j=1, \dots, N$ are constants. ϕ_j , $j=1, \dots, N$, are phase angles which are random variable realizations; these random variables are independent and uniformly distributed on the interval $(0, 2\pi)$. α is a decay rate. The c_j , $j=0, \dots, N$, are constants which determine the amplitudes of the excitation. All the values of c_j are taken as equal to c in all cases for the examples. ω_j , $j=1, \dots, N$, are equally spaced in the interval including the characteristic frequency of the system being analyzed.

The forcing function defined above was generated at discrete times. Specifically, $f(t)$ was evaluated at the times $t=t_1=l\Delta t$, $l=0, \dots, N-1$. A computer program, named FORCE, which generates the excitation of Equation 8-1 was used in these numerical examples.

Three distinct signal types were identified in the numerical examples. The first type used a computer program, named BILIN, to compute linear and nonlinear response. BILIN can be used to find the displacement, velocity, and acceleration response of a given bilinear hysteretic system to an arbitrary input. It also computes the energy dissipated by the structure during the response. The second type used a computer program, named TIMEVA, to compute the response. This program computes a linear time dependent response defined by Equations 5-1 and 5-2 with α , β , c_0 , and k_0 constants. The third type used a computer program named BLNMDF to compute the MDF structure response.

White noise was used whenever measurement noise was added to the signals. The white noise is normally distributed, $N(0, \sigma_n^2)$. A subroutine named NOISE was used to generate the noise signal. The noise signals were added to the generated input and response signals in the following manner. First, the excitation and response signals were generated using programs FORCE, BILIN, BLNMDF, and TIMVA. Then noise/signal ratios were selected and used to obtain the variances of the noise signals. The noise signals were generated as sequences of independent random variables, and directly added to the excitation and response. These noisy signals were then used as inputs to do the identification. Note, no filtering procedure was used on the simulated measured signals during the identification process.

Three basic models were used to represent the hysteretic systems. These are the second order linear, time invariant, third order linear, time invariant, and second order linear, time

varying models. All the model parameters were identified. The identification procedures and formulations were described previously. Different identification approaches may be applied for the same model.

8.1 Example 1

This example solves a parameter identification problem using the direct time domain approach, summarized in Equations 3-4 through 3-12. The parameters of the shock input are listed in Table 8.1. A typical forcing function history generated using these parameters is shown in Figure 8-1a. The derivative of the forcing function is shown in Figure 8-1b.

The notations for the parameters used in specifying the numerical examples are those used in the text. Some additional notations are defined here. c is the viscous damping in an SDF system. k is the initial stiffness in a bilinear hysteretic structure. k_y is the yield stiffness of a bilinear hysteretic structure. z_y is the yield displacement of a bilinear hysteretic structure. z_{max} is the maximum displacement of an SDF structure.

In this numerical example, two basic problem types are solved. These are summarized below.

- (1) An input is generated using Equation 8-1. The input is used to excite a linear SDF system with viscous damping. The structural input and response are stored, and no noise signals are added to the input and response. Then the input and response are used to identify the model parameters, a_j , $j=0, \dots, M+1$, from Equation 3-5.
- (2) An input is generated as in 1, above, but here the response of a bilinear hysteretic system is computed. No noise signals are added to the input and response. The input and response are used to identify the model parameters, a_j , $j=0, \dots, M+1$.

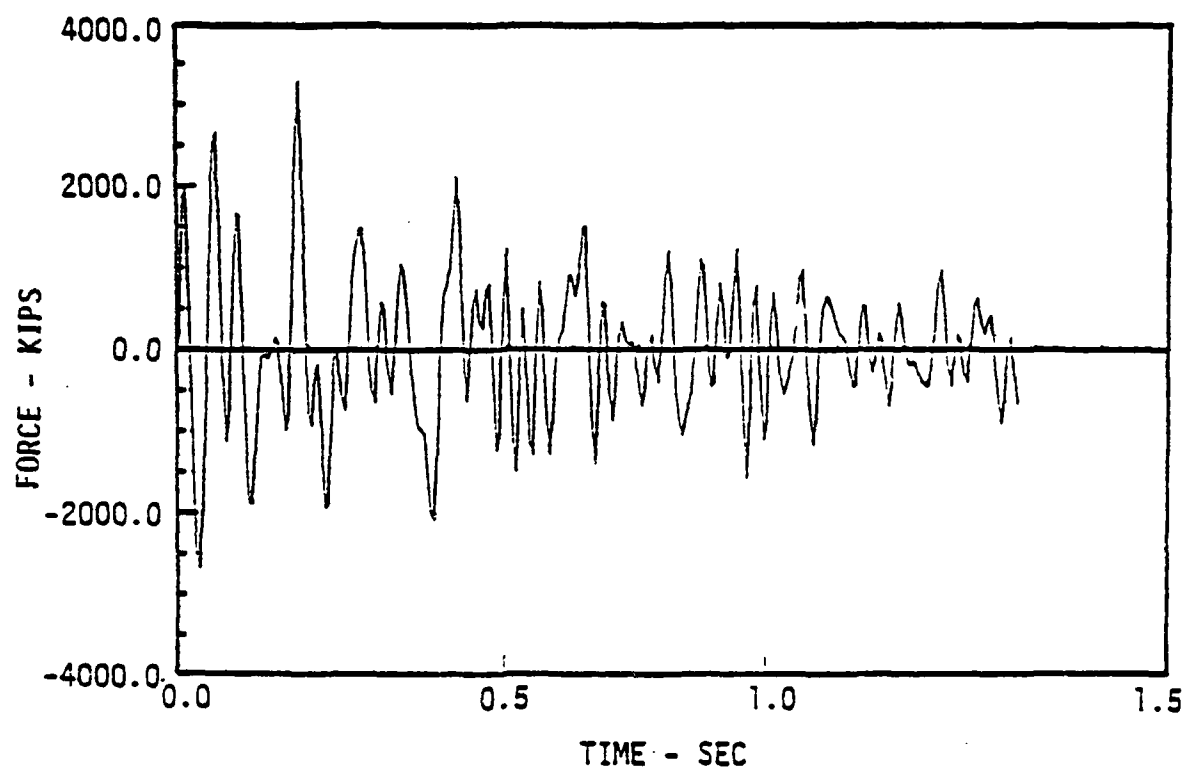


Figure 8-1a. Decaying exponential forcing function for Example 1.

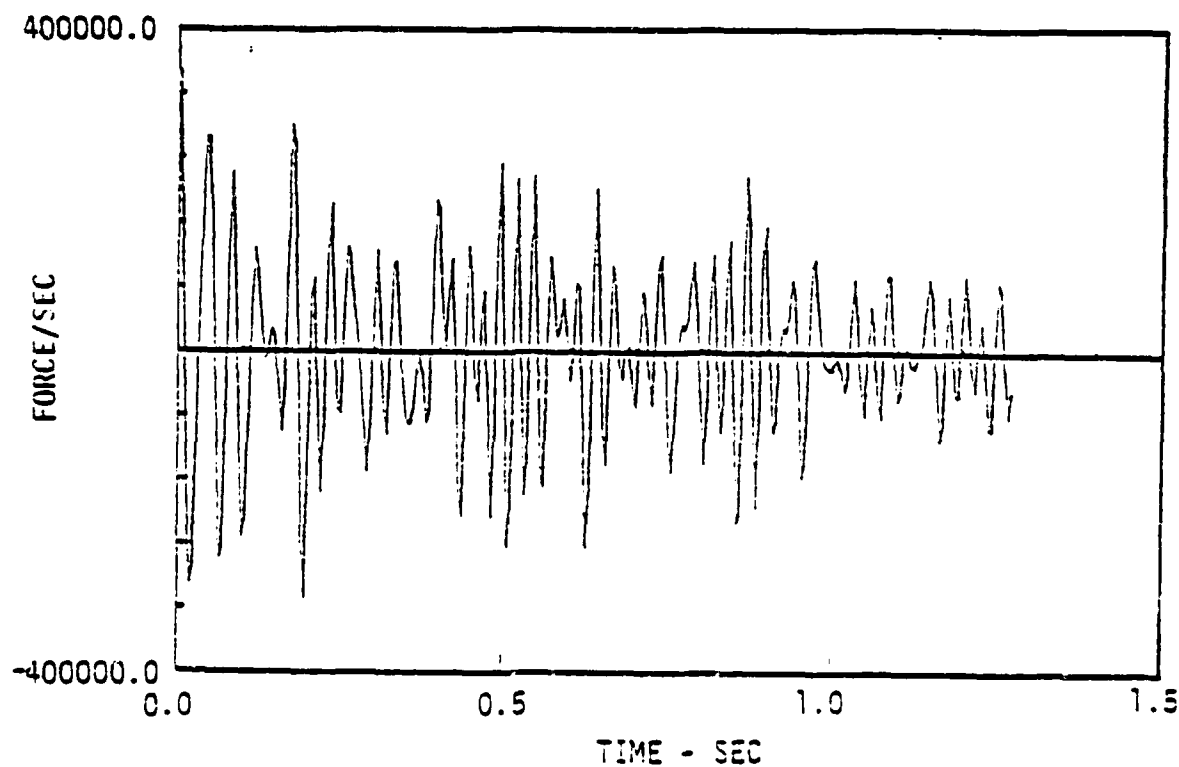


Figure 8-1b. Derivative of forcing function in Figure 8.1a.

For these two basic problems eight system identification problems are solved. In cases one and five, problem type one (above) is considered. In case one, a second order model ($M=0$), Equation 2-3) is identified. In case five, a third order model ($M=1$) is identified. In cases two through four and six through eight, problem type two (above) is considered. In cases two through four, a second order model ($M=0$) is identified. In cases six through eight, a third order model ($M=1$) is identified. The successive cases involve increasing degrees of yielding. In these eight cases, the parameters of the second order model, a_0 , a_1 , and a_2 ($M=1$) are identified.

Once the parameters of Equation 3-5 have been estimated, the energy dissipated by the model is computed; and this is compared to the energy dissipated by the actual system as computed in BILIN. This computation is the one discussed in Chapter 2 and given by Equation 2-7b. The energy computations are performed in programs ENER2, for second-order systems, and ENER3, for third-order systems. The computations are performed using an incremental form of the governing Equation 3-3.

The responses of some SDF systems to the shock input in Figure 8-1a were computed. First, the response of a linear system was computed for analysis in cases 1 and 5. The computed displacement response is plotted versus time in Figure 8-2a. The SDF structure spring restoring force versus displacement is plotted in Figure 8-2b. The very slightly nonlinear response of an SDF structure was computed for analysis in cases 2 and 6, but this response is not shown. A more nonlinear response was computed for analysis in cases 3 and 7. The displacement response versus time is plotted in Figure 8-3a, and the spring restoring force versus displacement is shown in Figure 8-3b. The first figure shows a residual plastic displacement as the

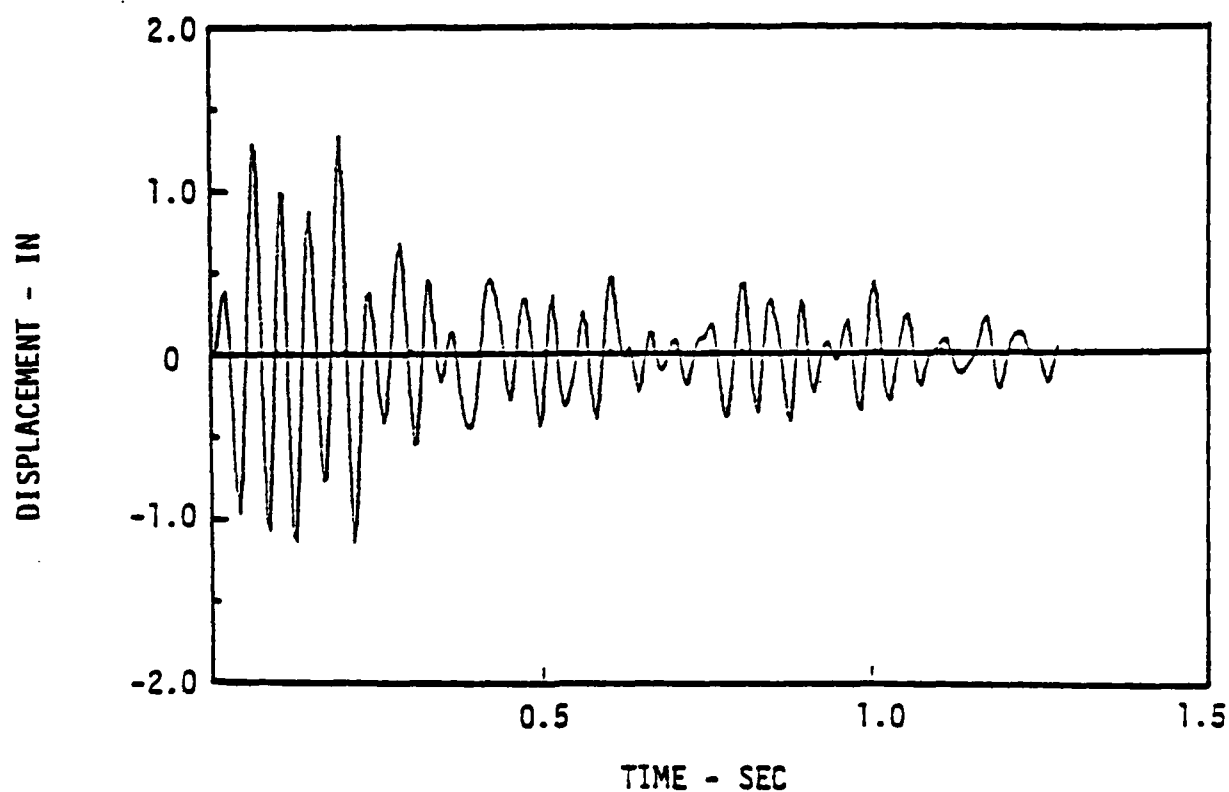


Figure 8-2a. Response of a linear system to the force in Figure 8-1a. $k = \infty$.

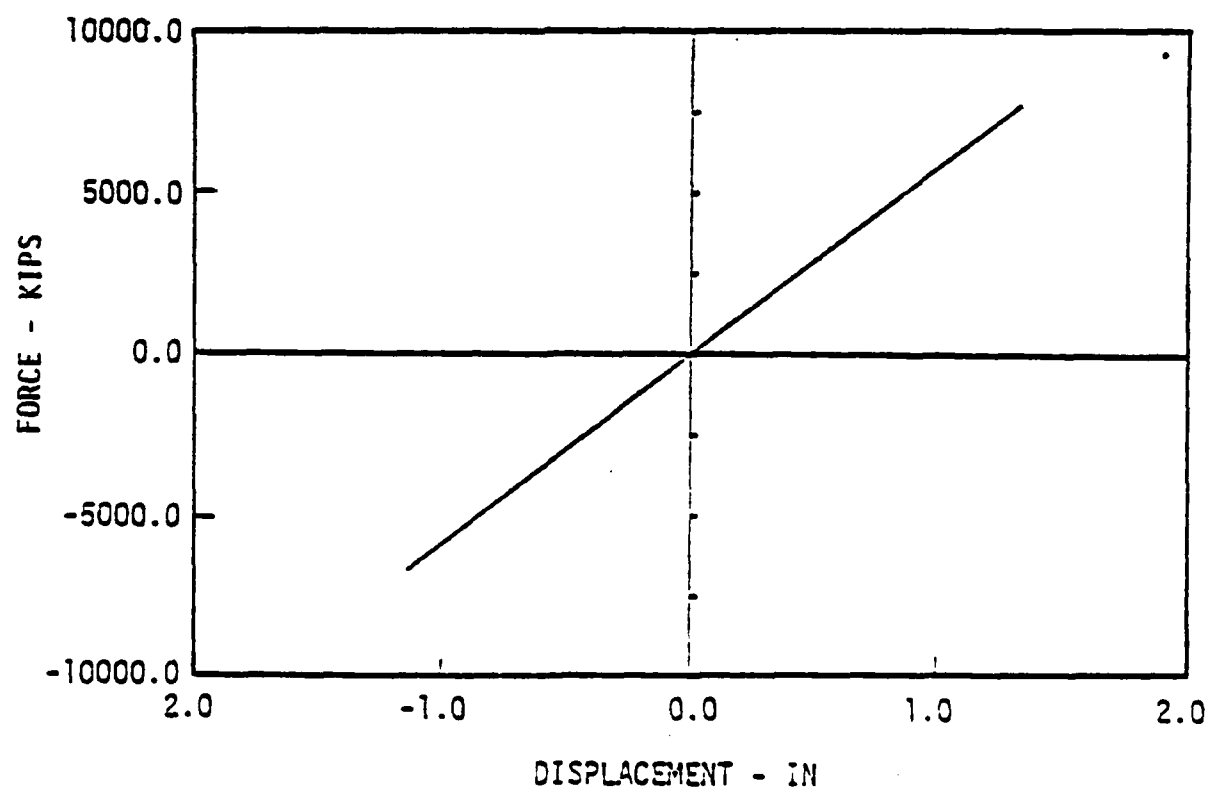


Figure 8-2b. Spring restoring force versus displacement for linear system.

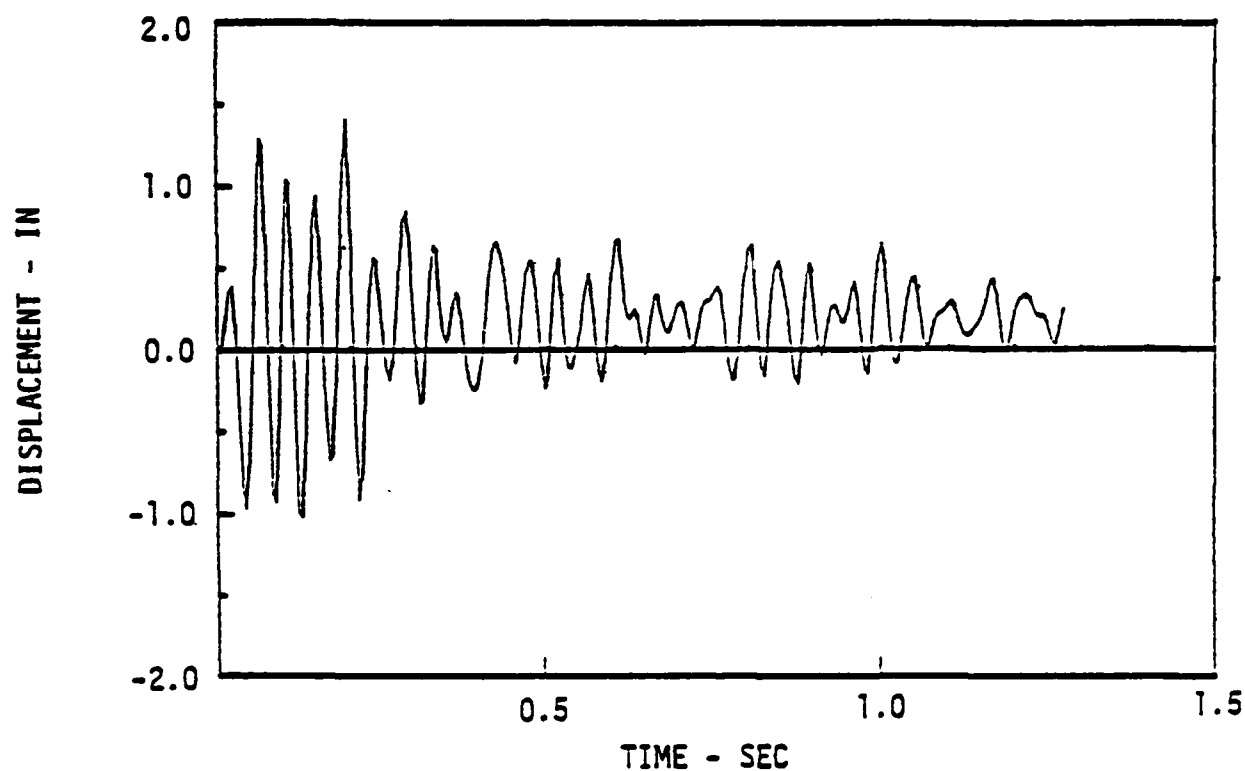


Figure 8-3a. Response of nonlinear system to the force in Figure 8-1a. $k_y = 7000$

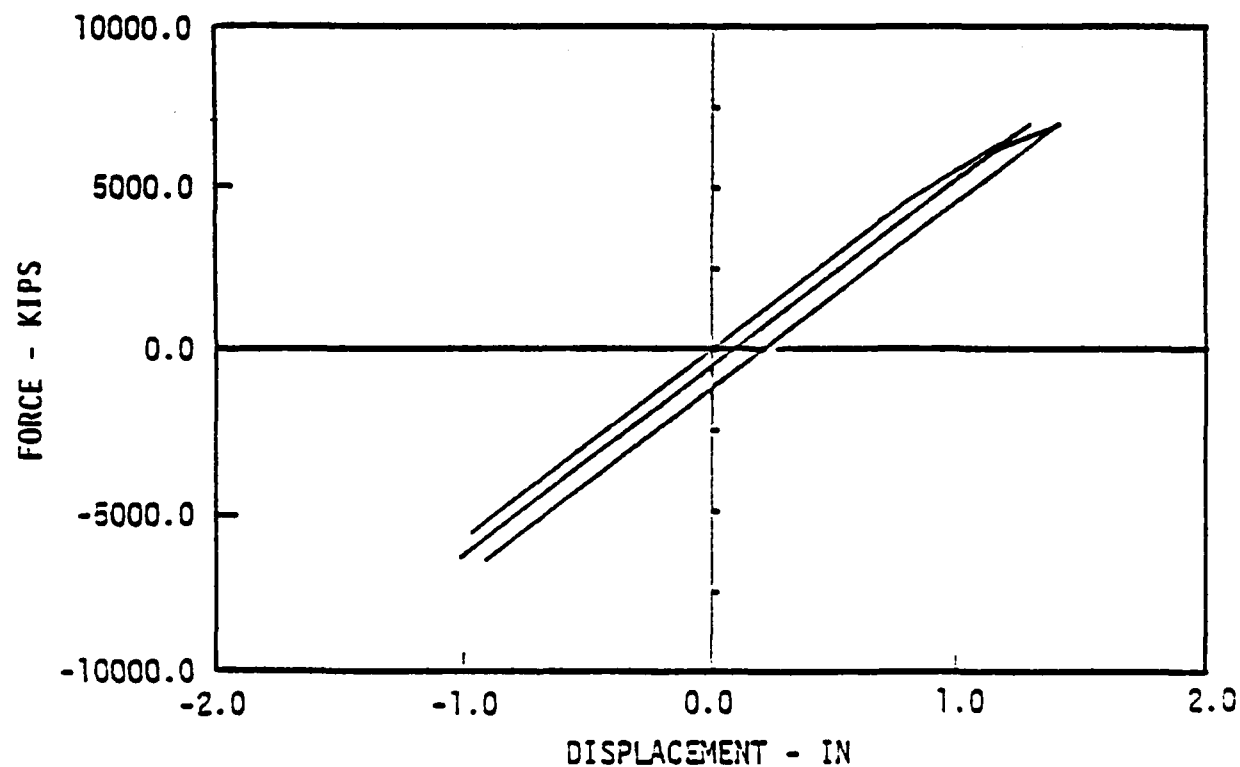


Figure 8-3b. Spring restoring force versus displacement for nonlinear system.

response vibrations diminish. The second graph shows the permanent set as lateral displacement of the horizontal axis intercept. Finally, a very nonlinear response was computed for analysis in cases 4 and 8. The displacement response versus time is shown in Figure 8-4a and the spring restoring force versus displacement is shown in Figure 8-4b. A considerable permanent set is evident, as the motion diminishes, from the first figure. The second figure shows that large plastic deformations occur in the structure in both directions of motion.

The energy dissipated by each structural system is listed with the structural parameters in Table 8.1. E_D is that energy dissipated due to the action of the inelastic spring and the action of the viscous damper.

Using the forcing function input described above, and the computed responses, the parameters of the structural systems were identified. The results of the parameter identifications are given in Table 8.1. The energy dissipated when the identified systems respond to the shock input is listed in Table 8.1 next to the identified parameters.

Figures 8-5a through 8-9b show the computed responses of some of the identified systems. The figure titles indicate which systems generate the responses shown. The top (or "a") figures show the computed responses versus time. The bottom (or "b") figures show the computed restoring forces, spring force plus damper force, versus displacements.

Figure 8-10 compares three responses. These are: 1) the actual nonlinear structural response obtained using BILIN in the slightly nonlinear cases 2 and 6, 2) the response executed by the identified model described in case 2, and 3) the response executed by the identified model described in case 6. The two latter responses practically overlay and very nearly equal the actual response.

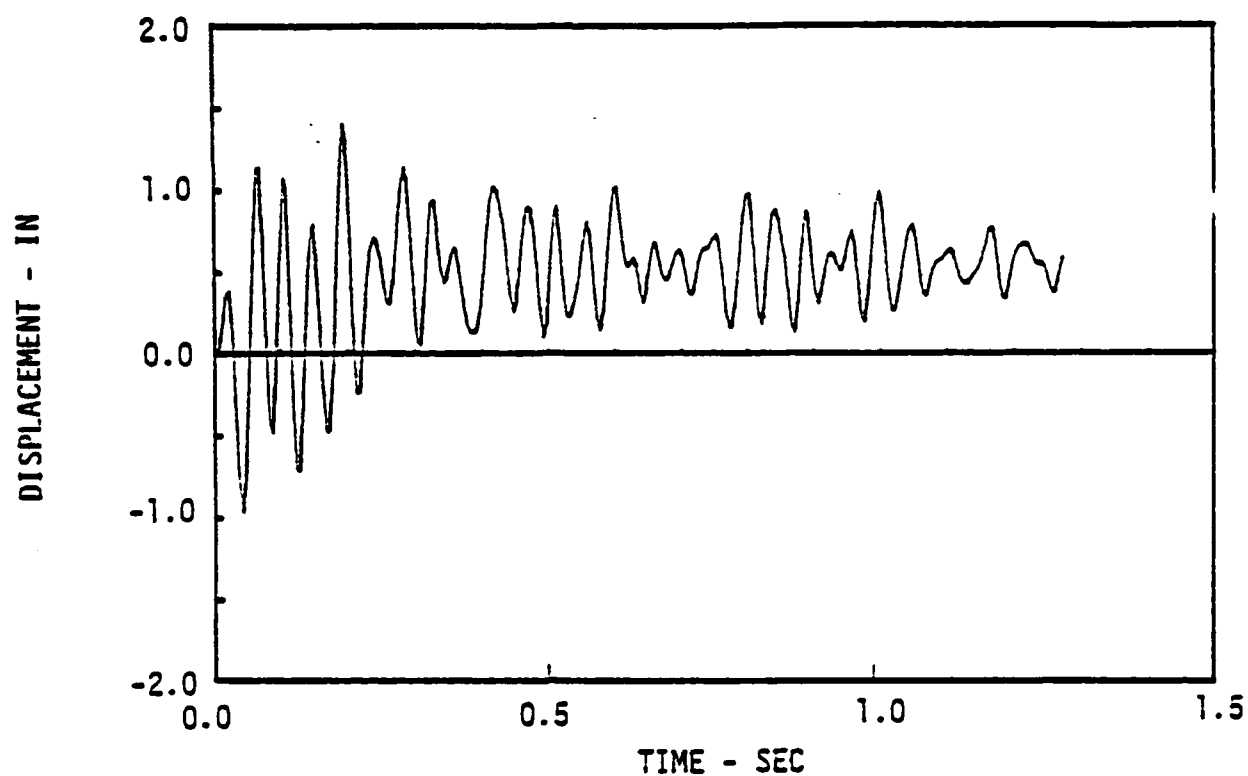


Figure 8-4a. Response of nonlinear system to the force in Figure 8-1a. $k_y = 5000$

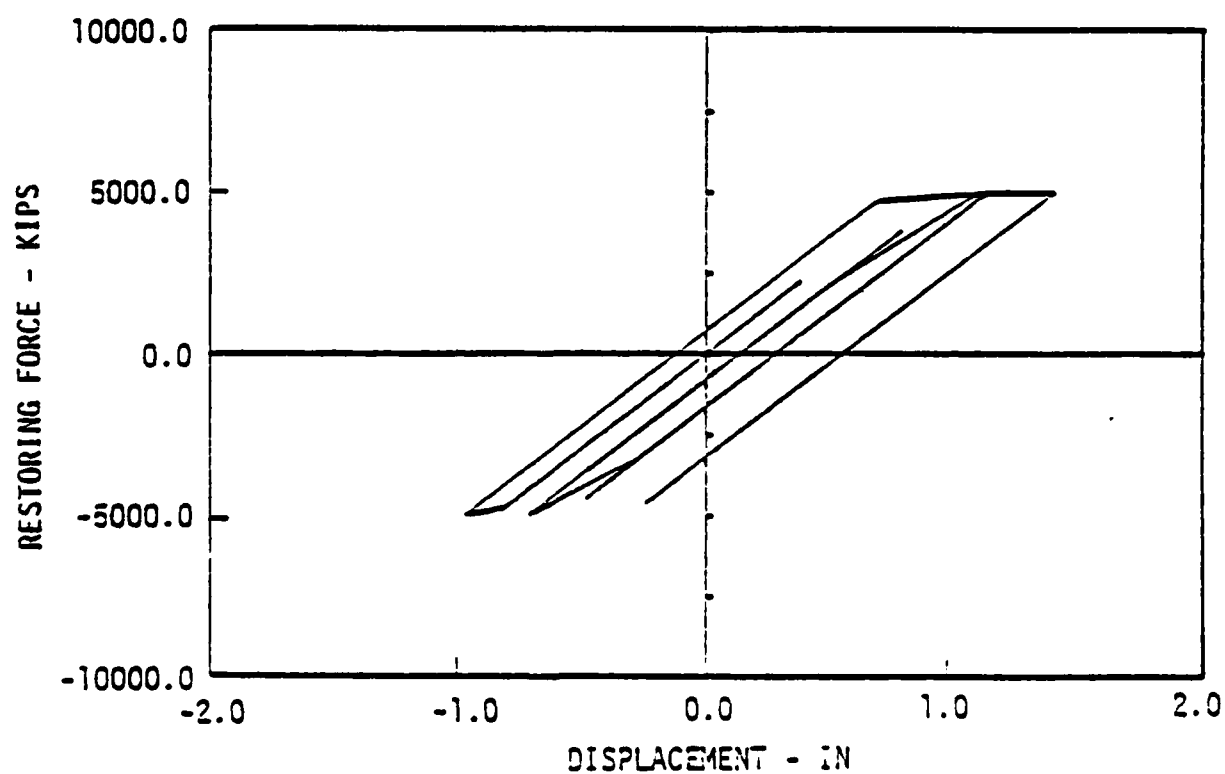


Figure 8-4b. Spring restoring force versus displacement for nonlinear system.

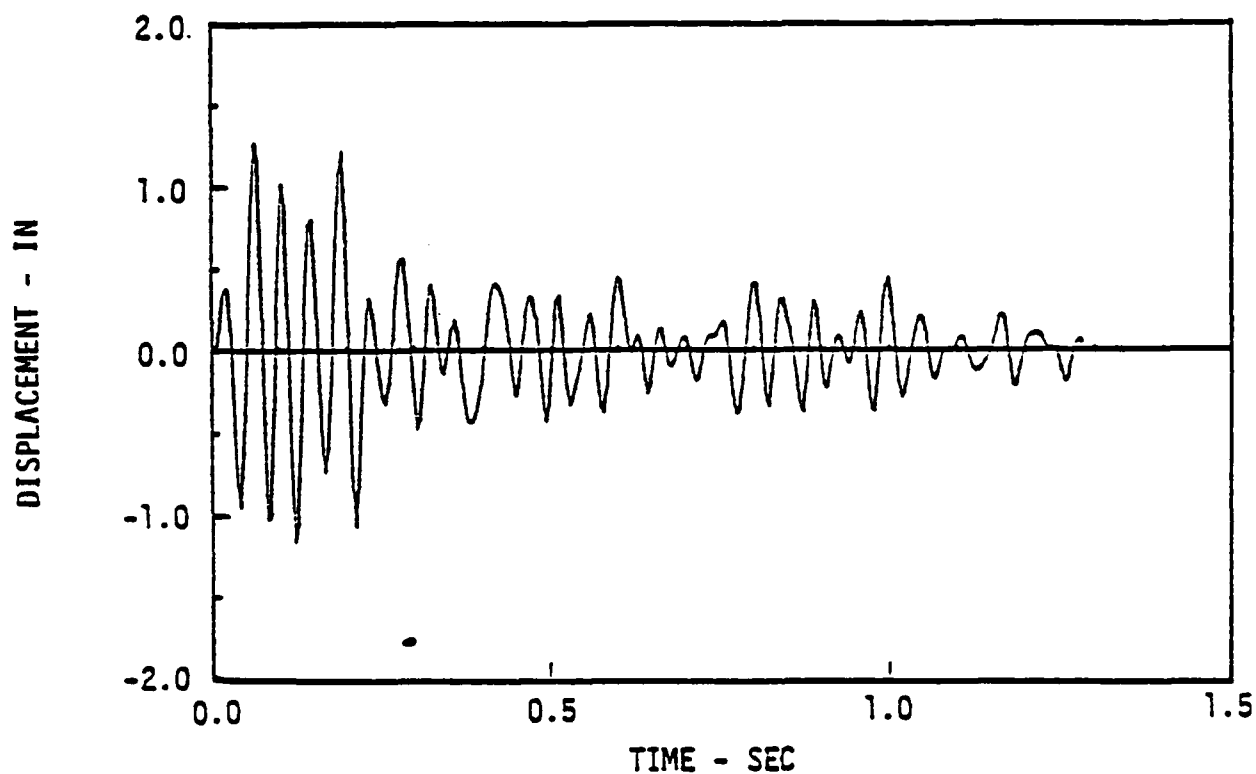


Figure 8-5a. Displacement response of identified system to force in Figure 8-1a. (Case 2)

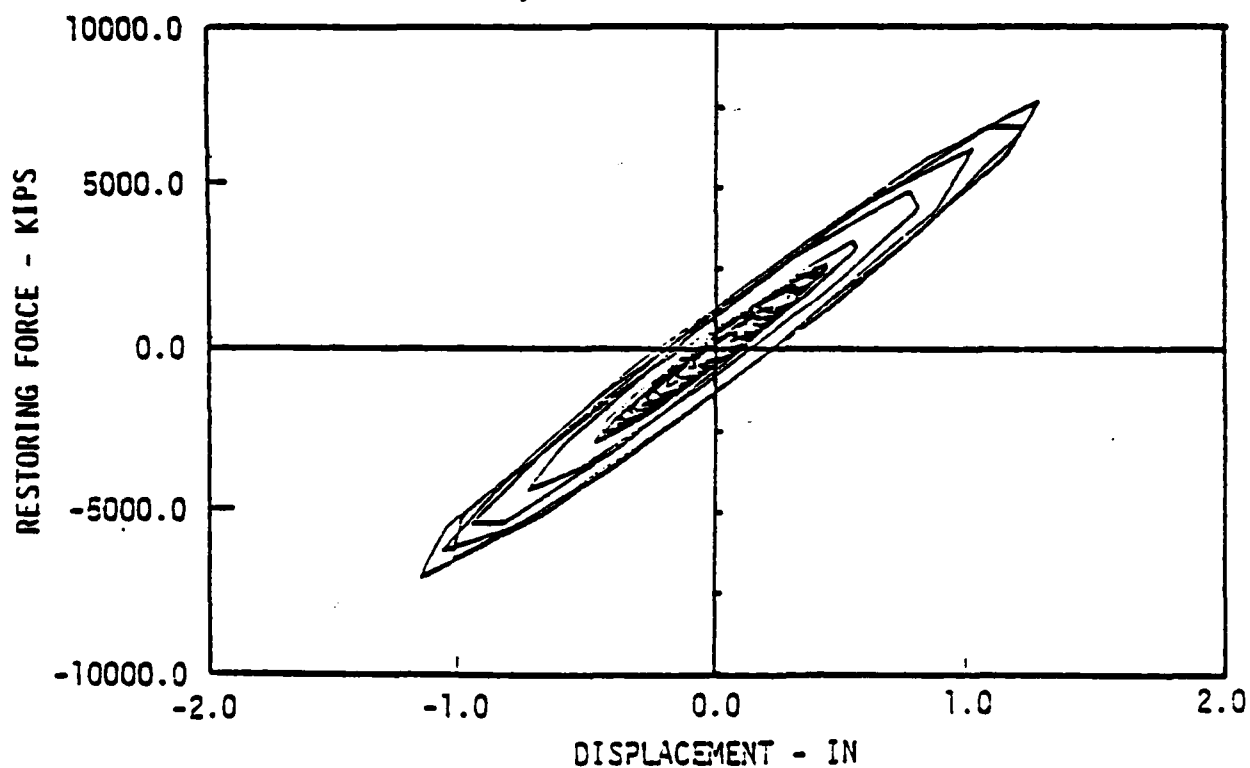


Figure 8-5b. Spring plus damper restoring force versus displacement for identified system. (Case 2)

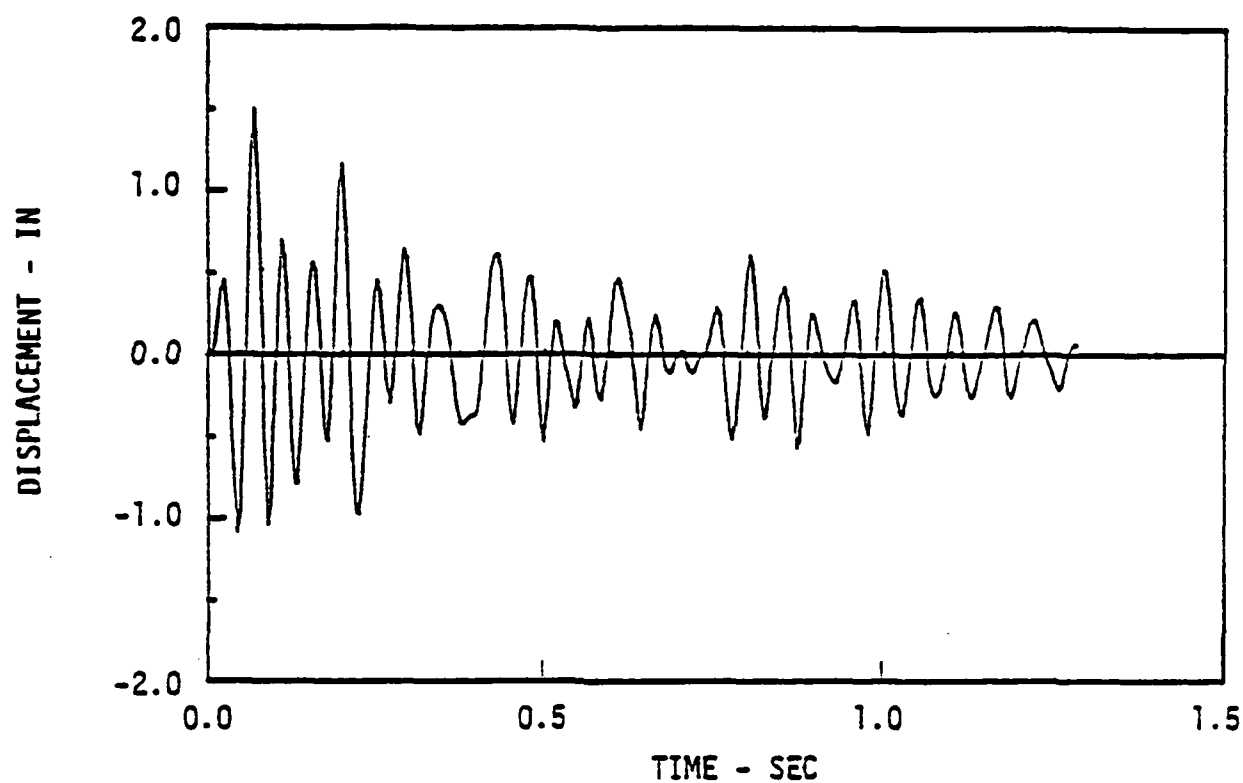


Figure 8-6a. Displacement response of identified system to force in Figure 8-1a. (Case 3)

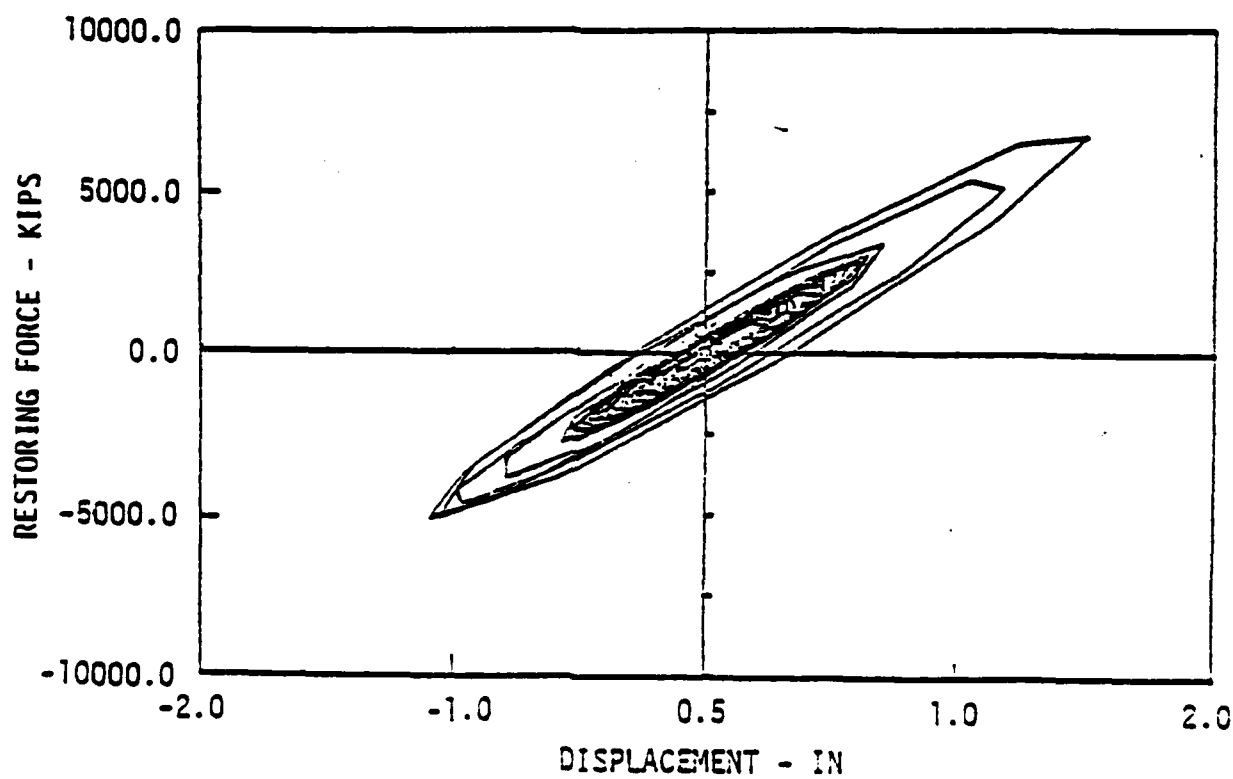


Figure 8-6b. Spring plus damper restoring force versus displacement for identified system. (Case 3)

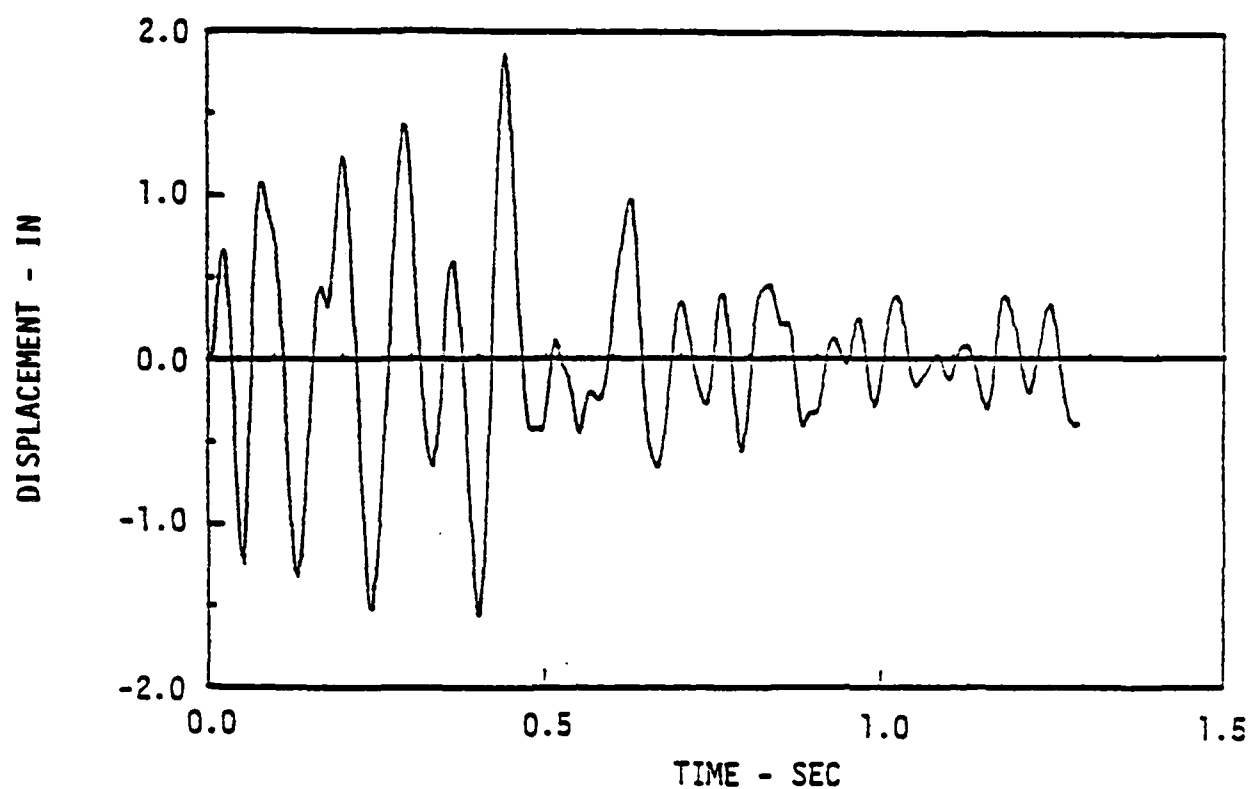


Figure 8-7a. Displacement response of identified system to force in Figure 8-1a. (Case 4)

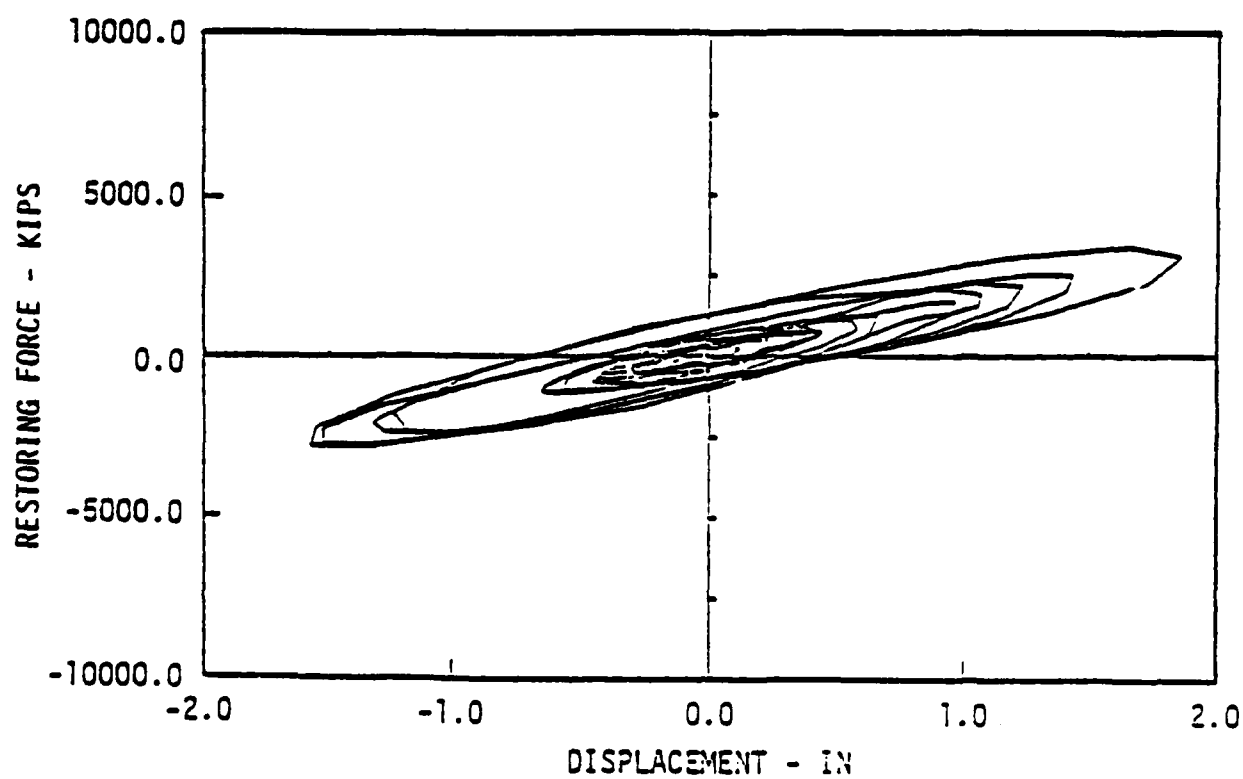


Figure 8-7b. Spring plus damper restoring force versus displacement for identified system. (Case 4)

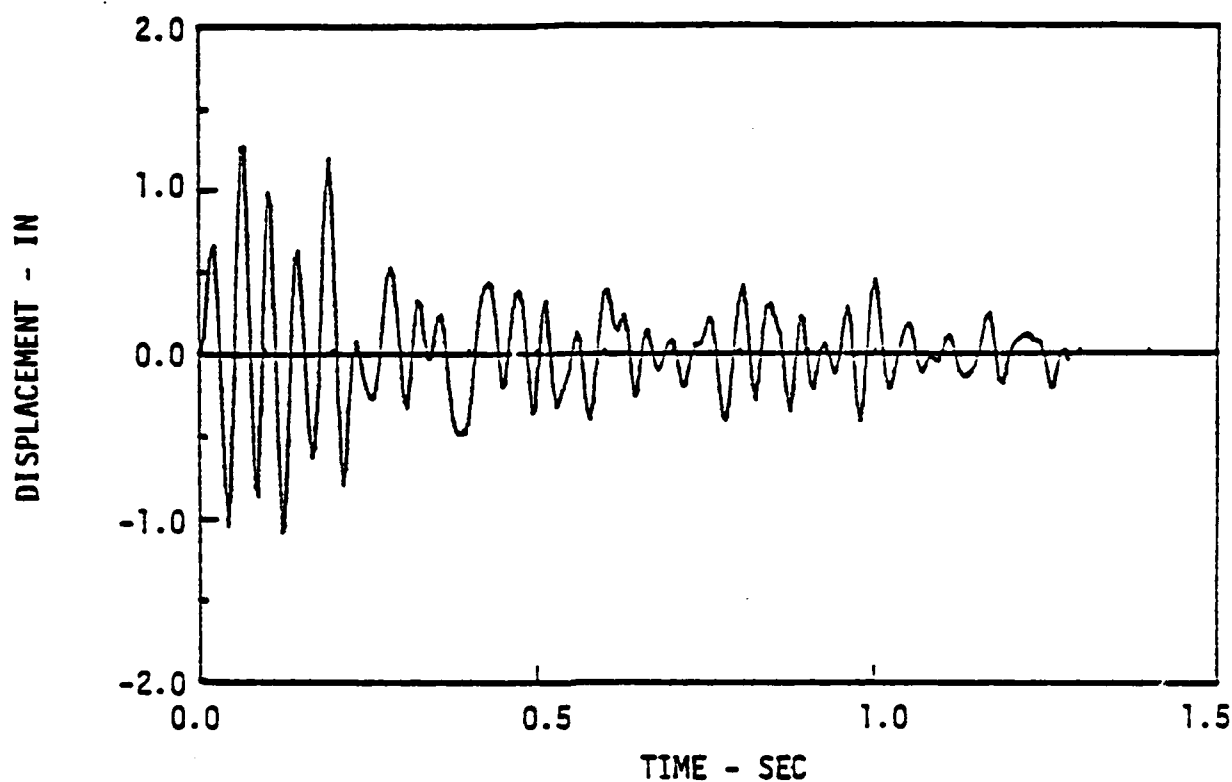


Figure 8-8a. Displacement response of identified system to force in Figure 8-1a. (Case 7)

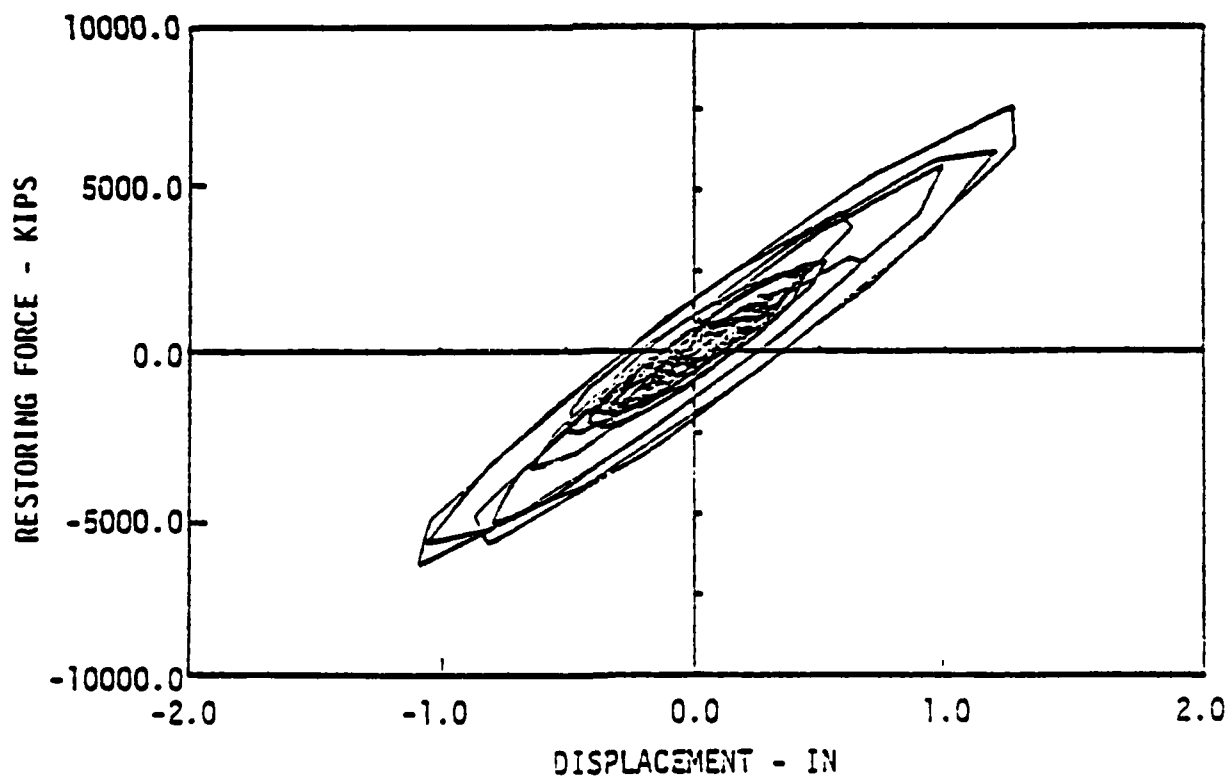


Figure 8-8b. Total restoring force versus displacement for identified system. (Case 7)

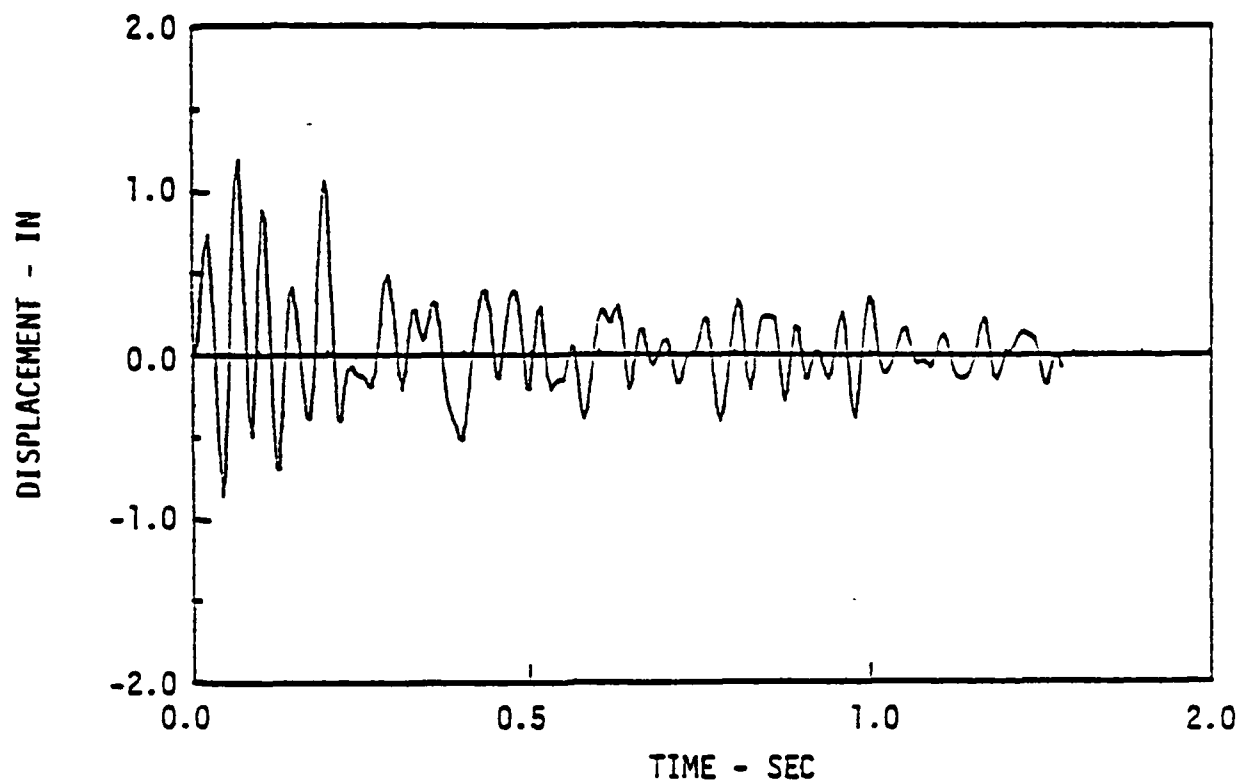


Figure 8-9a. Displacement response of identified system to force in Figure 8-1a. (Case 8)

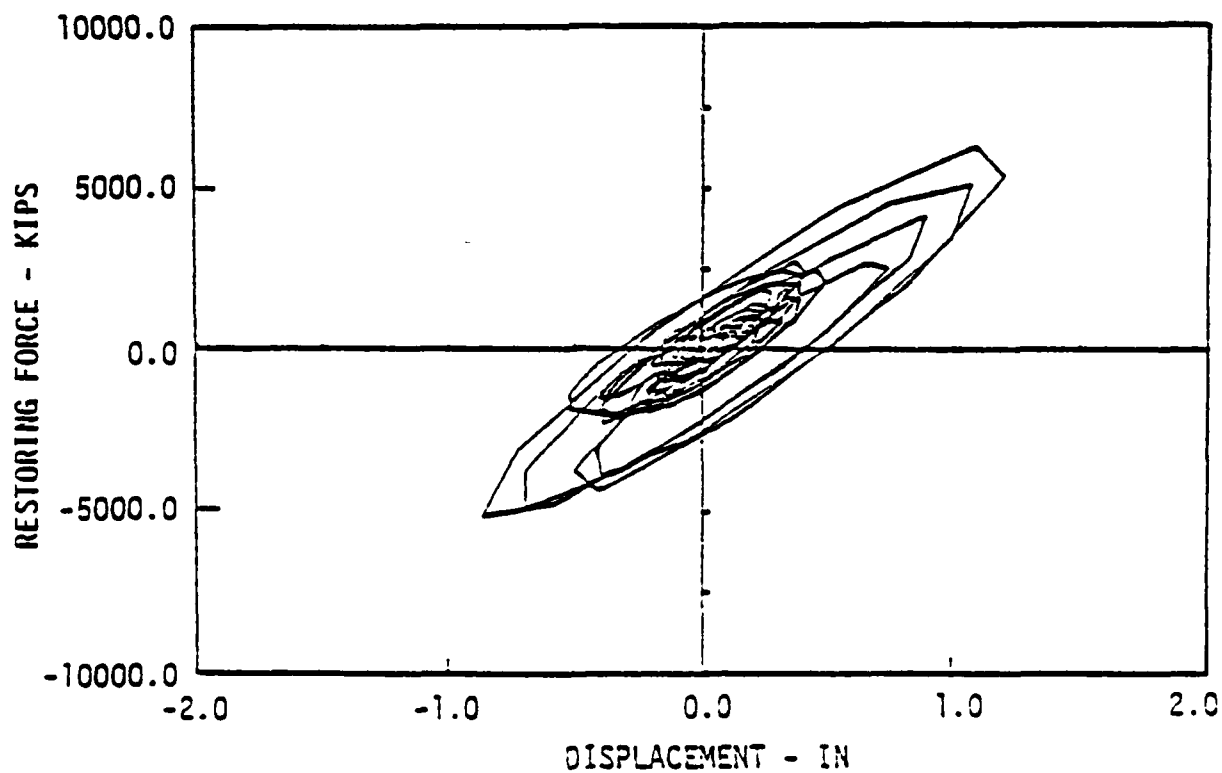


Figure 8-9b. Total restoring force versus displacement for identified system. (Case 8)

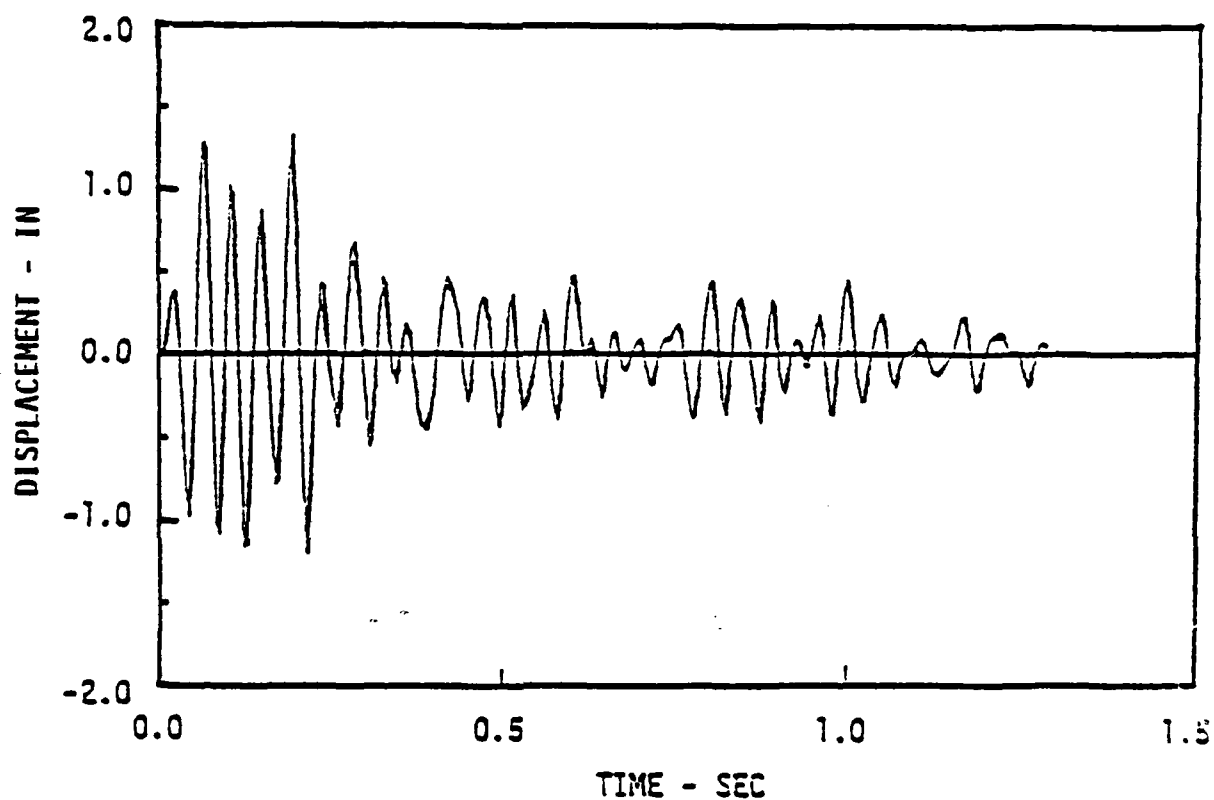


Figure 8-10. The comparison between measured response (light line) and identified response (dark line) for both second-order (case 3) and third-order (case 7) approximate systems. (The identified responses are practically the same.)

TABLE 8.1. PARAMETERS AND RESULTS FOR EXAMPLE 1

Input (Structural Excitation)

Case Number	N	α	c	ω_1	ω_N	n	Δt
1 through 8	50	1.0	300	32.4	1256.4	256	0.005

Structure Parameters

Case Number	m	c	k	k_y	z_y	E_D
1,5	0.259	7.77	5829	-	∞	23292
2,6	0.259	7.77	5829	0	7700	23588
3,7	0.259	7.77	5829	0	7000	23674
4,8	0.259	7.77	5829	0	5000	21959

Identification Parameters and Results

Case Number	M	a_0	a_1	a_2	E_D
1	2	5829	7.77		21533
2	2	5825	7.79		21533
3	2	4574	8.13		21779
4	2	1620	9.69		23844
5	3	5829	7.77	0.0	21533
6	3	5823	7.85	0.0	21498
7	3	2527	99.65	0.0158	20824
8	3	610	108.11	0.0175	18666

Figure 8-11a compares the actual nonlinear response of cases 3 and 7 to the second-order ($M=0$) model response of case 3. Figure 8-11b compares the actual nonlinear response of cases 3 and 7 to the third-order ($M=1$) model response of case 7. Both models simulate response amplitudes quite well; the third-order model is slightly closer than the second-order model in that the third-order model provides a slightly better phase match to the actual response than the second-order model.

In this numerical example, no cases are included where noise was added to the forcing function input and/or the acceleration response. Such cases were analyzed, but the results were so poor that they are not summarized here. These results showed that the direct, time domain parameter identification technique is not effective in parameter analysis when recording noise is present.

The numerical examples summarized here show that the direct, time domain parameter identification technique can be used effectively when the measured signals are noise free. This is best confirmed by reference to Figures 8-10, 8-11a, and 8-11b. These show that the linear model response can be made to match the nonlinear response well.

The energy dissipation results, summarized in Table 8.1, show that the third-order models provide the best simulation for a nonlinear hysteretic system.

8.2 Example 2.

In this example, a sequence of parameter identification problems is solved using the frequency domain approach. Three programs, FREQID, PUR3, and PUR, were written to execute the parameter identifications.

FREQID performs approximate frequency domain parameter identification for second and third order linear models. It

AD-A136 342

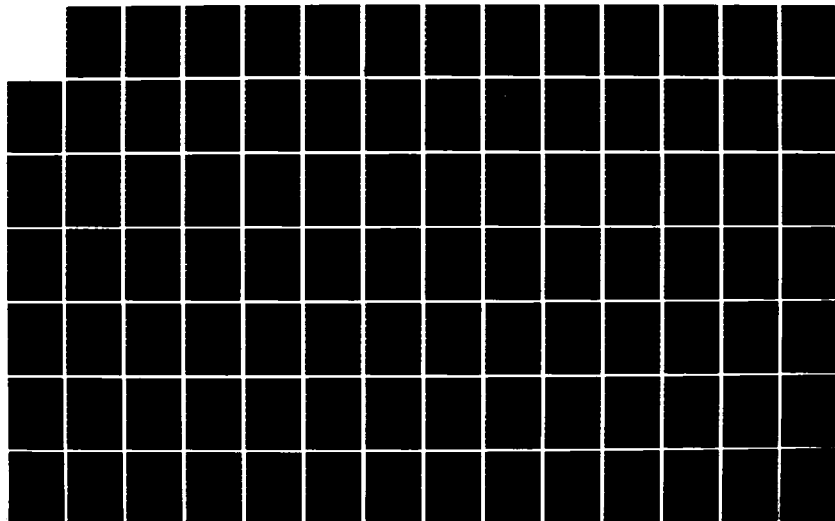
IDENTIFICATION OF DAMAGE IN HYSTERETIC STRUCTURES(U)
NEW MEXICO UNIV ALBUQUERQUE DEPT OF CIVIL ENGINEERING
M L WANG ET AL. JUL 83 AFOSR-TR-83-1230 AFOSR-81-0086

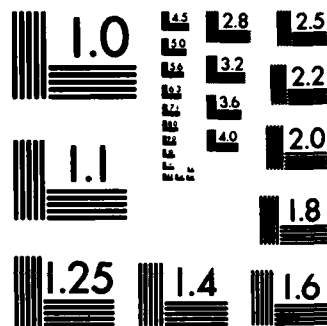
2/3

UNCLASSIFIED

F/G 13/13

NL





MICROCOPY RESOLUTION TEST CHART
NATIONAL BUREAU OF STANDARDS-1963-A

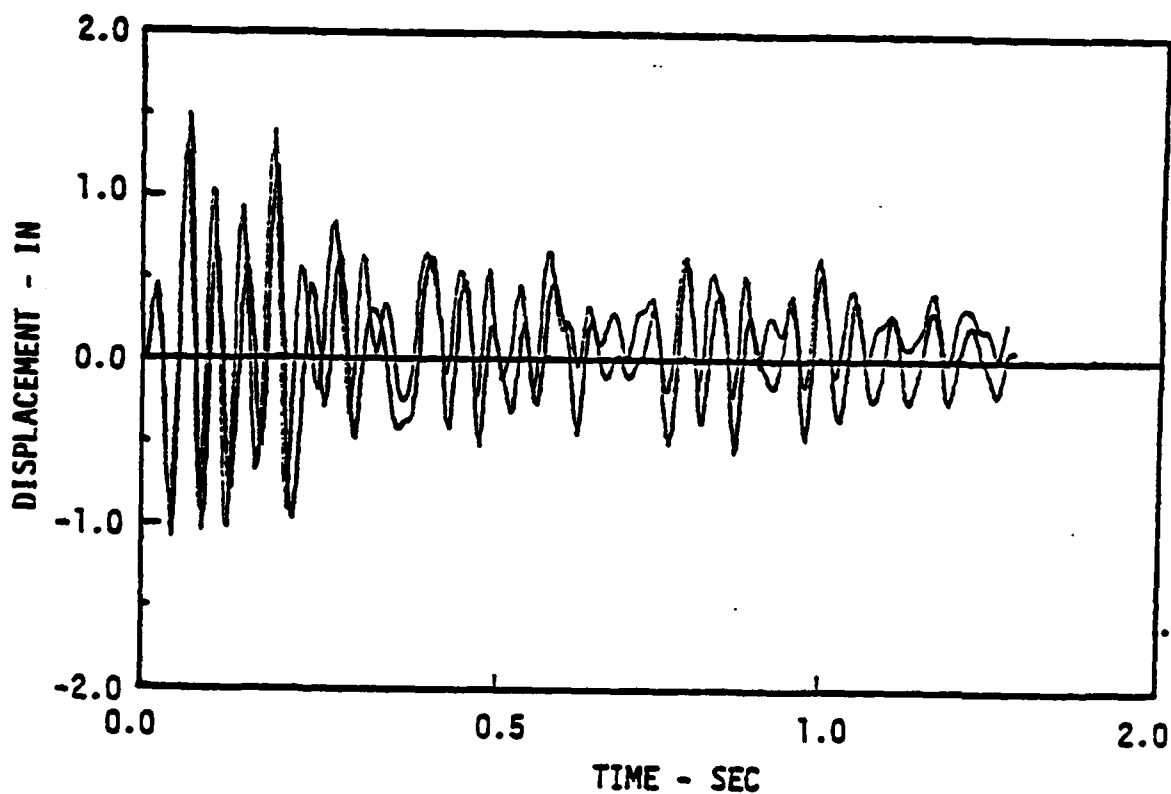


Figure 8-11a. The comparison between measured response (light line) and identified response for second-order system. (Case 3)

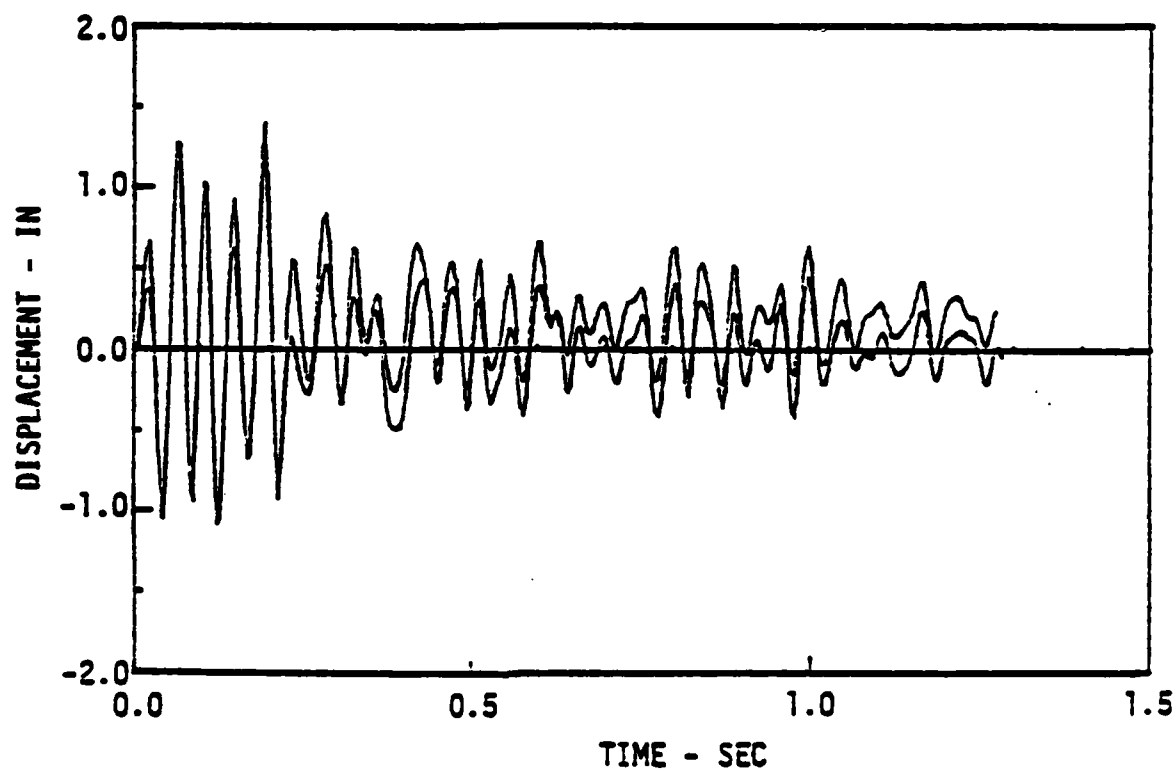


Figure 8-11b. The comparison between measured response (light line) and identified response for third-order system. (Case 7)

accepts both an input signal from FORCE and a response signal from BILIN or TIMEVA. When desired, the white noise signals are added to the corresponding input data. Then FREQID performs the necessary Fourier transforms and other data operations. Following this, the parameter identification is executed. One operation required in the parameter identification is estimation of the characteristic frequency. This can be done simply by searching $Q(\omega) + \epsilon(\omega)$ for a minimum value. However, a more precise method for determining the minimum value of $Q(\omega) + \epsilon(\omega)$ defined in Equations 4-8 and 4-11 involves use of a least square method. In this improved method, $Q(\omega) + \epsilon(\omega)$ is used to identify the characteristic frequency and other parameters.

In FREQID, an important assumption was made for the third-order model, Equation 4-21. In particular, it was assumed that a_2 is small in value. The parameters of this model may be identified, without the assumption that a_2 is small, by the search technique. The computer program PUR3 was written for this purpose. A detailed description of this method was given in Chapter 5.

Program PUR performs parameter identification for second-order time varying linear systems. The approach is based on the procedure described in Chapter 5. The program accepts the inputs and responses generated in the programs FORCE and BILIN or TIMEVA, with or without noise. Four parameters, namely k_0 , α , c_0 , and β are identified. The program employs a search technique; the initial estimators can be chosen by using the identified parameters obtained from any of the methods.

Once the parameters have been estimated, the energy dissipated by the model is computed. This result together with the predicted response is compared to both the energy dissipated and the response of the actual system. The energy and response

computations are performed in program ENER2 and ENER3 for the second and third order system, respectively.

From the above description, the methods used in the determination of the system parameters can be summarized as follows:

- Method 1. Performs parameter identification for the second-order system in the frequency domain utilizing Equation 4-15. No fitting equation for $Q(\omega) + \epsilon(\omega)$ is applied.
- Method 2. Performs parameter identification for the third-order system in the frequency domain utilizing the equations from 4-29a to 4-31. No fitting equation for $Q(\omega) + \epsilon(\omega)$ is applied.
- Method 3. Performs parameter identification using the same approach as Method 1 except the input data $Q(\omega) + \epsilon(\omega)$ are replaced by the fitted polynomial equation. This additional analysis is done in a subroutine called FIT.
- Method 4. Performs parameter identification using the same approach as Method 2 and using the same procedure described in Method 3.
- Method 5. Performs parameter identification for the third-order system using the search method described in Chapter 5. The operation is executed in a program called PUR3. Prior estimates obtained from the above methods are used.
- Method 6. Performs parameter identification for the second-order time-varying parameter system in the frequency domain. The search method described in Chapter 5 is used. This method also requires prior estimators which can be obtained from the information supplied in Methods 1 through 5.

All the methods described above can be used to estimate the parameters for the linear and nonlinear systems even when noise is present. The duration of the excitation must be long enough to characterize the system parameters.

In the following numerical examples, four basic problems are solved. These cases involving different degrees of nonlinearity in the system response are summarized below.

- Case 1. An input excitation is generated using Equation 8-1. The input is used to excite a linear SDF system with viscous damping. The excitation and linear response are used to identify the model parameters. Noise signals can be added to the generated input and response, if required.
- Case 2. An excitation input is generated as in Case 1, but here the response of a bilinear hysteretic system is computed. Yielding occurs in the response. The degree of nonlinearity was designed using a comparison between the yield displacement of the bilinear system and the maximum displacement of the linear system. Let the yield displacement of the bilinear system be z_y . Let the maximum displacement of the linear system be z_{max} . In this case, z_{max} is taken as 6.7 and z_y is equal to 6.0.
- Case 3. Same as Case 2, but z_y is equal to 5.0.
- Case 4. Same as Case 2, but z_y is equal to 4.0.
- Case 5. An input excitation is generated as in Case 1. The input is used to excite a linear SDF system with time varying damping and stiffness. The excitation and response are used to identify the model parameters. Noise signals are added to the simulated input and response when required.

The example carries out the parameter identification using the methods described above. Specifically, methods 1 through 6 are used to identify the parameters. The parameters of the input excitation are listed in Table 8.2. The notation for the parameters was specified above.

TABLE 8.2. PARAMETERS OF THE FORCING FUNCTION

$$\begin{aligned}\alpha &= 0.1 & N &= 50 & c_j &= 10.0 & j &= 1, \dots, 50 \\ \omega_j &= (1.8 + 0.008j)\pi, & j &= 1, \dots, 50 \\ \Delta t &= 0.05 & n &= 1024\end{aligned}$$

A typical forcing function history generated by using these parameters is shown in Figure 8-12. Actual forcing functions measured in the field usually contain a certain amount of noise. Inputs with noise to signal ratios of six and eight percent are shown in Figures 8-13 and 8-14, respectively.

The response of some SDF systems to the forcing input were computed. The energy dissipated in each structure is listed with the structural parameters in Tables 8.3A and 8.3B. All cases were described above. The notation of the system parameters is as follows: k is the initial stiffness; c is viscous damping; k_y is the yield stiffness; z_y is the yield displacement; z_{\max} is the maximum displacement of an SDF system; m is the mass of the SDF structure.

TABLE 8.3A. SYSTEM PARAMETERS

$$\begin{aligned}k &= 39.48 & c &= 1.257 & m &= 1.0 \\ z_{\max} &= 6.7 & k_y &= 0.0 & \Delta t &= 0.05 & n &= 1024\end{aligned}$$

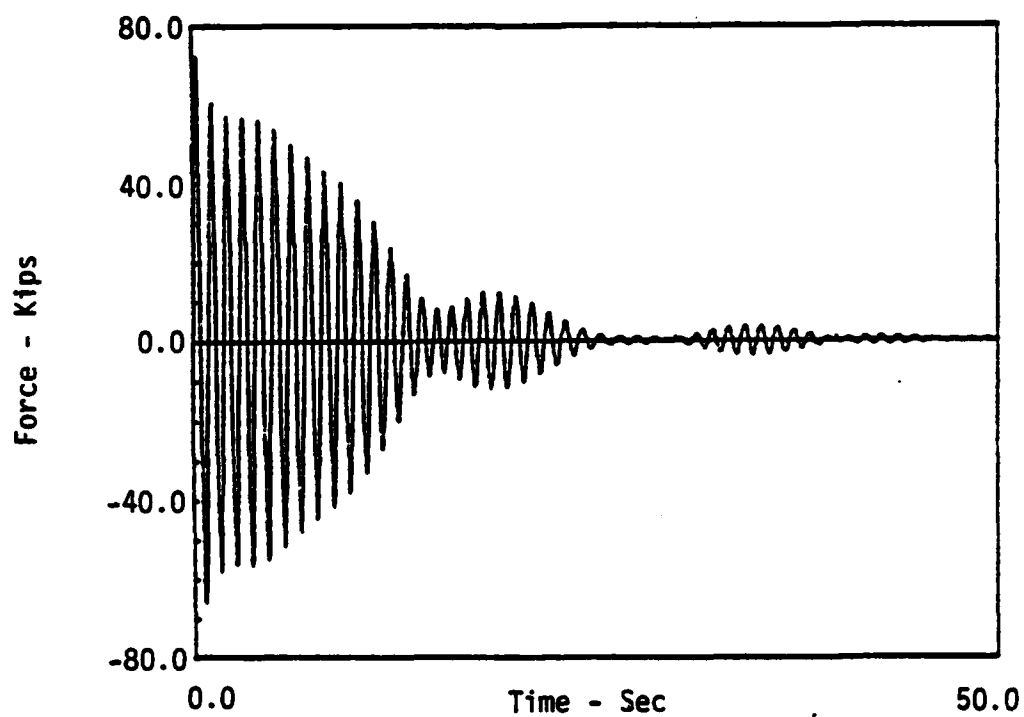


Figure 8-12. Signal used to simulate the actual input in Examples 2 and 3.

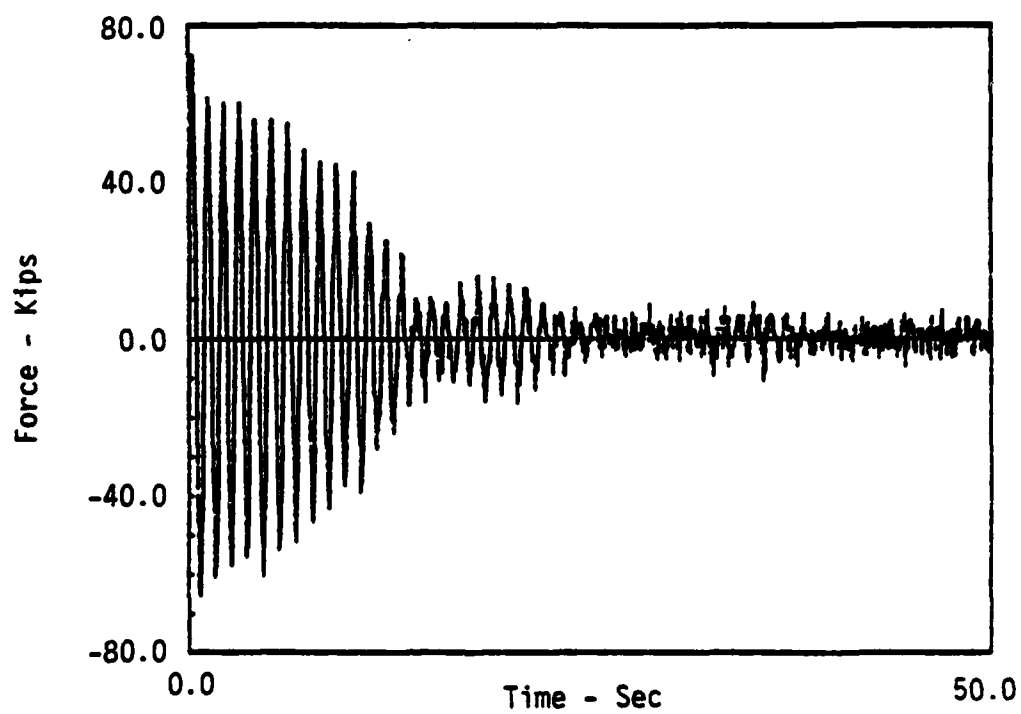


Figure 8-13. Signal used to simulate the measured input. (Includes 6% noise)

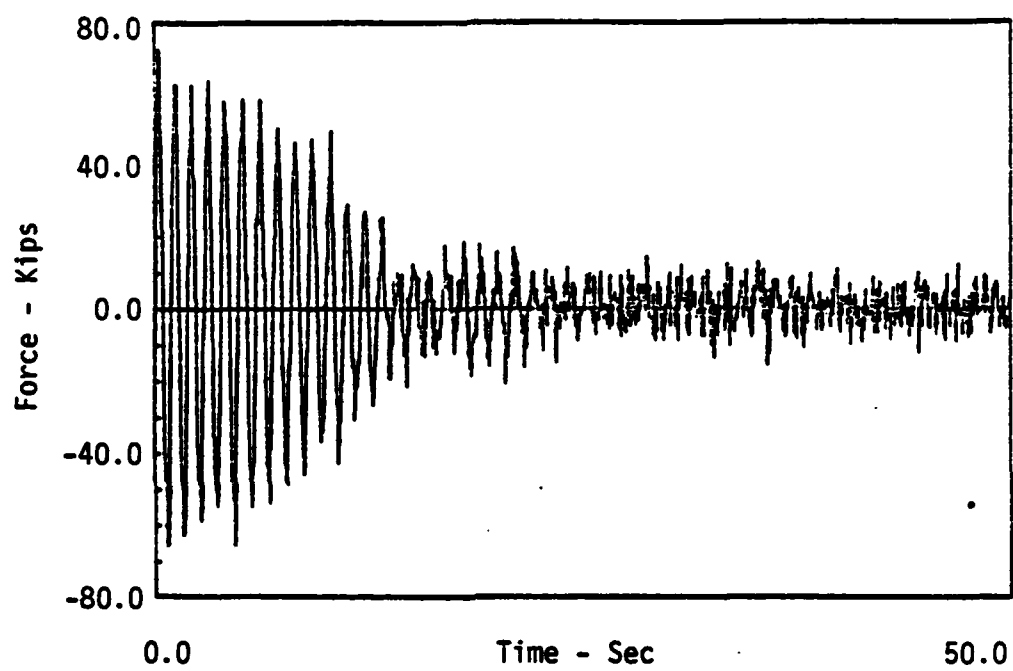


Figure 8-14. Signal used to simulate the measured input. (Includes 10% noise)

TABLE 8.3B. ENERGY DISSIPATION FOR CASE 1 THROUGH CASE 4

Cases	z_y	Damping Energy Dissipated	Spring Energy Dissipated	Total Energy Dissipated
Case 1	∞	11028.20	0.0	11028.2
Case 2	6	10199.30	405.21	10604.0
Case 3	5	8364.27	1186.74	3551.0
Case 4	4	6300.53	1924.48	8225.0

First, the response of a linear system (case 1) was computed. Then, a slightly nonlinear response of an SDF structure was computed for analysis in case 2. The displacement response versus time for case 2 is plotted in Figure 8-15. The spring restoring force versus displacement is shown in Figure 8-16. A small plastic deformation is shown. The total restoring force versus displacement is plotted in Figure 8-17. The measured responses for case 2 with a certain amount of noise are plotted in Figures 8-18 and 8-19. Figure 8-18 shows a measured signal with six percent noise to signal ratio. Figure 8-19 shows a measured signal with ten percent noise to signal ratio. Two more severe nonlinear responses were computed for analysis in cases 3 and 4.

The displacement response versus time for case 4 is plotted in Figure 8-20, and the measured response for case 4 with ten percent noise to signal ratio is shown in Figure 8-21. The spring restoring force versus displacement is shown in Figure 8-22. A considerable permanent set is evident in Figure 8-20. Figure 8-22 shows that plastic deformation occurs in the structure in both directions of motion.

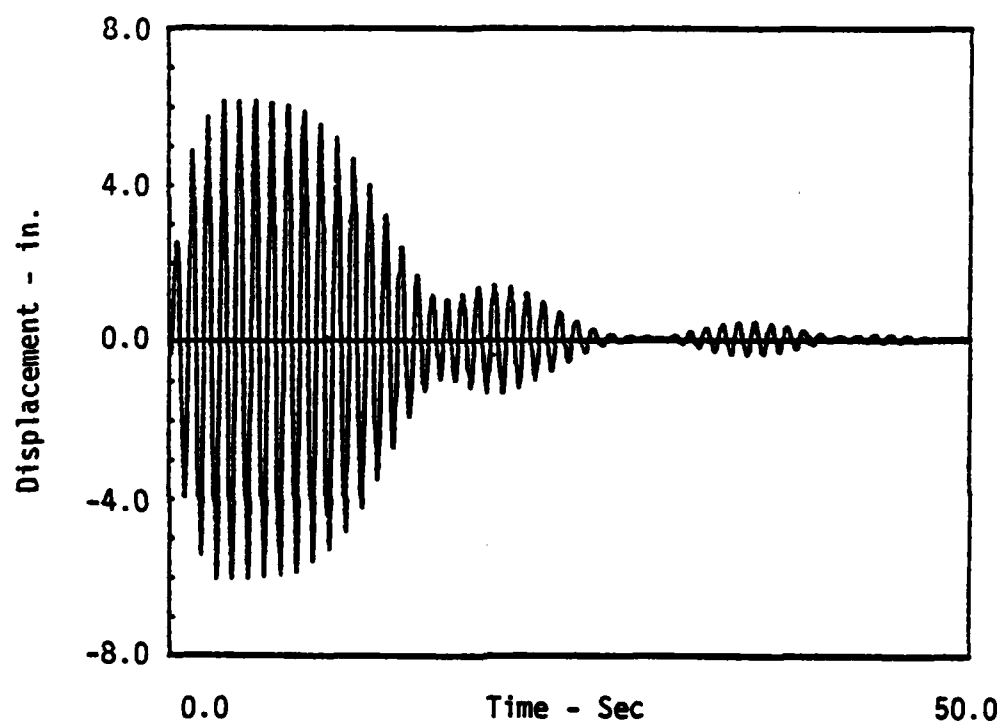


Figure 8-15. Displacement response of nonlinear SDF system to force in Figure 8-12. (Case 2)

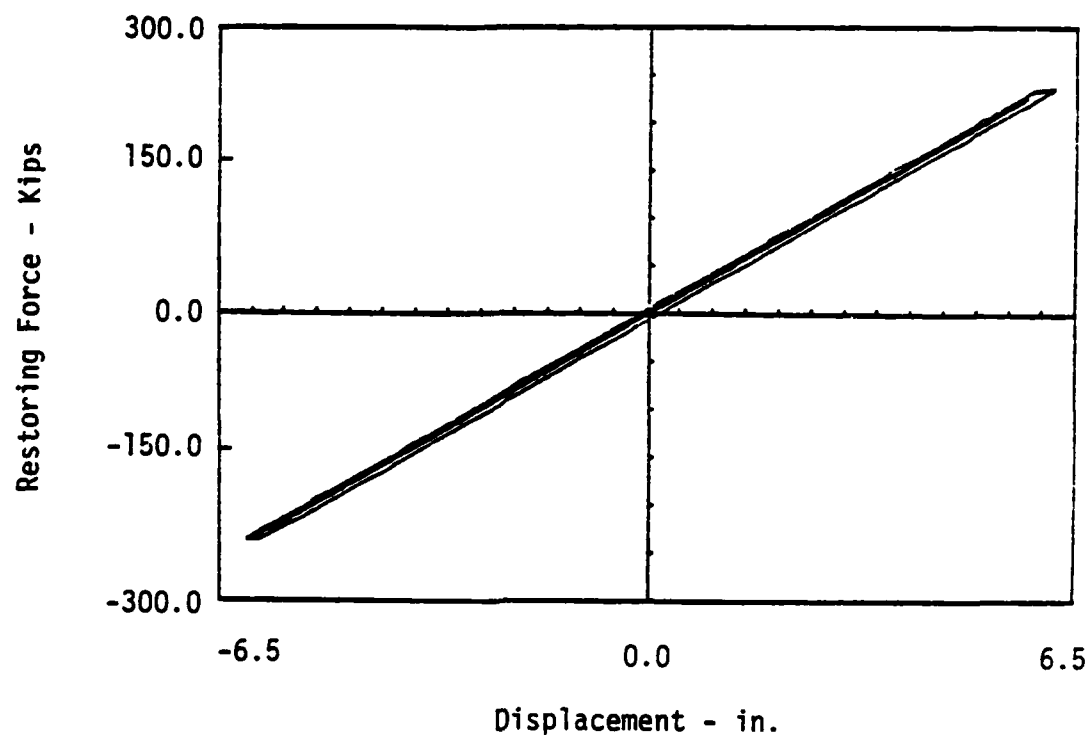


Figure 8-16. Spring restoring force versus displacement for nonlinear system (Case 2)

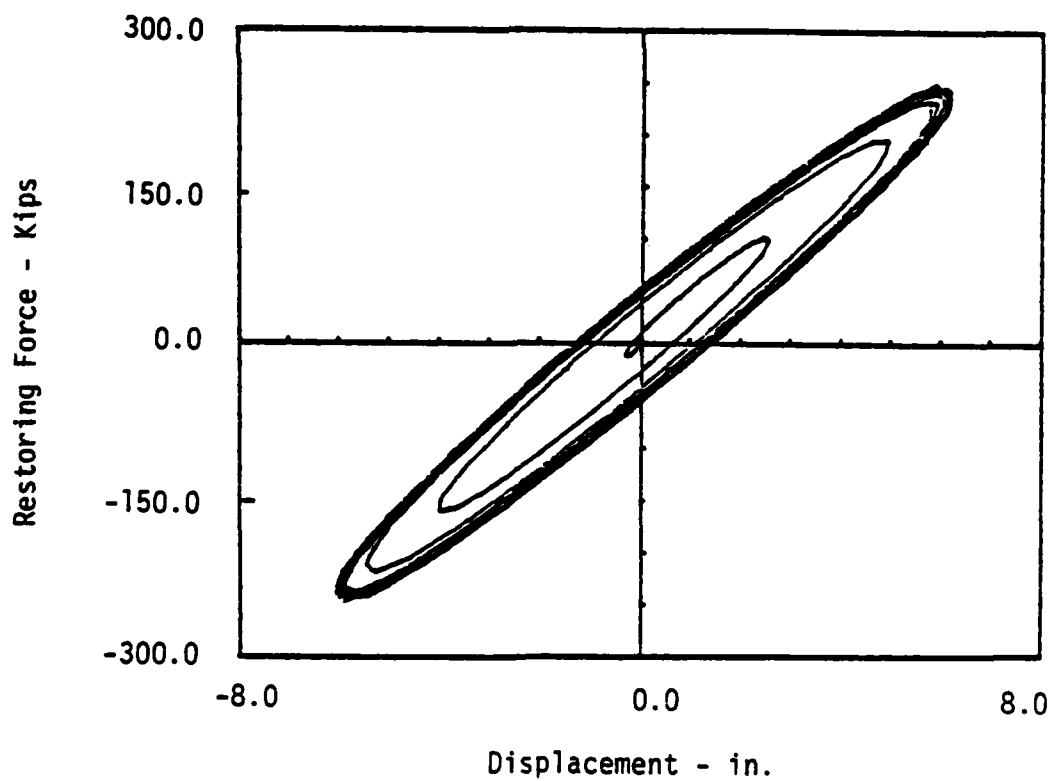


Figure 8-17. Spring plus damper restoring force versus displacement. (Case 2)

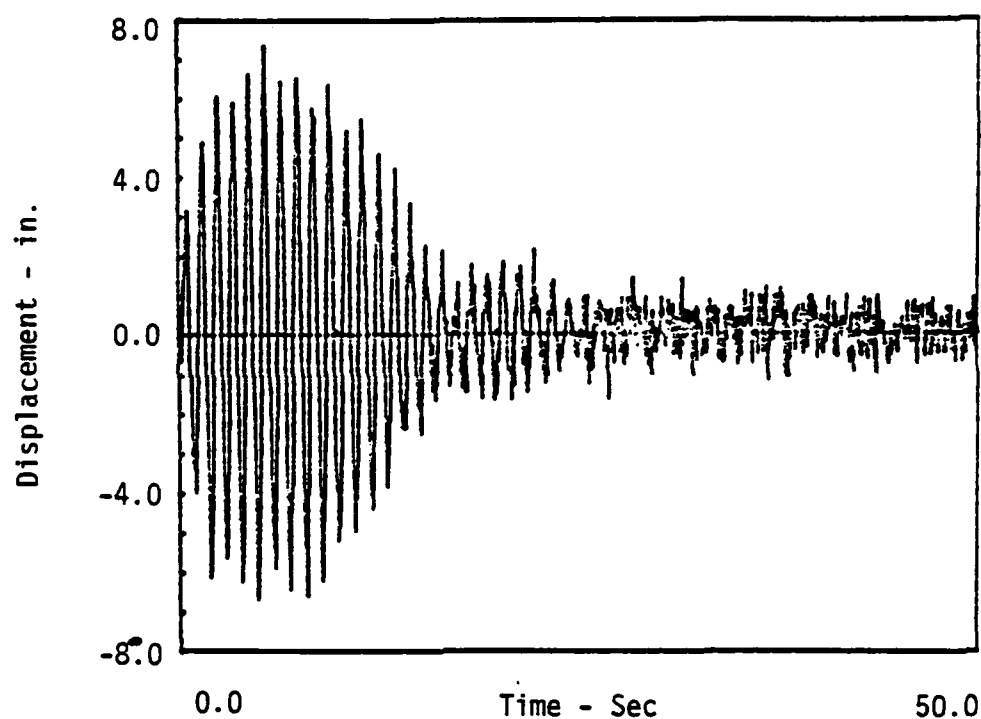


Figure 8-18. Signal used to simulate measured displacement response. Signal of Figure 8-15 plus 6% noise.

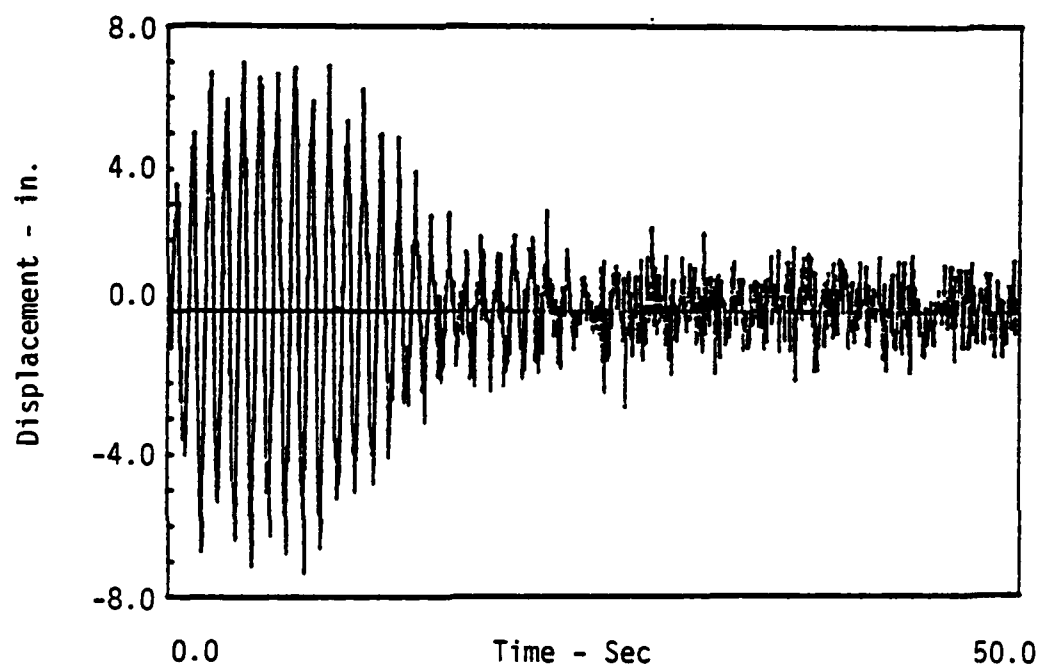


Figure 8-19. Signal used to simulate measured displacement response. (10% noise)

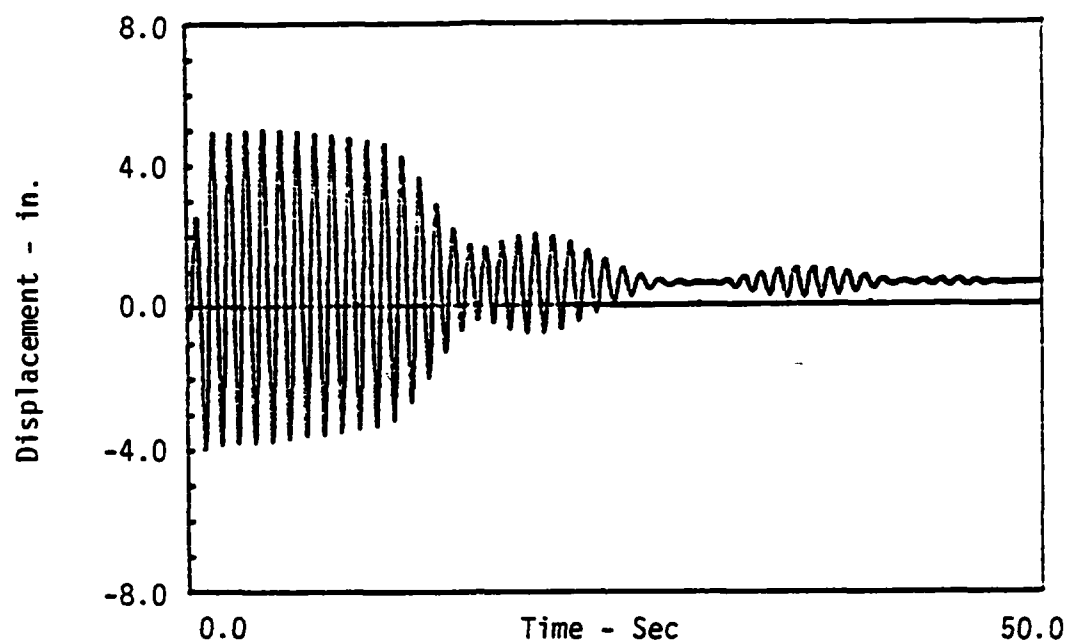


Figure 8-20. Displacement response of nonlinear system to the force in Figure 8.15 for Case 4

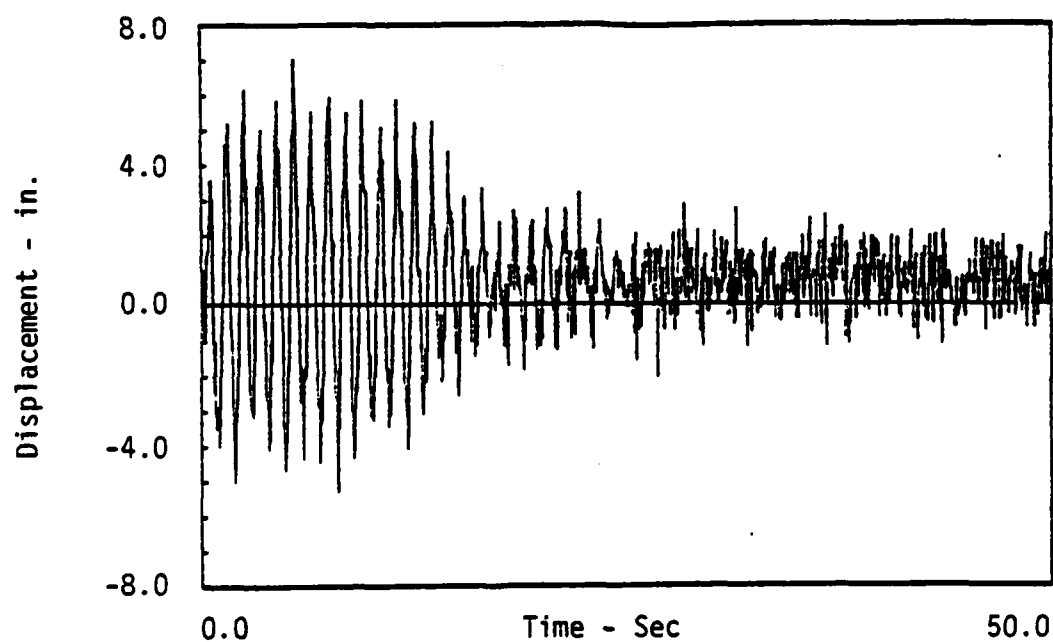


Figure 8-21. Displacement response (Case 4) plus 10% noise.

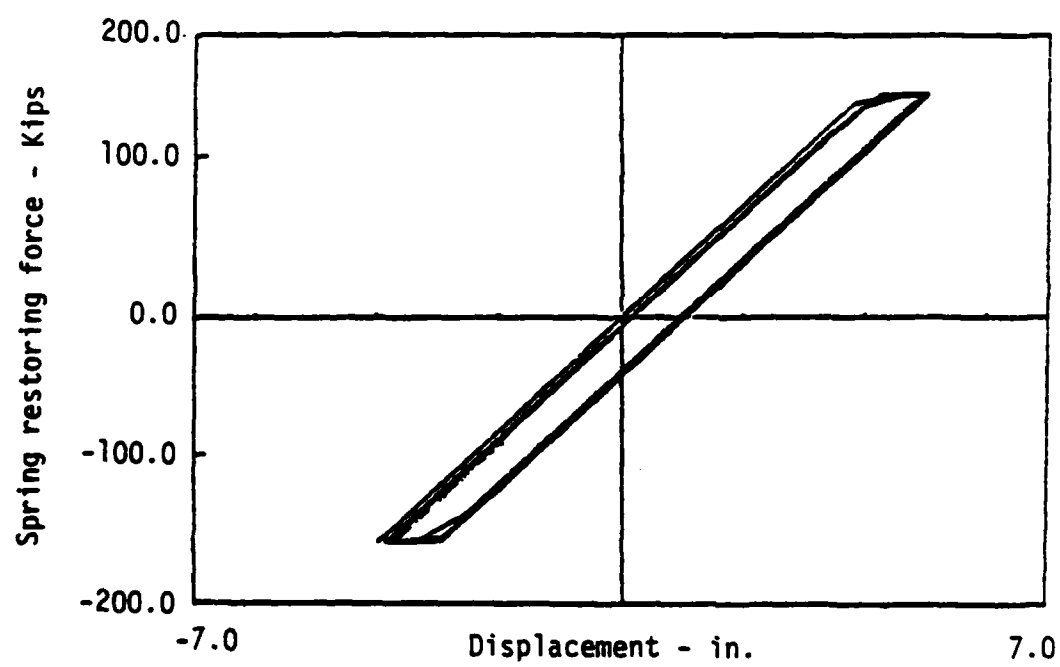


Figure 8-22. Spring restoring force versus displacement for nonlinear system (Case 4)

Using the forcing function input, described above, and the computed responses, the parameters of the structures were identified. The results of the parameter identification are given in Tables 8.4 through 8.7. These results provide the identified parameters in the noise-free case. The energy dissipated by the identified system is listed next to the identified parameters. For method 6, the parameters a_0 , a_1 , a_2 , and a_3 identify with the parameters k_0 , β , c_0 , and α , respectively.

TABLE 8.4. IDENTIFIED PARAMETERS AND ENERGY DISSIPATED
FOR CASE 1

Method	a_0	a_1	a_2	a_3	Energy
1	39.17	1.26			11210.0
2	39.17	1.28	0.0		11090.0
3	40.01	1.28			10720.0
4	40.01	2.48	0.0236		9270.0
5	39.50	1.26	0.0		11200.0
6	39.33	0.0	1.274	0.0	10741.0

TABLE 8.5. IDENTIFIED PARAMETERS AND ENERGY DISSIPATED
FOR CASE 2

Method	a_0	a_1	a_2	a_3	Energy
1	33.27	1.45			7968.0
2	33.27	3.98	0.05		7028.0
3	35.84	1.28			10500.0
4	35.84	3.57	0.042		7690.0
5	34.27	3.68	0.062		10370.0
6	36.56	0.001	1.094	0.022	10077.0

TABLE 8.6. IDENTIFIED PARAMETERS AND ENERGY
DISSIPATED FOR CASE 3

Method	a_0	a_1	a_2	a_3	Energy
1	33.27	1.35			7802.0
2	33.27	2.98	0.032		7368.0
3	35.32	1.41			9482.0
4	35.32	2.74	0.027		8185.0
5	32.54	2.98	0.042		8324.0
6	40.21	-0.0013	1.589	-0.018	9661.0

TABLE 8.7. IDENTIFIED PARAMETERS AND ENERGY
DISSIPATED FOR CASE 4

Method	a_0	a_1	a_2	a_3	Energy
1	33.27	1.67			7376.0
2	33.27	2.28	0.014		7053.0
3	34.61	1.75			7703.0
4	34.61	2.50	0.018		7486.0
5	30.30	3.95	0.066		7598.0
6	40.26	-0.0018	1.708	0.001	8186.5

Section 4.0 demonstrated that when the higher order linear model is used to simulate the actual system behavior, the parameter a_0 must be estimated first in the identification procedures, methods 1 through 4. The estimation of this parameter can be executed either by simply searching for a minimum in $Q(\omega) + \epsilon(\omega)$, or by using a curve-fit to $Q(\omega) + \epsilon(\omega)$, and then finding the minimum of the curve. Figure 8-23 shows a realization of $Q(\omega)$ for a specific case. This is the ratio of the Fourier transform moduli of the structure input and response. An example of the quantity $Q(\omega) + \epsilon(\omega)$ is shown in Figure 8-24. It

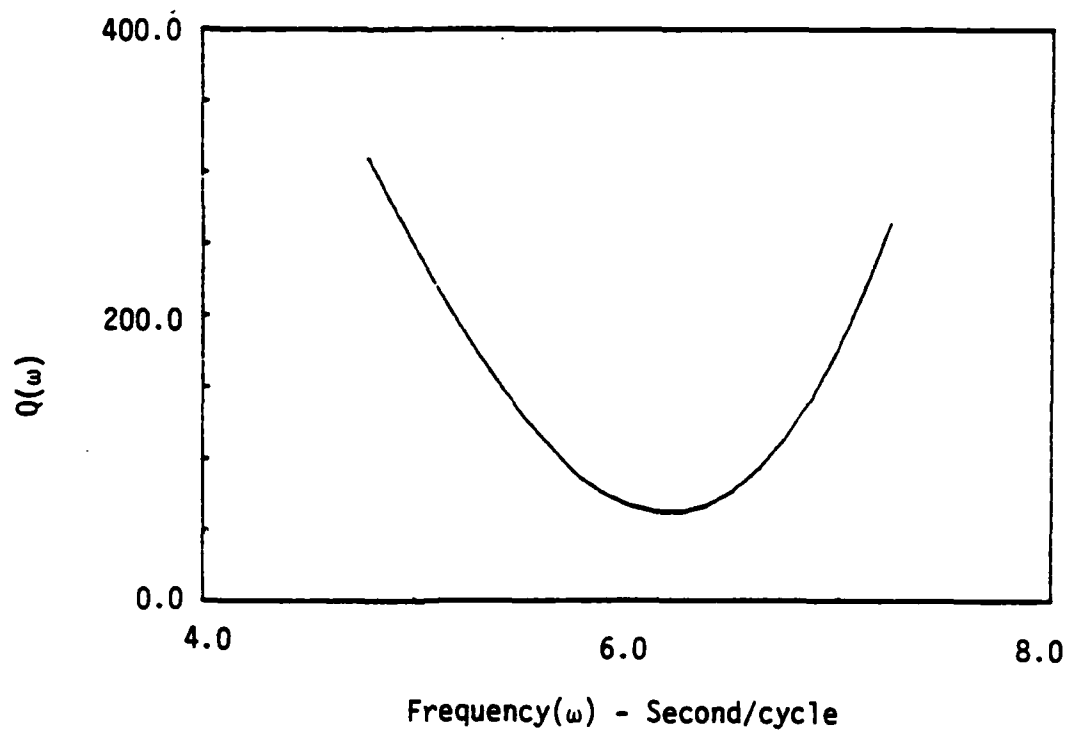


Figure 8-23. A realization of $Q(\omega)$.

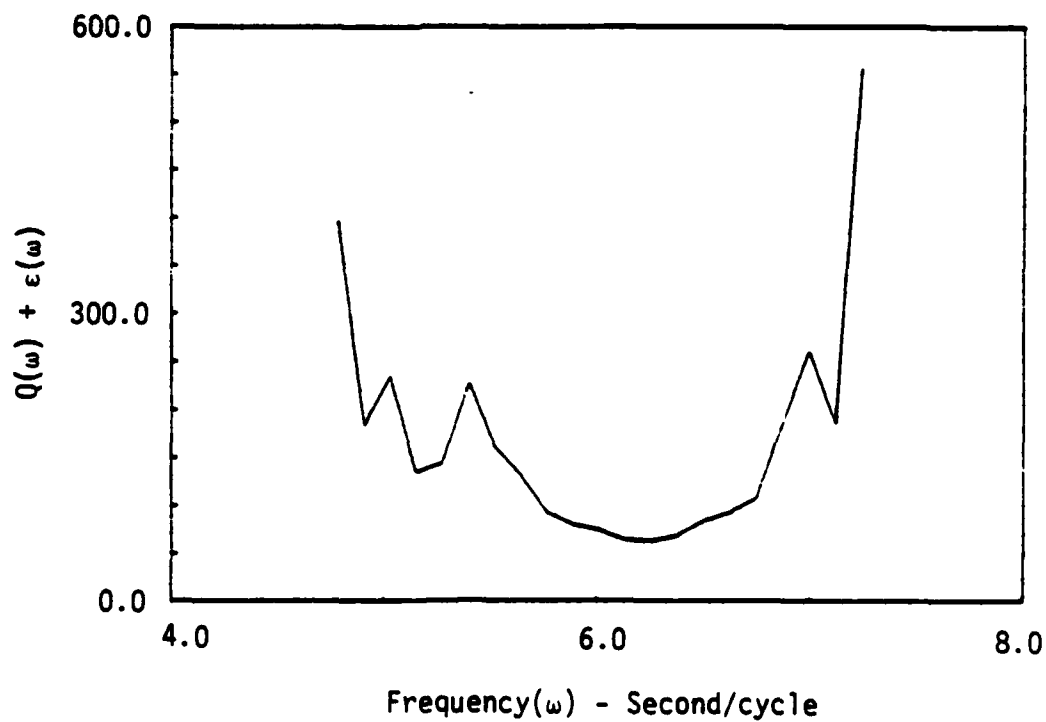


Figure 8-24. A realization of $Q(\omega) + \epsilon(\omega)$.

is apparent from this diagram why the use of a curve-fit provides better results.

Figures 8-25 through 8-27 show comparisons between the responses of the identified systems computed by different methods, and the actual response of the bilinear hysteretic system in case 2. The responses of the identified systems match the response of the actual system so closely that it is difficult to distinguish the two responses in these figures. More identified responses for case 4 are shown in Figures 8-28 through 8-30. The model responses do not match the actual response as closely when residual deformation exists in the actual structure since the models cannot accumulate permanent deformation. However, peak responses in the models match the actual system response quite well.

In this example, noise was added to the forcing function and response signals; then the system parameters were identified. The results are summarized in Tables 8.8 and 8.9.

TABLE 8.8. IDENTIFIED PARAMETERS AND ENERGY DISSIPATED
FOR CASE 1 WITH TEN PERCENT NOISE TO SIGNAL RATIO

Method	a_0	a_1	a_2	a_3	Energy
1	39.17	1.37			11022.0
2	39.17	1.45	0.003		10900.0
3	39.93	1.42			10300.0
4	39.33	2.44	0.022		9497.0
5	34.30	2.98	0.051		11710.0
6	38.44	0.0	1.286	0.0	10929.0

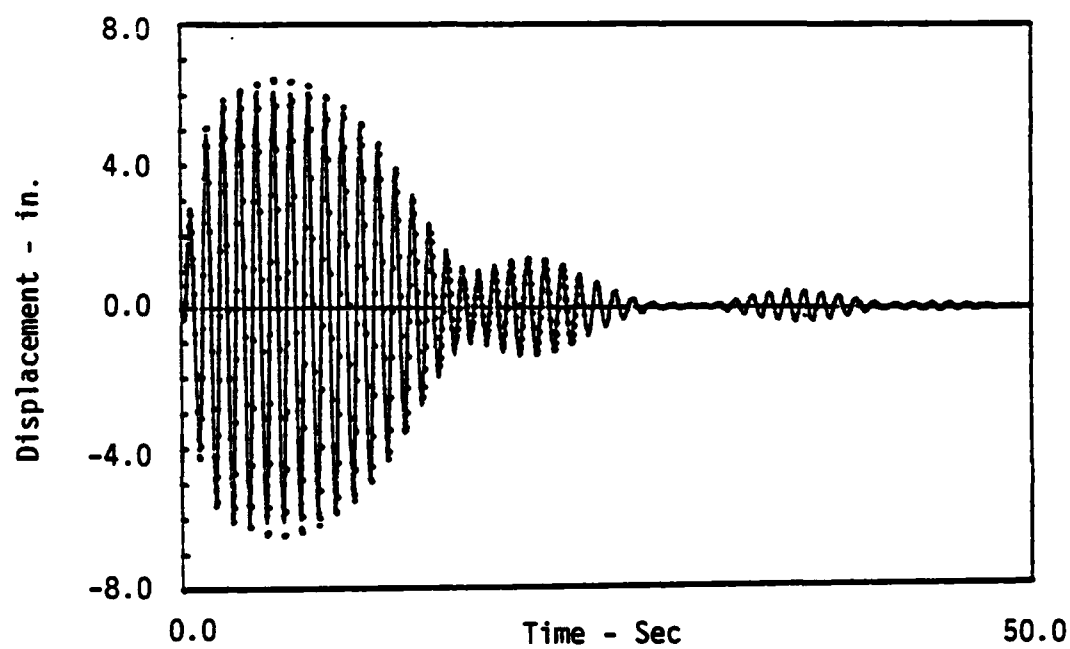


Figure 8-25. The comparison between noise-free response (solid) and second-order identified response (dot) for Case 2.

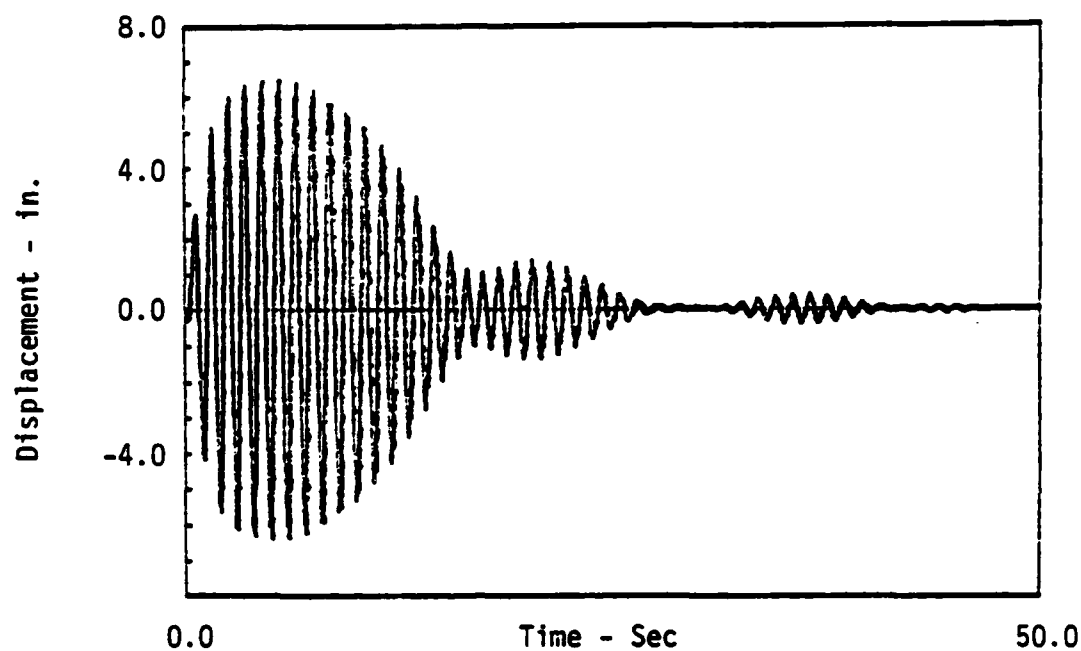


Figure 8-26. The comparison between noise-free response (heavy) and third-order identified response (light) for Case 2

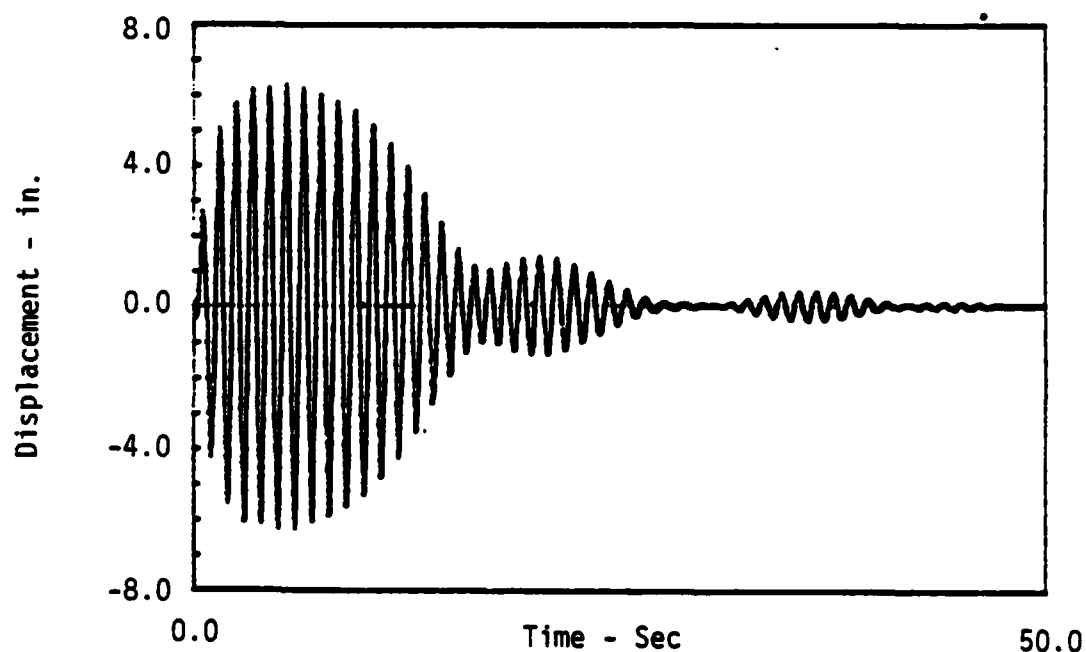


Figure 8-27. The comparison between noise-free response (heavy) and second-order time varying parameters identified response for Case 2

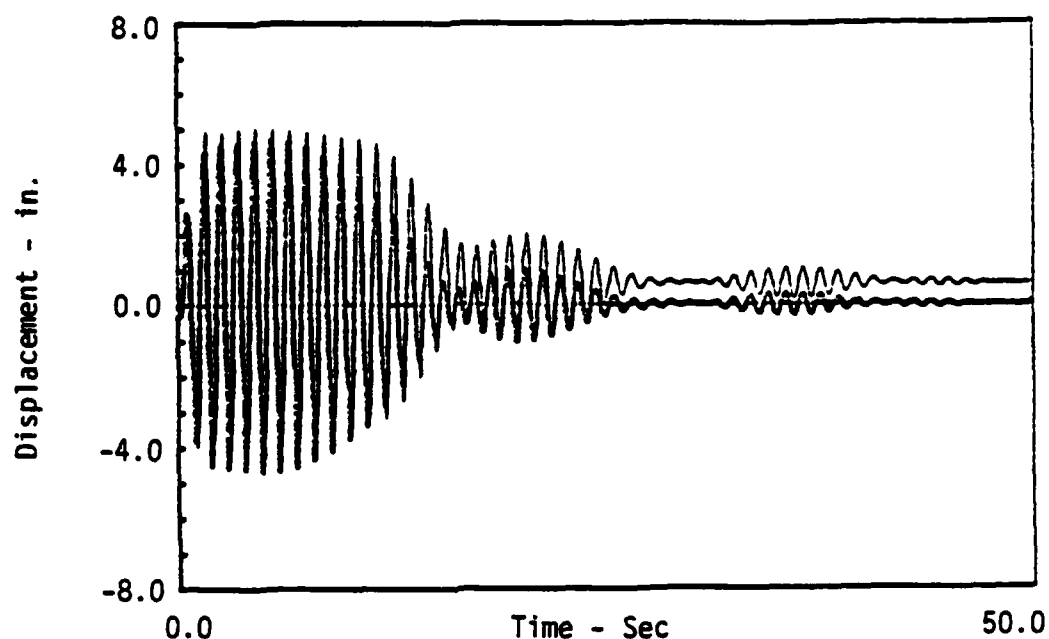


Figure 8-28. Comparison between actual response (thin line) and model (method 3) response (thick line)

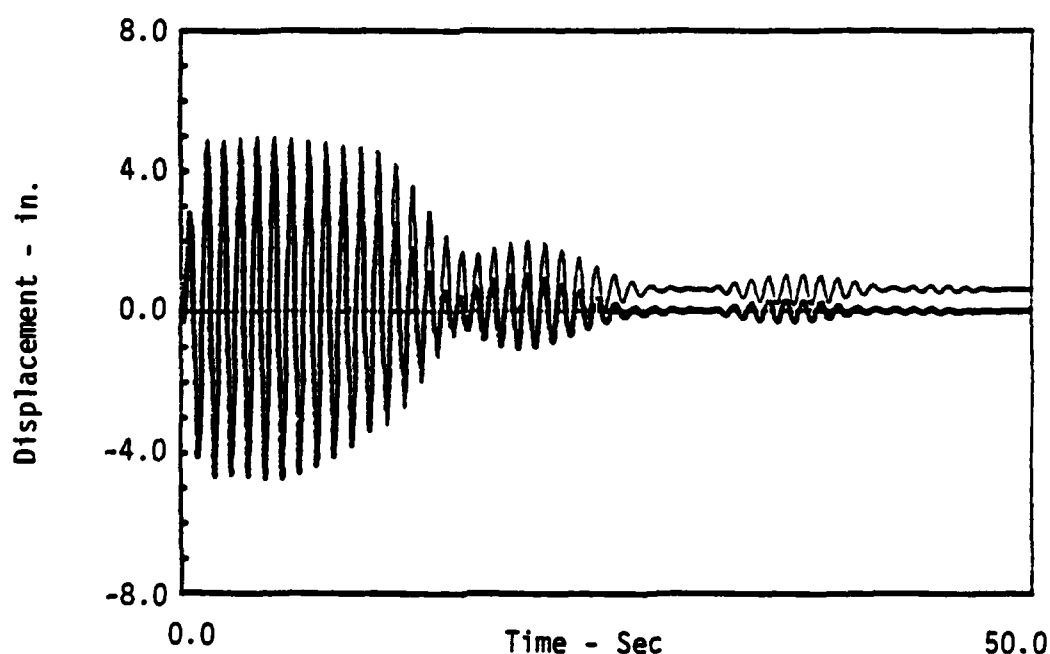


Figure 8-29. Comparison between actual response (thin line) and model (method 5) response (thick line)

TABLE 8.9. IDENTIFIED PARAMETERS AND ENERGY DISSIPATED
FOR CASE 4 WITH TEN PERCENT NOISE TO SIGNAL RATIO

Method	a_0	a_1	a_2	a_3	Energy
1	33.27	1.89			7092.0
2	33.27	1.42	0.021		9980.0
3	32.02	1.95			6476.0
4	32.02	2.60	0.021		6803.0
5	34.46	2.70	0.043		11400.0
6	32.83	0.0026	1.543	0.011	7016.0

These results show that the parameter identification procedure is still effective when noise is present.

8.3 Example 3

In this example, a parameter identification problem is solved using the frequency domain approach. The methods used to identify the parameters were described in section 8.2, namely methods 1 through 6. The same forcing function as illustrated in Example 3 is used. The only difference in this example is that the response was simulated by a second-order time varying parameter system. Unlike the responses simulated in Example 2, this example is a linear system with time dependent stiffness and damping. The parameters of the system and total energy dissipated are listed in Table 8.10.

TABLE 8.10. SYSTEM PARAMETERS FOR CASE 5

$$\begin{aligned}
 k_0 &= 39.48 & c_0 &= 1.257 \\
 \beta &= -0.01 & \alpha &= 0.01 \\
 \text{Total Energy} &= 9799.0
 \end{aligned}$$

The definitions of the symbols are the same as in Equation 5-2. This case was described in section 8.2 as case 5.

The displacement response versus time for case 5 is shown in Figure 8-31. The total restoring force versus displacement for this case is illustrated in Figure 8-32. Note that the major axis of the loops depicted in the diagram have different slopes. This occurs because the system stiffness diminishes with time. The parameters identified using methods 1 through 6 together with the total energy dissipated in the corresponding systems are shown in Table 8-11.

TABLE 8.11. IDENTIFIED PARAMETERS AND ENERGY DISSIPATED
FOR CASE 5

Method	a_0	a_1	a_2	a_3	Energy
1	34.70	1.36			9266.0
2	34.70	3.25	0.039		7883.0
3	37.15	1.29			10960.0
4	37.15	2.82	0.031		9074.0
5	34.31	2.97	0.05		11160.0
6	37.56	- 0.006	1.23	0.019	9120.2

It is shown that methods 1 through 6 can also be used to identify model parameters when noise is present. The results obtained when the measured signals contain noise are shown in Table 8.12

TABLE 8.12. IDENTIFIED PARAMETERS AND ENERGY DISSIPATED
FOR CASE 5 WITH SIX PERCENT NOISE TO SIGNAL RATIO

Method	a_0	a_1	a_2	a_3	Energy
1	34.70	1.38			9419.0
2	34.70	2.75	0.03		8623.0
3	37.34	1.31			11180.0
4	37.34	2.24	0.021		10280.0
5	34.32	2.49	0.038		11040.0
6	38.30	- 0.007	1.254	0.025	9245.6

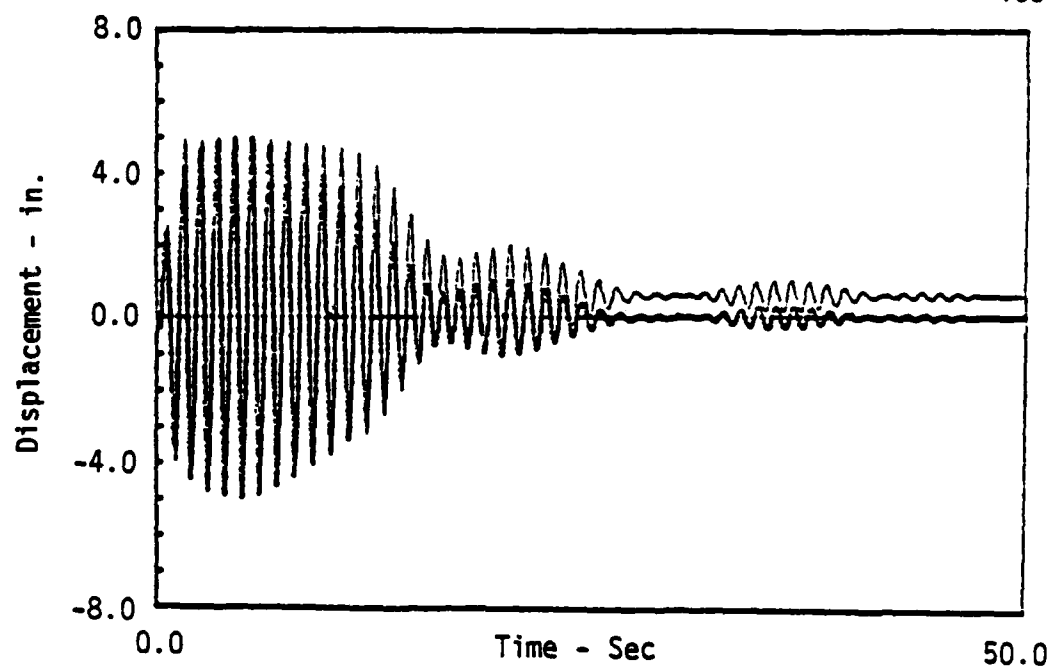


Figure 8-30. Comparison between actual response (thin line) and model (method 6) response (thick line)

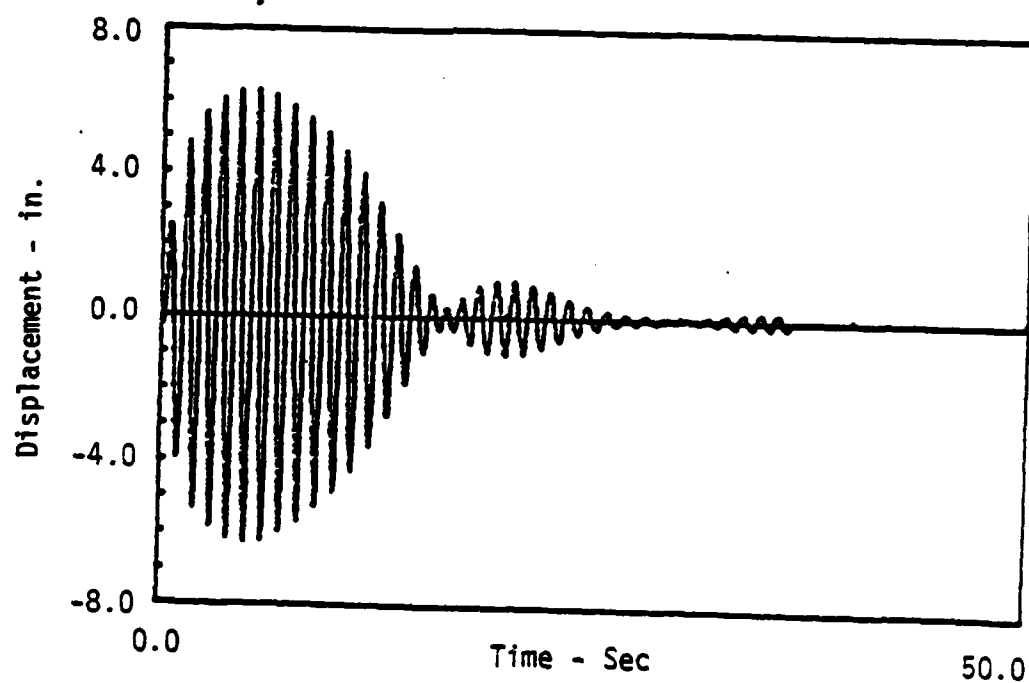


Figure 8-31. Displacement response of second-order time varying parameter system to force in Figure 8-15 (Case 5)

Figures 8-33, 8-35, and 8-36 compare the identified system responses to the response of the actual system. The simulated and actual responses match quite well in all cases. The model including time parameters provides the best match. Figure 8-34 shows the total restoring force versus displacement. A change in slope of the major axis of the loops is observed. This behavior matches the real system behavior shown in Figure 8-32.

8.4 Example 4

In this example, a two degree-of-freedom (2DF) system is considered and its parameters are identified by using the procedure outlined in Chapter 6. The system is a shear-beam lumped mass structure as shown in Figure 6-1.

The parameters of the input excitation are listed in Table 8.13. The notation for the parameters is the same as in previous examples. A typical forcing function generated using these parameters is shown in Figure 8-37. In some of the following analyses noise is contained in the measured data. An input with noise to signal ratio of eight percent is shown in Figure 8-38.

TABLE 8.13. PARAMETERS OF THE FORCING FUNCTION

$$\begin{aligned} \alpha &= 0.1 & N &= 50 & c_j &= 10.0 & j &= 1, \dots, 50 \\ \Delta t &= 0.05 & n &= 1024 & \omega_j &= (1.6 + 0.04 j)\pi, & j &= 1, \dots, 50 \end{aligned}$$

The response signals used to represent the measured signals were generated by computer program BLNMDF. BLNMDF generated the displacement, velocity, and acceleration response of a bilinear MDF system. First, the response of a linear system (case 1) was computed. Then, a nonlinear response was computed for analysis in case 2.

The structural parameters used in cases 1 and 2 in this numerical example are given in Table 8.14. The numerical subscripts on the parameters refer to the story and mass numbers

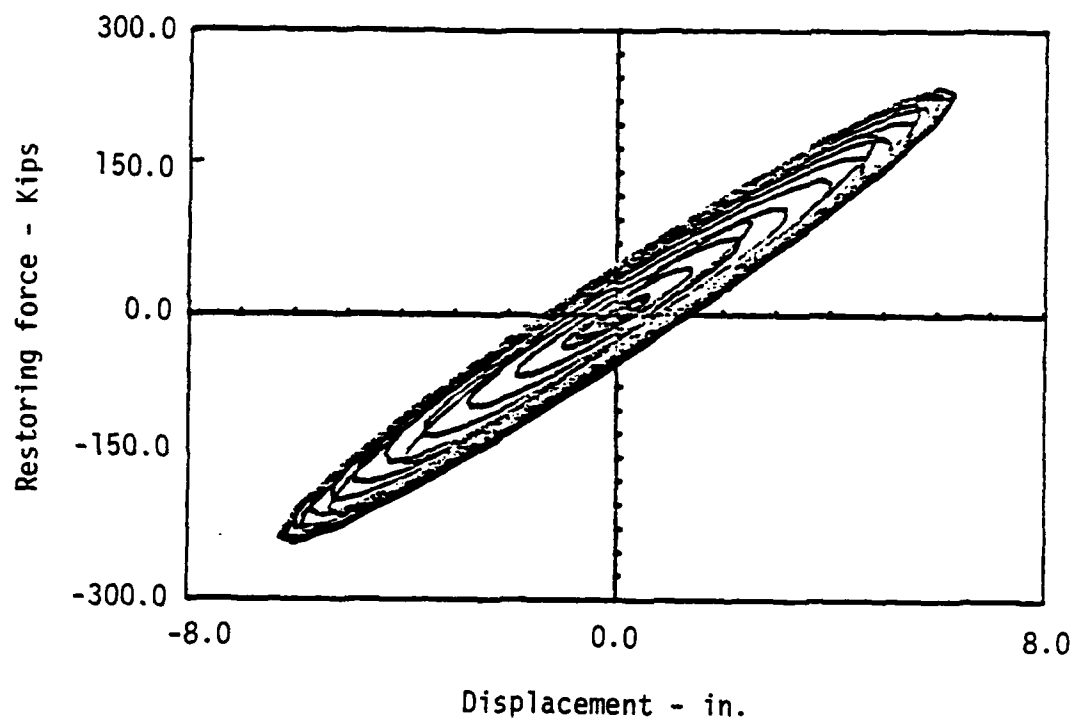


Figure 8-32. Total restoring force versus displacement for time varying parameter system (Case 5)

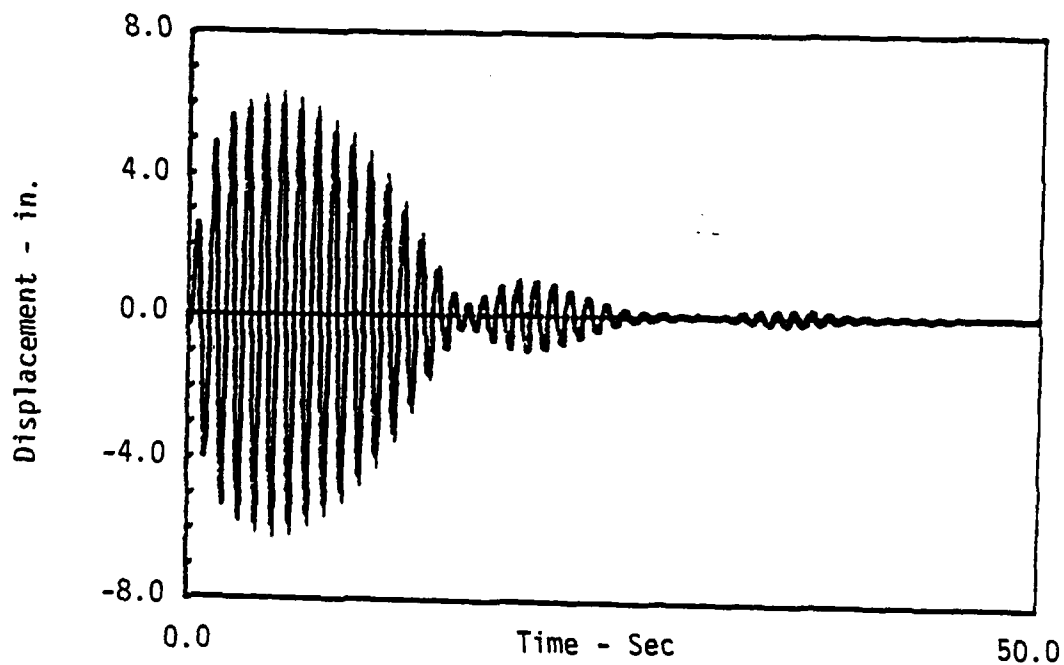


Figure 8-33. The comparison between measured response (light) and the identified response (dark) by method 6 for Case 5

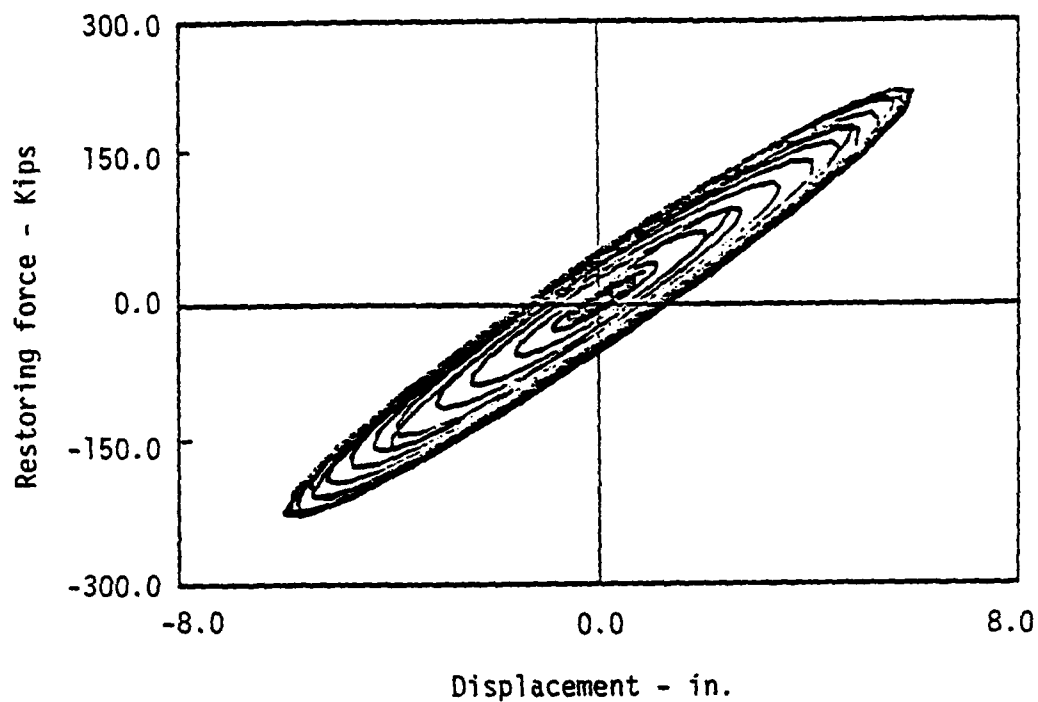


Figure 8-34. Total restoring force versus displacement after the identification by using method 6 for Case 5.

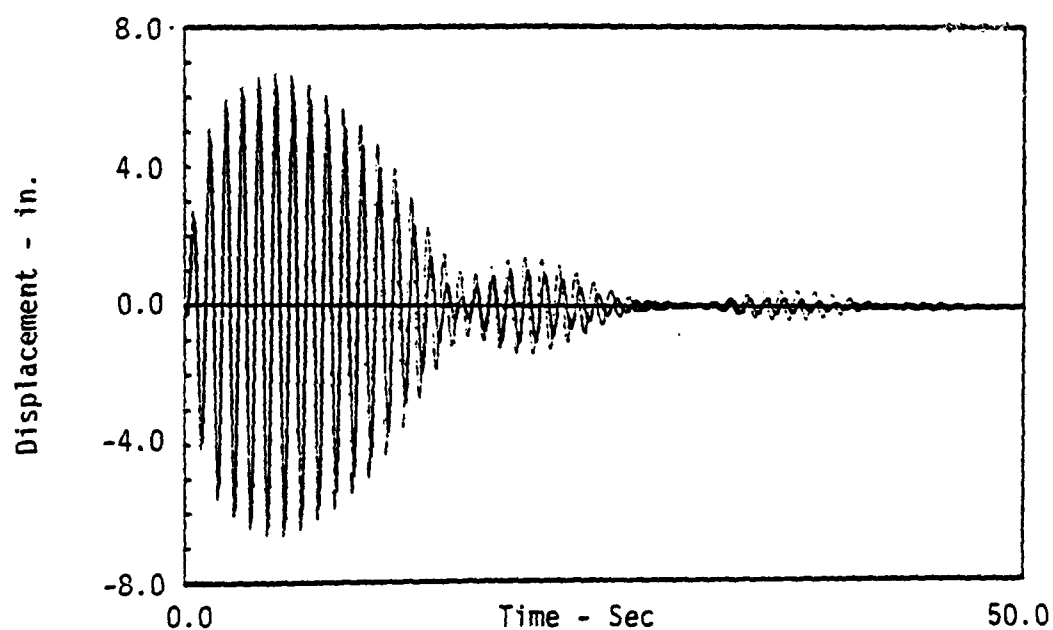


Figure 8-35. Comparison between measured response (heavy) and second-order identified response (light) using method 3 for Case 5.

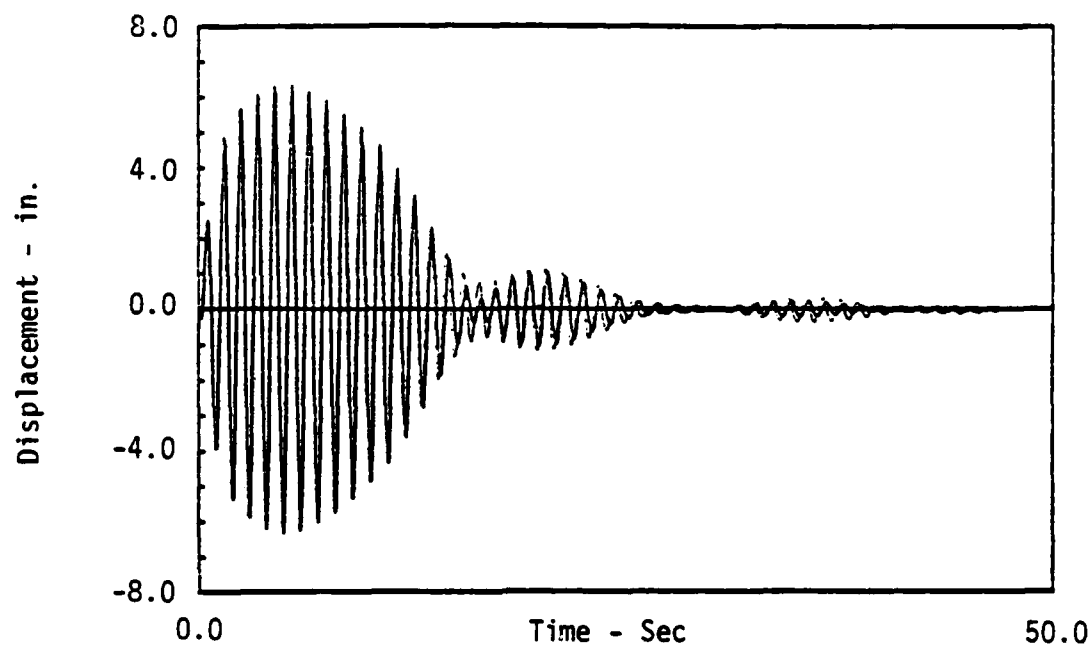


Figure 8-36. Comparison between measured response (heavy) and the third-order response (light) using method 4 for Case 5.

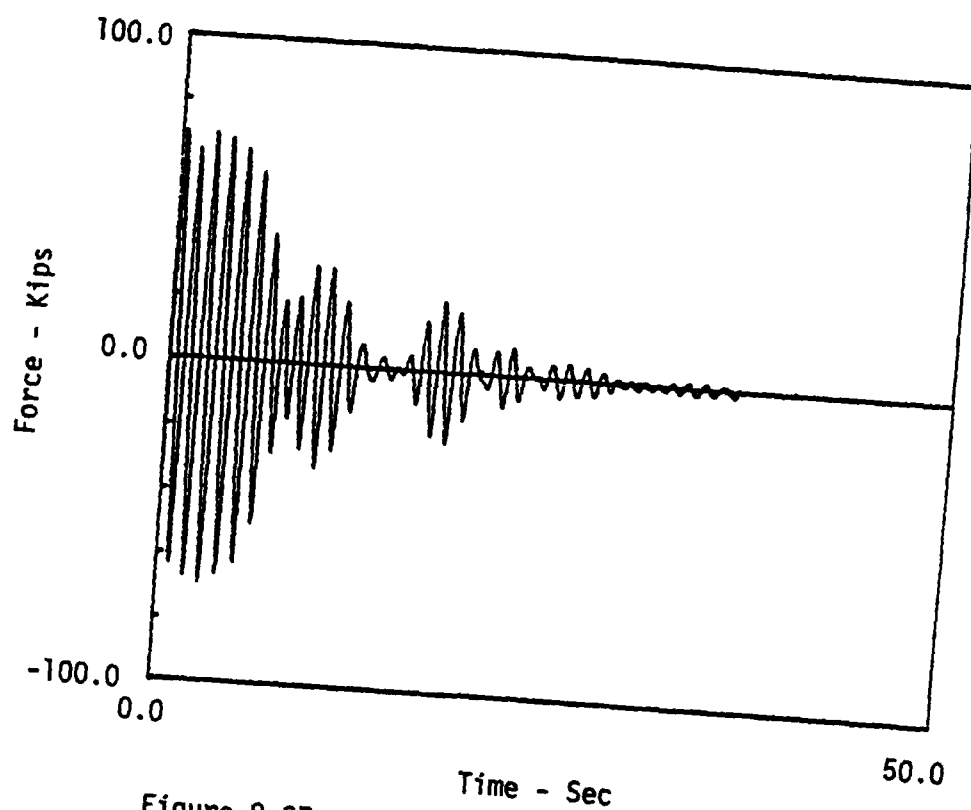


Figure 8-37. Typical input used to represent forcing function in Example 4.

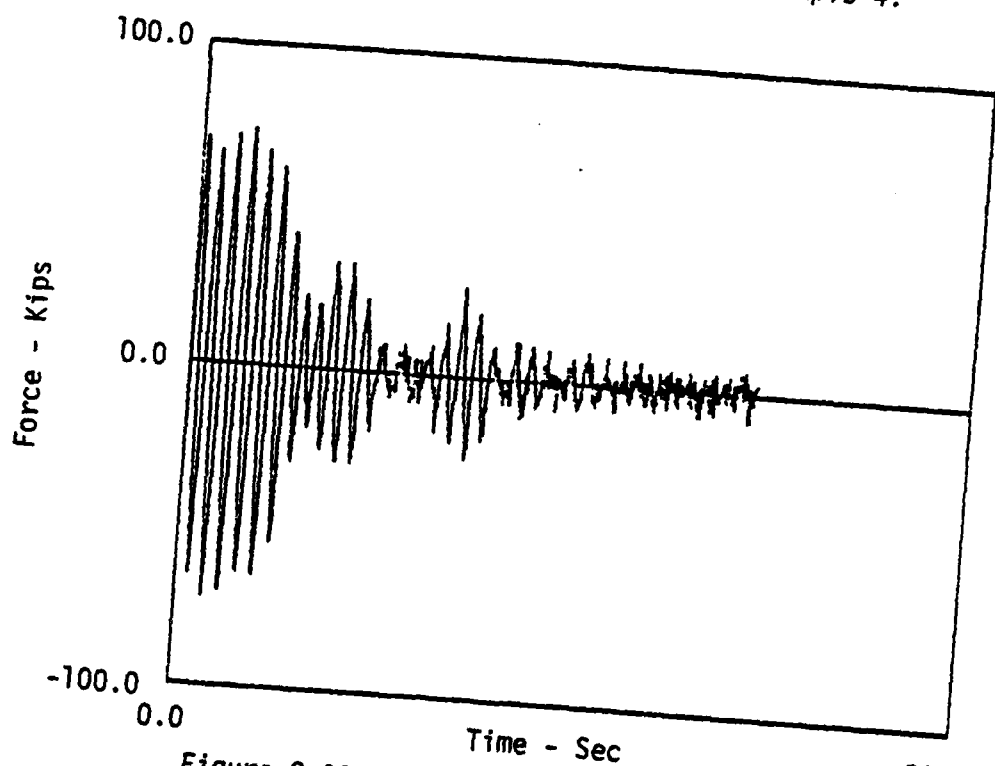


Figure 8-38. Input including eight percent noise.

TABLE 8.14. SYSTEM PARAMETERS (cases 1 and 2)

$k_1 = 39.48$	$c_1 = 1,257$	$m = 1.0$
$k_2 = 39.48$	$c_2 = 1.257$	$m = 1.0$
$\Delta t = 0.05$	$n = 1024$	$y_{d1} = 1.2, y_{d2} = 1.0$ (for case 2)

in the 2DF system. Since yielding only occurs in case 2 the yield level parameters are only used in case 2.

The displacement response versus time for case 1 is plotted in Figures 8-39 and 8-40. Note, the displacement is relative displacement with respect to each degree-of-freedom. The relative displacement histories for case 2 are shown in Figures 8-41 and 8-42. Figures 8-43 and 8-44 show the measured signals with ten percent noise to signal ratio corresponding to the actual response measurements in Figures 8-41 and 8-42.

The energy dissipated by the structure during the structural responses of cases 1 and 2 are presented in Table 8.15. Energy quantities dissipated in both first and second stories are given. Note that similar amounts of energy are dissipated in the linear and nonlinear structures.

TABLE 8.15. ENERGY DISSIPATION

	<u>First Story</u>	<u>Second Story</u>	<u>Total</u>
Case 1 (Linear)	527.80	53.00	580.80
Case 2 (Nonlinear)	447.20	105.10	552.30

The program MDFID performs a frequency domain parameter identification for the second and third order linear model. It accepts both an input signal from FORCE and response signals from BLNMDF. The white noise signals are added to the corresponding input data whenever noises are included in the analysis. It should be noted that when noise signals are included in the responses, a different signal is added for each degree-of-freedom.

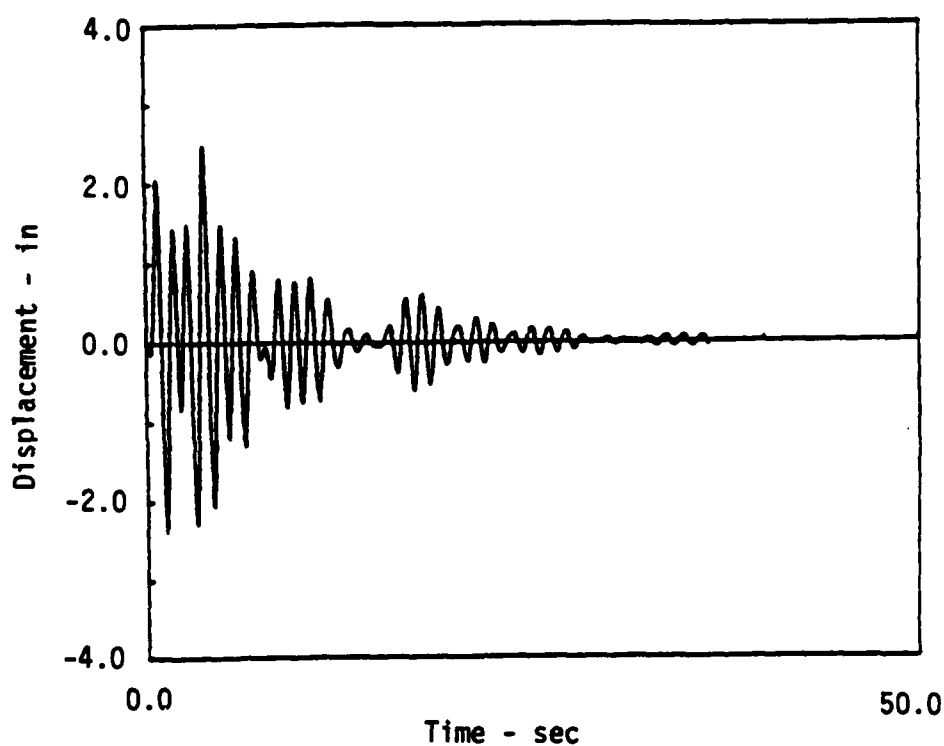


Figure 8-39. Relative displacement response between base and mass 1 in 2 DF structure. Case 1 (linear)

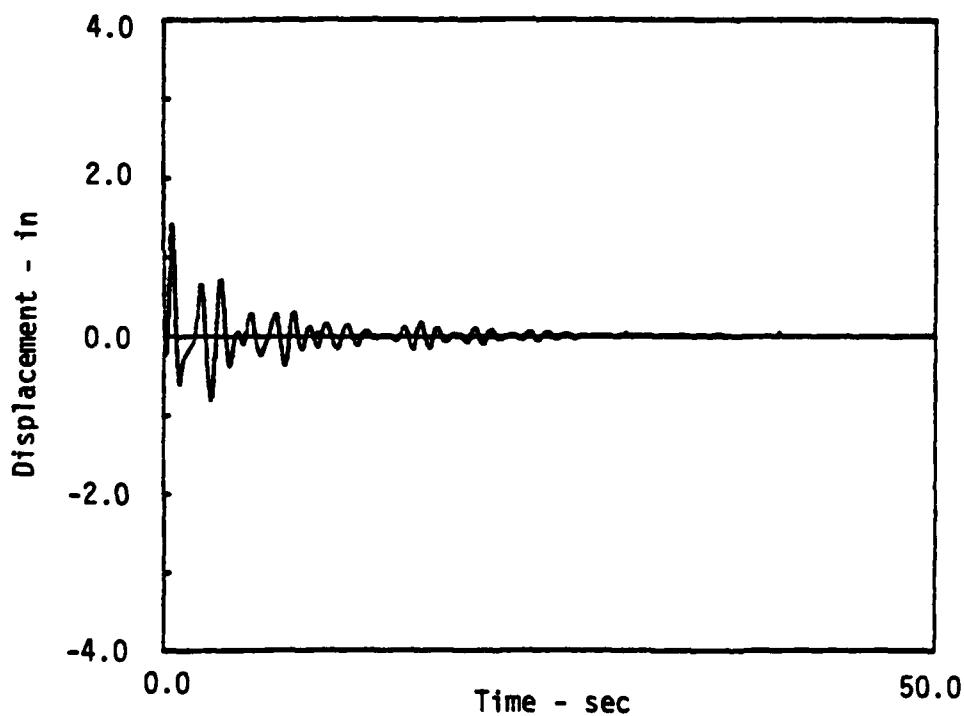


Figure 8-40. Relative displacement response between mass 1 and mass 2 in 2DF structure. Case 1 (linear)

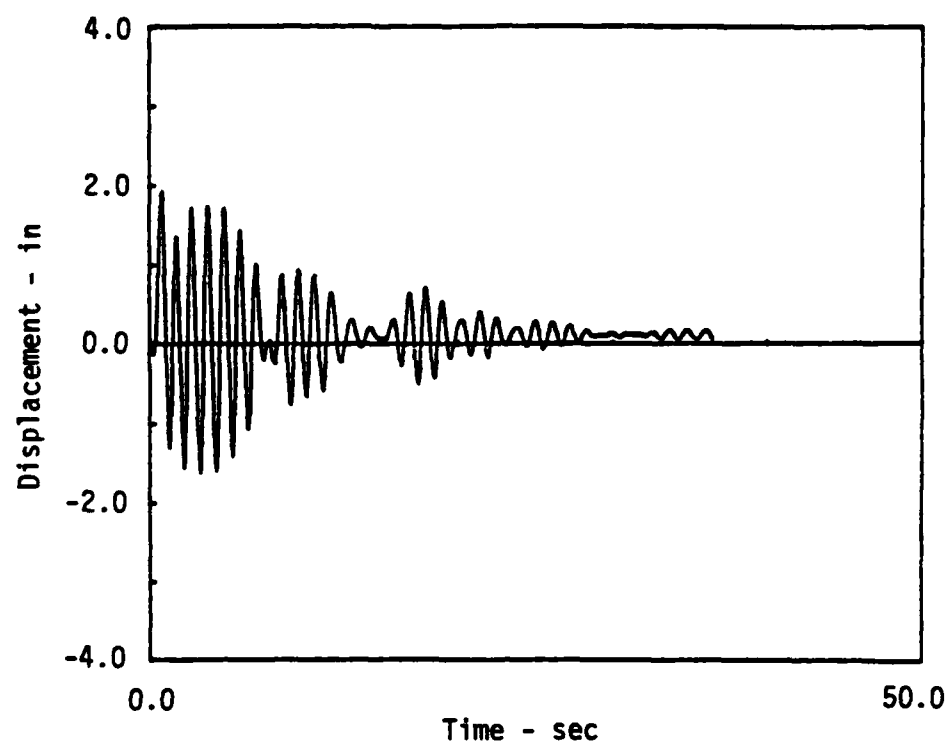


Figure 8-41. Relative displacement response between base and mass 1 in 2DF structure. Case 2 (nonlinear)

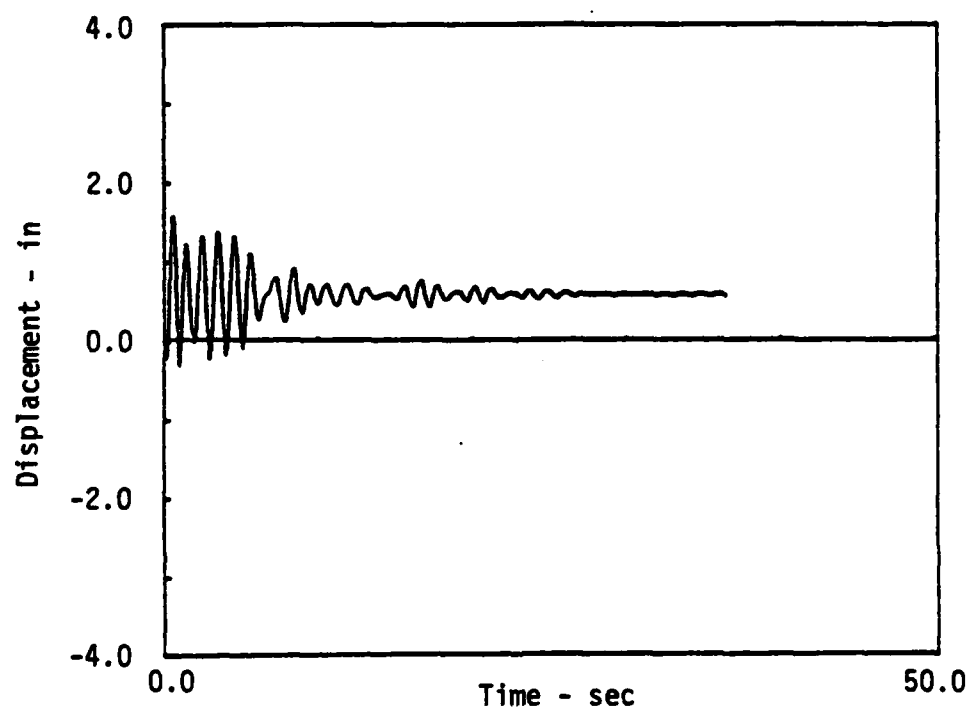


Figure 8-42. Relative displacement response between mass 1 and mass 2 in 2DF structure. Case 2 (nonlinear)

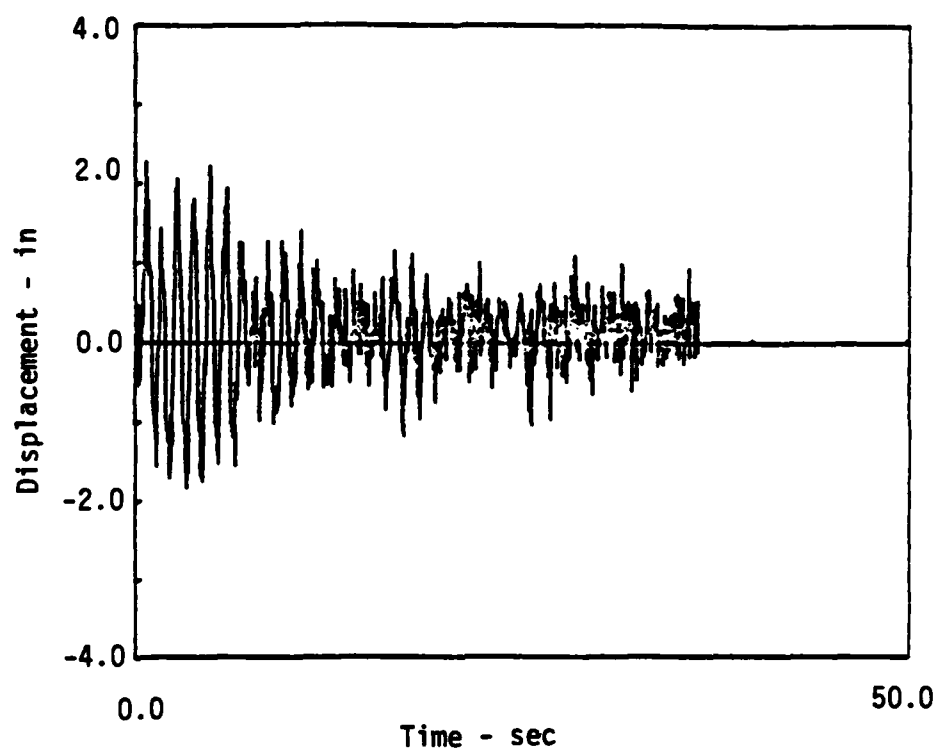


Figure 8-43. Relative displacement response between base and mass 1 in 2DF structure plus 10 percent noise. (corresponding to Figure 8-41)

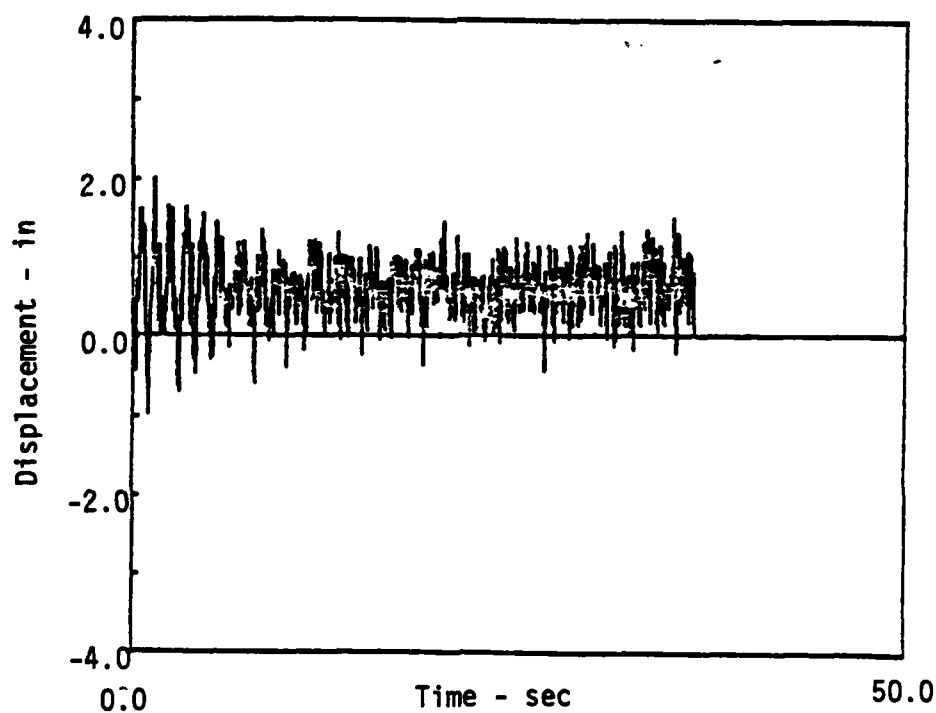


Figure 8-44. Relative displacement response between mass 1 and mass 2 in 2DF structure plus 15 percent noise. (corresponding to Figure 8-42)

MDFID performs the necessary Fourier transforms and other data operations. Then the parameter identification is executed. Once the parameters are known, the energy dissipated in each degree-of-freedom is calculated.

The parameters identified using the program MDFID are listed in Tables 8.16 through 8.19. The system parameters identified for case 1 (linear response) where no noise is included in the measured signals, are given in Table 8.16. The system parameters identified for case 1, where noise is included in the measured signals, are given in Table 8.17.

TABLE 8.16. IDENTIFIED PARAMETERS AND ENERGY DISSIPATED
FOR CASE 1 WITHOUT NOISE

Convergence Criteria = 4 percent

order	k_1	k_2	c_1	c_2	a_1	a_2	E_1	E_2	E_T
second	41.79	42.10	1.29	0.90	--	--	570.9	42.17	613.0
third	41.30	43.21	1.76	0.605	0.0093	0.0014	634.5	29.66	664.2

TABLE 8.17. IDENTIFIED PARAMETERS AND ENERGY DISSIPATED
FOR CASE 1 WITH NOISE

Convergence Criteria = 4 percent

order	k_1	k_2	c_1	c_2	a_1	a_2	E_1	E_2	E_T
second	44.37	38.4	1.30	0.90	--	--	563.1	56.22	619.3
third	43.45	39.07	1.38	0.96	0.0005	0.0037	592.7	42.80	635.5

The system parameters identified for case 2 (nonlinear) where no noise is included in the measured signals are given in Table 8.18. The system parameters identified for case 2, where noise is included in the measured signals, are given in Table 8.19. Each table lists a convergence criterion used in obtaining the parameter estimates. These quantities reflect a limit on the

change in parameter value required in the computation before the identification computation is terminated. The smallest convergence criteria values yield the most accurate results.

TABLE 8.18. IDENTIFIED PARAMETERS AND ENERGY DISSIPATED
FOR NONLINEAR CASE (CASE 2) WITHOUT NOISE

Convergence Criterion = 4 percent

order	k_1	k_2	c_1	c_2	a_1	a_2	E_1	E_2	E_T
second	29.04	33.87	1.81	1.81	--	--	861.3	81.43	948.73
third	29.07	32.30	2.11	1.89	0.0082	0.0048	676.10	140.60	816.70

TABLE 8.19. IDENTIFIED PARAMETERS AND ENERGY DISSIPATED
FOR CASE 2 WITH NOISE

Convergence Criterion = 2 percent

order	k_1	k_2	c_1	c_2	a_1	a_2	E_1	E_2	E_T
second	35.33	19.91	1.21	1.38	--	--	434.8	142.6	577.3
third	35.67	18.671	1.20	1.31	0.0033	0.001	397.1	133.2	530.3

Comparisons among Tables 8.14, 8.16 and 8.17 show that the parameters obtained using the program MDFID provide good estimates of the actual system parameters. The structural responses predicted using the second and third order models are shown in Figures 8-45 through 8-48 where they are compared with the actual responses. Model responses and energy dissipated were computed using computer program HDMDF. Figure 8-45 shows the relative displacement response between the base and mass 1 for the second order model (parameters from Table 8.16) and the actual response (Figure 8-39). The responses are almost identical. Figure 8-46 shows the corresponding relative displacement responses between masses 1 and 2. Figure 8-47 shows the relative displacement response between the base and mass 1 for the third order model (parameters from Table 8.16) and the actual response (Figure 8-39). The responses are almost identical. Figure 8-46 shows

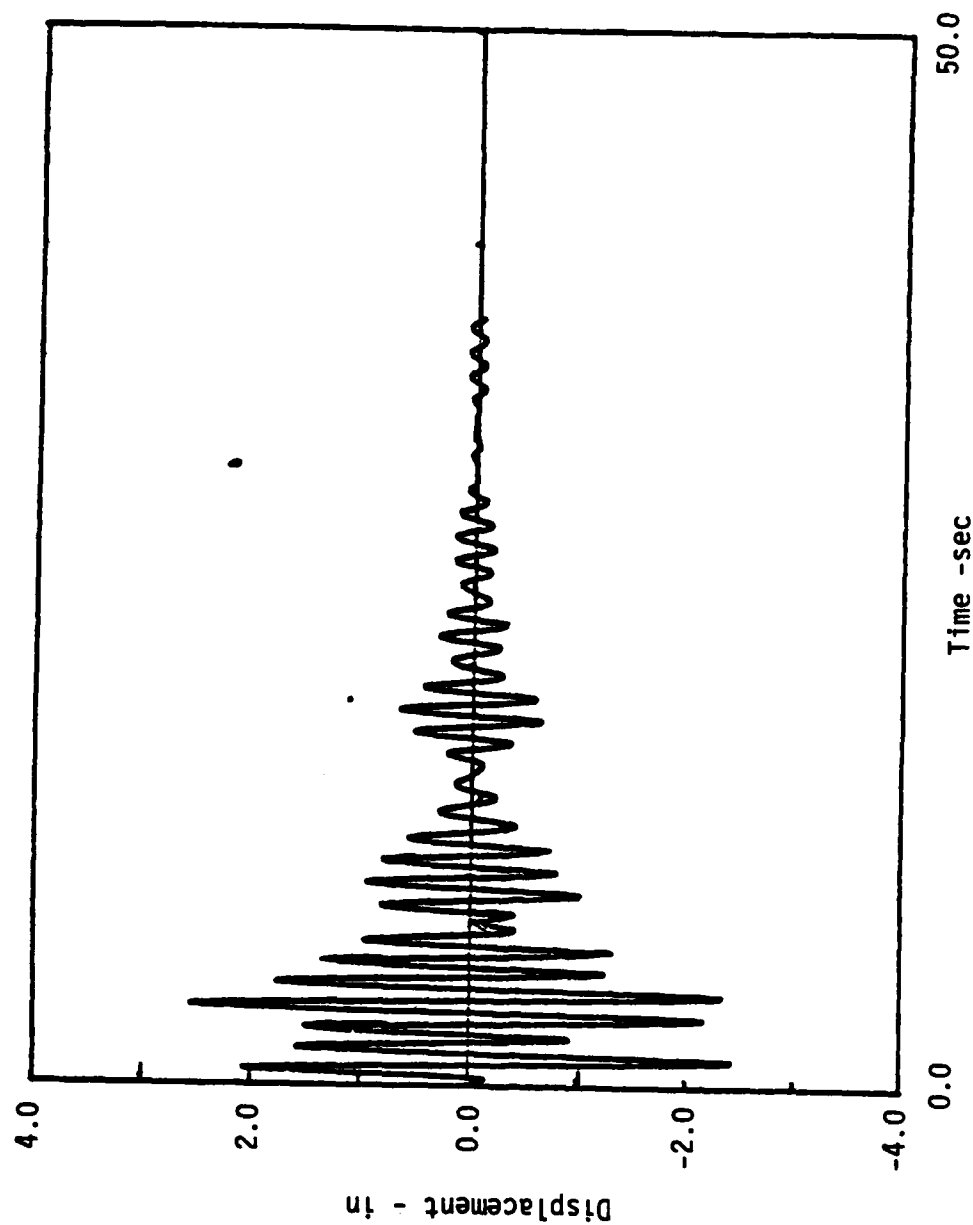


Figure 8.45. Comparison of second order model and actual relative displacement response between base and mass 1. (Case 1)

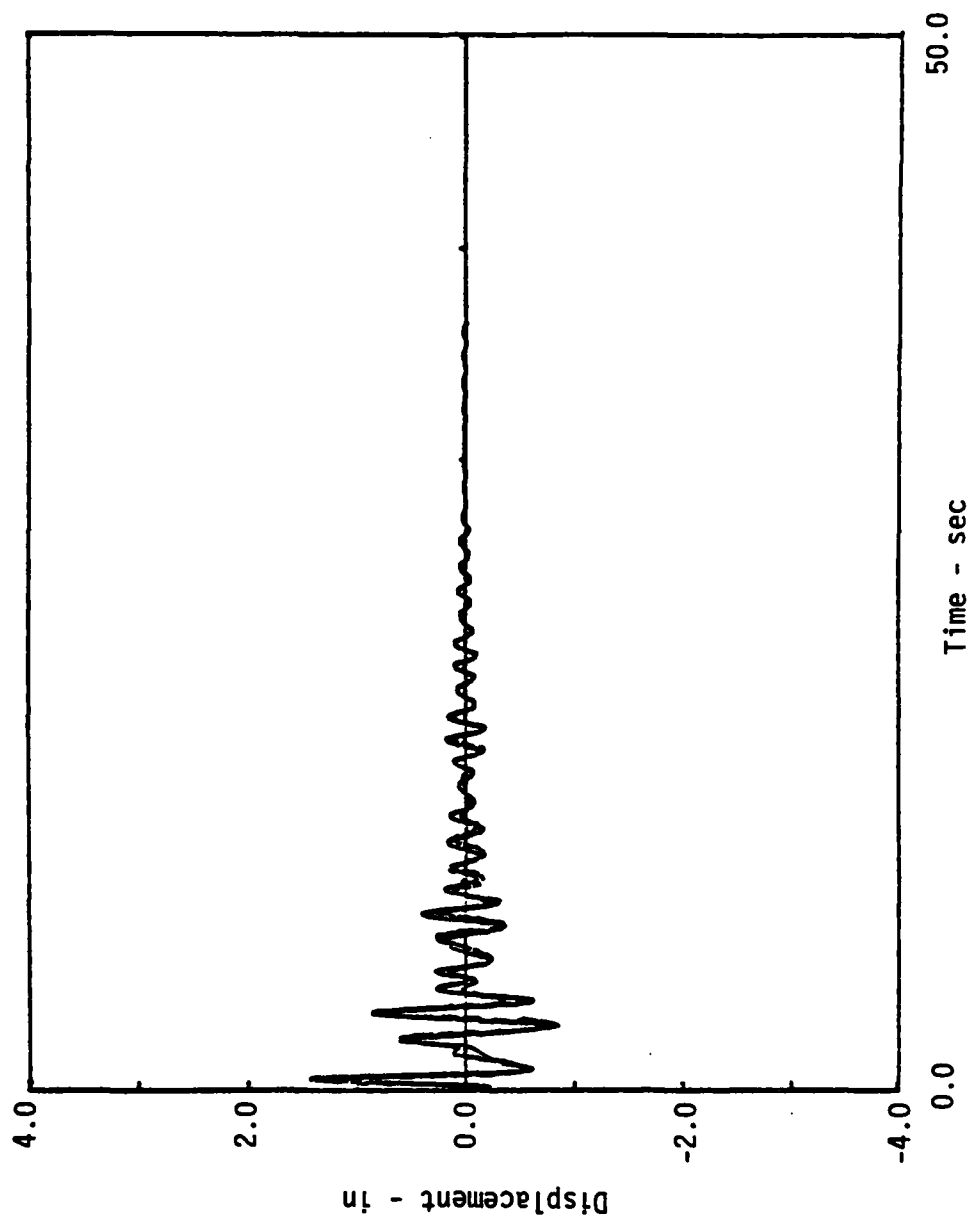


Figure 8-46. Comparison of second order model and actual relative displacement response between mass 1 and mass 2. (Case 1)

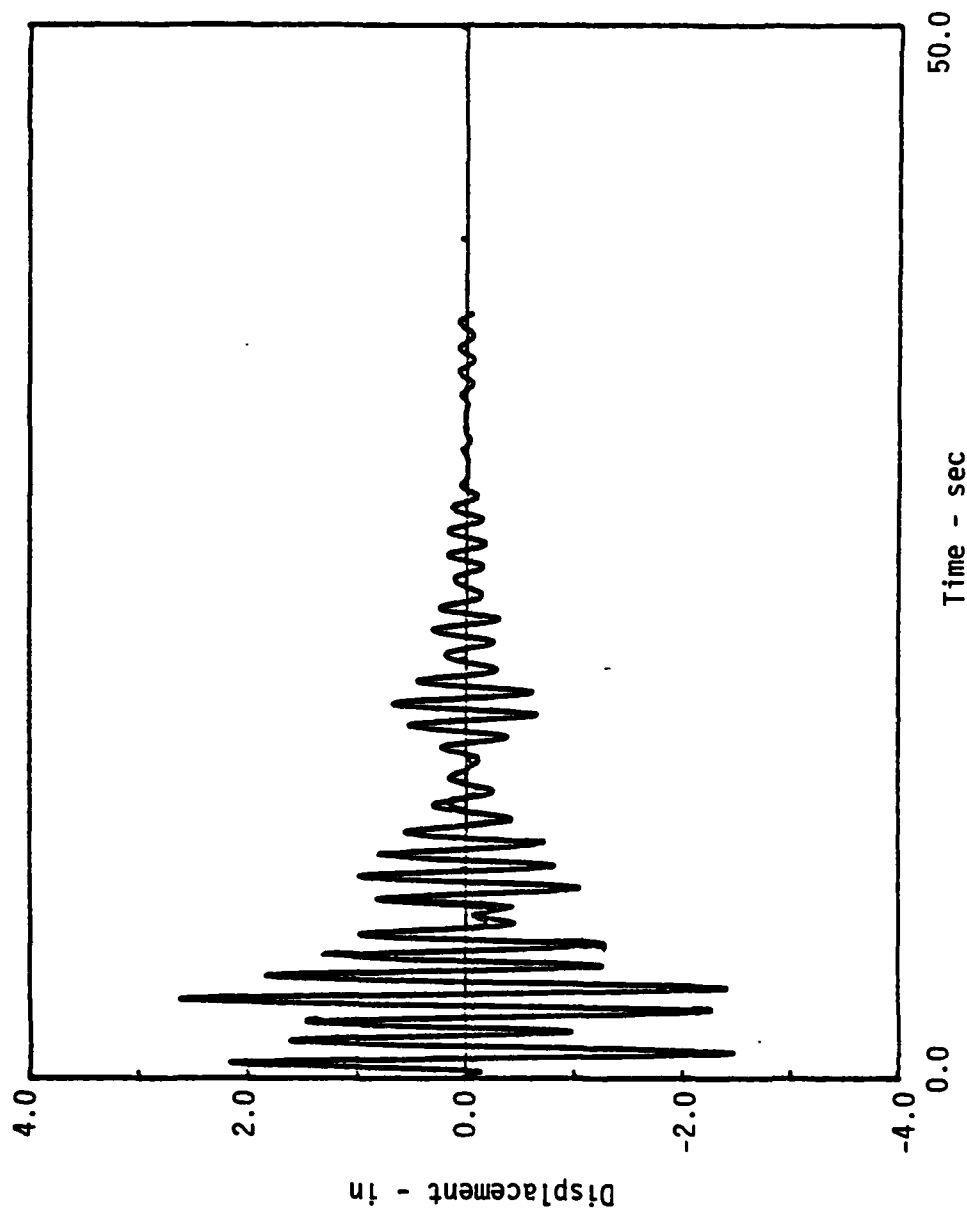


Figure 8-47. Comparison of third order model and actual relative displacement response between base and mass 1. (Case 1)

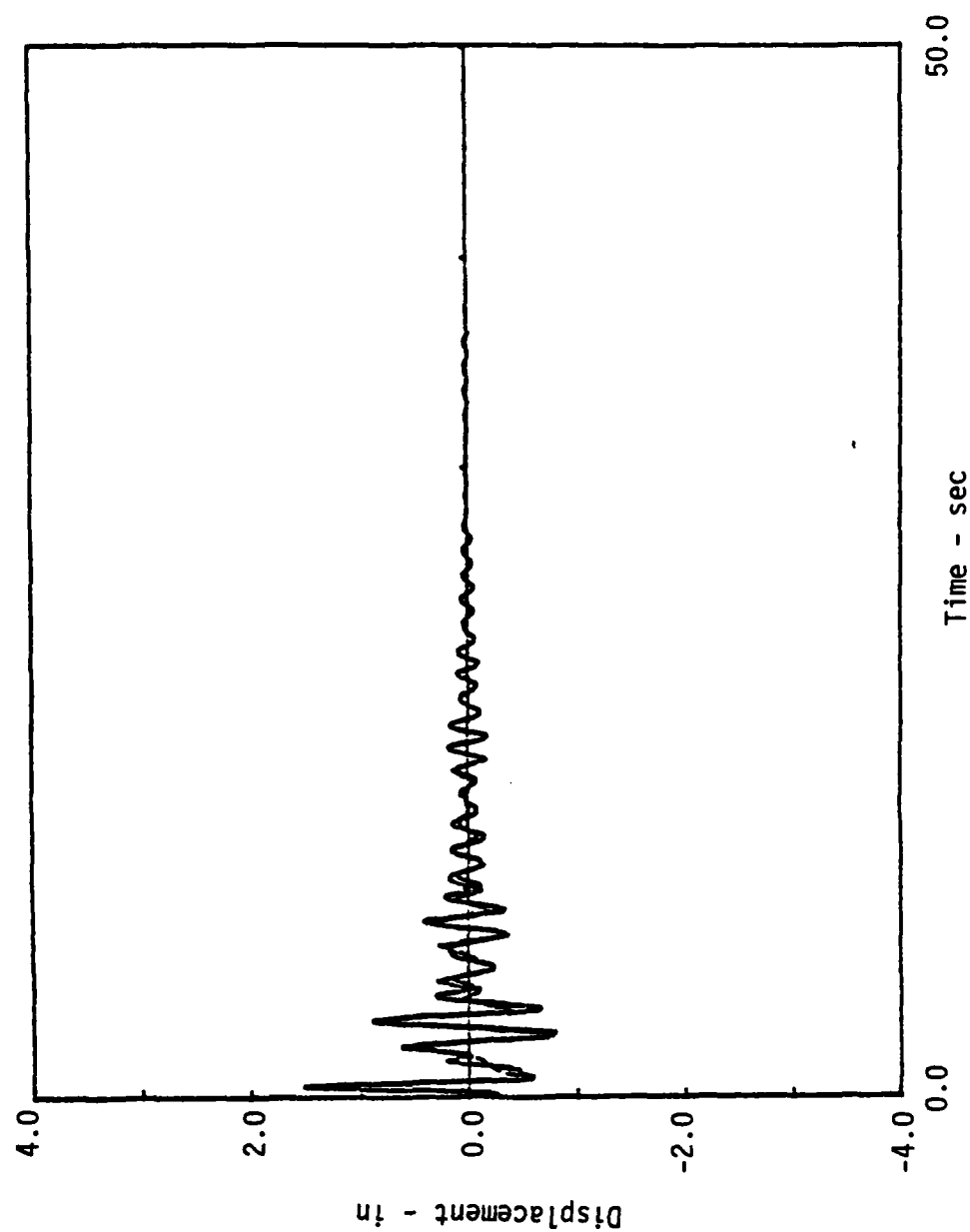


Figure 8-48. Comparison of third order model and actual relative displacement response between mass 1 and mass 2. (Case 1)

the corresponding relative displacement responses between masses 1 and 2. Figure 8-47 shows the relative displacement response between the base and mass 1 for the third order model (parameters from Table 8.16) and the actual response (Figure 8-39). Again, responses are almost identical. Figure 8-48 shows the corresponding relative displacement responses between masses 1 and 2.

The energy dissipated during structural response was computed using the second and third order models in program HDMDF, using the parameters identified in the presence of no noise and the parameters identified in the presence of noise. The results are given in Table 8.16 and 8.17. In both cases good agreement with the actual energy dissipated is found.

Comparison among Tables 8.14, 8.18 and 8.19 show that the parameters obtained using the program MDFID are changed. This change reflects the system nonlinearity. The structural responses predicted using the second and third order models for case 2 are shown in Figures 8-49 through 8-52 where they are compared with the actual nonlinear responses. Model responses and energy dissipated were computed using computer program HDMDF. Figures 8-49 and 8-50 show the relative displacement responses for the second order model (parameters from Table 8.19) and the actual responses (Figures 8-41 and 8-42). The model responses do not match the actual response as closely when residual deformation exists in the actual structure since the models cannot accumulate permanent deformation. However, peak responses in the model match the actual system response quite well. Figures 8-51 and 8-52 show the relative displacement responses for the third order model (parameters from Table 8.19) and the actual responses (Figures 8-41 and 8-42). Again, responses are not closely predicted by the model. However, peak responses of the model match the actual response very well.

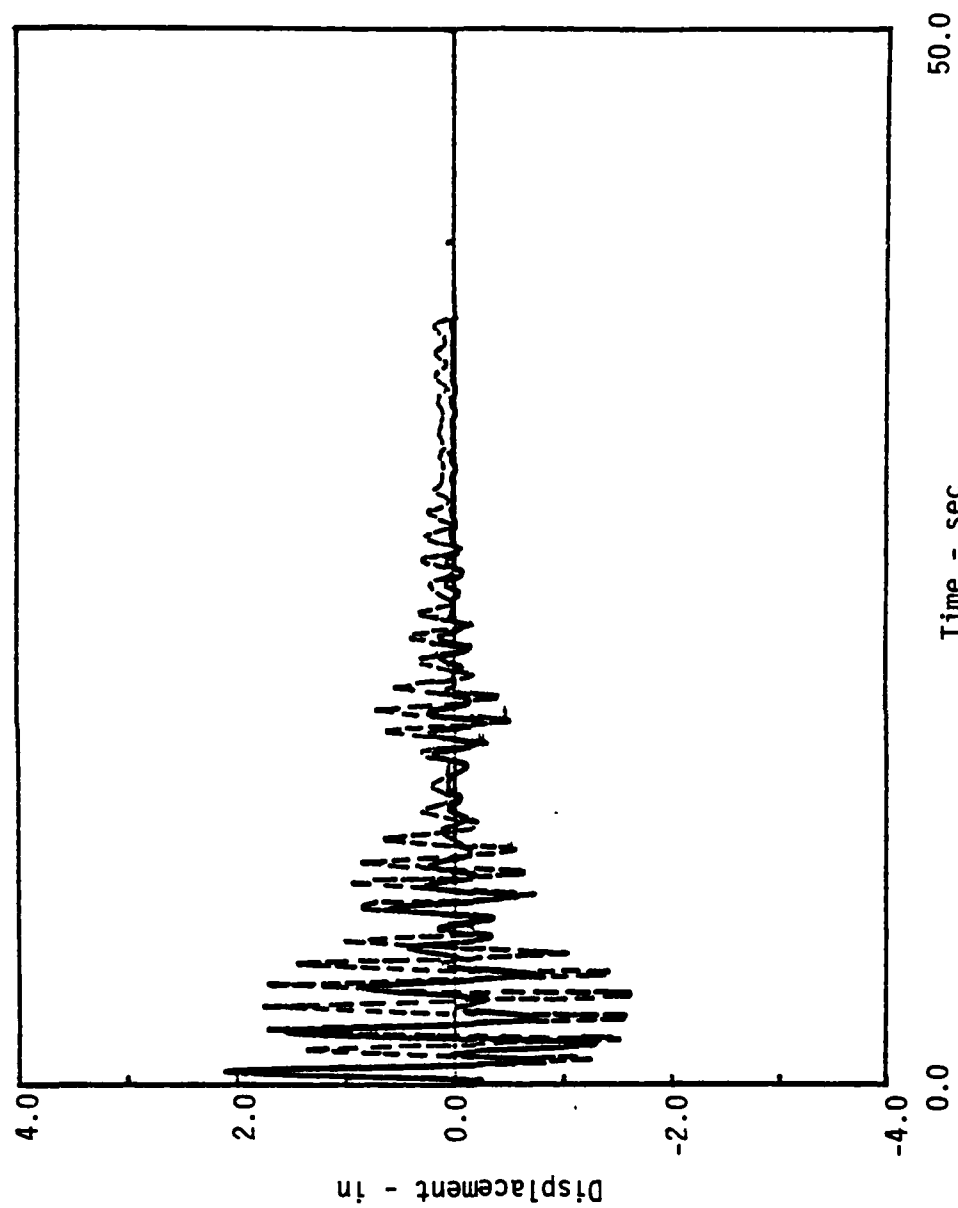


Figure 8-49. Comparison of second order model and actual relative displacement response between base and mass 1. (Case 2)

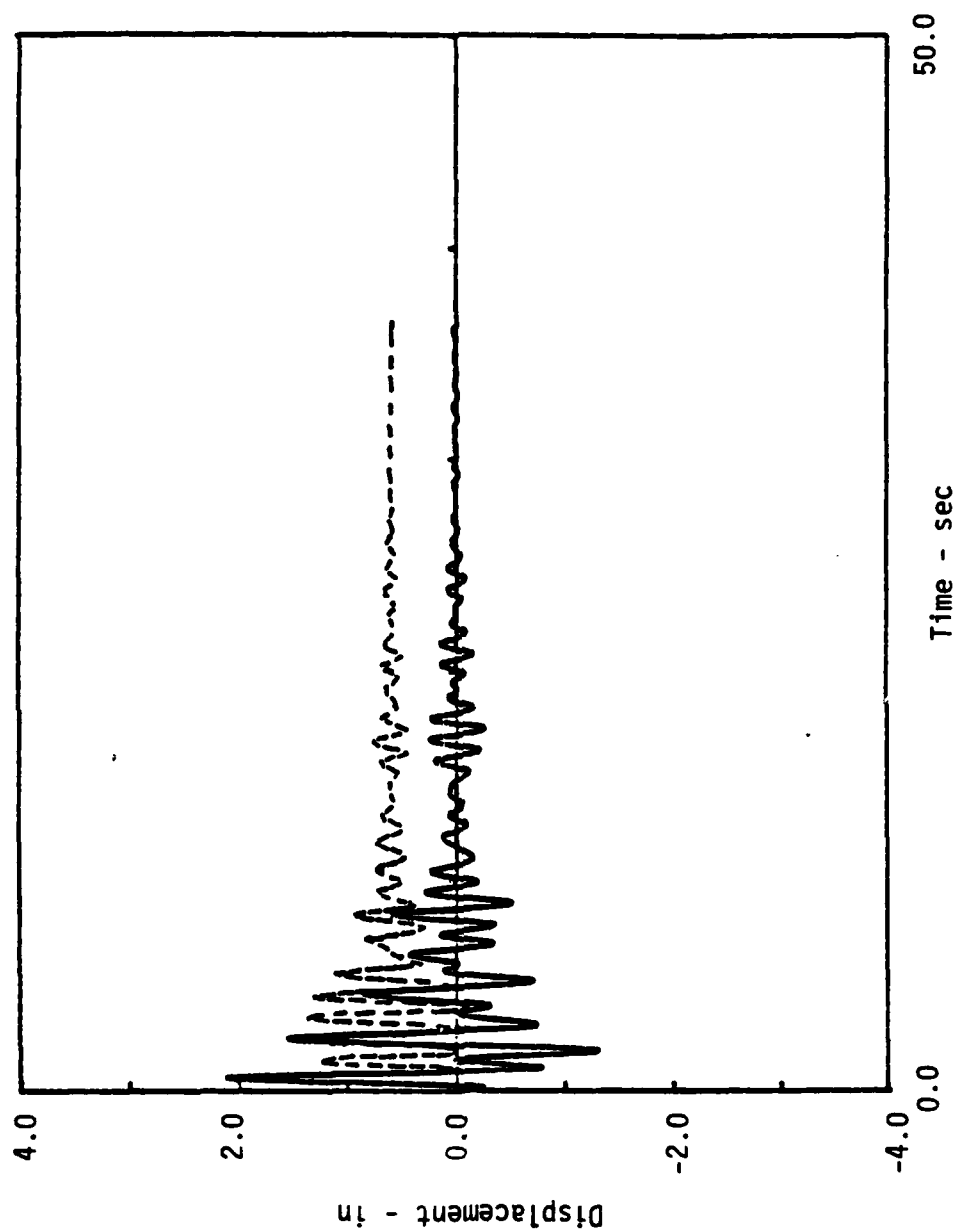


Figure 8-50. Comparison of second order model and actual relative displacement response between mass 1 and mass 2. (Case 2)

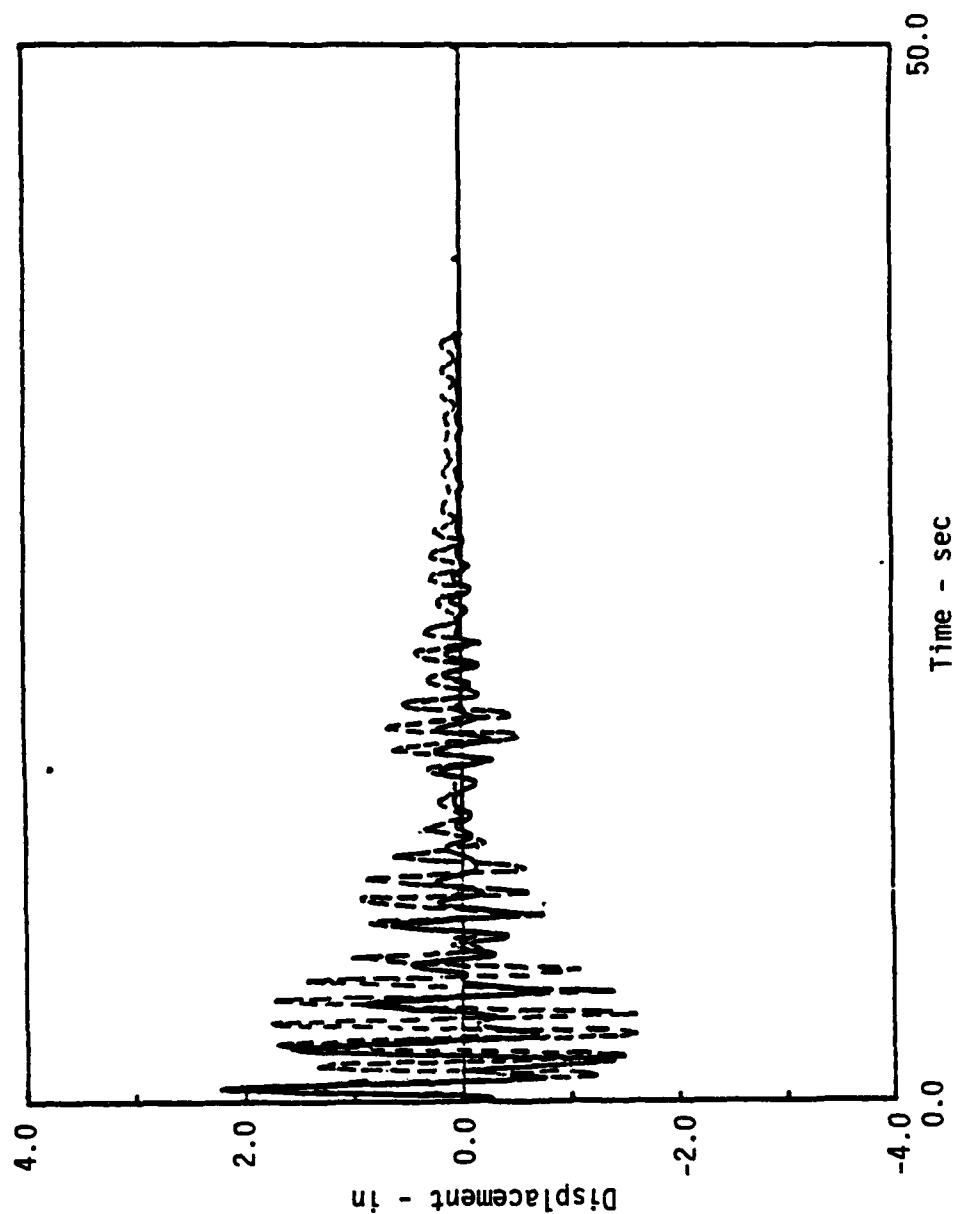


Figure 8-51. Comparison of third order model and actual relative displacement response between base and mass 1. (Case 2)

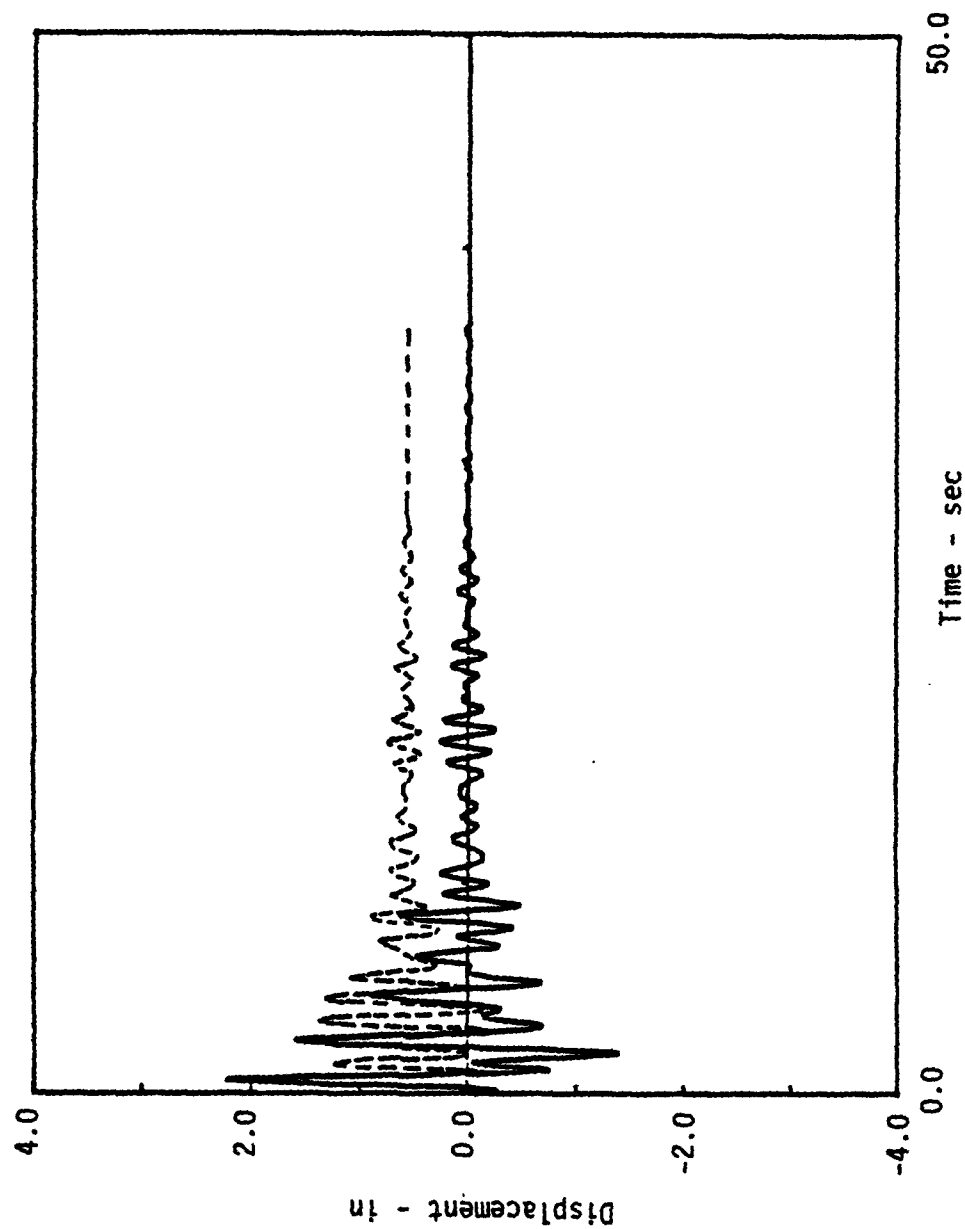


Figure 8-52. Comparison of third order model and actual relative displacement response between mass 1 and mass 2. (Case 2)

Consideration of the entire collection of results shows that the third order model provides the best simulation of nonlinear system behavior when the criteria of peak response and energy dissipated are used.

CHAPTER 9

SUMMARY AND CONCLUSIONS

The objective of this study was to develop approximate linear models for the simulation of inelastic system response and the measurement of damage accumulation in a structure. It was assumed that energy dissipated is related to the accumulation of damage. The model parameters were identified; then the energy dissipated during a strong motion was calculated. The displacement response and the energy dissipated in each model were compared with the displacement response and energy dissipated in the actual structure.

Three basic models were considered in this study. These are second and third order linear models with constant coefficients, and a second order linear model with time-varying parameters. The parameters of the models were estimated using two basic approaches, namely time domain and frequency domain approaches. The time domain approach was first introduced to estimate the model parameters by using the least squares method through which the modeling error is minimized with respect to the measured data. One reason for not using the time domain approach throughout this investigation is that the parameters identified using the time domain approach are inaccurate when noise signals are present.

Then, the frequency domain approach was used to identify the model parameters. In this approach, both analytical and search techniques were applied to find the system parameters. A good set of initial guesses of the parameters was an important concern when the search technique was used to execute the identification process.

Several numerical examples were solved, and some of them are summarized. Experience obtained in solving the numerical examples lead to the following conclusions.

- (1) Linear and nonlinear hysteretic SDF systems can, in some respects, be accurately modeled using second-and third-order linear differential equations with constant coefficients, and a second-order linear differential equation with time-varying coefficients. Specifically, the models provide accurate simulation when displacement response and energy dissipated criteria are used.
- (2) A direct, time domain approach can be used to identify model parameters when the force input and acceleration response measurements are not noisy.
- (3) The frequency domain approach can be used to identify model parameters of all three models when the force and response measurements are noisy.
- (4) The second order model with time-varying coefficients provides the best simulation of system response and energy dissipated among the three models considered.
- (5) The parameters of both single-degree-of-freedom (SDF) and multi-degree-of-freedom (MDF) systems can be identified. The numerical examples show that one and two degree-of-freedom systems can be identified. For the model presented in Chapter 6, it is anticipated that some difficulty would exist in identifying the parameters of a system with three or more degrees of freedom due to the number of parameters involved.
- (6) The energy dissipated in a structural system is related to system damage.

While the procedure developed in this investigation provides means for the simulation of response and the estimation of damage in inelastic structures, some improvements can be made. The systems considered in this study are one and two-degree-of-freedom; future investigations should include many degree-of-freedom structures. The models used in this study do not permit the accumulation of plastic deformation; future investigations should consider models that allow plastic deformation to accumulate. The tests that are summarized in Chapter 7 show that material damage is related to energy dissipated; future experiments should be performed, and a mathematical model characterizing the results should be developed. Finally, analyses should be performed to establish the spacial distribution of energy dissipated in actual structural members.

REFERENCES

1. Lutes, L. D., "Equivalent Linearization for Random Vibration," Journal of the Engineering Mechanics Division, ASCE, Vol. 96, No. 6M3, June 1970, pp. 227-242.
2. Lutes, L. D. and Hsieh, J., "High Order Equivalent Linearization in Random Vibration," Proceedings, Third Engineering Mechanics Division, Special Conference, Austin, Texas, September 17-19, 1979, pp. 60-63.
3. Wen, Y. K., "Stochastic Response Analysis of Hysteretic Structures," Proceedings of the Specialty Conference on Probabilistic Mechanics in Structural Reliability, ASCE, Tucson, Arizona, January 1979.
4. Wen, Y. K., "Method for Random Vibration of Hysteretic Systems," Journal of Engineering Mechanics, Div. Proc. of ASCE, Vol. 102, No. EM2, April 1976, pp. 249-263.
5. Baber, T. T. and Wen, Y. K., "Random Vibration of Hysteretic Degrading Systems," Journal of the Engineering Mechanics Division, ASCE Vol. 7, No. EM6, December 1981.
6. Baber, T. T. and Wen, Y. K., "Equivalent Linearization of Hysteretic Structures," Proceedings of the Specialty Conference on Probabilistic Mechanics and Structural Reliability, ASCE, Tucson, Arizona, January 1979.
7. Wafa, F., "Peak Response of Hysteretic Structures," Ph.D. Dissertation, Department of Civil Engineering, University of New Mexico, Albuquerque, NM, August 1981.
8. Paez, Thomas L., Ming-Liang Wang, and Ju, Frederick D., "Diagnosis of Damage in SDF Structures," University of New Mexico Research Rep., March 1982.
9. Udawadia, F. E. and Trifunac, M. D., "Time and Amplitude Dependent Response of Structures," Earthquake Engineering and Structural Dynamics, Vol. 2, 1974, pp. 359-378.
10. Iemura, H. and Jennings, D. C., "Hysteretic Response of a Nine-Story Reinforced Concrete Building," Earthquake Engineering and Structural Dynamics, Vol. 3, 1974, pp. 285-201.
11. Townsend, William H. and Hansen, Robert D., "Reinforced Concrete Connective Hysteresis Loops," Reinforced Concrete Structures in Seismic Zones, ACI Publication SP-53, 1974.

12. Uzumeri, S. M., "Strength and Ductility of Cast-in-Place Beam-Column Joints," Reinforced Concrete Structures in Seismic Zones, ACI Publication SP-53, 1974.
13. Yao, J. T. P., "Damage Assessment and Reliability Evaluation of Existing Structures," Journal of Engineering Structures, Vol. 1, October 1979, pp. 245-251.
14. Wiggins, H. H., Jr., and Moran, D. F., "Earthquake Safety in the City of Long Beach Based on the Concept of Balanced Risk," J. H. Wiggins Company, Redondo Beach, California, September 1971.
15. Culver, C. G., Lew, H. S., Hart, G. C., and Pinkham, C. W., "Natural Hazards Evaluation of Existing Buildings, National Bureau of Standards, Building Science Series No. 61, Jan. 1975.
16. Bresler, B., Anson, J. M., Comartin, C.D., and Thomases, D. E., "Practical Evaluation of Structural Reliability," Preprint 80-596, ASCE Convention, Florida, Oct. 27-31, 1980.
17. Ishizuka, M., Fu, K. S., and Yao, J. T. P., "SPERIL-I: Computer-Based Structural Damage Assessment System," Report No. CE-STR-81-36, School of Civil Engineering, Purdue University, Oct. 1981.
18. Ishizuka, M., Fu, K. S., and Yao, J. T. P., "Computer-Based Systems for the Assessment of Structural Damage," Presented at IABSE Colloquium on Informatics in Structural Engineering, Bergamo, Italy, 6-8 Oct. 1982.
19. Ishizuka, M., Fu, K. S., Yao, J. T. P., "Inference Method for the Damage Assessment of Existing Structures," Technical Report No. CE-STR-80-17, School of Civil Engineering, Purdue University, West Lafayette, IN, Oct. 1978.
20. Ang H-S., Wen, Y. K., "Prediction of Structural Damage under Random Earthquake Excitation," Earthquake Ground Motion and Its Effects on Structures, ASME, AMD, Vol. 53, November 1982.
21. Rudd, J. L., Yang, J. N., and Manning, S. D., "Damage Assessment of Mechanically Fastened Joints in the Small Crack Size Range," Proceeding of the Ninth U.S. National Congress of Applied Mechanics, Cornell University, June 21-25, 1982.

REFERENCES (Continued)

22. Yao, J. T. P., "Damage Assessment of Existing Structures," Journal of the Engineering Mechanics, ASCE, Vol. 106, No. EM4, August 1980, pp. 785-799.
23. Toussi, S., and Yao, J. T. P., "Identification of Hysteretic Behavior for Existing Structures," Technical Report No. CE-STR-80-19, School of Civil Engineering, Purdue University, West Lafayette, IN, December 1980.
24. Toussi, S., and Yao, J. T. P., "Hysteresis Identification of Multi-Story Buildings," Technical Report No. CE-STR-81-5, School of Civil Engineering, Purdue University, West Lafayette, IN, May 1981.
25. Chen, S. J. Hong, and Yao, J. T. P., "Damage Assessment of Existing Structures," Proceedings, Third ASCE EMD Specialty Conference, University of Texas, Austin, Texas, 17-19 September 1979, pp. 661-664.
26. Yao, J. T. P., Toussi, S., and M. A. Sozen, "Damage Assessment from Dynamic Response Measurements," Presented at the Symposium on Structural Reliability and Damage Assessment, Ninth U.S. National Congress of Applied Mechanics, Cornell University, Ithaca, NY, June 1982.
27. Astrom, K.J., and P. Eykhoff, "System Identification--A Survey," Automatica, Vol. 7, Pergamon Press, Great Britain, 1971, pp. 123-162.
28. Bekey, G. A., "System Identification--An Introduction and a Survey," Simulation, Oct. 1970, pp. 151-166.
29. Bowles, R. L. and T. A. Straeter, "System Identification of Vibrating Structures," ASME, 1972, pp. 23-44.
30. Collins, J. D., Young, J. P., and L. Keifling, "Methods and Application of System Identification in Shock and Vibration," System Identification of Vibrating Structures, ASME, New York, 1972, pp. 45-72.
31. Sage, A. P., "System Identification, Methodology, Future Prospects," System Identification of Vibrating Structures, ASME, 1972, pp. 1-21.
32. Rodeman, R. and J. T. P. Yao, "Structural Identification--Literature Review," School of Engineering, Purdue University, Tech. Report No. CE-STR-73-3, Dec. 1973.

33. Chen, S. H., "Methods of System Identification in Structural Engineering," Thesis, Purdue University, Aug. 1976.
34. Hart, G. C. and J. T. P. Yao, "System Identification in Structural Dynamics," *Journal of the Engineering Mechanics Division, ASCE*, Vol. 103, EM6, Dec. 1977, pp. 1089-1104.
35. Ting, E. C., Chen, S. J. H., and J. T. P. Yao, "System Identification, Damage Assessment and Reliability Evaluation of Structures," School of Engineering, Purdue Univ., Tech. Report NO. CE-STR-78-1, Feb. 1978.
36. Liu, S. C. and J. T. P. Yao, "Structural Identification Concept," *Journal of the Structural Division, ASCE*, Vol. 104, ST12, Dec. 1978, pp. 1845-1859.
37. Cole, H. A., Jr., "On-Line Failure Detection and Damping Measurement of Aerospace Structures by Random Decrement Signatures," NASA CR-2205, March 1973.
38. Cole, H. A., Jr., "A Method for Detecting Structural Deterioration in Bridges," N74-32346, Neilson Engineering and Research, July 1974.
39. Kennedy, C. C. and C. D. P. Pancu, "Use of Vectors in Vibration Measurement and Analysis," *Journal of the Aeronautical Sciences*, Vol. 14, No. 11, Nov. 1947, pp. 603-625.
40. Bert, C. W., "Material Damping: An Introductory Review of Mathematical Models, Measures, and Experimental Techniques," *Journal of Sound and Vibration*, Vol. 29, No. 2, pp. 129-153.
41. Bert, C. W., and R. R. Clary, "Evaluation of Experimental Methods for Determining Dynamic Stiffness and Damping of Composite Materials," ASTM Special Publication 546, 1974, pp. 250-264.
42. Bishop, R. E. D., and G. M. C. Gladwell, "An Investigation into the Theory of Resonance Testing," *Philosophical Transactions of the Royal Society of London, Series A*, Vol. 255, Mathematics and Physical Sciences, Jan. 1963, pp. 242-280.
43. Lewis, R. C., and D. L. Wrisley, "A System for the Excitation of Pure Natural Modes in Complex Structures," *Journal of the Aeronautical Sciences*, N. 1950, pp. 705-722.

REFERENCES (Continued)

44. Schiff, A. J., "Identification of Large Structures Using Data from Ambient and Low Level Excitations," System Identification of Vibrating Structures, ASME, 1972, pp. 87-120.
45. Smith, S. and A. A. Woods, Jr., "A Multiple Driver Technique for Vibration Testing of Complex Structures," The Shock and Vibration Bulletin, Jan. 1972.
46. Traill-Nash, R. W., "On the Excitation of Pure Natural Modes in Aircraft Resonance Testing," Journal of the Aerospace Sciences, Dec. 1958, pp. 775-777.
47. Nord, A. R., "Modal Analysis of Three Composite Flywheels," Tech. Report #SAND79-0459, Sandia Laboratories, Albuquerque, NM, April 1979.
48. Distefano, N., and A. Rath, "System Identification in Non-linear Structural Dynamics," Computer Methods in Applied Mechanics and Engineering, Vol. 5, 1975, pp. 353-372.
49. Distefano, N., and A. Rath, "Sequential Identification of Hysteretic and Viscous Models in Structural Seismic Dynamics," Computer Methods in Applied Mechanics and Engineering, Vol. 6, 1975, pp. 219-232.
50. Flannelly, W. G., and A. Berman, "The State of the Art of System Identification of Aerospace Structures," System Identification of Vibrating Structures, ASME, 1972, pp. 121-132.
51. Ibanez, P., "Identification of Dynamic Structural Models from Experimental Data," UCLA School of Engineering and Applied Science Report, UCLA 7225.
52. Ibanez, P., "Identification of Dynamic Parameters of Linear and Nonlinear Structural Models from Experimental Data," Nuclear Engineering and Design, Vol. 25, 1973, pp. 30-41.
53. Ibrahim, R. A. and A. D. S. Barr, "Parametric Vibration, Part I. Mechanics of Linear Problems," Shock and Vibration Digest, Naval Research Lab., Vol. 10, No. 2, Feb. 1978, pp. 15-22.
54. Ibrahim, R. A. and A. D. S. Barr, "Parametric Vibration, Part II. Mechanics of Nonlinear Problems," Shock and Vibration Digest, Naval Research Lab., Vol. 10, No. 3, March 1978, pp. 9-24.

REFERENCES (Continued)

55. Ibrahim, R.A., "Parametric Vibration, Part III. Current Problems (1)," Shock and Vibration Digest, Naval Research Lab., Vol. 10, No. 4, April 1978, pp. 41-57.
56. Ibrahim, R. A., "Parametric Vibration, Part IV. Current Problems (2)," Shock and Vibration Digest, Naval Research Lab., Vol. 10, No. 5, May 1978, pp. 19-34.
57. Ibrahim, R. A. and J. W. Roberts, "Parametric Vibration, Part V. Stochastic Problems," Shock and Vibration Digest, Naval Research Lab., Vol. 10, No. 6, June 1978, pp. 17-38.
58. Ibrahim, S.R. and E. C. Mikulick, "A Method for the Direct Identification of Vibration Parameters from the Free Response," The Shock and Vibration Bulletin, Naval Research Lab., Sept. 1977, pp. 183-198.
59. Milne, R. D. and A. Simpson, "Reconciliation of Calculated and Measured Natural Frequencies and Normal Modes," Journal of Sound and Vibration, Vol. 30, No. 1, 1973, pp. 45-63.
60. Raggett, J. D., "Estimating Damping of Real Structures," Journal of the Structural Division, ASCE, Vol. 101, ST9, Sept. 1975, pp. 1823-1835.
61. Udawadia, F. E. and P. C. Shaw, "Identification of Structures Through Records Obtained During Strong Earthquake Ground Motion," Journal of Engineering for Industry, Vol. 98, Nov. 1976, pp. 1347-1262.
62. Wells, W. R., "Application of Modern Parameter Estimation Methods to Vibrating Structures," The Shock and Vibration Bulletin, Naval Research Lab., Sept. 1977, pp. 155-159.
63. Brieman, L., Prabability and Stochastic Processes: With a View Toward Applications, Houghton Mifflin, Boston, 1969.
64. Caravani, P. and W. T. Thomson, "Identification of Damping Coefficients in Multidimensional Linear Systems," Journal of Applied Mechanics, Trans. of the ASME, Vol. 44, No. 1, March 1977, pp. 135-140.
65. Caravani, P. and W. T. Thomson, "Identification of Damping Coefficients in Multidimensional Linear Systems," Journal of Applied Mech nics, Trans. of the ASME, Vol. 41, No. 2, June 1974, pp. 379-383.

REFERENCES (Continued)

66. Wang, M. L., Paez, T. L., Ju, F. D., "Mathematical Models for Damageable Structures," The Bureau of Engineering Research, The University of New Mexico, Albuquerque, NM, February 1983.
67. Wang, M. L., Paez, T. L., Ju, F. D., "Models for Damage Diagnoses in SDF Structures," Proceedings of the Symposium on The Interaction of Non-Nuclear Munitions with Structures, Colorado Springs, CO, May 1983.
68. Kandianis, F., "Frequency Response of Structures and the Effects of Noise on Its Estimates from the Transient Response," Journal of Sound and Vibration, Vol. 15, No. 2, 1971, pp. 203-215.
69. Spooner, D. C. and Dougill, J. W., "A Quantitative Assessment of Damage Sustained in Concrete during Compressive Loading," Magazine of Concrete Research, Vol. 27, No. 92, September 1975, pp. 151-160.
70. Spooner, D. C., Pomeroy, C. D., and Dougill, J. W., "Damage and Energy Dissipation in Cement Pastes in Compression," Magazine of Concrete Research, Vol. 28, No. 94, March 1976, pp. 21-29.
71. Karsan, I. Demir and Jirsa, James D., "Behavior of Concrete under Compressive Loading," Journal of the Structural Division, ASCE, December 1969.
72. Distefano, N. and B. Pena-Pardo, "System Identification of Frames Under Seismic Loads," Journal of the Engineering Mechanics Division, ASCE, December 1969.
73. Engels, R. C. and L. Meirovitch, "Response of Periodic Structures by Modal Analysis," Journal of Sound and Vibration, Vol. 56, No. 4, 1978, pp. 481-493.
74. Bendat, J. S., "Solutions for the Multiple Input-Output Problem," Journal of Sound and Vibration, Vol. 44, No. 3, 1976, pp. 311-325.
75. Bendat, J. S., "System Identification from Multiple Input/Output Data," Journal of Sound and Vibration, Vol. 49, No. 3, 1976, pp. 293-308.
76. Murakami, H. and J. E. Luco, "Seismic Response of a Periodic Array of Structures," Journal of the Engineering Mechanics Division, ASCE, Vol. 103, EM5, Oct. 1977, pp. 965-977.

REFERENCES (Concluded)

77. Mustain, R. W., "Survey of Modal Vibration Test/Analysis Techniques," Society of Automotive Engineers, Aerospace Engineering and Manufacturing Meeting, San Diego, Dec. 1976.
78. Newland, D. E., An Introduction to Random Vibration and Spectral Analysis, Longman Publishing, 1976.
79. Jenkins, G. M. and D. G. Watts, Spectral Analysis and Its Applications, Holden Day, San Francisco, 1969.
80. Hoel, P. G., S. C. Port, and C. J. Stone, Introduction to Stochastic Processes, Houghton Mifflin, Boston, 1972.
81. Lin, Y. K., Probabilistic Theory of Structural Dynamics, Krieger Publishing, Huntington, NY, 1976.
82. Karel Rektorys, Editor, Survey of Applicable Mathematics, The MIT Press, Cambridge, MA, 1969.

APPENDIX

COMPUTER PROGRAMS

```

C
C
C *****
C *          PROGRAM "BILIN"          *
C *****
C
C SN: EXCITATION NOISE
C RN: RESPONSE NOISE
C MAXIMUN DISPLACEMENT EAQUL TO 6.7
C INDEX=1 MEANS NOISE PRESENTED
C
C DIMENSION SF(1024),DD(1024),SN(1024),RN(1024)
C DIMENSION AA(1024),RESF(1024),SK1(1024),SPI(1024)
C CALL OPSYS('ALLOC','RH1',10)
C CALL OPSYS('ALLOC','FD1',15)
C CALL OPSYS('ALLOC','RH2',25)
C INDEX=1
C N=1024
C SM=1.0
C SC=1.256637
C SK=39.48
C YSTI=0.0
C YDIS=4.0
C DT=0.05
C READ(10,50) (SF(I),SN(I),I=1,N)
C READ(25,55) (RN(I),I=1,N)
C CALL BILIN(SF,SC,SM,SK,YSTI,YDIS,DT,N,DD,ENED,SPI)
C IF(INDEX.EQ.1) GO TO 45
C DO 12 I=1,N
C   T=DT*(I-1)
C   RESF(I)=SF(I)-SM*AA(I)
C   WRITE(15,50)T,DD(I)
12 CONTINUE
C   GO TO 60
45 DO 40 I=1,N
C   T=DT*(I-1)
C   SF(I)=SF(I)+SN(I)
C   DD(I)=DD(I)+RN(I)
40 WRITE(15,50)T,DD(I)
50 FORMAT(2E12.4)
55 FORMAT(E12.4)
60 WRITE(6,*)ENED,ENED1,ENED2
C STOP
C END
C
C SUBROUTINE FOR GENERATING THE BILINEAR
C HYSTERETIC SYSTEM.
C C7 : DAMPING
C SM7: MASS
C SK7: STIFFNESS
C A7 : YIELDING STIFFNESS
C V7 : YIELDING DISPLACEMENT
C D9 : TIME INCREMENT

```

```

C      V : OUTPUT DISPLACEMENT
C      V1 : OUTPUT VELOCITY
C      V0 : OFFSET DISPLACEMENT
C      V2 : OUTPUT ACCELERATION
C      ENED:ENERGY DISSIPATED
C      SPI:SPRING RESTORING FORCE
C      ENED1:TOTAL SPRING ENERGY DISSIPATED
C      ENED2:TOTAL DAMPING ENERGY DISSIPATED
C
      SUBROUTINE BILIN(F,C7,SM7,SK7,A7,V7,D9,N,V,ENED,SPI)
      DIMENSION V(N),V0(1024),V1(1024),V2(1024),F(N)
      DIMENSION SPI(1024)
      U7=SK7*V7
      SK9=1.0-A7/SK7
C
C      INITIALIZE VARIABLES
C
      V(1)=0.
      V0(1)=0.
      V1(1)=0.
      V2(1)=F(1)/SM7
C
C      START THE RESPONSE CYCLE
C
      Q1=6.0*SM7/D9**2
      Q2=3.0*C7/D9
      Q3=6.0*SM7/D9
      Q4=3.0*SM7
      Q5=3.0*C7
      Q6=0.5*D9*C7
      Q7=3.0/D9
      Q8=3.0
      Q9=0.5*D9
      SK8=SK7
      NM=N-1
      ENED=0.0
      ENED1=0.0
      ENED2=0.0
      DO 1199 I=1,NM
      I1=I+1
      U1=Q1+Q2+SK8
      U2=Q3*V1(I)+Q4*V2(I)
      U3=Q5*V1(I)+Q6*V2(I)
      V5=(F(I1)-F(I)+U2+U3)/U1
      V6=Q7*V5-Q8*V1(I)-Q9*V2(I)
      V(I1)=V(I)+V5
      V1(I1)=V1(I)+V6
C
C      COMPUTE THE STIFFNESS AT T+DT
C
      X0=SK7*(V(I1)-V0(I))
      X1=A7*(V(I1)-V7)+U7

```

```

      X2=A7*(V(I1)+V7)-U7
      IF(X0.GT.X1)GO TO 1150
      IF(X0.LT.X2)GO TO 1160
      SK8=SK7
      V0(I1)=V0(I)
      GO TO 1170
1150  IF (V1(I1).GT.0.0)SK8=A7
      IF (V1(I1).LE.0.0)SK8=SK7
      V0(I1)=(V(I1)-V7)*SK9
      GO TO 1170
1160  IF (V1(I1).LT.0.0)SK8=A7
      IF (V1(I1).GE.0.0)SK8=SK7
      V0(I1)=SK9*(V(I1)+V7)
1170  SPI(I1)=SK7*(V(I1)-V0(I1))
      V2(I1)=(F(I1)-C7*V1(I1)-SPI(I1))/SM7
      ENED=ENED+D9*0.5*(V1(I)*(F(I)-SM7*V2(I))+V1(I)*
+ (F(I)-SM7*V2(I)))
      ENED1=ENED1+D9*0.5*(V1(I)*SPI(I)+V1(I1)*SPI(I1))
      ENED2=ENED2+D9*0.5*(V1(I)*C7*V1(I)+V1(I1)*C7*V1(I1))
1199  CONTINUE
      RETURN
      END

```

C
C
C
C
C
C
C
C
C
C
C

```

*****
*          PROGRAM " TIMEVA "          *
*****

```

```

SOLVE FOR THE SECOND O.D.E.
(TIME VARIED PARAMETERS)
SN: INPUT NOISE
YN: RESPONSE NOISE
ALPHA: TIME VARIED COEFFICIENT FOR K
BATA: TIME VARIED COEFFICIENT FOR C

```

```

      READ(5,*) CO,AKO,ALPHA,BATA
      CALL OPSYS('ALLOC','RH1',15)
      CALL OPSYS('ALLOC','RH3',65)
      CALL OPSYS('ALLOC','RH2',13)
      CALL OPSYS('ALLOC','ID3',67)
      DIMENSION DY(2),Y(2),F(42),SN(1024),YN(1024)
      DIMENSION SF(1024),TS(1024),S(1024),INDEX(1024)
      DIMENSION Y3(1024),V(1024)
      EXTERNAL SPLINE
      COMMON /ARRAY/ TS,SF,S,INDEX
      NTS=1024
      DT=0.05
      READ(15,8) (SF(I),SN(I),I=1,NTS)
      READ(13,33) (YN(I),I=1,NTS)
      DO 2 I=1,NTS
      TS(I)=DT*(I-1)
2  CONTINUE

```



```

      CALL SPCOEF(NTS,TS,SF,S,INDEX)
      SM=1.0
      N=2
      TT=NTS*DT
      T=0.0
      Y(1)=0.
      Y(2)=0.0
      ENER=0.0
10  L=3
      M=0
50  CALL RUNGE(T,DT,N,Y,DY,F,L,M,J)
      IF(M-1)75,10,75
75  GO TO (100,200,999),L
100 FQ=-FF(T)
      DY(1)=Y(2)
      DY(2)=- (1.+ALPHA*T)*AKO*Y(1)- (1.+BATA*T)*CO*Y(2)+FQ
      GO TO 50
200 I=T/DT+1.1
      Y3(I)=(1.+ALPHA*T)*AKO*Y(1)+(1.+BATA*T)*CO*Y(2)
      V(I)=Y(2)
      IF((I-1).EQ.0) GO TO 111
      ENER=ENER+DT*0.5*((Y3(I)*V(I))+(Y3(I-1)*V(I-1)))
      GO TO 250
111 ENER=DT*0.5*(Y3(1)*V(1))

C
C      NOISE CASE
C
C 112 SF(I)=SF(I)+SN(I)
C      YKK=Y(1)+YN(I)
250 WRITE(65,800)Y(1),Y3(I)
      IF(T-TT)260,999,999
260 GO TO 50
800 FORMAT(2E12.4)
      8 FORMAT(2E12.4)
      33 FORMAT(E12.4)
999 WRITE(6,*) ENER
      STOP
      END

C
C      REAL FUNCTION FF
C
      FUNCTION FF(T)
      DIMENSION TT(1024),FT(1024),SS(1024),INDE(1024)
      COMMON /ARRAY/ TT,FT,SS,INDE
      N=1024
      QA=SPLINE(N,TT,FT,SS,INDE,T)
      FF=QA
      RETURN
      END

C
C      SOLVING N-TH ORDER ODE
C

```

```

SUBROUTINE RUNGE(T,DT,N,Y,DY,F,L,M,J)
DIMENSION DY(2),Y(2),F(42)
GO TO (100,110,300),L
100 GO TO (101,110),IG
101 J=1
L=2
DO 106 K =1,N
K1=K+3*N
K2=K1+N
K3=N+K
F(K1)=Y(K)
F(K3)=F(K1)
106 F(K2)=DY(K)
GO TO 406
110 DO 140 K=1,N
K1=K
K2=K+5*N
K3=K2+N
K4=K+N
GO TO (111,112,113,114),J
111 F(K1)=DY(K)*DT
Y(K)=F(K4)+.5*F(K1)
GO TO 140
112 F(K2)=DY(K)*DT
GO TO 124
113 F(K3)=DY(K)*DT
GO TO 134
114 Y(K)=F(K4)+(F(K1)+2.*(F(K2)+F(K3))+DY(K)*DT)/6.
GO TO 140
124 Y(K)=.5*F(K2)
Y(K)=Y(K)+F(K4)
GO TO 140
134 Y(K)=F(K4)+F(K3)
140 CONTINUE
GO TO (170,180,170,180),J
170 T=T+.5*DT
180 J=J+1
IF(J-4)404,404,299
299 M=1
GO TO 406
300 IG=1
GO TO 405
404 IG=2
405 L=1
406 RETURN
END

```

C
C
C
C
C
C

```

*****
*          PROGRAM " URAND"          *
*****

```

```

C      THIS PROGRAM IS FOR GENERATING THE RANDOM SIGNAL
C
      CALL OPSYS('ALLOC','RH2',66)
      CALL OPSYS('ALLOC','RH1',65)
      CALL OPSYS('ALLOC','RH4',77)
      REAL*8 URAND
      REAL S(1024),SS(1024),DS(1024),T(1024),TPF(1024)
      REAL EPS(1024),SF(1024),OUN(1024),RENOI(1024)
      DIMENSION PS(1024),IND(1024),PHI(1024)
      DOUBLE PRECISION FD(1024)
      EXTERNAL URAND

C      INITIALIZATION
C      WHEN INDEX=1 SHOWS NO DERIVATIVE FOR FORCE,
C      OTHERWISE WILL GO TO DERIVATIVE INCLUDING NOISE
C
      RATIO : NOISE/SIGNAL RATIO
      S(I)  : FORCE
      DS(I) : DERIVATIVE OF THE FORCE
      SF(I) : FORCE + NOISE
      FD(I) : DERIVATIVE OF (FORCE+NOISE)
      ZETA  : DAMPING OF THE SYSTEM
      ALPHA : DECAY RATIO
      NT    : TOTAL NUMBER OF POINT
      FN     : NATURAL FREQUENCY
      NF     : NUMBER OF POINT IN THE FREQUENCY BAND
      INDEX=0
      RATIO=0.0036
      ZETA=0.1
      DT=0.05
      NF=50
      NT=1024
      NN=NT+1
      NSEED=0
      ALPHA=0.1
      C=10.0
      PI=4.000*DATAN(1.000)
      FN=2.*PI

C      CALCULATE THE FREQUENCY AND TIME
C
      F1=FN-(2.*ZETA*FN)
      IF(F1.LT.0.0) F1=0.0
      F2=FN+(2.*ZETA*FN)
      FB=F2-F1
      DF=(F2-F1)/NF
      F3=F1-(DF/2.0)

C      S1: VARIANCE OF THE FORCE NOISE
C      S2: VARIANCE OF THE OUTPUT NOISE
C
      S1=FB*RATIO*C*C/(2.*DF)

```

```

      S2=PI*RATIO*C*C/(8.*DF*(FN**3)*ZETA)
      DO 8 K=1,NF
      TPF(K)=F3+(K*DF)
      PHI(K)=2.*PI*URAND(NSEED)
8     CONTINUE
      DO 9 J=1,NT
      T(J)=(J-1)*DT
9     CONTINUE
C
C     GENERATE THE EXCITATION AND ITS FIRST DERIVATIVES
C
      DO 11 J=1,NT
      S(1)=0.
      SS(1)=0.
      DO 11 K=1,NF
      S(J)=S(J)+1.*C*COS(TPF(K)*T(J)-PHI(K))
      SS(J)=SS(J)+1.*C*TPF(K)*SIN(TPF(K)*T(J)-PHI(K))
11    CONTINUE
      DO 12 J=1,NT
      S(J)=S(J)*EXP(-ALPHA*T(J))
      DS(J)=-SS(J)*EXP(-ALPHA*T(J))-S(J)*ALPHA
12    CONTINUE
C
C     GENERATE THE RANDOM EXCITATION INCLUDES NOISE.
C     OUN:FORCE NOISE, EPS: RESPONSE NOISE.
C
      CALL NOISE(OUN,NN,S1,1)
      CALL NOISE(RENOI,NN,S2,2)
      CALL NOISE(EPS,NN,S2,NSEED)
      IF(INDEX.EQ.1) GO TO 40
C     FD(1)=0.0
C     DO 15 I=2,NT
C     FD(I)=DS(I)+(OUN(I+1)-OUN(I-1))/(2.0*DT)
C 15    CONTINUE
35    DO 38 J=1,NT
38    WRITE(65,22) S(J),DS(J)
      GO TO 18
40    DO 42 I=1,NT
      WRITE(77,21)RENOI(I)
      WRITE(66,21)EPS(I)
42    WRITE(65,13)S(I),OUN(I)
13    FORMAT(2E12.4)
17    FORMAT(9X,'TIME',11X,'FORCE',1X,'FIRST DERIVATIVE',/)
21    FORMAT(1E12.4)
22    FORMAT(2E12.4)
18    STOP
      END
C
      SUBROUTINE NOISE(DPS,N,S2,NSEED)
C
C     THIS SUBROUTINE GENERATES A SEQUENCE OF WHITE NOISE

```

```

C      IT'S LENGTH IS N, MEAN ZERO, VARIANCE S2
C
      REAL*8 URAND
      REAL X(12),DPS(N)
      C=SQRT(S2)
      DPS(1)=0.0
      DO 2 I=2,N
      DPS(I)=0.0
      DO 1 J=1,12
      X(J)=URAND(NSEED)
1     DPS(I)=DPS(I)+X(J)
2     DPS(I)=(DPS(I)-6.0)*C
      RETURN
      END
      REAL FUNCTION URAND*8(IY)
      INTEGER IY

C
C      URAND IS A UNIFORM NUMBER GENERATOR BASED ON THE
C      THEORY AND SUGGESTIONS GIVEN IN D.E. KNUTH (1969).
C
      INTEGER IA,IC,ITWO,M2,M,MIC
      DOUBLE PRECISION HALFM
      REAL S
      DOUBLE PRECISION DATAN,DSQRT
      DATA M2/0/,ITWO/2/
      IF (M2 .NE. 0) GO TO 20

C
C      IF FIRST ENTRY, COMPUTE MACHINE INTEGER
C      WORD LENGTH.
C
      M = 1
10    M2 = M
      M = ITWO*M2
      IF (M .GT. M2) GO TO 10
      HALFM = M2

C
C      COMPUTE MULTIPLIER AND INCREMENT FOR
C      LINEAR CONGRUENTIAL METHOD
C
      IA = 8*IDINT(HALFM*DATAN(1.DO)/8.DO) + 5
      IC = 2*IDINT(HALFM*(0.5DO-DSQRT(3.DO)/6.DO)) + 1
      MIC = (M2 - IC) + M2

C
C      S IS THE SCALE FACTOR FOR CONVERTING TO
C      FLOATING POINT.
C
      S = 0.5/HALFM

C
C      COMPUTE NEXT RANDOM NUMBER
C
20    IY = IY*IA
C

```

```

C      THE FOLLOWING STATEMENT IS FOR COMPUTERS WHICH
C      DO NOT ALLOW INTEGER OVERFLOW ON ADDITION
C
C      IF (IY .GT. MIC) IY = (IY - M2) - M2
C
C      IY = IY + IC
C
C      THE FOLLOWING STATEMENT IS FOR COMPUTERS WHERE
C      THE WORD LENGTH FOR ADDITION IS GREATER THAN
C      FOR MULTIPLICATION
C
C      IF (IY/2 .GT. M2) IY = (IY - M2) - M2
C
C      THE FOLLOWING STATEMENT IS FOR COMPUTERS WHERE
C      INTEGER OVERFLOW AFFECTS THE SIGN BIT
C
C      IF (IY .LT. 0) IY = (IY + M2) + M2
C      URAND = FLOAT(IY)*S
C      RETURN
C      END
C
C
C      *****
C      *                PROGRAM " BLNMDF"                *
C      *****
C
C      THIS PROGRAM GENERATE THE MDF BILINEAR
C      HYSTERETIC STRUCTURE RESPONSE
C
C      N      : NUMBER OF DEGREE OF FREEDOM
C      NT     : NUMBER OF TIME STEP
C      DT     : TIME INCREMENT
C      MC(I)  : MASS FOR EACH DEGREE OF FREEDOM
C      CC(I)  : DAMPING FOR EACH DEGREE OF FREEDOM
C      KC(I)  : STIFFNESS FOR THE SYSTEMS
C      AC(I)  : YIELD STIFFNESS
C      ZOI(I) : INITIAL DISPLACEMENT
C      ZOF(I) : FINAL DISPLACEMENT
C      Z1I(I) : INITIAL VELOCITY
C      Z1F(I) : FINAL VELOCITY
C      Z2F(I) : FINAL VELOCITY
C      PSF(I) : FINAL PERMANENT DISPLACEMENT
C
C      CALL OPSYS('ALLOC','MDF1',10)
C      CALL OPSYS('ALLOC','MDF2',20)
C      CALL OPSYS('ALLOC','RH1',23)
C      CALL OPSYS('ALLOC','RH2',25)
C      CALL OPSYS('ALLOC','RH3',40)
C      CALL OPSYS('ALLOC','RH4',46)
C      DIMENSION DUMV1(2),DUMV2(2),DUMM1(2,2),DUMM2(2,2)
C      DIMENSION DLO(2),DL1(2),RU(2),RL(2),PSI(2),YD(2)

```

```

DIMENSION CC(2),AC(2),Q(2),PSF(2),FF(1024),RN(1024)
DIMENSION CM(2,2),RV(2),DZO(2),DZ1(2),DZ2(2)
DIMENSION ZOI(2),Z1I(2),Z2I(2),F(1024,2),ZOF(2)
DIMENSION A1(2,2),A2(2,2),A3(2,2),A4(2),A5(2)
DIMENSION AKMC(2),AMC(2),AKC(2),AMM(2,2),AKM(2,2)
DIMENSION A11(2,2),A22(2),ZM(2),ZS(2),ZN(2),ZT(2)
DIMENSION A11I(2,2),ENED1(1024),ENED2(1024),DN(1024)
DIMENSION Z1F(2),Z2F(2),FN(1024)

```

C
C
C

```
INOISE=1 MEANS NOISE INCLUDED
```

```

INOISE=0
N=2
NT=1024
DT=0.05
AMC(1)=1.0
AMC(2)=1.0
CC(1)=1.256
CC(2)=1.256
AKC(1)=39.48
AKC(2)=39.48
AC(1)=0.0
AC(2)=0.0
ZOI(1)=0.0
ZOI(2)=0.0
Z1I(1)=0.0
Z1I(2)=0.0
YD(1)=1.2
YD(2)=1.0
N1=NT-1
ENED1(1)=0.0
ENED2(1)=0.0

```

C
C
C
C
C

```

READ THE FORCE VECTOR
FN(I): INPUT NOISE
RN(I): RESPONSE NOISE

```

```

READ(23,33)(FF(I),FN(I),I=1,NT)
READ(25,35)(RN(I),I=1,NT)
READ(46,35)(DN(I),I=1,NT)
33 FORMAT(2E12.4)
35 FORMAT(E12.4)
DO 30 I=1,NT
F(I,1)=0.0
30 F(I,2)=FF(I)

```

C
C
C

```
FORM THE MM AND CM MATRICES
```

```

DO 1111 I=1,N
DO 1111 J=1,N
AKM(I,J)=0.
AMM(I,J)=0.

```

```

1111 CM(I,J)=0.
C
C   FORM MASS MATRIX
C
      DO 1112 I=1,N
1112 AMM(I,I)=AMC(I)
C
C   FORM DAMPING MATRIX
C
      DO 1113 I=1,N
      IP=I+1
      CM(I,I)=CC(I)
      IF(I.EQ.N)GO TO 1113
      CM(I,I)=CM(I,I)+CC(IP)
      CM(I,IP)=-CC(IP)
      CM(IP,I)=-CC(IP)
1113 CONTINUE
C
C   FORM CONSTANTS VECTORS AND MATRICES
C   FOR ITERATION.
C
      CD1=DT/2.0
      CD2=6.0/DT
      CD3=6.0/(DT**2)
      CD4=3.0/DT
      D1=DT/2.0
      D2=DT*DT/6.0
      D3=DT*DT/2.0
      DO 1119 I=1,N
      A4(I)=AC(I)/(AKC(I)-AC(I))
      A5(I)=(AKC(I)-AC(I))/AKC(I)
      DO 1119 J=1,N
      A1(I,J)=AMM(I,J)+D1*CM(I,J)
      A2(I,J)=DT*CM(I,J)
1119 CONTINUE
C
C   INVERSE THE MASS MATRIX
C
      CALL MATINV(AMM,A3,N)
C
C   INITIATE KM AND RESPONSE VECTORS
C
      DO 1130 I=1,N
      IP=I+1
      AKM(I,I)=AKC(I)
      IF(I.EQ.2) GO TO 1130
      AKM(I,I)=AKM(I,I)+AKC(IP)
      AKM(I,IP)=-AKC(IP)
      AKM(IP,I)=-AKC(IP)
1130 CONTINUE
C
C   SET INITIAL CONDITIONS

```



```

C
      DO 1132 I=1,N
      ZOI(I)=0.
      Z1I(I)=0.
1132  PSI(I)=0.
      DO 1133 I=1,N
1133  DUMV1(I)=F(1,I)
C
C      FIND INITIAL ACCELERATION Z2I
C
      CALL MVM(A3,DUMV1,Z2I,N)
C
C      WRITE INITIAL VALUES
C
      WRITE(6,3)
      T=0.0
      WRITE(40,100) FF(1)
      WRITE(10,14)(ZOI(I),I=1,N)
      WRITE(20,14)(PSI(I),I=1,N)
C
C      START THE RESPONSE COMPUTATION
C
      DO 8999 IND=1,N1
      T=IND*DT
C
C      COMPUTE DZ2
C
      DO 1121 I=1,N
      DO 1121 J=1,N
1121  DUMM1(I,J)=A1(I,J)+D2*AKM(I,J)
      CALL MATINV(DUMM1,DUMM2,N)
      DO 1212 I=1,N
      DO 1212 J=1,N
1212  DUMM1(I,J)=A2(I,J)+D3*AKM(I,J)
      CALL MVM(DUMM1,Z2I,DUMV1,N)
      DO 1213 I=1,N
      DO 1213 J=1,N
1213  DUMM1(I,J)=DT*AKM(I,J)
      CALL MVM(DUMM1,Z1I,DUMV2,N)
      DO 1214 I=1,N
1214  DUMV1(I)=-(DUMV1(I)+DUMV2(I))+
      +(F(IND+1,I)-F(IND,I))
      CALL MVM(DUMM2,DUMV1,DZ2,N)
C
C      COMPUTE DZ1 AND DZ0
C
      DO 1221 I=1,N
      DZ1(I)=DT*Z2I(I)+DZ2(I)*D1
1221  DZ0(I)=D3*Z2I(I)+D2*DZ2(I)+DT*Z1I(I)
C
C      COMPUTE Z1F AND ZOF
C

```

```

C      DO 100 I=1,N
C      DO 100 J=1,N
C 100  A11(I,J)=AKM(I,J)+CD3*AMM(I,J)+CD4*CM(I,J)
C      DO 110 I=1,N
C      ZM(I)=CD2*Z1I(I)+3.0*Z2I(I)
C      ZS(I)=3.0*Z1I(I)+CD1*Z2I(I)
C 110  CONTINUE
C      CALL MVM(AMM,ZM,ZN,N)
C      CALL MVM(CM,ZS,ZT,N)
C      DO 120 I=1,N
C 120  A22(I)=F(IND+1,I)-F(IND,I)+ZN(I)+ZT(I)
C      CALL MATINV(A11,A11I,N)
C      CALL MVM(A11I,A22,DZO,N)
C      DO 140 I=1,N
C 140  DZ1(I)=CD4*DZO(I)-3.0*Z1I(I)-CD1*Z2I(I)
C      DO 1231 I=1,N
C      Z1F(I)=Z1I(I)+DZ1(I)
C 1231 ZOF(I)=Z0I(I)+DZO(I)
C
C      COMPUTE THE END OF STEP KM MATRIX
C
C      DLO(1)=ZOF(1)
C      DL1(1)=Z1F(1)
C      IF(N.EQ.1)GO TO 1245
C      DO 1241 I=2,N
C      DLO(I)=ZOF(I)-ZOF(I-1)
C 1241 DL1(I)=Z1F(I)-Z1F(I-1)
C 1245 CONTINUE
C      DO 1251 I=1,N
C      RU(I)=AKC(I)*(A4(I)*PSI(I)+YD(I))
C 1251 RL(I)=AKC(I)*(A4(I)*PSI(I)-YD(I))
C      DO 1272 I=1,N
C      QCC=AKC(I)*(DLO(I)-PSI(I))
C      IF(QCC.GT.RU(I))GO TO 1258
C      IF(QCC.LT.RL(I))GO TO 1265
C      AKMC(I)=AKC(I)
C      PSF(I)=PSI(I)
C      GO TO 1271
C 1258 IF(DL1(I).LE.0.)GO TO 1260
C      AKMC(I)=AC(I)
C      GO TO 1261
C 1260 AKMC(I)=AKC(I)
C 1261 PSF(I)=A5(I)*(DLO(I)-YD(I))
C      GO TO 1271
C 1265 IF(DL1(I).GE.0.)GO TO 1267
C      AKMC(I)=AC(I)
C      GO TO 1268
C 1267 AKMC(I)=AKC(I)
C 1268 PSF(I)=A5(I)*(DLO(I)+YD(I))
C 1271 Q(I)=AKC(I)*(DLO(I)-PSF(I))
C 1272 CONTINUE
C      DO 1281 J=1,N

```

```

      JP=J+1
      AKM(J,J)=AKMC(J)
      IF(J.EQ.N)GO TO 1281
      AKM(J,J)=AKM(J,J)+AKMC(JP)
      AKM(J,JP)=-AKMC(JP)
      AKM(JP,J)=-AKMC(JP)
1281  CONTINUE
C
C      COMPUTE THE RESTORING FORCE VECTOR
C
      DO 1291 I=1,N
      RV(I)=Q(I)
      IF(I.LT.N)RV(I)=RV(I)-Q(I+1)
1291  CONTINUE
C
C      COMPUTE Z2F
C
      CALL MVM(CM,Z1F,DUMV1,N)
      DO 1311 I=1,N
1311  DUMV2(I)=F(IND+1,I)-DUMV1(I)-RV(I)
      CALL MVM(A3,DUMV2,Z2F,N)
C
C      PRINT THE RESULTS
C
      WRITE(6,3)
      IF(INOISE.NE.1) GO TO 555
      ZNOISE=ZOF(1)+RN(IND+1)
      YNOISE=ZOF(2)+DN(IND+1)
      WRITE(10,14)ZNOISE,YNOISE
      YF=FF(IND+1)+FN(IND+1)
      WRITE(40,100)YF
      GO TO 558
555  WRITE(10,14)ZOF(1),ZOF(2)
      WRITE(40,100)F(IND+1,2)
558  WRITE(20,14)(PSF(I),I=1,N)
      IP=IND+1
      DIS=ZOF(2)-ZOF(1)
      REV=Z1F(2)-Z1F(1)
      REACC=Z2F(2)-Z2F(1)
      ENED1(IP)=Z1F(1)*(CC(1)*Z1F(1)+AKC(1)*ZOF(1))
      ENED2(IP)=REV*(CC(2)*REV+AKC(2)*DIS)
C
C      INITIATE THE NEXT COMPUTATION CYCLE
C
      DO 1341 I=1,N
      ZOI(I)=ZOF(I)
      Z1I(I)=Z1F(I)
      Z2I(I)=Z2F(I)
      PSI(I)=PSF(I)
1341  CONTINUE
8999  CONTINUE
      CALL SIMP(ENED1,ENER1,DT,NT)

```

```

      CALL SIMP(ENED2,ENER2,DT,NT)
      ENER=ENER1+ENER2
      WRITE(6,17) ENER1,ENER2,ENER
3    FORMAT(/)
14   FORMAT(2E12.4)
17   FORMAT(3E12.4)
100  FORMAT(1E12.4)
      STOP
      END

```

C
C
C

FIND THE AREA UNDER THE CURVE

```

      SUBROUTINE SIMP(X,E,D,N)
      DIMENSION X(1024)
      N2=N/2-1
      E=X(1)
      DO 1 I=1,N2
      IA=2*I
      IB=IA+1
      E=E+4.0*X(IA)
      E=E+2.0*X(IB)
1    CONTINUE
      N3=N-1
      E=E+0.5*X(N3)+1.5*X(N)
      E=D*E/3.0
      RETURN
      END

```

C
C
C

SUBROUTINE MULTIPLICATION

```

      SUBROUTINE MVM(A,B,C,N)
      DIMENSION A(2,2),B(2),C(2)
      DO 1 I=1,N
      C(I)=0.
      DO 1 J=1,2
      C(I)=A(I,J)*B(J)+C(I)
1    CONTINUE
      RETURN
      END

```

```

C *****
C *                PROGRAM "TIMID"                *
C *****
C MAIN PROGRAM FOR LEAST-SQUARE STRUCTURE
C IDENTIFICATION
C
C EXTERNAL SUBS
C EXTERNAL MULTI
C DIMENSION C(720,2),D(10,10),AT(2,720),CM(2,2)
C DIMENSION F(720,1),AA(2,1),CA(720,1),ERR(720,1)
C DIMENSION CMS(2,2),DIA(2,1),CMS1(2,2),UM(2,2)
C DIMENSION CM1(2,2),CT(2,720),ERRT(1,720),AJN(2,2)
C DOUBLE PRECISION AT,CM,CT,AA,C,F,CA,ERR,ERRT
C DOUBLE PRECISION AJN,CM1,CMS,DIA,CMS1,UM
C CALL OPSYS('ALLOC','ID1',33)
C
C DATA FILE NEED TO CHANGE ACCORDING THE
C SYSTEM USED
C N NUMBER OF POINTS FOR THE IDENTIFICATION
C IM NUMBER OF COLUMN
C
C CALL OPSYS('ALLOC','ID1',34)
C READ(5,*) N,M,IM
C DO 10 I=1,N
10 READ(33,15) (C(I,J), J=1,IM)
C DO 11 I=1,N
11 READ(34,16) (F(I,1))
C CALL TRAN(C,N,IM,AT)
C CALL MULTI(AT,IM,N,C,IM,CMS1)
C DO 8 I=1,IM
C DO 8 J=1,IM
8 CM(I,J)=CMS1(I,J)
C WRITE(6,30)
C DO 3 I=1,IM
3 WRITE(6,4) (CMS1(I,J), J=1,IM)
C CALL INVER(CMS1,IM,D,M,DETER)
C CALL MULTI(CM,IM,IM,CMS1,IM,UM)
C WRITE(6,33)
C DO 5 I=1,IM
5 WRITE(6,7) (UM(I,J), J=1,IM)
C CALL MULTI(CMS1,IM,IM,AT,N,CT)
C CALL MULTI(CT,IM,N,F,1,AA)
C WRITE(6,34)
C DO 22 I=1,IM
22 WRITE(6,12) AA(I,1)
C CALL MULTI(C,N,IM,AA,1,CA)
C CALL SUBS(F,N,1,CA,ERR)
C CALL TRAN(ERR,N,1,ERRT)
C CALL MULTI(ERRT,1,N,ERR,1,VAR)
C VAR=VAR/(N-IM)
C DEV=SQRT(VAR)

```

```

WRITE(6,17)
WRITE(6,37) DEV
4 FORMAT(2E16.6)
7 FORMAT(2E16.6)
12 FORMAT(E16.6)
15 FORMAT(2E12.4)
16 FORMAT(1E16.6)
17 FORMAT (5X,'THE DEVIATION IS',/)
20 FORMAT(6E12.4)
24 FORMAT(6E12.4)
30 FORMAT(5X,'MATRIX Z',/)
31 FORMAT(5X,'INVERSE MATRIX',/)
32 FORMAT(5X,'INVERSE MATRIX IMPROVED',/)
33 FORMAT(5X,'UNIT MATRIX FOR CHECKING',/)
34 FORMAT(5X,'IDENTIFIED PARAMETERS',/)
35 FORMAT(5X,'MATRIX CT',/)
37 FORMAT(E18.6)
STOP
END

```

C
C
C

THIS SUBROUTINE IS FOR MATRIX INVERSION

```

SUBROUTINE INVER(A,N,B,M,DET)
DOUBLE PRECISION A(2,2),B(2,2),IPVOT(2),INDEX(2,10)
DOUBLE PRECISION T,PIVOT(2)
COMMON IPVOT,INDEX,PIVOT
EQUIVALENCE (IROW,JROW),(ICOL,JCOL)

```

C
C
C

INITIALIZATION

```

DET=1.0D0
DO 7 J=1,N
7 IPVOT(J)=0
DO 135 I=1,N

```

C
C
C

SEARCH FOR PIVOT ELEMENT

```

T=0.0D0
DO 9 J=1,N
IF(IPVOT(J)-1) 13,9,13
13 DO 23 K=1,N
IF(IPVOT(K)-1)43,23,81
43 IF(DABS(T)-DABS(A(J,K))) 83,23,23
83 IROW=J
ICOL=K
T=A(J,K)
23 CONTINUE
9 CONTINUE
IPVOT(ICOL)=IPVOT(ICOL)+1

```

C
C
C

PUT PIVOT ELEMENT ON DIAGONAL

```

      IF(IROW-ICOL) 73, 109, 73
73  DET=-DET
      DO 12 L=1,N
      T=A(IROW,L)
      A(IROW,L)=A(ICOL,L)
12  A(ICOL,L)=T
      IF(M) 109,109,33
33  DO 2 L=1,M
      T=B(IROW,L)
      B(IROW,L)=B(ICOL,L)
      2 B(ICOL,L)=T
109 INDEX(I,1)=IROW
      INDEX(I,2)=ICOL
      PIVOT(I)=A(ICOL,ICOL)
      DET=DET*PIVOT(I)
C
C      DIVIT PIVOT ROW BY PIVOT ELEMENT
C
      A(ICOL,ICOL)=1.
      DO 205 L=1,N
205 A(ICOL,L)=A(ICOL,L)/PIVOT(I)
      IF(M) 347,347,66
66  DO 52 L=1,M
52  B(ICOL,L)=B(ICOL,L)/PIVOT(I)
C
C      REDUCE NON-PIVOT ROW
C
347 DO 135 LI=1,N
      IF(LI-ICOL) 21,135,21
21  T=A(LI,ICOL)
      A(LI,ICOL)=0.000
      DO 89 L=1,N
89  A(LI,L)=A(LI,L)-A(ICOL,L)*T
      IF(M) 135,135,18
18  DO 68 L=1,M
68  B(LI,L)=B(LI,L)-B(ICOL,L)*T
135 CONTINUE
C
C      INTERCHANGE COLUMNS
C
222 DO 3 I=1,N
      L=N-I+1
      IF(INDEX(L,1)-INDEX(L,2)) 19,3,19
19  JROW=INDEX(L,1)
      JCOL=INDEX(L,2)
      DO 549 K=1,N
      T=A(K,JROW)
      A(K,JROW)=A(K,JCOL)
      A(K,JCOL)=T
549 CONTINUE
      3 CONTINUE
81  RETURN

```

END

C
C
C

THIS SUBROUTINE IS FOR MATRIX MULTIPLICATION

```

SUBROUTINE MULTI(A,N,M,B,L,C)
DIMENSION A(N,M),B(M,L),C(N,L)
DOUBLE PRECISION A,B,C
DO 5 I=1,N
DO 5 J=1,L
C(I,J)=0.0DO
DO 5 K=1,M
5 C(I,J)=C(I,J)+A(I,K)*B(K,J)
RETURN
END
SUBROUTINE MULTIA(TA,N,M,TB,L,TC)
DIMENSION TA(N,M),TB(M,L),TC(N,L)
DOUBLE PRECISION TA,TB,TC
DO 15 I=1,N
DO 15 J=1,L
TC(I,J)=0.0DO
DO 15 K=1,M
15 TC(I,J)=TC(I,J)+TA(I,K)*TB(K,J)
RETURN
END

```

C
C
C

THIS SUBROUTINE IS FOR MATRIX TRANSFORMATION

```

SUBROUTINE TRAN(A,N,IM,AT)
DIMENSION A(N,IM),AT(IM,N)
DOUBLE PRECISION A,AT
DO 3 I=1,N
DO 3 J=1,IM
3 AT(J,I)=A(I,J)
RETURN
END

```

C
C
C

THIS SUBROUTINE IS FOR MATRIX SUBSTRACTION

```

SUBROUTINE SUBS(A,N,IN,B,C)
DOUBLE PRECISION A(N,IN),B(N,IN),C(N,IN)
DO 101 I=1,N
DO 101 J=1,IN
101 C(I,J)=A(I,J)-B(I,J)
RETURN
END

```

C
C

SUBROUTINE SET(A,IM,B,DIA)

```

DIMENSION A(IM,IM),B(IM,IM),DIA(IM,1)
DOUBLE PRECISION A,B,DIA
DO 3 J=1,IM
DO 3 I=1,IM

```



```

      B(I,J)=A(I,J)/A(J,J)
      DIA(J,1)=A(J,J)
3    CONTINUE
      RETURN
      END

```

C
C
C
C

THIS SUBROUTINE IS FOR IMPROVING THE ACCURACY
OF THE MATRIX INVERSION.

```

      SUBROUTINE RIVISE(A,A1,IM,AIN)
      DOUBLE PRECISION A(2,2),A1(2,2),AIN(2,2),AJN(2,2)
      DOUBLE PRECISION UN(2,2),UN1(2,2),SA1(2,2)
      DOUBLE PRECISION ERR(2,2),AA1(2,2)
      UN1(1,1)=1.0DO
      UN1(2,2)=1.0DO
      UN1(3,3)=1.0DO
      UN1(4,4)=1.0DO
      UN1(1,2)=0.0DO
      UN1(1,3)=0.0DO
      UN1(1,4)=0.0DO
      UN1(2,1)=0.0DO
      UN1(2,3)=0.0DO
      UN1(2,4)=0.0DO
      UN1(3,1)=0.0DO
      UN1(3,2)=0.0DO
      UN1(3,4)=0.0DO
      UN1(4,1)=0.0DO
      UN1(4,3)=0.0DO
      DO 30 I=1,IM
      DO 30 J=1,IM
30    UN(I,J)=UN1(I,J)*2.0DO
      ICOUNT=1
      2    CALL MULTI(A,IM,IM,A1,IM,AA1)
      CALL SUBS(UN,IM,IM,AA1,SA1)
      CALL MULTI(A1,IM,IM,SA1,IM,AIN)
      CALL MULTI(A,IM,IM,AIN,IM,AJN)
      ERRSM=0.0DO
      DO 5 I=1,IM
      DO 5 J=1,IM
      ERR(I,J)=AJN(I,J)-UN1(I,J)
      ERRSM=ERRSM+DABS(ERR(I,J))
      5    CONTINUE
      IF(ERRSM.LT.1.0D-7) GO TO 20
      ICOUNT=ICOUNT+1
10    DO 15 I=1,IM
      DO 15 J=1,IM
15    A1(I,J)=AIN(I,J)
      GO TO 2
20    RETURN
      END

```

```

      SUBROUTINE INVERS(B,N,A)
      DOUBLE PRECISION A(N,N),B(N,N),C(18,18)

```

```

      DOUBLE PRECISION AMAX,TEMP,PIVOT
      DIMENSION INDEX(4,2)
      IF(N.GT.40) WRITE(6,101)
101  FORMAT(20X,'MATRIX INVERSION IS LIMITED TO A
      +40 X 40 MATRIX')
      IF(N.GT.40) GO TO 134
103  FORMAT(/,'    MATRIX INVERSION'//)
104  FORMAT('    THE MATRIX (XT*X)',/)
106  FORMAT('  ROW', I3,1X,1P4E16.7/(8X,1P4E16.7))
128  FORMAT('    THE INVERSE OF MATRIX (XT*X)',/)
131  FORMAT('    THE UNIT MATRIX')
133  FORMAT('    ZERO PIVOT')
      DO 90 I=1,N
      DO 90 J=1,N
      A(I,J)=B(I,J)
  90  CONTINUE
      WRITE(6,103)
      WRITE(6,104)
      DO 105 I=1,N
105  WRITE(6,106) I,(A(I,J),J=1,N)
      DO 107 I=1,N
      DO 107 J=1,N
107  B(I,J)=A(I,J)
      DO 108 I=1,N
108  INDEX(I,1)=0
      II=0
109  AMAX=-1.0D0
      DO 110 I=1,N
      IF(INDEX(I,1)) 110,111,110
111  DO 112 J=1,N
      IF(INDEX(J,1)) 112,113,112
113  TEMP=DABS(A(I,J))
      IF(TEMP-AMAX) 112,112,114
114  IROW=I
      ICOL=J
      AMAX=TEMP
112  CONTINUE
110  CONTINUE
      IF(AMAX) 225,115,116
116  INDEX(ICOL,1)=IROW
      IF(IROW-ICOL) 119,118,119
119  DO 120 J=1,N
      TEMP=A(IROW,J)
      A(IROW,J)=A(ICOL,J)
120  A(ICOL,J)=TEMP
      II=II+1
      INDEX(II,2)=ICOL
118  PIVOT=A(ICOL,ICOL)
      A(ICOL,ICOL)=1.0D0
      PIVOT=1.0D0/PIVOT
      DO 121 J=1,N
121  A(ICOL,J)=A(ICOL,J)*PIVOT

```

```

DO 122 I=1,N
IF(I-ICOL) 123,122,123
123 TEMP=A(I,ICOL)
A(I,ICOL)=0.0DO
DO 124 J=1,N
124 A(I,J)=A(I,J)-A(ICOL,J)*TEMP
122 CONTINUE
GO TO 109
125 ICOL=INDEX(II,2)
IROW=INDEX(ICOL,1)
DO 126 I=1,N
TEMP=A(I,IROW)
A(I,IROW)=A(I,ICOL)
126 A(I,ICOL)=TEMP
II=II-1
225 IF(II) 125,127,125
127 WRITE(6,128)
DO 129 I=1,N
129 WRITE(6,106) I,(A(I,J),J=1,N)
DO 130 I=1,N
DO 130 J=1,N
C(I,J)=0.0DO
DO 130 K=1,N
130 C(I,J)=C(I,J)+B(I,K)*A(K,J)
WRITE(6,131)
DO 132 I=1,N
132 WRITE(6,106) I,(C(I,J),J=1,N)
GO TO 134
115 WRITE(6,133)
134 RETURN
END

```

C
C
C
C
C
C
C
C
C

```

*****
*          PROGRAM " ENER2"          *
*****
THIS PROGRAM COMPUTES ENERGY DISSIPATED IN A
2ND ORDER SYSTEM , A0,A1 COEFF GENERATED
IN IDENTIFICATION PROGRAM
DT DELTA T
N NO OF PTS

```

```

DIMENSION F(1024),XINT(1024)
REAL K1,K2,L1,L2
CALL OPSYS('ALLOC','RH1',55)
CALL OPSYS('ALLOC','ID1',57)
READ(5,*)N
READ(5,*)DT,A0,A1,AMS
READ(55,90)(F(I),I=1,N)
XINT(1)=0.0
NM=N-1
C1=-A1/AMS
C2=-A0/AMS

```

```

C3=1.0/AMS
Y0=0.0
Z0=0.0
DO 999 I=1,NM
T=DT*(I-1)
K1=DT*Z0
L1=DT*(C1*Z0+C2*Y0+C3*F(I))
K2=DT*(Z0+L1)
L2=DT*(C1*(Z0+L1)+C2*(Y0+K1)+C3*F(I+1))
Y1=Y0+0.5*(K1+K2)
Z1=Z0+0.5*(L1+L2)
IP=I+1
XINT(IP)=Z1**2
Y0=Y1
Z0=Z1
WRITE(57,92)T,Y0
999 CONTINUE
CALL SIMP(XINT,ENED,DT,N)
ENED=A1*ENED+0.5*A0*Y1**2
WRITE(6,12)ENED
12 FORMAT(5X,7HENED = ,E12.4)
90 FORMAT(E12.4)
91 FORMAT(1E12.4)
92 FORMAT(2E12.4)
STOP
END
SUBROUTINE SIMP(X,E,D,N)
DIMENSION X(1024)
N2=N/2-1
E=X(1)
DO 1 I=1,N2
IA=2*I
IB=IA+1
E=E+4.0*X(IA)
E=E+2.0*X(IB)
1 CONTINUE
N3=N-1
E=E+0.5*X(N3)+1.5*X(N)
E=D*E/3.0
RETURN
END

C
C
C *****
C *          PROGRAM " ENER3 "          *
C *****
C THIS PROGRAM USES THE INCREMENTAL EQUATIONS
C TO COMPUTE THE ENERGY DISSIPATED
C IN A 3RD ORDER SYSTEM
C N NO OF PTS
C DT DELTA T
C A0,A1,A2 COEFF FROM ID PROGRAM

```

```

C      AO COMPARE TO STIFFNESS
C      ENED TOTAL ENERGY DISSIPATED
C      ENED1 SPRING ENERGY DISSIPATED
C
      CALL OPSYS('ALLOC','ID2',21)
      DIMENSION F(1024),FD(1024),XINT(1024)
      DIMENSION ESP(1024),XINT1(1024)
      READ(5,*)N
      READ(5,*)DT,A0,A1,A2,AMS
      CALL OPSYS('ALLOC','RH1',55)
111 READ(55,91)(F(I),FD(I),I=1,N)
C      CONVERT
      A0=A0/(A2*AMS)
      A1=A1/(A2*AMS)
      B1=1.0/(A2*AMS)
      B2=1.0/AMS
      A2=1.0/A2
C      CONSTANTS
      R0=24.0/DT**3
      R1=4.0
      R2=12.0/DT
      R3=24.0/DT**2
      S0=12.0/DT**2
      S1=DT
      S2=6.0
      S3=12.0/DT
      U0=4.0/DT
      U1=DT**2/6.0
      U2=DT
      U3=4.0
      Q1=24.0/DT**3+12.0*A2/DT**2+4.0*A1/DT+A0
      Q2=4.0+A2*DT+A1*DT**2/6.0
      Q3=12.0/DT+6.0*A2+A1*DT
      Q4=24.0/DT**2+12.0*A2/DT+4.0*A1
      Y0=0.0
      Y1=0.0
      Y2=0.0
      Y3=B1*F(1)+B2*FD(1)
      XINT(1)=0.0
      ESP(1)=0.0
      NM=N-1
      DO 999 I=1,NM
      T=DT*(I-1)
      DF=B1*(F(I+1)-F(I))+B2*(FD(I+1)-FD(I))
      DZ0=(DF+Q2*Y3+Q3*Y2+Q4*Y1)/Q1
      DZ1=U0*DZ0-U1*Y3-U2*Y2-U3*Y1
      DZ2=S0*DZ0-S1*Y3-S2*Y2-S3*Y1
      Y0=Y0+DZ0
      Y1=Y1+DZ1
      Y2=Y2+DZ2
      Y3=B1*F(I+1)+B2*FD(I+1)-A2*Y2-A1*Y1-A0*Y0
      IP=I+1

```

```

XINT(IP)=Y1*(F(IP)-AMS*Y2)
WRITE(21,91)T,Y0
999 CONTINUE
CALL SIMP(XINT,ENED,DT,N)
WRITE(6,12)ENED
12 FORMAT(5X,7HENED = ,E12.4)
90 FORMAT(E12.5)
91 FORMAT(2E12.4)
STOP
END
SUBROUTINE SIMP(X,E,D,N)
DIMENSION X(1024)
N2=N/2-1
E=X(1)
DO 1 I=1,N2
IA=2*I
IB=IA+1
E=E+4.0*X(IA)
E=E+2.0*X(IB)
1 CONTINUE
N3=N-1
E=E+0.5*X(N3)+1.5*X(N)
E=D*E/3.0
RETURN
END

```

C
C
C
C
C
C

```

*****
*                PROGRAM " FREQID"                *
*****

```

FREQUENCY DOMAIN SYSTEM IDENTIFICATION

```

REAL DD(1024),F(1024),W(1024),COE(4),QT(20)
DIMENSION S(1024),INDEX(1024),QQ(1024),X2(22,1)
DIMENSION X1(22,2),XT1(2,22),XP(2,2),XPI(2,2)
DIMENSION XTT(2,22),B(2,1)
COMPLEX FT(1024),DDF(1024)
CALL OPSYS('ALLOC','FD1',10)
CALL OPSYS('ALLOC','ID1',8)
COMMON /ARRAY/W,QQ,S,INDEX
EXTERNAL SPLINE
EXTERNAL QF
EXTERNAL MATINV

```

C
C
C
C

WHEN INDE=1 SHOWS THE PROGRAM WILL GO TO
THE THIRD ORDER SYSTEM

```

INDE=1
ID=0
KDEX=0
MP=2
M=10

```

```

N=1024
NT=N/2
NTP=NT+1
DT=0.05
C2=1.0
PI=3.1415926535
NS=N/2
CA=PI/NS

```

```

C
C
C

```

```

      GET THE INPUT FROM THE FILE AND FFT THE INPUT

```

```

      READ(10,15) (F(I),DD(I),I=1,N)
15  FORMAT(2E12.4)
      IF(KDEX.NE.1) GO TO 13

```

```

C
C
C

```

```

      SMOOTH THE FUNCTION

```

```

      DO 9 I=1,NS
      IM=N-I+1
      CMULT=0.5*(1.0-COS((I-1)*CA))
      F(IM)=CMULT*F(IM)
      DD(IM)=CMULT*DD(IM)
      9  CONTINUE
13  TT=N*DT

```

```

C
C
C

```

```

      DO THE FOURIER TRANSFORM

```

```

      DO 20 I=1,N
      FT(I)=CMPLX(F(I),0.0)*TT
      DDF(I)=CMPLX(DD(I),0.0)*TT
20  CONTINUE
      CALL FFT1(FT,M,N,-1.)
      CALL FFT1(DDF,M,N,-1.0)

```

```

C
C
C

```

```

      CALCULATE THE DF AND FREQUENCY

```

```

      DF=2.0*PI/TT
      DO 24 I=1,N
      W(I)=(I-1)*DF
24  CONTINUE
      IF(ID.EQ.1) GO TO 33
      GO TO 45

```

```

C
C
C
C
C
C

```

```

      IDENTIFICATION PROCESS
      SECOND ORDER SYSTEM

```

```

      CHANGE F.T. OF ACCELERATION TO F.T. OF DISPLACEMENT

```

```

33  DO 55 I=2,N
      DDF(I)=-DDF(I)/(W(I)**2)
55  CONTINUE
45  DO 50 I=40,60

```

```

      FF=CABS(FT(I))
      ZF=CABS(DDF(I))
      QQ(I)=FF**2/(ZF**2)
      WRITE(8,88)W(I),QQ(I)
50  CONTINUE
      GO TO 200

C
C
C      FIND THE MINIMUM OF THE QQ(I) AND IT'S FREQUENCY

      SMAL=QQ(30)
      KN=30
      DO 60 I=31,70
      IF(SMAL.LE.QQ(I)) GO TO 60
      SMAL=QQ(I)
      QMIN=QQ(I)
      KN=I
60  CONTINUE
      WM=KN*DF

C
C
C      CALCULATE THE STIFFNESS

      CO=C2*WM**2
      WRITE(6,*)KN,WM,CO,QMIN

C
C
C      USE FIT TO FIND THE REAL MINIMUM

      AS=0.9*WM
      AF=1.1*WM
      IS=AS/DF
      IF=AF/DF
      IJ=IS-1
      ITT=(IF-IS)+1
      DO 67 I=1,ITT
      IK=I+IJ
      QT(I)=QQ(IK)
67  CONTINUE

C
C
C      POLYNOMIAL FITTING BY LEAST SQUARE METHOD

      QT : INPUT VALUES
      ITT: TOTAL PTS OF QT
      AS: START FREQUENCY
      AF: FIANL FREQUENCY
      COE(I): COEFFICIENTS OF POLYNOMIAL

      CALL FIT1(QT,3,ITT,AS,AF,COE)
      WM=-COE(2)/(2.0*COE(3))
      CO=C2*WM**2
      WRITE(6,*)ITT,WM,CO

C
C
C      SET THE RANGE OF FREQUENCY AND FIT THE
      DATA BY CUBIC SPLINE

```



```

C
QA=0.9
QB=1.1
WA=QA*WM
WB=QB*WM
IF(INDE.EQ.1) GO TO 80
CALL SPCOE(NT,W,QQ,S,INDEX)
DO 70 I=1,NT
QQ(I)=-QQ(I)
70 CONTINUE

C
C
C
DO THE INTEGRATION AND CALCULATE THE DAMPING

CALL SIMP(QF,WA,WB,1.0E-5,ANS,ERROR,AREA,IFLAG)
QIN=5.*ANS/(WM**7)
Q3=(QB**3)-(QA**3)
Q5=(QB**5)-(QA**5)
Q7=(QB**7)-(QA**7)
QP=(-5./3.)*Q3+2.*Q5-(5./7.)*Q7
CI=((WM**2)/Q5)*(QIN+(C2**2)*QP)
CC=SQRT(CI)
WRITE (6,*) CO,CC,ANS,IFLAG
GO TO 200

C
C
C
C
C
INDENTIFICATION FOR THIRD ORDER SYSTEM

CALCULATE THE FREQUENCY BAND FOR IDENTIFICATION

80 IA=WA/DF
IB=WB/DF
II=IA-1
NF=(IB-IA)+1
WRITE(6,*)NF,IA,IB

C
C
C
FORMING THE IDENTIFICATION MATRIX

DO 100 I=IA,IB
J=I-II
EU=W(I)**2
EV=-2.*C2*(W(I)**4)
EE=WM**2-(W(I)**2)
EW=(C2**2)*(EE**2)
QQ(I)=COE(1)+COE(2)*W(I)+COE(3)*(W(I)**2)
X1(J,1)=EU
X1(J,2)=EV
X2(J,1)=QQ(I)-EW
100 CONTINUE
DO 105 I=1,2
DO 105 J=1,2
XP(I,J)=0.0
DO 105 K=1,NF
XP(I,J)=XP(I,J)+X1(K,I)*X1(K,J)

```

```

105 CONTINUE
    DO 104 I=1,2
    DO 104 K=1,NF
    XT1(I,K)=X1(K,I)
104 CONTINUE
    CALL MATINV(XP,MP,XPI)
    DO 106 I=1,2
    WRITE(6,15) (XPI(I,J),J=1,2)
106 CONTINUE
    DO 110 I=1,2
    DO 110 J=1,NF
    XTT(I,J)=0.0
    DO 110 K=1,2
110 XTT(I,J)=XTT(I,J)+XPI(I,K)*XT1(K,J)
    DO 118 I=1,2
118 WRITE(6,37)(XTT(I,J),J=1,NF)
    DO 115 I=1,2
    B(I,1)=0.0
    DO 115 K=1,NF
115 B(I,1)=B(I,1)+XTT(I,K)*X2(K,1)
    DO 119 I=1,2
119 WRITE(6,*) B(I,1)
    CK=SQRT(B(1,1))
    CL=B(2,1)/CK
    WRITE(6,*)CK,CL
    35 FORMAT(24H REAL PART IMAGINAL PART)
    37 FORMAT(6E12.4)
    88 FORMAT(2E12.4)
200 STOP
    END

```

C
C
C
C
C

FUNCTION QF IS A CONTINUOUS FUNCTION.
THE DATA QQ(I) WAS ARRANGED SO THAT THE FUNCTION
COULD BE CALLED IN ANY TIME.

```

FUNCTION QF(WW)
DIMENSION W(1024),QQ(1024),S(1024),INDEX(1024)
COMMON /ARRAY/W,QQ,S,INDEX
N=512
X=WW
QT=SPLINE(N,W,QQ,S,INDEX,X)
QF=QT*(X**2)
RETURN
END

```

```

C
C *****
C *          PROGRAM NAME "PUR"          *
C *****
C THIS PROGRAM IDENTIFIES THE PARAMETERS OF A
C TIME VARYING SECOND-ORDER LINEAR MODEL BY
C USING THE PERTURBATION METHOD AND ITERATIVE
C NEWTON- RAPHSON PROCEDURE. IT MAY ALSO USE
C THE POLYNOMIAL FITTING APPROACH.
C
C COMPLEX FF(1024),FD(1024)
C COMPLEX ZZ(1024),HD,Z(1024),HABS(512)
C DIMENSION DD(1024),F(1024),HMOD(512),HZ(512)
C DIMENSION EK(3),COE(4),S(9),INDEX(9),AS(9)
C COMMON/ARRAY/FF,FD
C CALL OPSYS('ALLOC','FD1',10)
C CALL OPSYS('ALLOC','RH1',7)
C CALL OPSYS('ALLOC','NFL',4)
C EXTERNAL MATINV
C
C SM      : SYSTEM MASS
C ALPHA   : DAMPING COEFFICIENT
C BETA    : STIFFNESS COEFFICIENT
C ZETA    : DAMPING RATIO
C C1      : INITIAL GUESS 'DAMPING'
C C2      : INITIAL GUESS 'ALPHA*C1'
C C3      : INITIAL GUESS 'STIFFNESS'
C C4      : INITIAL GUESS 'BETA*C3'
C ESLON   : ACCURACY MEASURE(FOR ESLON1-ESLON4)
C W1-W4   : ACCURACY MEASURE FOR NEWTON METHOD
C DA1-DA4 : INCREMENT VALUES
C
C SM=1.0
C C1=1.5
C C2=0.02
C C3=37.5
C C4=-0.01
C ZETA=0.1
C ESLON1=0.02
C ESLON2=0.02
C ESLON3=0.02
C ESLON4=0.02
C WN=SQRT(C3/SM)
C DA1=0.01
C DA2=0.001
C DA3=1.0
C DA4=0.01
C W1=0.01
C W2=0.01
C W3=0.01
C W4=0.01
C PI=3.1415926535

```

```

DT=0.05
M=10
N=2**M
NT=N/8
TT=DT*N
DW=2.*PI/TT
NS=N/2
CA=PI/NS

C
C
C   READ IN THE TIME DOMAIN RESPONSE
C
C   READ(10,80) (F(I),DD(I),I=1,N)
C
C   WINDOW THE DATA
C
C   DO 3 I=1,NS
C     IM=N-I+1
C     CMULT=0.5*(1.0-COS((I-1)*CA))
C     F(IM)=CMULT*F(IM)
C     DD(IM)=CMULT*DD(IM)
3   CONTINUE

C
C
C   FFT THE INPUT AND RESPONSE
C
C   DO 8 I=1,N
C     FF(I)=CMPLX(F(I),0.0)*TT
C     ZZ(I)=CMPLX(DD(I),0.0)*TT
8   CONTINUE
C   CALL FFT1(FF,M,N,-1.0)
C   CALL FFT1(ZZ,M,N,-1.0)

C
C
C   FIND THE MOD(H)
C
C   DO 9 I=1,NT
C     FA=CABS(FF(I))
C     ZA=CABS(ZZ(I))
C     HMOD(I)=ZA/FA
9   CONTINUE

C
C
C   CALCULATE THE DERIVATIVE OF FF
C
C   DO 12 I=1,N
C     TC=(I-1)*DT
C     F(I)=F(I)*TC
C     FD(I)=CMPLX(F(I),0.0)*TT
12  CONTINUE
C   CALL FFT1(FD,M,N,-1.)
C   DO 13 I=1,N
13  FD(I)=FD(I)*CMPLX(0.0,-1.)

C
C
C   FIND THE NUMBER OF PTS NEEDED IN THE BAND

```

```

NC=(1.0*ZETA*WN)/DW
NW=WN/DW
NS=NW-NC
NF=NW+NC
AA1=C1
AA2=C2
AA3=C3
AA4=C4
26 L=1
28 WRITE(6,89)C1,C2,C3,C4
   ICOUNT=2
   ISTEAD=ICOUNT
   AC1=C1
   AC2=C2
   AC3=C3
   AC4=C4

C
C
C
C
29 WN=SQRT(C3/SM)
   NC=(1.0*ZETA*WN)/DW
   NW=WN/DW
   NS=NW-NC
   NF=NW+NC
   CALL PURT(DW,NT,C1,C2,C3,C4,HZ)

C
C
C
   FIND E(ERROR MEASURE)

   EE=0.0
   DO 30 I=NS,NF
   E=HMOD(I)-HZ(I)
   EE=EE+(E**2)
30 CONTINUE
   EK(ICOUNT)=EE
   IF(ICOUNT.EQ.3) GO TO 50
   GO TO (31,32,33,34),L
31 IF(ICOUNT.EQ.1) GO TO 40
   C1=C1-DA1
   ICOUNT=ICOUNT-1
   GO TO 29
40 C1=AC1+DA1
   ICOUNT=ISTEAD+1
   GO TO 29
32 IF(ICOUNT.EQ.1) GO TO 41
   C2=C2-DA2
   ICOUNT=ICOUNT-1
   GO TO 29
41 C2=AC2+DA2
   ICOUNT=ISTEAD+1
   GO TO 29
33 IF(ICOUNT.EQ.1) GO TO 42

```

```

      C3=C3-DA3
      ICOUNT=ICOUNT-1
      GO TO 29
42  C3=AC3+DA3
      ICOUNT=ISTEA+1
      GO TO 29
34  IF(ICOUNT.EQ.1) GO TO 43
      C4=C4-DA4
      ICOUNT=ICOUNT-1
      GO TO 29
43  C4=AC4+DA4
      ICOUNT=ISTEA+1
      GO TO 29

```

C
C
C

CALCULATE THE FIRST AND SECOND DERIVETIVES

```

50  GO TO(60,61,62,63),L
60  TD=DA1
      AV=AC1
      W=W1
      GO TO 70
61  TD=DA2
      AV=AC2
      W=W2
      GO TO 70
62  TD=DA3
      AV=AC3
      W=W3
      GO TO 70
63  TD=DA4
      AV=AC4
      W=W4
      GO TO 70
70  DEK=(EK(3)-EK(1))/(2.0*TD)
      DDEK=(EK(3)-2.*EK(2)+EK(1))/(TD**2)

```

C
C
C

DO THE NEWTON RAPHSON METHOD

```

      ACC=AV-(DEK/DDEK)
      WE=ABS((ACC-AV)/ACC)
      WD=WE-W
      IF(WD.LE.0.0) GO TO 87
99  GO TO(101,102,103,104),L
101 C1=ACC
      GO TO 28
102 C2=ACC
      GO TO 28
103 C3=ACC
      GO TO 28
104 C4=ACC
      GO TO 28
87  GO TO(92,93,94,95),L

```

```

92 C1=ACC
   GO TO 85
93 C2=ACC
   GO TO 85
94 C3=ACC
   GO TO 85
95 C4=ACC
85 L=L+1
   IF(L.EQ.5) GO TO 100
   GO TO 28

```

C
C
C

COMPARE THE PARAMETERS

```

100 CD1=ABS((AA1-C1)/C1)
    CD2=ABS((AA2-C2)/C2)
    CD3=ABS((AA3-C3)/C3)
    CD4=ABS((AA4-C4)/C4)
    IF(CD1.GT.ESLON1) GO TO 81
    IF(CD2.GT.ESLON2) GO TO 81
    IF(CD3.GT.ESLON3) GO TO 81
    IF(CD3.GT.ESLON4) GO TO 81
    WRITE(6,*) C1,C2,C3,C4
    GO TO 88
81  AA1=C1
    AA2=C2
    AA3=C3
    AA4=C4
    GO TO 26
80  FORMAT(2E12.4)
82  FORMAT(3E13.4)
89  FORMAT(4E12.4)
150 FORMAT(2E16.6)
88  STOP
    END

```

C
C
C

PERTURBATION METHOD

```

SUBROUTINE PURT(DW,NT,C1,C2,C3,C4,HA)
COMPLEX FF(1024),FD(1024),HABS(512),Z(512)
COMPLEX HD,H,HDEV,H1,H2,H3,H4
DIMENSION HA(NT)
COMMON/ARRAY/FF,FD
SM=1.0
DO 14 I=1,NT
W=(I-1)*DW
HD=CMPLX((C3-SM*(W**2)),W*C1)
H=1.0/HD
HDEV=CMPLX((2.*SM*W),-C1)/(HD**2)
H1=H*FF(I)
H2=C2*H*(H1+W*(HDEV*FF(I)+H*FD(I)))
H3=CMPLX(0.0,-C4)*H*(HDEV*FF(I)+H*FD(I))
Z(I)=H1+H2+H3

```



```

NCUV=7
M=10
M1=1.0
M2=1.0

C
C
C   INITIAL GUESS

C(1)=30.0
C(2)=1.5
C(3)=0.01
C(4)=25.0
C(5)=2.0
C(6)=0.01
DC(1)=1.0
DC(2)=0.05
DC(3)=0.001
DC(4)=1.0
DC(5)=0.05
DC(6)=0.001
ACUR=0.02
PI=3.1425926
CA=PI/NS
TT=DT*NT
DW=2.0*PI/TT
NW=30
NWA=30
W1=NWA*DW
DO 111 I=1,NW
111 W(I)=W1+(I-1)*DW
W2=W(NW)
DO 112 I=1,NID
112 CT(I)=C(I)
MC=M1+M2

C
C
C   READ INPUT AND REPOSE THEN FFT

READ(10,12) (Y1(I),Y2(I),I=1,NT)
READ(14,16) (F2(I),I=1,NT)

C
C
C   COMPUTE THE RELATIVE DISPLACEMENT AND
   SMOOTH THE INPUT FUNCTION WHEN IF NECESSARY

DO 37 I=1,NT
37 Y2(I)=Y2(I)-Y1(I)
   IF(ISMOTH.NE.1) GO TO 39
DO 36 I=1,NS
   IM=NT-I+1
   CMULT=0.5*(1.0-COS((I-1)*CA))
   Y1(IM)=CMULT*Y1(IM)
   Y2(IM)=CMULT*Y2(IM)
   F2(IM)=CMULT*F2(IM)
36 CONTINUE

```

```

39 DO 18 I=1,NT
C
C   CALCULATE THE FFT
C
Y1FT(I)=CMPLX(Y1(I),0.0)*TT
Y2FT(I)=CMPLX(Y2(I),0.0)*TT
F2FT(I)=CMPLX(F2(I),0.0)*TT
18 CONTINUE
CALL FFT1(Y1FT,M,NT,-1.0)
CALL FFT1(Y2FT,M,NT,-1.0)
CALL FFT1(F2FT,M,NT,-1.0)
C
C   FIND MODULI OF Y1FT,Y2FT
C
NB=NW+NWA
DO 20 I=NWA,NB
Y1(I)=CABS(Y1FT(I))
Y2(I)=CABS(Y2FT(I))
WW=(I-1)*DW
C 20 WRITE(13,17)WW,Y1(I),Y2(I)
20 CONTINUE
IF(IORDER.EQ.2) GO TO 122
GO TO 123
C
C   CHANGE THE ORDER OF INITIAL VALUES
C
122 NID=4
C(1)=C(1)
C(2)=C(2)
C(3)=C(4)
C(4)=C(5)
DC(1)=DC(1)
DC(2)=DC(2)
DC(3)=DC(4)
DC(4)=DC(5)
DO 133 I=1,NID
CT(I)=C(I)
133 CONTINUE
C
C   IDENTIFICATION START
C
123 DO 99 INDEX=1,NCY
ICOUNT=1
DO 98 IDX=1,NID
CC(IDX)=C(IDX)
105 DO 97 IX=1,NCUV
CT(IDX)=C(IDX)-(4-IX)*DC(IDX)
IF(IX.EQ.1) CTI=CT(IDX)
DO 96 IW=1,NW
C
C   COMPUTE COEFFICIENTS
C

```

```

IF(IORDER.EQ.2)GO TO 200
B1=CMPLX(1.0,W(IW)*CT(3))
B2=CMPLX(1.0,W(IW)*CT(6))
B11=(W(IW))**2*MC*B1
B22=(W(IW))**2*M2*B2
A(1,1)=CMPLX(CT(1)-REAL(B11),CT(2)*W(IW)-AIMAG(B11))
A(1,2)=-(W(IW))**2*M2*B1
A(2,1)=-B22
A(2,2)=CMPLX(CT(4)-REAL(B22),CT(5)*W(IW)-AIMAG(B22))
CALL MATINV(A,2,AINV)
B(1,1)=B1
B(1,2)=B1
B(2,1)=CMPLX(0.0,0.0)
B(2,2)=B2
CALL MULTI(AINV,2,2,B,NCOL,H)
GO TO 205

```

C
C
C

CALCULATION FOR SECOND ORDER

```

200 AA(1,1)=CMPLX(CT(1)-MC*(W(IW))**2,CT(2)*W(IW))
AA(2,2)=CMPLX(CT(3)-M2*(W(IW))**2,CT(4)*W(IW))
AA(1,2)=CMPLX(-M2*(W(IW))**2,0.0)
AA(2,1)=AA(1,2)
BB(1,1)=CMPLX(1.0,0.0)
BB(1,2)=CMPLX(1.0,0.0)
BB(2,1)=CMPLX(0.0,0.0)
BB(2,2)=CMPLX(1.0,0.0)
CALL MATINV(AA,2,AAIN)
CALL MULTI(AAIN,2,2,BB,NCOL,H)
205 H12=H(1,2)
H22=H(2,2)
Y1T(IW)=CABS(H12*F2FT(NWA+IW-1))
Y2T(IW)=CABS(H22*F2FT(NWA+IW-1))
Y11(IW)=Y1(NWA+IW-1)
Y22(IW)=Y2(NWA+IW-1)

```

C
C
C

CALCULATE THE ERROR TERM

```

EPS1(IW)=Y11(IW)-Y1T(IW)
EPS2(IW)=Y22(IW)-Y2T(IW)
96 CONTINUE
E2(IX)=0.0

```

C
C
C

SUMMATION OF ERROR

```

DO 121 I=1,NW
121 E2(IX)=E2(IX)+EPS1(I)**2+EPS2(I)**2
C WRITE(6,12) CT(IDX),E2(IX)
97 CONTINUE
C WRITE(6,25)
C

```

C

FIT THE E2(IX) IN A POLYNOMIAL EQUATION BY

```

C      USING THE LEAST SQUARE METHOD AND THEN FIND
C      THE CORRESPONDING FREQUENCY WHERE THE CURVE
C      HAS A MINIMUM
C
C      CALL FIT1(E2,3,NCUV,CTI,DC(IDX),COE)
C
C      CHECK THE CURVATURE
C
103  CT(IDX)=-COE(2)/(2.0*COE(3))
      C(IDX)=CT(IDX)
      CCOUNT(ICOUNT)=CT(IDX)
      ICOUNT=ICOUNT+1
98   CONTINUE
C     ERROR(INDEX)=E2(NCUV)
C     ACU=ABS(ERROR(INDEX-1)-ERROR(INDEX))/ERROR(INDEX)
C     IF(ACU.LT.1.0E-3) GO TO 100
      DO 191 I=1,NID
      RATIO=ABS(CCOUNT(I)-CC(I))/CC(I)
      IF(RATIO.LE.ACUR) GO TO 191
      GO TO 95
191  CONTINUE
      GO TO 100
95   WRITE(6,19)(C(I),I=1,NID)
99   CONTINUE
100  WRITE(6,*)(C(I),I=1,NID)
      GO TO 87
12   FORMAT(2E12.4)
16   FORMAT(E12.4)
17   FORMAT(3E12.4)
19   FORMAT(6E12.4)
23   FORMAT(4E12.4)
25   FORMAT(/)
87   STOP
      END
C
C      MATRIX MULTIPLICATION
C
      SUBROUTINE MULTI(TA,N,M,TB,L,TC)
      COMPLEX TA(N,M),TB(M,L),TC(N,L)
      DO 15 I=1,N
      DO 15 J=1,L
      TC(I,J)=0.0
      DO 15 K=1,M
15   TC(I,J)=TC(I,J)+TA(I,K)*TB(K,J)
      RETURN
      END
C
C
C      *****
C      *          PROGRAM "MDFID"          *
C      *****
C      A COMPUTER PROGRAM FOR THE ANALYSIS OF THE

```

AD-A136 342

IDENTIFICATION OF DAMAGE IN HYSTERETIC STRUCTURES(U)
NEW MEXICO UNIV ALBUQUERQUE DEPT OF CIVIL ENGINEERING
M L WANG ET AL. JUL 83 AFOSR-TR-83-1230 AFOSR-81-0086

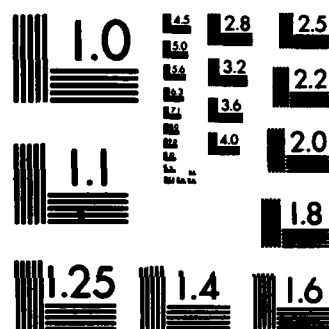
3/3

UNCLASSIFIED

F/G 13/13

NL

END



MICROCOPY RESOLUTION TEST CHART
NATIONAL BUREAU OF STANDARDS-1963-A

```

C      LINEAR RESPONSE OF HIGH ORDER MDF SYSTEM
C
C      MM      =HIGHEST DERIVATIVES
C      NT      =NUMBER OF POINTS ANALYZED
C      DT      =TIME STEP
C      A(J,K,L)=(AJ)
C      XO(J,K)=JTH DERIVATIVES OF STATE VECTOR AT TIME T
C      DX(J,K)=DELTA OF JTH DERIVATIVES
C      XN(J,K)=JTH DERIVATIVES OF STATE VECTOR AT TIME T+DT
C      F(J,K) =JTH FORCE AT TIME K
C
C      DIMENSION A(4,2,2),XO(4,2),DX(4,2),XN(4,2),CA(2,2)
C      DIMENSION CB(2,2),F(2,1024),DM(2,2),AMI(2,2),FT(5)
C      DIMENSION DV(2),DU(2),DW(2),DN(2,2),DR(2),FF(1024)
C      DIMENSION FK(5),DD(4,2),DE(4,2),DF(2),FD(1024)
C      DIMENSION ENED1(1024),ENED2(1024),FDD(2,1024)
C      CALL OPSYS('ALLOC','RH1',10)
C      CALL OPSYS('ALLOC','MDF2',16)
C
C      SPECIFY DATA(AJ)=A(J,K,L)
C
C      A(1,1,1)=29.07
C      A(1,1,2)=0.0
C      A(1,2,1)=0.0
C      A(1,2,2)=32.3
C      A(2,1,1)=2.11
C      A(2,1,2)=0.0
C      A(2,2,1)=0.0
C      A(2,2,2)=1.89
C      A(3,1,1)=1.0+1.0
C      A(3,1,2)=1.0
C      A(3,2,1)=1.0
C      A(3,2,2)=1.0
C      A(4,1,1)=0.0082*A(3,1,1)
C      A(4,1,2)=0.0082*A(3,1,2)
C      A(4,2,1)=0.0048*A(3,2,1)
C      A(4,2,2)=0.0048*A(3,2,2)
C
C      M=4 MEANS THIRD-ORDER; M=3 MEANS SECOND-ORDER
C
C      M=4
C      MM=M-1
C      DT=0.05
C      NT=1024
C      ENED1(1)=0.0
C      ENED2(1)=0.0
C      AM1=1.0
C      AM2=1.0
C      DO 14 I=1,M
C      DO 14 J=1,2
C      XO(I,J)=0.0

```

```

14 CONTINUE
C
C   READ THE INPUT
C
  READ(10,18)(FF(I),FD(I),I=1,NT)
18 FORMAT(2E12.4)
  DO 20 I=1,NT
    F(2,I)=FF(I)
    F(1,I)=FF(I)
  20 CONTINUE
    IF(M.NE.4) GO TO 91
    DO 93 I=1,NT
      FDD(1,I)=FD(I)*A(4,1,2)
      FDD(2,I)=FD(I)*A(4,2,2)
  93 CONTINUE
C
C   FIND A(M) AND ITS INVERSE
C
  91 DO 121 I=1,2
    DO 121 J=1,2
  121 DM(I,J)=A(M,I,J)
    CALL MATINV(DM,2,AMI)
C
C   FACTOR COMPUTATION
C
  FT(M)=1.0
  DO 131 J=2,M
    JJ=M+1-J
  131 FT(JJ)=FT(JJ+1)*FLOAT(J)
C
C   CALCULATE THE CONSTANT VALUES OF EQ 13
C
  DO 141 K=1,2
    DO 141 L=1,2
  141 CA(K,L)=0.0
    DO 151 J=1,MM
      AC=(DT** (M-J))/FT(J)
      DO 150 K=1,2
        DO 150 L=1,2
      150 CA(K,L)=CA(K,L)+AC*A(J,K,L)
  151 CONTINUE
    DO 161 K=1,2
      DO 161 L=1,2
    161 DM(K,L)=CA(K,L)
      CALL MULT(AMI,DM,CA,2)
      DO 171 K=1,2
    171 CA(K,K)=CA(K,K)+1.0
      CALL MATINV(CA,2,DM)
      CALL MULT(DM,AMI,CA,2)
C
C   FACTOR COMPUTATION

```



```

C      FK(1)=1.0
      DO 173 J=2,5
      FK(J)=FK(J-1)*FLOAT(J-1)
173  CONTINUE
C
C      START THE COMPUTATION LOOP
C
      WRITE(16,26)T,XO(1,1),XO(1,2)
      DO 999 INDEX=2,NT
      T=(INDEX-1)*DT
C
C      SOLVE EQ 13
      (CALCULATE THE DIFFERENCES OF MTH DERIVATIVES)
C
      DO 181 J=1,2
181  DW(J)=0.0
      DO 191 J=1,MM
      LIM=M-J
      DO 183 L=1,2
183  DV(L)=0.0
      DO 185 K=1,LIM
      AC=(DT**K)/FK(K+1)
      JK=J+K
      DO 184 L=1,2
184  DV(L)=DV(L)+AC*XO(JK,L)
185  CONTINUE
      DO 186 K=1,2
      DO 186 L=1,2
186  DN(K,L)=A(J,K,L)
      CALL MULV(DN,DV,DU,2)
      DO 187 I=1,2
187  DW(I)=DU(I)+DW(I)
191  CONTINUE
      DO 201 I=1,2
      DF(I)=F(I,INDEX)-F(I,INDEX-1)+
      +(FDD(I,INDEX)-FDD(I,INDEX-1))
      DO 211 I=1,2
211  DV(I)=DF(I)-DW(I)
      CALL MULV(CA,DV,DW,2)
      DO 221 I=1,2
221  DX(M,I)=DW(I)
C
C      SOLVE EQ 7
      (CALCULATE THE DIFFERENCES OF JTH DERIVATIVES)
C
      DO 261 J=1,MM
      DO 230 I=1,2
230  DV(I)=0.0
      LIM=M-J
      DO 231 K=1,LIM
      AC=(DT**K)/(FK(K+1))

```

```

      JK=J+K
      DO 228 L=1,2
228  DV(L)=DV(L)+AC*XO(JK,L)
231  CONTINUE
      AC=(DT** (M-J))/FT(J)
      DO 241 I=1,2
241  DX(J,I)=DV(I)+AC*DX(M,I)
261  CONTINUE

```

C
C
C

SOLVE EQ 14(SOLUTIONS)

```

      DO 271 J=1,MM
      DO 269 L=1,2
269  XN(J,L)=XO(J,L)+DX(J,L)
271  CONTINUE

```

C
C
C
C

SOLVE EQ 16
(CALCULATE THE HIGHEST DERIVATIVES)

```

      DO 281 I=1,2
281  DW(I)=0.0
      DO 291 J=1,MM
      DO 285 K=1,2
      DV(K)=XN(J,K)
      DO 285 L=1,2
285  DM(K,L)=A(J,K,L)
      CALL MULV(DM,DV,DU,2)
      DO 286 K=1,2
286  DW(K)=DU(K)+DW(K)
291  CONTINUE
      DO 301 K=1,2
301  DW(K)=F(K,INDEX)+FDD(K,INDEX)-DW(K)
      CALL MULV(AMI,DW,DV,2)
      DO 311 K=1,2
311  XN(M,K)=DV(K)

```

C
C
C
C
C
C

WRITE(6,*)XN(M,1),XN(M,2)

PRINT OUT THE DISPLACEMENT

```

      XRE=XN(1,2)-XN(1,1)
      WRITE(16,26)T,XN(1,1),XN(1,2)
      VEL1=XN(2,1)
      VEL2=XN(2,2)-XN(2,1)
      REACC=XN(3,2)-XN(3,1)

```

C
C
C

STORE VALUES AND SET XO EQUAL TO XN

```

      ENED1(INDEX)=XN(2,1)*(F(2,INDEX)-
+2.0*AM1*XN(3,1)-AM2*XN(3,2))
      ENED2(INDEX)=XN(2,2)*(F(2,INDEX)-

```

```

+AM1*XN(3,1)-AM2*XN(3,2))
DO 321 J=1,M
DO 321 K=1,2
321 X0(J,K)=XN(J,K)
999 CONTINUE
CALL SIMP(ENED1,ENER1,DT,NT)
CALL SIMP(ENED2,ENER2,DT,NT)
ENER=ENER1+ENER2
WRITE(6,26) ENER1,ENER2,ENER
22 FORMAT(2E12.4)
26 FORMAT(3E12.4)
STOP
END

```

C
C
C

COMPUTE THE AREA UNDER THE CURVE

```

SUBROUTINE SIMP(X,E,D,N)
DIMENSION X(1024)
N2=N/2-1
E=X(1)
DO 1 I=1,N2
IA=2*I
IB=IA+1
E=E+4.0*X(IA)
E=E+2.0*X(IB)
1 CONTINUE
N3=N-1
E=E+0.5*X(N3)+1.5*X(N)
E=D*E/3.0
RETURN
END

```

C
C
C

MATRIX MULTIPLICATION

```

SUBROUTINE MULT(A,B,C,N)
DIMENSION A(N,N),B(N,N),C(N,N)
DO 1 I=1,N
DO 1 J=1,N
C(I,J)=0.0
DO 1 K=1,N
C(I,J)=C(I,J)+A(I,K)*B(K,J)
1 CONTINUE
RETURN
END

```

C
C

```

SUBROUTINE MULV(A,B,C,N)
DIMENSION A(N,N),B(N),C(N)
DO 1 I=1,N
C(I)=0.0
DO 1 J=1,N
C(I)=C(I)+A(I,J)*B(J)

```

```

1  CONTINUE
   RETURN
   END

C
   SUBROUTINE MATINV(C,N,D)
C   MATRIX INVERSION C-INPUT  D-OUTPUT
   DIMENSION C(N,N),D(N,N)
   DO 10 J=1,N
   DO 10 K=1,N
10  D(J,K)=0.0
   DO 11 K=1,N
11  D(K,K)=1.0
   P1=1.0
   DO 55 I=1,N
   P2=C(I,I)
   DO 40 J=1,N
   C(I,J)=C(I,J)/P2
40  D(I,J)=D(I,J)/P2
   DO 51 IC=1,N
   P3=-C(IC,I)
   DO 50 K=1,N
   IF(IC-I)21,51,21
21  C(IC,K)=C(I,K)*P3+C(IC,K)
50  D(IC,K)=D(I,K)*P3+D(IC,K)
51  CONTINUE
   P1=P2*P1
   IF((I+2)-N)55,53,55
53  DET=P1*((C(I+1,I+1)*C(I+2,I+2))-
+ (C(I+2,I+1)*C(I+1,I+2)))
55  CONTINUE
   DO 70 IT=1,N
   DO 70 IS=1,N
70  C(IT,IS)=D(IT,IS)
   RETURN
   END

```

```

C *****
C *                SELECTED SUBROUTINES                *
C *****
C
C SUBROUTINE SPCOEF(N,XN,FN,S,INDEX)
C DIMENSION XN(N),FN(N),S(N),INDEX(N)
C DIMENSION RHO(1024),TAU(1024)
C NM1=N-1
C
C ARRANGE THE NODES XN IN INCREASING ORDER.
C STORE THE ORDER IN THE ARRAY INDEX.
C
C DO 1 I=1,N
1  INDEX(I)=I
C DO 3 I=1,NM1
C   IP1=I+1
C   DO 2 J=IP1,N
C     II=INDEX(I)
C     IJ=INDEX(J)
C     IF(XN(II).LE.XN(IJ))GO TO 2
C     ITEMP=INDEX(I)
C     INDEX(I)=INDEX(J)
C     INDEX(J)=ITEMP
C   2 CONTINUE
C   3 CONTINUE
C   NM2=N-2
C
C CALCULATE THE ELEMENTS OF THE ARRAYS RHO AND TAU.
C
C RHO(2)=0.0
C TAU(2)=0.0
C DO 4 I=2,NM1
C   IIM1=INDEX(I-1)
C   II=INDEX(I)
C   IIP1=INDEX(I+1)
C   HIM1=XN(II)-XN(IIM1)
C   HI=XN(IIP1)-XN(II)
C   TEMP=(HIM1/HI)*(RHO(I)+2.0)+2.0
C   RHO(I+1)=-1.0/TEMP
C   D=6.0*((FN(IIP1)-FN(II))/HI-
C 4   +(FN(II)-FN(IIM1))/HIM1)/HI
C   TAU(I+1)=(D-HIM1*TAU(I)/HI)/TEMP
C
C COMPUTE ARRAY OF SECOND DERIVATIVES S FOR
C THE NATURAL SPLINE
C
C S(1)=0.0
C S(N)=0.0
C DO 5 I=1,NM2
C   IB=N-I
C 5  S(IB)=RHO(IB+1)*S(IB+1)+TAU(IB+1)
C RETURN

```

```

END
FUNCTION SPLINE(N,XN,FN,S,INDEX,X)
DIMENSION XN(N),FN(N),S(N),INDEX(N)

C
C
C
C
C
C
IF X.LT.XN(INDEX(1)), APPROXIMATE FUNCTION BY
THE STRAIGHT LINE WHICH PASSES THROUGH THE POINT
(XN(INDEX(1)),FN(INDEX(1)))AND WHOSE
SLOPE AGREES WITH THE SPLINE AT THAT POINT

I1=INDEX(1)
IF(X.GE.XN(I1))GO TO 1
I2=INDEX(2)
H1=XN(I2)-XN(I1)
SPLINE=FN(I1)+(X-XN(I1))*((FN(I2)-FN(I1))
+/H1-H1*S(2)/6.0)
RETURN

C
C
C
C
C
C
IF X.GE.XN(INDEX(N)), APPROXIMATE FUNCTION BY
THE STRAIGHT LINE WHICH PASSES THROUGH THE POINT
(XN(INDEX(N)),FN(INDEX(N))) AND WHOSE SLOPE AGREES
WITH THE SLOP OF THE SPLINE AT THAT POINT.

1 IN=INDEX(N)
IF(X.LE.XN(IN))GO TO 2.
INM1=INDEX(N-1)
HN1=XN(IN)-XN(INM1)
SPLINE=FN(IN)+(X-XN(IN))*((FN(IN)-FN(INM1))
+/HN1+HN1*S(N-1)/6.0)
RETURN

C
C
C
C
FOR XN(INDEX(1)).LE.X.LE.XN(INDEX(N)) CALCULATE
SPLINE FIT.

2 DO 3 I=2,N
II=INDEX(I)
IF(X.LE.XN(II))GO TO 4
3 CONTINUE
4 L=I-1
IL=INDEX(L)
ILP1=INDEX(L+1)
A=XN(ILP1)-X
B=X-XN(IL)
HL=XN(ILP1)-XN(IL)
SPLINE=A*S(L)*(A**2/HL-HL)/6.0+B*S(L+1)*
+(B**2/HL-HL)/6.0-(A*FN(IL)+B*FN(ILP1))/HL
RETURN
END

C
C
C
C
C
FFT PROGRAM

*****
MULTIPLIED BY T WHEN USING THE FORWARD FFT

```

```

C      DIVIDED BY DT FOR BACKWARD FFT
C      SIGN =-1. FOR DFT, SIGN=1. FOR IDFT
C      *****
C
C      SUBROUTINE FFT1(A,N,NB,SIGN)
C      COMPLEX A(NB),U,W,T
C
C      DIVIDE ALL ELEMENT BY NB
C
C      DO 1 J=1,NB
1  A(J)=A(J)/NB
C
C      REORDER SEQUENCE
C
C      NBD2=NB/2
C      NBM1=NB-1
C      J=1
C      DO 4 L=1,NBM1
C      IF(L.GE.J) GO TO 2
C      T=A(J)
C      A(J)=A(L)
C      A(L)=T
2  K=NBD2
3  IF(K.GE.J) GO TO 4
C      J=J-K
C      K=K/2
C      GO TO 3
4  J=J+K
C      CALCULATE FFT
C
C      PI=3.141592653589793
C      DO 6 M=1,N
C      U=(1.0,0.0)
C      ME=2**M
C      K=ME/2
C      W=CMPLX(COS(PI/K),SIGN*SIN(PI/K))
C      DO 6 J=1,K
C      DO 5 L=J,NB,ME
C      LPK=L+K
C      T=A(LPK)*U
C      A(LPK)=A(L)-T
5  A(L)=A(L)+T
6  U=U*W
C      RETURN
C      END
C
C      SUBROUTINE SIMP(QF,A,B,ACC,ANS,ERROR,AREA,IFLAG)
C
C      SIMP IS AN ADAPTIVE, ITERATIVE CODE BASED
C      ON SIMPSON'S RULE. IT IS DESIGNED TO EVALUATE THE
C      DEFINITE INTEGRAL OF A CONTINUOUS FUNCTION WITH
C      FINITE LIMITS OF INTEGRATION.

```

C F - NAME OF FUNCTION WHOSE INTEGRAL IS DESIRED.
 C THE FUNCTION NAME F MUST APPEAR IN AN EXTERNAL
 C STATEMENT IN THE CALLING PROGRAM.
 C A,B - LOWER AND UPPER LIMITS OF INTEGRATION.
 C ANS- APPROXIMATE VALUE OF THE INTEGRAL OF F(X)
 C FROM A TO B.
 C AREA - APPROXIMATE VALUE OF THE INTEGRAL OF
 C ABS(F(X)) FROM A TO B.
 C ERROR - ESTIMATED ERROR OF ANS. USER MAY WISH
 C TO EXTRAPOLATE BY FORMING ANS+ERROR TO GET WHAT IS
 C OFTEN A MORE ACCURATE RESULT, BUT NOT ALWAYS.
 C ACC - DESIRED ACCURACY OF ANS. CODE TRIES TO MAKE
 C ABS(ERROR).LE.ACC*ABS(AREA).
 C IFLAG = 1 FOR NORMAL RETURN.
 C = 2 IF IT IS NECESSARY TO GO TO 30 LEVELS OR
 C USE A SUBINTERVAL TOO SMALL FOR MACHINE WORD
 C LENGTH. ERROR MAY BE UNRELIABLE IN THIS CASE.
 C = 3 IF MORE THAN 2000 FUNCTION EVALUATIONS
 C ARE USED. ROUGH APPROXIMATIONS ARE USED TO
 C COMPLETE THE COMPUTATIONS AND ERROR IS
 C USUALLY UNRELIABLE.

DIMENSION FV(5),LORR(30),F1T(30),F2T(30),F3T(30)
 DIMENSION ARESTT(30),ESTT(30),EPST(30),PSUM(30)
 DIMENSION DAT(30)

C SET U TO APPROXIMATELY THE UNIT ROUND-OFF OF
 C SPECIFIC MACHINE (HERE IBM 360/67)

U = 9.0E-7

C INITIALIZE

FOURU=4.0*U
 IFLAG=1
 EPS=ACC
 ERROR=0.0
 LVL=1
 LORR(LVL)=1
 PSUM(LVL)=0.0
 ALPHA=A
 DA=B-A
 AREA=0.0
 AREST=0.0
 FV(1)=QF(ALPHA)
 FV(3)=QF(ALPHA+0.5*DA)
 FV(5)=QF(ALPHA+DA)
 KOUNT=3
 WT=D/6.0
 EST='*(FV(1)+4.0*FV(3)+FV(5))

C


```

C      'BASIC STEP'. HAVE ESTIMATE EST OF INTEGRAL
C      ON (ALPHA,ALPHA+DA). BISECT AND COMPUTE
C      ESTIMATES ON LEFT AND RIGHT HALF INTERVALS.
C      SIMILARLY TREAT INTEGRAL OF ABS(F(I)). SUM IS
C      BETTER VALUE FOR INTEGRAL AND DIFF/15.0 IS
C      APPROXIMATELY ITS ERROR.
C
1      DX=0.5*DA
      FV(2)=QF(ALPHA+0.5*DX)
      FV(4)=QF(ALPHA+1.5*DX)
      KOUNT=KOUNT+2
      WT=DX/6.0
      ESTL=WT*(FV(1)+4.0*FV(2)+FV(3))
      ESTR=WT*(FV(3)+4.0*FV(4)+FV(5))
      SUM=ESTL+ESTR
      ARESTL=WT*(ABS(FV(1))+ABS(4.0*FV(2))+ABS(FV(3)))
      ARESTR=WT*(ABS(FV(3))+ABS(4.0*FV(4))+ABS(FV(5)))
      AREA=AREA+((ARESTL+ARESTR)-AREST)
      DIFF=EST-SUM
C
C      IF ERROR IS ACCEPTABLE, GO TO 2. IF INTERVAL
C      IS TOO SMALL OR TOO MANY LEVELS OR TOO MANY
C      FUNCTION EVALUATIONS, SET A FLAG
C      AND GO TO 2 ANYWAY.
C
      IF(ABS(DIFF).LE.EPS*ABS(AREA))GO TO 2
      IF(ABS(DX).LE.FOURU*ABS(ALPHA))GO TO 5
      IF(LVL.GE.30)GO TO 5
      IF(KOUNT.GE.2000)GO TO 6
C
C      HERE TO RAISE LEVEL. STORE INFORMATION TO
C      PROCESS RIGHT HALF INTERVAL LATER. INITIALIZE FOR
C      'BASIC STEP' SO AS TO TREAT LEFT HALF INTERVAL.
C
      LVL=LVL+1
      LORR(LVL)=0
      F1T(LVL)=FV(3)
      F2T(LVL)=FV(4)
      F3T(LVL)=FV(5)
      DA=DX
      DAT(LVL)=DX
      AREST=ARESTL
      ARESTT(LVL)=ARESTR
      EST=ESTL
      ESTT(LVL)=ESTR
      EPS=EPS/1.4
      EPST(LVL)=EPS
      FV(5)=FV(3)
      FV(3)=FV(2)
      GO TO 1
C
C      ACCEPT APPROXIMATE INTEGRAL SUM. IF IT WAS ON

```

```

C      A LEFT INTERVAL GO TO 'MOVE RIGHT'.  IF A RIGHT
C      INTERVAL, ADD RESULTS TO FINISH AT THIS LEVEL.
C      ARRAY LORR (MNEMONI" FOR LEFT OR RIGHT TELLS
C      WHETHER LEFT OR RIGHT INTERVAL AT EACH LEVEL.
C
2      ERROR=ERROR+DIFF/15.0
3      IF(LORR(LVL).EQ.0)GO TO 4
      SUM=PSUM(LVL)+SUM
      LVL=LVL-1
      IF(LVL.GT.1)GO TO 3
      ANS=SUM
      RETURN

C      'MOVE RIGHT'.  RESTORE SAVED INFORMATION TO
C      PROCESS RIGHT HALF INTERVAL.
C
4      PSUM(LVL)=SUM
      LORR(LVL)=1
      ALPHA=ALPHA+DA
      DA=DAT(LVL)
      FV(1)=F1T(LVL)
      FV(3)=F2T(LVL)
      FV(5)=F3T(LVL)
      AREST=ARESTT(LVL)
      EST=ESTT(LVL)
      EPS=EPST(LVL)
      GO TO 1

C      ACCEPT 'POOR' VALUE.  SET APPROPRIATE FLAGS.
C
5      IFLAG=2
      GO TO 2
6      IFLAG=3
      GO TO 2
      END

C
C      SUBROUTINE SPCOEF(N,XN,FN,S,INDEX)
      DIMENSION XN(N),FN(N),S(N),INDEX(N)
      DIMENSION RHO(1024),TAU(1024)
      NM1=N-1

C      ARRANGE THE NODES XN IN INCREASING ORDER.
C      STORE THE ORDER IN THE ARRAY INDEX.
C
      DO 1 I=1,N
1      INDEX(I)=I
      DO 3 I=1,NM1
      IP1=I+1
      DO 2 J=IP1,N
      II=INDEX(I)
      IJ=INDEX(J)

```

```

IF(XN(II).LE.XN(IJ))GO TO 2
ITEMP=INDEX(I)
INDEX(I)=INDEX(J)
INDEX(J)=ITEMP
2 CONTINUE
3 CONTINUE
NM2=N-2

C
C
C
C
CALCULATE THE ELEMENTS OF THE ARRAYS
RHO AND TAU.

RHO(2)=0.0
TAU(2)=0.0
DO 4 I=2,NM1
IIM1=INDEX(I-1)
II=INDEX(I)
IIP1=INDEX(I+1)
HIM1=XN(II)-XN(IIM1)
HI=XN(IIP1)-XN(II)
TEMP=(HIM1/HI)*(RHO(I)+2.0)+2.0
RHO(I+1)=-1.0/TEMP
D=6.0*((FN(IIP1)-FN(II))/HI
+-(FN(II)-FN(IIM1))/HIM1)/HI
4 TAU(I+1)=(D-HIM1*TAU(I)/HI)/TEMP

C
C
C
C
COMPUTE ARRAY OF SECOND DERIVATIVES S FOR
THE NATURAL SPLINE.

S(1)=0.0
S(N)=0.0
DO 5 I=1,NM2
IB=N-I
5 S(IB)=RHO(IB+1)*S(IB+1)+TAU(IB+1)
RETURN
END
FUNCTION SPLINE(N,XN,FN,S,INDEX,X)
DIMENSION XN(N),FN(N),S(N),INDEX(N)

C
C
C
C
C
IF X.LT.XN(INDEX(1)), APPROXIMATE FUNCTION
BY THE STRAIGHT LINE WHICH PASSES THROUGH THE
POINT (XN(INDEX(1)),FN(INDEX(1))) AND WHOSE SLOPE
AGREES WITH THE SLOPE OF THE SPLINE AT THAT POINT.

I1=INDEX(1)
IF(X.GE.XN(I1))GO TO 1
I2=INDEX(2)
H1=XN(I2)-XN(I1)
SPLINE=FN(I1)+(X-XN(I1))*((FN(I2)-FN(I1))
+/H1-H1*S(2)/6.0)
RETURN

C
C
IF X.GE.XN(INDEX(N)), APPROXIMATE FUNCTION BY

```

```

C      THE STRAIGHT LINE WHICH PASSES THROUGH THE POINT
C      (XN(INDEX(N)),FN(INDEX(N))) AND WHOSE SLOPE
C      AGREES WITH THE SLOPE OF THE SPLINE AT THAT POINT.
C
1      IN=INDEX(N)
      IF(X.LE.XN(IN))GO TO 2
      INM1=INDEX(N-1)
      HNM1=XN(IN)-XN(INM1)
      SPLINE=FN(IN)+(X-XN(IN))*((FN(IN)-FN(INM1))/HNM1
+HNM1*S(N-1)/6.0)
      RETURN
C
C      FOR XN(INDEX(1)).LE.X.LE.XN(INDEX(N))
C      CALCULATE SPLINE FIT.
C
2      DO 3 I=2,N
      II=INDEX(I)
      IF(X.LE.XN(II))GO TO 4
3      CONTINUE
4      L=I-1
      IL=INDEX(L)
      ILP1=INDEX(L+1)
      A=XN(ILP1)-X
      B=X-XN(IL)
      HL=XN(ILP1)-XN(IL)
      SPLINE=A*S(L)*(A**2/HL-HL)/6.0+B*S(L+1)*(B**2/HL-HL)
+ /6.0-(A*FN(IL)+B*FN(ILP1))/HL
      RETURN
      END
C
C      THIS SUBROUTINE IS FOR N*N MATRIX INVERSION
C
C      SUBROUTINE INVERS(B,N,A)
C
      DOUBLE PRECISION A(2,2),B(2,2),C(2,2)
      DOUBLE PRECISION AMAX,TEMP,PIVOT
      DIMENSION INDEX(4,2)
      IF(N.GT.40) GO TO 134
      DO 90 I=1,N
      DO 90 J=1,N
      A(I,J)=B(I,J)
90      CONTINUE
      DO 107 I=1,N
      DO 107 J=1,N
107      B(I,J)=A(I,J)
      DO 108 I=1,N
108      INDEX(I,1)=0
      II=0
109      AMAX=-1.0DO
      DO 110 I=1,N
      IF(INDEX(I,1)) 110,111,110
111      DO 112 J=1,N

```

```

        IF(INDEX(J,1)) 112,113,112
113 TEMP=DABS(A(I,J))
        IF(TEMP-AMAX) 112,112,114
114 IROW=I
        ICOL=J
        AMAX=TEMP
112 CONTINUE
110 CONTINUE
        IF(AMAX) 225,115,116
116 INDEX(ICOL,1)=IROW
        IF(IROW-ICOL) 119,118,119
119 DO 120 J=1,N
        TEMP=A(IROW,J)
        A(IROW,J)=A(ICOL,J)
120 A(ICOL,J)=TEMP
        II=II+1
        INDEX(II,2)=ICOL
118 PIVOT=A(ICOL,ICOL)
        A(ICOL,ICOL)=1.0D0
        PIVOT=1.0D0/PIVOT
        DO 121 J=1,N
121 A(ICOL,J)=A(ICOL,J)*PIVOT
        DO 122 I=1,N
        IF(I-ICOL) 123,122,123
123 TEMP=A(I,ICOL)
        A(I,ICOL)=0.0D0
        DO 124 J=1,N
124 A(I,J)=A(I,J)-A(ICOL,J)*TEMP
122 CONTINUE
        GO TO 109
125 ICOL=INDEX(II,2)
        IROW=INDEX(ICOL,1)
        DO 126 I=1,N
        TEMP=A(I,IROW)
        A(I,IROW)=A(I,ICOL)
126 A(I,ICOL)=TEMP
        II=II-1
225 IF(II) 125,127,125
127 DO 130 I=1,N
        DO 130 J=1,N
        C(I,J)=0.0D0
        DO 130 K=1,N
130 C(I,J)=C(I,J)+B(I,K)*A(K,J)
        GO TO 134
115 WRITE(6,133)
133 FORMAT('          ZERO PIVOT')
134 RETURN
        END

```

C
C
C
C

LEAST SQUARE POLYNOMIAL FITTING

```

C      Y : INPUT
C      MP : DEGREE OF POLYNOMIAL
C      N : NUMBER OF POINT FOR THE FITTING
C      X1 : THE LOW X-AXIS VALUE
C      X2 : THE UPPER X-AXIS VALUE
C      A(I): THE COEFFICIENT OF THE POLYNOMIAL
C      A(1): THE CONSTANT COEFFICIENT
C
      SUBROUTINE FIT1(Y,MP,N,X1,X2,A)
      DIMENSION XX(20,3),Y(20),X(20),XP(3,3),A(3)
      DIMENSION EPS(20),D(3,3),B(3)
      DX=(X2-X1)/FLOAT(N-1)
      DO 10 I=1,N
10     X(I)=X1+FLOAT(I-1)*DX
      DO 1 I=1,N
      XX(I,1)=1.0
      DO 1 J=2,MP
1     XX(I,J)=X(I)**(J-1)
      DO 2 I=1,MP
      DO 2 J=I,MP
      XP(I,J)=0.0
      DO 2 K=1,N
2     XP(I,J)=XP(I,J)+XX(K,I)*XX(K,J)
      DO 3 I=2,MP
      IM=I-1
      DO 3 J=1,IM
3     XP(I,J)=XP(J,I)
      CALL MATINV(XP,MP,D)
      DO 4 I=1,MP
      B(I)=0.0
      DO 4 J=1,N
4     B(I)=B(I)+XX(J,I)*Y(J)
      DO 5 I=1,MP
      A(I)=0.0
      DO 5 J=1,MP
5     A(I)=A(I)+D(I,J)*B(J)
      RETURN
      END
C
C      MATRIX INVERSION
C
      SUBROUTINE MATINV(C,N,D)
C      MATRIX INVERSION C-INPUT D-OUTPUT
      DIMENSION C(N,N),D(N,N)
      DO 10 J=1,N
      DO 10 K=1,N
10     D(J,K)=0.0
      DO 11 K=1,N
11     D(K,K)=1.0
      P1=1.0
      DO 55 I=1,N
      P2=C(I,I)

```

```
DO 40 J=1,N
C(I,J)=C(I,J)/P2
40 D(I,J)=D(I,J)/P2
DO 51 IC=1,N
P3=-C(IC,I)
DO 50 K=1,N
IF(IC-I)21,51,21
21 C(IC,K)=C(I,K)*P3+C(IC,K)
50 D(IC,K)=D(I,K)*P3+D(IC,K)
51 CONTINUE
P1=P2*P1
IF((I+2)-N)55,53,55
53 DET=P1*((C(I+1,I+1)*C(I+2,I+2))-
+(C(I+2,I+1)*C(I+1,I+2)))
55 CONTINUE
DO 70 IT=1,N
DO 70 IS=1,N
70 C(IT,IS)=D(IT,IS)
RETURN
END
```

FILM

2-84

DTIC